SIGNAL TRANSDUCTION IN THE BARLEY POWDERY MILDEW FUNGUS

Gemma D. Priddey

Linacre College

A thesis submitted for the degree of Doctor of Philosophy at the University of Oxford

June 2003



Be your own light, your own refuge.
Believe only that which you test for yourself.
Do not accept authority merely because it comes from a great man,
or is written in a sacred book,
for truth is different for each man and woman.

-Buddha

ABSTRACT
Signal transduction in the barley powdery mildew fungus

Gemma Priddey, Linacre College
Thesis submitted for the degree of Doctor of Philosophy
Trinity Term 2003

Barley powdery mildew disease is caused by the highly specialised phytopathogenic fungus, *Blumeria graminis* f.sp. *hordei*. Disease is spread prolifically by the production of asexual conidia. Following contact with the barley leaf surface, a short, primary germ tube (PGT) emerges, followed by elaboration of a second-formed germ tube, the appressorial germ tube (AGT). This second-formed germ tube elongates, swells and hooks to form an appressorium, which allows direct penetration of the barley cuticle and infection of the host.

Infection structure differentiation in *B. graminis* is a highly regulated and complex process. It demands the coordinated perception of multiple external signals, but little is known about how these signals are integrated and transduced within the fungus. Protein kinase A (PKA) and cAMP signalling are known to play important, but complex, roles during infection structure development. However, signalling via cAMP alone is not sufficient to promote progression through infection structure differentiation.

This study describes the characterization of two *B. graminis* protein kinase C genes, *pkc*1 and *pkc*-like. PKC activity was identified in *B. graminis* protein extracts. Efforts to find an inhibitor specific for *B. graminis* PKC were unsuccessful. However, phorbol ester, a PKC agonist, invoked both appressorium formation when applied to spores *in vivo* and PKC activity in protein extracts. In addition, real-time PCR confirmed the differentially regulated transcript profiles of both *pkc*1 and *pkc*-like, revealing a peak in transcript levels just prior to PGT emergence for *pkc*1, and during PGT differentiation for the *pkc*-like gene.

Two mitogen-activated protein (MAP) kinases, *mpk*1 and *mpk*2, were characterized. MAP kinase activity was detected in conidial protein extracts. The MAP kinase kinase (MEK) inhibitor, PD98059, inhibited *B. graminis* germling morphogenesis. However, a MAP kinase agonist failed to show any effect on germling differentiation. In addition, real-time PCR confirmed the differentially regulated transcript profiles of both *mpk*1 and *mpk*2, and revealed a peak in transcript levels during appressorial germ tube elongation and swelling for both genes.

The "model" phytopathogenic fungus, *Magnaporthe grisea*, was employed as a "surrogate host" for the functional analysis of the *B. graminis* MAP kinase gene, *mpk*1. Firstly, the *mpk*1 promoter was sequenced and a plasmid construct made comprising the *mpk*1 gene under the control of the *mpk*1 promoter. This, and the control construct, that is the *M. grisea PMK1* gene under the control of the *PMK1* promoter, were transformed into *M. grisea* Δ*pmk1*. Southern analysis identified transformants for phenotypic studies. These showed that whereas Δ*pmk1* was complemented by *M. grisea PMK1* in the control experiments, *B. graminis mpk*1 failed to complement Δ*pmk1*. Expression studies showed that there was no expression of *mpk*1 in an *mpk*1 transformant.

ACKNOWLEDGEMENTS

The research reported in this thesis was funded by a special BBSRC CASE studentship in association with Aventis.

Many **BIG** thanks to Sarah Gurr for her support, encouragement and contagious enthusiasm throughout my undergraduate and D.Phil days. I would also like to thank Professor Nick Talbot and Dr Mick Kershaw (University of Exeter) for their assistance with the *Magnaporthe* work. Also thanks to Dr Catherine Pears and Dr Louis Mahadevan (Department of Biochemistry, Oxford University) for useful discussions on kinases. I am also very grateful to John Baker for help with photographs and for being wonderfully accommodating – especially during "time-courses"!

HUGE amounts of gratitude to everyone in the Gurr lab for being such wonderful friends. Thank you thank you thank you to Ziguo for his molecular biology wizardry and for providing an alternative view in any situation – in and out of the lab! Thanks to Pushpa for helping me to "walk", to Zena for providing a positive aura and to Julie for words of wisdom and encouragement - and for Hickory Dickory Dock cake. Thanks to Molly for the BBQ's, to Suzanne for helping to introduce me to the world of mildew, to Alison for getting me started on signalling and to Hannah for the "Japanese" and the alien outfit. A proliferation of praise also goes to Keith for being there through the good times and through the rants, to Emma for calmness via cocktails, to Cath for her vibrant attitude and for introducing us to Settlers, and to Susie for the laughs! Here's to many more games evenings!

And to Mum and Dad - for making it possible for me to pursue my goals and for always being there for me. Thanks to Rob for a life-time of inspiration. And many^{many}x☺ thanks to Martin for being instrumental in the creation of many happy memories.

CONTENTS

Abstract
Acknowledgements
Contents
Abbreviations

CHAPTER 1 – INTRODUCTION

1.1 THE POWDERY MILDEWS 1
1.1.1 Economic impacts 1
1.1.2 Taxonomy 2
1.1.3 Host specialisation 2
1.1.4 *Blumeria graminis* f.sp. *hordei* reproduction 3
1.1.5 Establishment of infection 4
1.1.6 Host response to *Blumeria graminis* f.sp. *hordei* infection 5
1.1.7 Host resistance 7
1.1.8 Methods of control 9
1.1.8.1 Chemical control 9

1.2 MAGNAPORTHE GRISEA 10
1.2.1 Host range, economic impact and description 10
1.2.2 Reproduction 11
1.2.3 Establishment of infection 11
1.2.4 Methods of control 13
1.2.4.1 Resistant crop cultivars 13
1.2.4.2 Cultural practices 14
1.2.4.3 Chemical control 14

1.3 APPRESSORIUM FORMATION 14
1.3.1 Attachment 15
1.3.2 Germination 15
1.3.3 Signals for appressorium formation 16
1.3.4 Perception of signals for appressorium differentiation 18
1.3.5 Signal transduction 19

1.4 OBJECTIVES 23

CHAPTER 2 – MATERIALS AND METHODS

2.1 PLANT AND FUNGAL MATERIAL 25
2.1.1 Plant material 25
2.1.2 Fungal material: Isolate, maintenance and inoculation 25
2.1.2.1 Blumeria graminis f.sp. *hordei* 25
2.1.2.2 Magnaporthe grisea 26
2.1.3 Collection of fungal material 26
2.1.3.1 Ungerminated conidia 26
2.1.3.2 Stage-specific material 26
From the host 26
From agar 27
From cellulose membrane 27
From cellophane 27

2.2 CHEMICALS AND SOLUTIONS 27

2.3 LIGHT MICROSCOPY 28

2.3.1 Preparation of surfaces for assay of *Blumeria graminis* f.sp. *hordei* and *Magnaporthe grisea* development 28
2.3.1.1 Barley epidermal peels 28
2.3.1.2 Cellulose membrane 29
2.3.1.3 Agar 29
2.3.2 Determination of development 29
2.3.3 Measurement of surface hydrophobicity 29

2.5 ENZYME ASSAYS 30
2.5.1 Fungal protein extraction and purification 30
2.5.1.1 Protein extraction 30
2.5.1.2 Protein purification 30
Ammonium sulphate precipitation 30
Column purification 31
2.5.1.3 Protein quantification 31
2.5.2 Protein kinase C activity (PKC) assay 31
2.5.2.1 Inhibitor IC_{50} value determination 32
2.5.3 cAMP-dependent protein kinase (PKA) assay 32
2.5.4 Mitogen-activated protein (MAP) kinase assay 32
2.5.4.1 SDS-polyacrylamide gel electrophoresis 32
2.5.4.2 Western blot analysis 33

2.6 DNA METHODS 34
2.6.1 Extraction of genomic DNA 34
2.6.2 Restriction endonuclease digests 34
2.6.3 DNA agarose electrophoresis 35
2.6.4 Extraction and purification of DNA from agarose gels 35
2.6.5 Transformation of *Escherichia coli* 35
2.6.5.1 Preparation of heat-shock competent cells 35
2.6.5.2 DNA ligation 36
2.6.5.3 Heat-shock transformation method 36
2.6.5.4 Purification of plasmid DNA from Escherichia coli 36
2.6.6 Transformation of *Magnaporthe grisea* 37
2.6.6.1 Protoplast preparation and transformation 37
2.6.6.2 Selection of transformants 37
2.6.7 Southern analysis 38
2.6.7.1 Southern blotting 38
2.6.7.2 Preparation of radiolabelled probes 38
2.6.7.3 Hybridisation, washing, autoradiography and stripping of Southern blots 38
2.6.8 Polymerase chain reaction (PCR) techniques 39
2.6.8.1 'Step-down' PCR 39
2.6.8.2 Amplification of DNA 41
2.6.8.3 DNA sequencing 41

2.7 RNA METHODS 42
2.7.1 Maintenance of ribonuclease free environment 42
2.7.2 Isolation of total RNA 42
2.7.3 cDNA synthesis 43
2.7.4 Reverse transcriptase PCR 43
2.7.5 Real-time PCR 44

2.8 SUPPLIERS 46

CHAPTER 3 - *BLUMERIA GRAMINIS* F.SP. *HORDEI* AND *MAGNAPORTHE GRISEA* DEVELOPMENT ON BARLEY AND ARTIFICIAL SURFACES

3.1 INTRODUCTION 48
- 3.1.1 *Blumeria graminis* f.sp. *hordei* infection structure differentiation 48
- 3.1.2 *Magnaporthe grisea* infection structure differentiation 48
- 3.1.3 The study of infection structure development 48
- 3.1.4 Objectives 50

3.2 RESULTS 51
- 3.2.1 Time-courses of *Blumeria graminis* f.sp. *hordei* and *Magnaporthe grisea* development on host and artificial surfaces 51
  - *3.2.1.1 Germination and differentiation of B. graminis f.sp. hordei on barley epidermis, 2% (w/v) water agar and cellulose membrane* 52
  - *3.2.1.2 Germination and differentiation of Magnaporthe grisea Guy11 and Δpmk1 on barley epidermis and cellulose membrane* 53
- 3.2.2 Surface hydrophobicity 55

3.3 DISCUSSION 57
- 3.3.1 *B. graminis* f.sp. *hordei* development on host barley epidermis and on the artificial surfaces of cellulose membrane and 2% water agar 57
  - *3.3.1.1 Stages of infection structure development* 57
  - *3.3.1.2 Germination* 58
  - *3.3.1.3 Differentiation* 58
- 3.3.2 *Magnaporthe grisea* development on host barley epidermis and on the artificial surface of cellulose membrane 59
  - *3.3.2.1 Stages of infection structure development* 60
  - *3.3.2.2 Germination* 60
  - *3.3.2.3 Differentiation* 61
- 3.3.3 *B. graminis* f.sp. *hordei* infection structure development versus *M. grisea* infection structure development 63
- 3.3.4 Summary 63

CHAPTER 4 - THE ROLE OF PROTEIN KINASE C IN THE EARLY DEVELOPMENT OF *BLUMERIA GRAMINIS* F.SP. *HORDEI*

4.1 INTRODUCTION 65
- 4.1.1 Protein kinase C 65
- 4.1.2 PKC structure 66
- 4.1.3 PKC and fungi 67
- 4.1.4 Objectives 68

4.2 RESULTS 69
- 4.2.1 Identification of *pkc*1 and *pkc*-like genes in *Blumeria graminis* f.sp. *hordei* 69
- 4.2.2 *pkc*1 and *pkc*-like phylogeny 70
- 4.2.3 *In vivo* detection of PKC activity in ungerminated *Blumeria graminis* f.sp *hordei* conidia 70
- 4.2.4 Investigation of the effects of inhibitors on *Blumeria graminis* f.sp. *hordei* PKC activity 71
  - *4.2.4.1 Purification of Blumeria graminis f.sp. hordei protein extracts* 72
    - *Ammonium sulphate precipitation* 72
    - *Column purification* 73
- 4.2.5 Investigation of the effects of agonists on *Blumeria graminis* f.sp. *hordei* PKC activity 73
  - *4.2.5.1 Phorbol 12-myristate 13-acetate* 73
  - *4.2.5.2 Dioctanoyl 1, 2-sn-glycerol* 74
- 4.2.6 Investigation into the effects of PKC agonists on *Blumeria graminis* f.sp. 74

hordei germling development
4.2.6.1 Phorbol 12-myristate 13-acetate 75
4.2.6.2 Dioctanoyl 1, 2-sn-glycerol 75
4.2.7 Expression of *pkc*1 and *pkc*-like gene during germling morphogenesis 76

4.3 DISCUSSION 78
4.3.1 Identification of *pkc*1 and *pkc*-like genes in *Blumeria graminis* f.sp. *hordei* 78
4.3.2 *pkc*1 and *pkc*-like phylogeny 79
4.3.3 The effect of inhibitors on *Blumeria graminis* f.sp. *hordei* 79
4.3.4 The effect of PKC agonists on *Blumeria graminis* f.sp. *hordei* PKC activity and germling development 81
4.3.5 *pkc*1 and *pkc*-like gene expression profiles 83
4.3.6 Summary 84

CHAPTER 5 - THE ROLE OF MITOGEN-ACTIVATED PROTEIN KINASES IN THE EARLY DEVELOPMENT OF *BLUMERIA GRAMINIS* F.SP. *HORDEI*

5.1 INTRODUCTION 85
5.1.1 Mitogen-activated protein kinase 85
5.1.2 MAP kinase activation and structure 85
5.1.3 ERKS, JNKs and p38 MAP kinases 87
5.1.4 MAP kinase inhibitors 87
5.1.5 MAP kinases and fungi 88
5.1.6 *Magnaporthe grisea* as a "surrogate host" 90
5.1.6 Objectives 91

5.2 RESULTS 92
5.2.1 Identification of *mpk*1 and *mpk*2 genes in *Blumeria graminis* f.sp. *hordei* 92
5.2.2 *mpk*1 and *mpk*2 phylogeny 93
5.2.3 *In vivo* detection of MAP kinase activity in *Blumeria graminis* f.sp *hordei* protein extracts 94
5.3.4 Investigation into the effects of MAP kinase signalling pathway antagonists on *Blumeria graminis* f.sp. *hordei* germling differentiation 95
5.2.5 Investigation into the effects of PD98059 on *Magnaporthe grisea* germling differentiation 97
5.2.6 Investigation into the effects of MAP kinase agonists on *Blumeria graminis* f.sp. *hordei* 98
5.2.7 Expression of *mpk*1 and *mpk*2 during germling morphogenesis 98

5.3 DISCUSSION 100
5.3.1 Identification of *mpk*1 and *mpk*2 genes in *Blumeria graminis* f.sp. *hordei* 100
5.3.2 MPK1 and MPK2 phylogeny 100
5.3.3 MAP kinase activity 102
5.3.4 The effect of MAP kinase antagonists on *Blumeria graminis* f.sp. *hordei* germling development 103
5.3.5 The effect of MAP kinase agonists on *Blumeria graminis* f.sp. *hordei* germling development 104
5.3.6 *mpk*1 and *mpk*2 gene expression profiles 104
5.3.7 Summary 106

CHAPTER 6 – COMPLEMENTATION OF THE *MAGNAPORTHE GRISEA* MITOGEN-ACTIVATED PROTEIN KINASE MUTANT Δ*pmk1* WITH *BLUMERIA GRAMINIS* F.SP. *HORDEI mpk*1

6.1 INTRODUCTION 107

6.1.1 Mitogen-activated protein kinases and *Saccharomyces cerevisiae* 107
6.1.2 *Magnaporthe grisea PMK1* 107
6.1.3 *Magnaporthe grisea* and complementation experiments 108
6.1.4 Objectives 109

6.2 RESULTS 110
6.2.1 The *mpk*1 promoter 110
6.2.2 Transformation vector construction: *mpk*1 and *PMK1* 110
6.2.3 Transformation 110
6.2.4 Southern blot analysis 111
6.2.5 Phenotypic analysis 112
6.2.5.1 In vitro phenotype 113
6.2.5.2 Germination and differentiation on barley epidermis 113
6.2.6 Expression analysis of transformants 115

6.3 DISCUSSION 117
6.3.1 Transformants 118
6.3.2 Phenotypic analysis 119
6.3.3 Expression analysis 119
6.3.4 Alternative transformation vector 120
6.3.5 Summary 120

CHAPTER 7 - DISCUSSION

7.1 INFECTION STRUCTURE FORMATION 122

7.2 SIGNAL TRANSDUCTION 126
7.2.1 Protein kinase C 126
7.2.2 Mitogen-activated protein kinase pathways 129
7.2.2.1 PMK1 homologues 129
7.2.2.2 MPS1 homologues 131
7.2.2.3 MAP kinase signalling in B. graminis f.sp. hordei 133
7.2.2.4 The function of Blumeria graminis f.sp. hordei mpk1 135
7.2.3 Upstream effectors, downstream targets and interacting pathways 137

7.3 THE FUTURE FOR SIGNAL TRANSDUCTION WORK IN *BLUMERIA GRAMINIS* F.SP. *HORDEI* 139

REFERENCES 142

APPENDIX 1 161

APPENDIX 2 162

ABBREVIATIONS

AGT	appressorial germ tube
bp	base pairs
Ca^{2+}	calcium
conc.	concentration
dH_2O	deionised water
DAG	diacylglycerol
DOG	dioctanoyl 1, 2-*sn*-glycerol
EGT	elongated germ tube
f.sp.	forma specialis
GT	germ tube
h	hours
hpi	hours post inoculation
IC_{50}	concentration providing 50% inhibition
MAP kinase	mitogen-activated protein kinase
MEK	mitogen-activated protein kinase kinase
min	minute
MPa	Mega Pascales
PCR	polymerase chain reaction
pers. comm.	personal communication
PGT	primary germ tube
PKA	protein kinase A
PKC	protein kinase C
PMA	phorbol 12, 13-myristate acetate
RH	relative humidity
rpm	revolutions per minute
RT-PCR	reverse transcriptase PCR
s	second
SE	standard error of the mean
SDW	sterile distilled water
SGT	short germ tube
SwGT	swollen germ tube
U	units of enzyme activity

Note on gene names:
The convention for naming fungal genes is adhered to within this thesis. That is, wild-type genes are given in lower case and are italicised, but with non-italicised numerals, e.g. *mpk*1. However, in the literature, other conventions are also used.

Specifically, wild-type genes are given in italics and are capitalised, e.g. *PMK1*, whereas mutants are given in italics and are lower case, e.g. *pmk1*. Thus for facility of comparison with previously published works, these two conventions are used within this thesis.

CHAPTER 1
INTRODUCTION

1.1 THE POWDERY MILDEWS

The powdery mildews are amongst the most common, widespread and conspicuous groups of phytopathogenic fungi (Agrios, 1997). They are characterised by spots or patches of white-grey powdery mildew growth (Figure 1.1) appearing on young shoots and stems, buds, flowers and young fruits, although leaves are the most commonly infected organ (Agrios, 1997). They have a host range covering almost 10 000 plant species in over 1600 genera of angiosperms, with the majority of powdery mildews infecting dicotyledonous plants (Braun, 1995). However, the most extensively studied of the powdery mildews is *Blumeria graminis* (syn. *Erysiphe graminis*) DC. Speer, the sole powdery to infect monocots (Jenkyn and Bainbridge, 1978; Aist and Bushnell, 1991).

1.1.1 Economic impacts

Their broad host range means that the total losses in plant growth and crop yield caused every year by powdery mildews surpasses the losses caused by any other single plant disease (Agrios, 1997). Actual losses depend on the time of disease epidemic onset and its severity, but at the extreme can reach up to 60% (James, 1991). Powdery mildews generally seem to cause the most damage in temperate latitudes, where economically important cereals are more frequently grown. In particular, barley powdery mildew has been a persistent problem in European agriculture (Wolfe and Schwarzbach, 1978). Yield losses of harvested grain resulting from infection by barley powdery mildew are typically 5-20%, although this can reach 40% following severe infections (Gair *et al.*, 1991). Infection reduces tiller number and grain number per ear early in the growing season, whereas later infections have a greater effect on grain weight (Lim and Gaunt, 1986).



Figure 1.1. *Blumeria graminis* f.sp. *hordei* growing on barley cultivar Golden Promise. The fungus is characterised by spots or patches of white-grey powdery mildew growth.

1.1.2 Taxonomy

The powdery mildews comprise a single family, the Erysiphaceae, within the order Erysiphales of the division Ascomycota (Braun, 1995; Braun *et al.*, 2002). Current taxonomic research into powdery mildews is based on morphological and molecular approaches, particularly comparison between the internal transcribed spacer (ITS) ribosomal DNA sequences. Using this system of classification, the cereal/grass powdery mildew previously referred to as *Erysiphe graminis* has been elevated to the separate genus *Blumeria*, containing the single species *B. graminis*. In addition to classification based on ITS sequence data, according to Braun *et al.* (2002), *B. graminis* differs from all species of *Erysiphe* because its anamorph possesses unique features, for example, digitate haustoria, secondary mycelia with bristle-like hyphae and bulbous swellings of the conidiophores, and because of the structure of the ascocarps.

1.1.3 Host specialisation

B. graminis is a highly specialized, obligate biotrophic pathogen and is unique amongst the powdery mildews in that it infects only grasses and cereals. Within the species, Marchal (1902) distinguished seven specialised forms (referred to as *formae specialis*; f.sp) on the basis of their exclusive infection of a single host genus: f.sp. *tritici* pathogenic on *Triticum* spp.; f.sp. *hordei* pathogenic on *Hordeum* spp.; f.sp. *avenae* pathogenic on *Avena* spp.; f.sp. *poae* pathogenic on *Poa* spp.; f.sp. *agropyri* pathogenic on *Agropyron* spp.; f.sp. *bromi* pathogenic on *Bromus* spp. However, Hardison (1944) recognized that, although powdery mildew isolates from wheat, barley and rye infected only their own crop, they were also capable of infecting several wild grass species in the genus *Agropyron*, thus invalidating the concept of narrow specialization. Further work demonstrated that wild grass species represent a biological "bridge" through which reservoirs of infection could be maintained between growing seasons, and highlighted the potential for interbreeding between different *formae speciales* (Hardison, 1944; Hiura, 1978; Wahl *et al.*, 1978).

1.1.4 *Blumeria graminis* f.sp. *hordei* reproduction

As with all powdery mildew fungi, *B. graminis* f.sp. *hordei* can reproduce both sexually and asexually. However, it is the asexual cycle (Figure 1.2) that is far more significant in terms of epidemic disease (Agrios, 1997). Asexual reproduction is by the production of prolific numbers of conidia and can occur throughout the growing season, particularly during the spring. Conidia are borne in long chains on conidiophores arising from the mycelium at a right angle with the host surface (Figure 1.2(f)). Conidiophores have a terminal generative cell and a swollen basal mother cell. The conidia are dispersed to other plants by air currents. After the successful establishment of infection by a conidium on a susceptible leaf surface, further conidia are produced within 4-6 days (Aist and Bushnell, 1991). The spread of an epidemic of powdery mildew is facilitated by close-growing plants, and favourable environmental conditions such as warm temperatures, high humidity and the absence of free water (Sivapalan, 1993; Bushnell, 2002). All contribute to the abundant production of conidia.

Sexual reproduction is common towards the end of the host's growing season or when environmental conditions are unfavourable (Agrios, 1997). Sexually-derived ascospore formation is recognised as a survival mechanism rather than a mechanism for epidemic spread of disease (Wolfe, 1984). Ascospores are produced within the cleistothecium, a spherical black fruiting structure of between 130-200 μm, with simple myceloid appendages which are thought to be involved in adhesion of the cleistothecium to the host plant (Blumer, 1967; Brun *et al.*, 2002).

In Europe, barley is typically sown in the autumn and in the spring, thus providing a host for *B. graminis* throughout the year. Volunteer plants may allow the continued asexual reproduction of *B. graminis* during the summer gap in the barley crop cycle, thus providing inoculum to initiate an autumn epidemic (Brown, 1994). During the autumn, ascospores are released from asci within the cleistothecia upon rehydration, and are wind-dispersed to autumn-sown barley seedlings, or susceptible wild grass relatives, where they establish infection

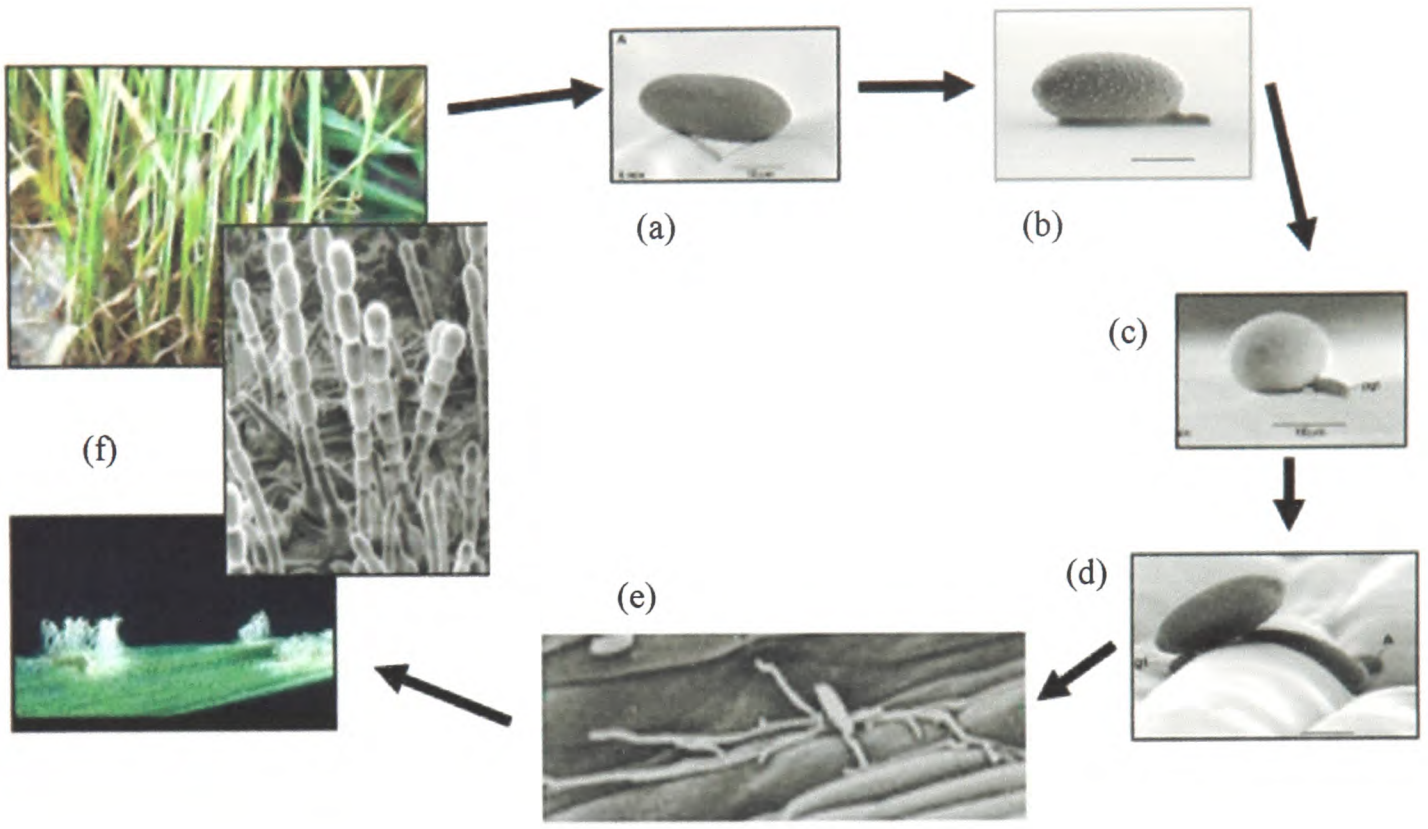


Figure 1.2. *Blumeria graminis* f.sp. *hordei* cycle of asexual reproduction (a) ungerminated conidia (b) and (c) differentiation of primary germ tube (PGT) (d) appressorial differentiation (e) elongating secondary hyphae ramify across the barley leaf surface (f) reproduction of further conidia. Scale bar (a) to (e) represents 10 μm.

(Webster, 1986). However, *B. graminis* ascospores are unable to survive the winter in Northern Europe, thus it is thought that their principle significance is to allow over-summering between spring and autumn-sown barley (Jenkyn and Bainbridge, 1978). Over-wintering occurs by the formation of colonies on the autumn-sown crops and/or susceptible wild grasses.

1.1.5 Establishment of Infection

B. graminis f.sp *hordei* infection structure differentiation involves a series of complex ordered processes that are initiated almost immediately after the conidia lands on the susceptible plant surface (Green *et al.*, 2002). Conidia (Figure 1.2(a)) are short-lived, ovaloid (14 μm x 28 μm), uninucleate and contain numerous large spherical vacuoles which occupy the majority of the spore volume. On surface contact, viable conidia will germinate to produce the primary germ tube (PGT) (Figure 1.2(b) and (c)) which is a short (5-10 μm), aseptate germ tube that emerges within 0.5-2 hours (h) after inoculation (Kunoh *et al.*, 1982). The PGT breaches the host cuticle, but not the host cell wall. It is thought to be involved in adhesion of the germling to the plant surface (Carver *et al.*, 1995b), water uptake from the host (Carver and Bushnell, 1983) which, under arid conditions, may be required to support further differentiation, and the perception of host surface characteristics in order to engage intracellular signalling resulting in the next phase of germling differentiation (Carver and Ingerson, 1987).

B. graminis differs from all other powdery mildew fungi in that its conidia form two germ tubes (Kunoh *et al.*, 1979; Kunoh, 1982). Indeed, some 3-3.5 h after the PGT has formed, a second germ tube, the appressorial germ tube (AGT), emerges. This elongates to a length of between 30 and 40 μm, becomes septate, swells and hooks to form an appressorial lobe (Figure 1.2(d)) (Carver *et al.*, 1995b). During the formation of the appressorium, the majority of the cytoplasm and a single nucleus from the conidial body migrate into the expanding germ tubes (McKeen, 1972). A second nucleus remains in the body of the conidium surrounded by residual cytoplasm.

Penetration by *B. graminis* occurs through a penetration peg (0.6 μm in diameter) formed at the hooked tip of the appressorium (Kunoh *et al.*, 1978). Penetration is thought to be mediated in part by the build up of turgor pressure of between 2 to 3 MPa within the AGT (Pryce-Jones *et al.*, 1999) and in part by the localised action of degradatory enzymes (Edwards and Allen, 1970). Specifically, esterases are released during conidial germination (Nicholson *et al.*, 1988; Kunoh *et al.*, 1990), cutinase activity has been identified in conidial exudates (Pascholati *et al.*, 1992), and hydrolytic enzymes, including esterases, lipases, protease, phosphatases, 1, 3-β-glucanase, chitinase and amylase have been identified in extracts from ungerminated and germinated conidia (Fric and Wolf, 1994).

Following successful penetration of the host cuticle and cell wall, the fungus begins to differentiate a uninucleate, multi-digitate haustorium between the host cell wall and the plasma membrane, at around 18 h post inoculation (hpi) (Aist and Bushnell, 1991). The haustorium is the only point of intracellular contact between the fungus and the plant (Manners and Gay, 1980, 1982) and is a highly specialised interface for the uptake of nutrients, largely in the form of glucose, from epidermal cells and mesophyll cells of the host into the pathogen. Within the fungus, glucose is rapidly converted to mannitol, and small amounts of trehalose and arabinitol (Edwards and Allen, 1966). Following haustorium formation, elongating secondary hyphae (ESH) ramify across the host surface resulting in the development of a colony (Figure 1.2(e)). Secondary haustoria are formed from the ESH.

1.1.6 Host response to *Blumeria graminis* f.sp. *hordei* infection

B. graminis is a highly specialised phytopathogenic fungus, and must evade recognition by the host and the host defence response at every step of its development. In general, successful evasion of the host defence responses results in the establishment of a compatible, disease-causing, interaction. Host recognition of the pathogen results in an incompatible interaction, or resistance. However, even in a compatible interaction, the observed infection frequency rarely exceeds 50% due to both the general background resistance of the host and

the induced resistance by the pathogen (Tim Carver, *pers. comm.*). Induced resistance is highly important in the successful penetration of the barley epidermal cells, with challenge of a host cell by the PGT reducing the probability of successful penetration of the AGT from 40% (if the PGT and AGT contact adjacent) cells to 7-8% (if the PGT and AGT contact the same cell) (Woolacott and Archer, 1984). In contrast, the presence of a haustorium within an epidermal cell renders that cell entirely susceptible to further challenge by *B. graminis*, a phenomenon known as "induced accessibility" whereas a prior, unsuccessful challenge renders the epidermal cell inaccessible to subsequent infection (Carver *et al.*, 1999; Lyngkaer and Carver, 1999a, b).

Infection of the barley leaf by *B. graminis* occurs almost exclusively in the epidermal layers (Kunoh and Ishikazi, 1975; Aist and Bushnell, 1991). Barley epidermal cells respond to the presence of the fungus and within 4 hpi, directly beneath the conidia, small cytoplasmic accumulations are observed in the epidermal cells. These are generated by cytoplasmic streaming at the point of interaction with the fungus and consist of rapidly moving organelles including mitochondria, endoplasmic reticulum-derived vesicles, Golgi bodies and polyribosomes, which indicate high metabolic and synthetic activities (Bushnell and Bergquist, 1975; Bushnell and Zeyen, 1976). By 6 hpi, the epidermal cells respond by forming a small papilla immediately beneath the PGT, and a larger papilla is produced in response to the AGT (Zeyen *et al.*, 2002).

Papilla are thought to prevent fungal penetration of the epidermal cell wall (Zeyen and Bushnell, 1979; Zeyen *et al.*, 2002), and may also serve as a site of accumulation of substances inhibitory to the development of the penetration peg (Edwards and Allen, 1970). In an incompatible reaction, the fungal penetration may be arrested by the papilla, whereas in a compatible interaction, the papilla is breached by the fungal penetration peg, resulting in the establishment of infection.

Electron microscope studies have given some indication as to the formation and composition of papilla. A thin, dense layer of osmophilic material, probably lipid,

from non-membrane-bound vesicles is deposited between the host cell wall and plasma membrane, followed by deposition of compacted and non-compacted layers of non-osmophilic, amorphous material (probably callose) by membrane-bound vesicles (Bushnell and Zeyen, 1976; Zeyen and Bushnell, 1979). Reactive oxygen species, including hydrogen peroxide, are thought to be involved in papilla formation (Hückelhoven *et al.*, 1999) and phenolic compounds have been identified.

1.1.7 Host resistance

Host resistance is generally considered to operate by three broad mechanisms, termed "monogenic" (vertical or race-specific) resistance, "polygenic" (or horizontal resistance) and "non-host" resistance. Polygenic resistance is a non-race-specific and a "durable" resistance against powdery mildews in barley and other cereals. It is an incomplete resistance, governed by the synergistic action of many genes acting against all races of the pathogen. Non-host resistance is resistance expressed by an entire plant species against all genetic variants of a pathogen (Heath, 2000). Non-host resistance is the mechanism which prevents infection by inappropriate *formae speciales* of *B. graminis* (Peterhänsel *et al.*, 1997). In addition, a general "background" resistance is believed to operate in nominally-compatible cereal-powdery mildew interactions (Bushnell, 2002).

For the majority of commercially grown crop species, race-specific resistance has long been the mainstay of disease control. Race-specific resistance is governed by the action of specific plant gene products against specific pathogens and is only effective against those pathogen isolates carrying a complementary avirulence (*Avr*) gene (Dangl and Jones, 2001). However, reliance on a single resistance (*R*) gene imposes a huge selection pressure on the pathogen to overcome these defence responses, though this can be reduced by combining multiple *R* genes from different genetic loci into a single cultivar.

The nature of the avirulence factors and the mode of recognition by the host are as yet unknown in the barley/powdery mildew interaction. Certain race-specific

resistance types, such as those at the *Mla*, *Mlc*, *Mlg* and *Mlh* loci, appear to block penetration, while others, such as *Mlat*, *Mlk*, *MlLa* and *Mlp* trigger the hypersensitive response (Bryngelsson and Collinge, 1992). Recently, the *Mla* resistance gene cluster has been identified and has undergone characterisation (reviewed in Jones, 2001). Around 30 *Mla* alleles have been identified, each recognising a different spectrum of races of powdery mildew, and by implication, different *Avr* genes. Most of these *Mla* species have been introduced into cultivated barley from the wild relative (*Hordeum spontaneum*) by plant breeders. Within an interval of 240 kb, there are at least 11 genes that encode nucleotide binding site and leucine rich repeat motifs (NBS-LRR), which are the predominant class of plant proteins and confer resistance to many plant pathogens (Ellis and Jones, 1998).

In contrast with the dominantly-acting *R* genes, a broad-spectrum resistance controlled by a single recessive gene has been identified and extensively researched in barley. Resistance is conferred to all tested *B. graminis* f.sp *hordei* isolates and is controlled by the *mlo* gene and has provided a durable form of resistance in European spring barley varieties for more than 20 years (Jørgensen, 1992; reviewed in Schulze-Lefert and Vogel, 2000). At the cytological level, resistance leads to the abortion of infection attempts during the penetration process through the epidermal cell wall. Attacked cells do not initiate a suicide response and therefore stay alive. Molecular isolation of *Mlo* confirmed that the resistant phenotype is caused by loss-of-function mutations in the wild-type gene (Büschges *et al.*, 1997). The Mlo protein has been identified as a 60 kDa novel plasma membrane-anchored seven transmembrane protein (Devoto *et al.*, 1999). Potential mechanisms for an *mlo*-controlled defense include the formation of cell-wall appositions (CWAs), which are concentric rings of new plant-cell-wall material that are deposited directly under fungal penetration pegs. Oxidative cross-linking is thought to reinforce the wall, with cross-linking occurring earlier during infection in *mlo* plants than in *Mlo* plants (von Röpenack *et al.*, 1998).

1.1.8 Methods of control

Barley powdery mildew disease has traditionally been controlled by the use of chemical fungicides and resistant host varieties. Since Roman times chemical fungicides have been employed to control powdery mildew. More recently, the potential for biological control of powdery mildews has been identified, but these are unlikely to be effective in intensive crop monoculture, one of the most important limiting factors being the efficacy of biological alternatives compared with fungicides (Bélanger and Labbé, 2002).

1.1.8.1 Chemical control

Prior to the 1960s fungicidal protectants and multi-site inhibitors were extensively used to control powdery mildew. Products contained dithiocarbamates, quinomethionate, but required high dose rates and were costly. However, since the 1960s, systemic fungicides have been introduced which initially proved highly effective. However, most have a single-site mode of action, focusing on the inhibition of sterol biosynthesis, which affects the formation of cell membranes and hyphal development (Siegel, 1981). This has led to the pathogen evolving resistance (Urech *et al.*, 1997). Furthermore, although many systemic fungicides have been developed, since they act at a limited number of target sites, a pathogen that is resistant to a fungicide at a given target site may be cross-resistant to all fungicides which act at that target (Blatter *et al.*, 1998). However, the combined use of fungicides based on different chemistries, particularly the sterol demethylation inhibitors (DMIs), and morpholine-type fungicides, has provided greater durability for these fungicides.

Throughout the 1990s a new generation of fungicides were developed based on the chemistry of strobilurins, such as azoxystrobin, and the 5, 7-dichloroquinoline compound, quinoxyfen (Holloman and Wheeler, 2002). The strobilurins act by disrupting electron transfer in the mitochondria through inhibition of the terminal cytochrome *c* oxidase (Holloman and Wheeler, 2002). The arrest of the respiratory chain results in the generation of reactive oxygen species (ROS), which would be fungicidial in the absence of mechanisms which would allow

their removal. However, the respiratory pathway in fungal mitochondria is thought to be branched, with an azoxystrobin-insensitive alternative pathway allows electrons to flow through an alternative oxidase. This ensures that some ATP is generated, and allows the deleterious effects of ROS to be moderated. The stobilurins actively stop germination of powdery mildew conidia, but have little curative or eradicant activity (Holloman and Wheeler, 2002).

Quinoxyfen acts against powdery mildews during the early stages of infection (Holloman *et al.*, 1997) stopping germination in some mildews and appressorium formation in others. However, quinoxyfen is not effective against appressoria arising from secondary hyphae (Holloman and Wheeler, 2002) and eradication of established colonies requires the combined use of eradicant, morpholine-based fungicides. Moreover, whilst quinoxyfen may perturb signal transduction (Wheeler *et al.*, 2003), the mode of action of quinoxyfen remains unclear. Resistance to quinoline fungicides was reported soon after their introduction (Ypema and Gold, 1999). However, quinoxyfen-resistant isolates have been demonstrated to be defective in conidiation, and the potential of such isolates to generate epidemics is limited (Hollman and Wheeler, 2002).

1.2 *MAGNAPORTHE GRISEA*

1.2.1 Host range, economic impact and description

Magnaporthe grisea (Herbert) Barr (anamorph, *Pyricularia grisea* Sacc formerly *Pyricularia oryzae* Cav.) (Rossman *et al.*, 1990) is a heterothallic ascomycete which causes leaf spot disease of more than 50 grasses, including economically important crops such as barley (*Hordeum vulgare*), wheat (*Triticum aestivum*), rice (*Oryza sativa*), maize (*Zea mays*) and millet (*Pennisetum americanum*) (Ou, 1985). These hosts each support pathogenic forms of the fungus that are normally restricted to one or a small number of very closely related species (Mackill and Bonman, 1986). However, *M. grisea* is best known as the causal agent of rice blast disease (reviewed in Talbot, 1995), being the most devastating disease of

cultivated rice and a serious problem in most rice-growing regions of the world. Indeed, several rice blast epidemics have occurred in different parts of the world, resulting in yield losses in these areas ranging from 50 to 90% of the expected crop (Agrios, 1997).

Rice blast affects leaves, on which it causes diamond-shaped white to grey lesions with dark green to brown borders surrounded by a yellow halo (Figure 1.3). These lesions may enlarge are kill entire leaves. Blast also affects, and can kill, the leaf collar and the stem nodes, and on occasion, the internodes and the panicle neck node (Agrios, 1997).

1.2.2 Reproduction

M. grisea can reproduce both sexually and asexually. However, the teleomorph stage has not been found in nature because almost all rice field isolates are of the male mating type (Agrios, 1997). However, it can be produced under laboratory conditions, which allows genetic analysis (Talbot, 1995). In the field though, *M. grisea* reproduces asexually (Figure 1.4) by producing tear drop-shaped three-celled conidia (Figure 1.4(a)), which are produced from lesions on aerial conidiophores (Figure 1.4(e)) during periods of high humidity and are carried to new hosts by wind or splash dispersal. At optimum temperatures, new blast lesions appear within 4 to 5 days. Conidia can be produced and released from a lesion within hours if weather conditions are wet and humid.

M. grisea overseasons as mycelium and conidia on diseased rice straw and seed, and possibly on weed hosts (Agrios, 1997). However, in the tropics, conidia are present in the air throughout the year.

1.2.3 Establishment of infection

M. grisea conidia do not remain viable for long, and thus must adhere to the host as quickly as possible in order to establish infection. To this end, the conidia (Figure 1.4(a)) release an adhesive, triggered by wetting, from a compartment in the spore apex (Hamer *et al.*, 1988). Germination (Figure 1.4(b)) is rapid with a

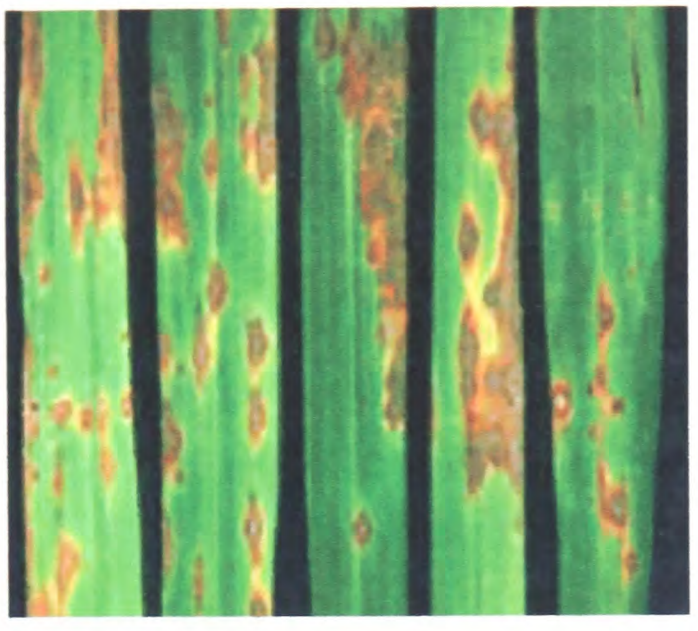


Figure 1.3. *Magnaporthe grisea* (rice blast) is characterised by diamond-shaped white to grey lesions with dark green to brown borders surrounded by a yellow halo.

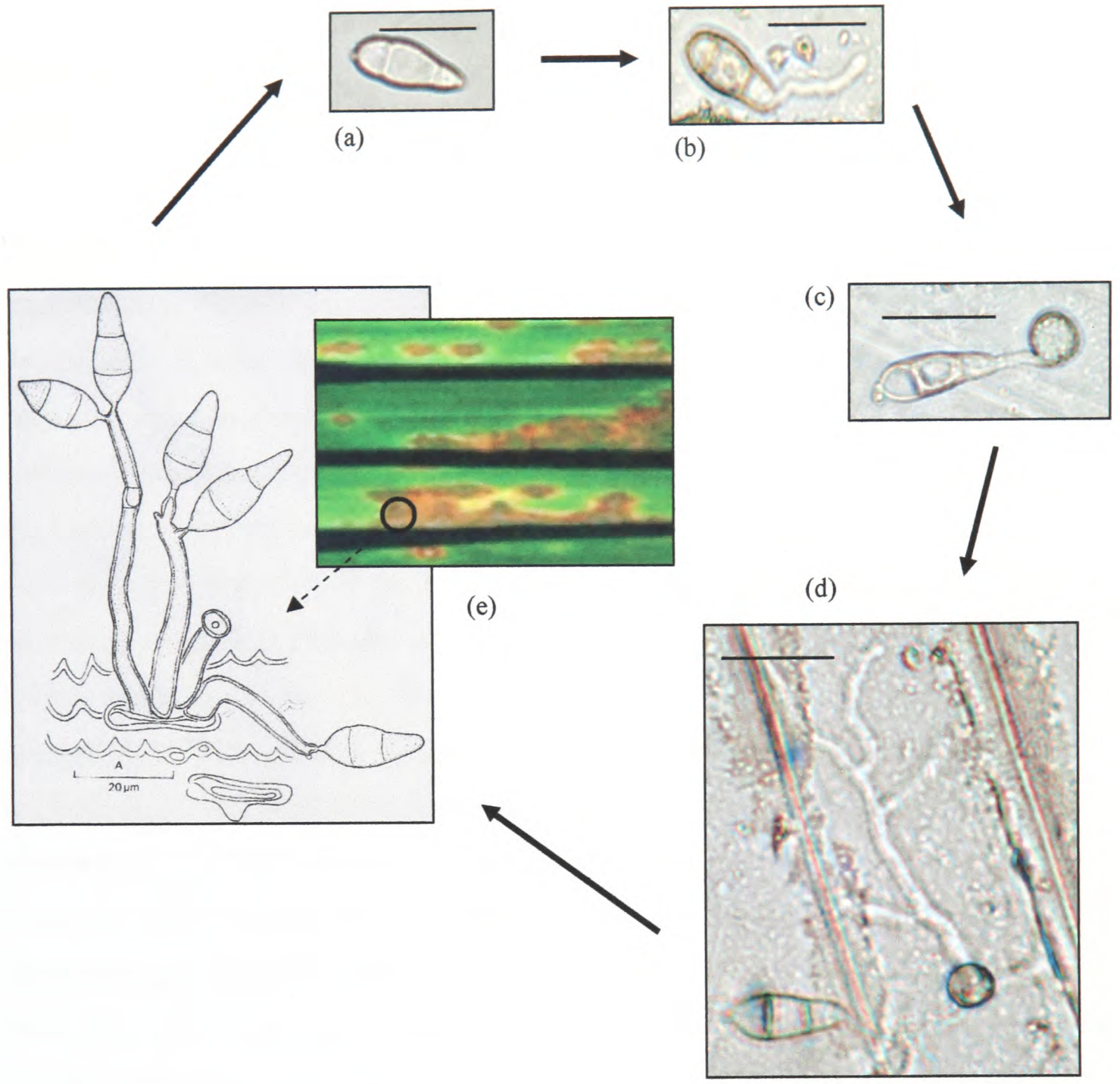


Figure 1.4. *Magnaporthe grisea* cycle of asexual reproduction (a) ungerminated conidia (b) germination (c) appressorial differentiation (d) *M. grisea* forms a narrow infection hypha within the first-encountered epidermal cell which is followed by a significant widening and change of direction of the hypha, before development into a bulbous and branched mycelium (e) conidia are produced from lesions on aerial conidiophores. e) shows conidiophores emerging from a stomata (taken from Webster, 1993) Scale bar (a) to (e) represents 20 µm.

germ tube emerging from one of the terminal cells within an hour of attachment to the plant surface (Howard *et al.*, 1994). The germ tube extends to between 10 and 30 μm, reaching maximum extension by about 4 h. Subsequently, the germ tube hooks and swells, marking the beginning of cellular differentiation (Howard *et al.*, 1994).

Swelling of the germ tube represents the initial step in formation of the appressorium. This is accompanied by a mitotic division which results in the production of two daughter nuclei, one which migrates to the incipient appressorium, and one which migrates to the cell of the conidium from which the mother cell originated (Bourett and Howard, 1990). Cell division is completed by the formation of a septum, after which the cell wall of the appressorium begins to thicken by the formation of an outer fibrillar layer over the existing cell wall and an inner-wall layer of melanin. The appressorium adheres itself to the leaf surface before inflating to its full potential to produce the mature, hemispherical appressorium. This inflation is caused by the accumulation of high concentrations (as high as 3.2 M) of glycerol contained within the melanin-pigmented cell wall (de Jong *et al.*, 1997). This creates an osmotic gradient which draws free water from the plant surface into the appressorium, generating an extremely high internal turgor pressure of up to 8 MPa (Howard and Ferrari, 1989; Howard *et al.*, 1991). By 8-10 hours after germination, differentiation of the appressorium is complete (Figure 1.4(c)) (Bourett and Howard, 1990). A penetration peg emerges from the appressorium and ruptures the leaf cuticle after 28 to 31 h, allowing entry to the epidermis.

Once inside the plant tissue, *M. grisea* forms a narrow (3 μm) infection hypha for the first 10-20 μm within the first-encountered epidermal cell. This is followed by a significant widening and change of direction of the hypha, before development into a bulbous and branched mycelium (Figure 1.4(d)) (Heath *et al.*, 1990). Intracellular growth involves the invagination of the plant plasma membrane around the mycelium, but elaboration into a true haustorial structure does not seem to occur (Heath *et al.*, 1992). It has been speculated that this is a biotrophic,

assimilative stage of development during which the fungus recovers from the energy intensive phase of plant penetration and shifts gene expression, and possibly its metabolic profile, ready for invasive growth (Urban *et al.*, 1999). However, this stage is short-lived and the fungus rapidly spreads throughout the rice leaf tissue. Measurement of sugar fluxes show that mannitol and arabitol appear specifically in the leaves infected with blast and are thought to be fungal storage compounds. Additionally, a high level of invertase activity and a corresponding flux of glucose and fructose levels also occur within the leaves (Hwang *et al.*, 1989).

1.2.4 Methods of control

Rice blast is presently controlled by planting of resistant culivars, cultural methods and by fungicide application. However, such methods are largely ineffective and far from ideal for durable disease management. Development of a stable blast resistant variety of rice has so far been unsuccessful due to the high level of genetic variability of the fungus in the field and quickly develops new pathotypes in response to resistant rice cultivars (Latterell and Rossi, 1986). No methods of biological control are currently available.

1.2.4.1 Resistant crop cultivars

Host cultivars that are resistant against leaf and panicle blast have been the most widely used method of disease control (Bonman *et al.*, 1992), but resistance (mainly race-specific resistance) has tended to be ephemeral because of pathogen variability. Forms of "partial resistance" (Marchetti, 1994; Roumen, 1994) have been identified but are little understood or used. Cultivars with multiple genes for blast resistance (Marchetti *et al.*, 1996) and "durable" forms of resistance in hybrid rice (Zhou *et al.*, 1999) have been described as offering better hopes of sustained activity against the pathogen. Marker-aided selection of resistance from recombinant populations have provided new tools for rice breeding and resulted in improved genetic analysis of resistance (Inukai *et al.*, 1996).

1.2.4.2 Cultural practices

Cultural methods are implemented in association with other agronomic practices and include avoidance of using excessive levels of nitrogenous fertilizer (Prabhu *et al.*, 1996), early planting and using fungicides. Avoidance of moisture stress to crops reduces disease severity.

1.2.4.3 Chemical control

Fungicidal control is largely practised in temperate or subtropical rice cultivation, mainly in Japan, China, South Korea, Taiwan and, increasingly, Vietnam. Substantial areas are also treated in Latin America (Colombia and Brazil), in India and in the USA, but little is used in other geographical areas either because of cost limitations, or because of lower or inconsistent disease pressures (CABI Crop Protection Compendium, 2002).

Currently, systemic fungicides are widely used. However, older organophosphorous products, such as edifenphos, are still utilized. The modern blasticides include isoprothiolane, probenazole, pyroquilon and tricyclazole (Filippi and Prabhu, 1997). In recent years, newer melanin biosynthesis inhibitors such as carpropamid (Motoyama *et al.*, 1999; Thieron *et al.*, 1999) or broad-spectrum fungicides like azoxystrobin (Lee and Beaty, 1999) have become increasingly popular.

1.3 APPRESSORIUM FORMATION

Phytopathogenic fungi have evolved a wide array of strategies to breach the plant wax cuticle and epidermal cell wall to gain access to nutrients. At one extreme, there are the necrotrophs, facultative parasites that may kill their hosts by secretion of copious amounts of cell wall degrading enzymes and toxins (Agrios, 1997; Dean, 1997). At the other extreme, many fungi have evolved elaborate mechanisms of gaining entry to their hosts through the formation of specialised infection structures, named "appressoria", from the Latin "apprimere", meaning

"to press against" (Dean, 1997). An appressorium is defined as a structure employed by fungal pathogens to press against and attach to the plant surface in preparation for infection (Hawksworth *et al.*, 1995). Appressoria may be visible as inconspicuous swellings of the germ tubes as in the basidiosporelings of rust fungi, or as discrete, swollen, lobed or dome-shaped cells, separated from the germ tube by a septum, as in, for example, *M. grisea*, *Colletotrichum* species (Deising *et al.*, 2000) and in *B. graminis*.

1.3.1 Attachment

Attachment of a conidium to the plant surface is an important factor in the infection structure differentiation process of a fungus and is the first step in committing a pathogen to the establishment of disease. Primarily, adhesion serves to anchor the spore to the plant surface, but may also be required for host recognition and subsequent fungal development (Hamer *et al.*, 1988). There is considerable variation in the apparent composition of the materials employed by plant pathogenic fungi to adhere to plant surfaces and also in the environmental cues that induce the spore to produce adhesive material. However, fungal adhesives are typically water-insoluble glycoproteins, and lipids and polysaccharides have also been detected in adhesive material and, in some fungi, have been shown to contribute to adhesion (Nicholson and Epstein, 1991; Nicholson, 1996). This has been the subject of several recent reviews (Dean, 1997; Tucker and Talbot, 2001).

1.3.2 Germination

Following successful attachment of a fungal spore to the plant surface, a series of developmental events occurs which determines whether an infection attempt will be successful, beginning with the process of germination. Spore germination is a prerequisite for infection structure formation, but does not necessarily result in appressorial differentiation. Indeed, phytopathogenic fungi have evolved so that the initiation of the infection process occurs in response to an environment in which the pathogenic lifestyle would be advantageous. Factors that influence infection structure differentiation include physical and chemical factors derived

from the host, and environmental factors such as the presence of water, humidity, light, temperature, as well as nutritional and sexual status status of the fungus (Jelitto *et al.*, 1994; Kronstad *et al.*, 1995; Mendgen, 1996; Hamer and Holden, 1997). The germ tube is normally the site and developmental stage in which perception of the host surface occurs. If the appropriate physical and chemical signals are not perceived correctly, the germ tube will remain undifferentiated and will eventually arrest growth. However, with detection of the appropriate signals, a complex series of developmental processes is triggered that results in appressorium formation.

In *M. grisea*, hydration alone is sufficient to induce spore germination, with germination being independent of the nature of the surfaces inoculated, as high levels of germination are observed on both solid and liquid surfaces (Xiao *et al.*, 1994b). However, contact stimulation is an important signal for the germination of *B. graminis* f.sp. *hordei* conidia, where the point of contact of a conidium with a surface can dictate the orientation and emergence of the primary and subsequent appressorial germ tube (Wright *et al.*, 2000).

1.3.3 Signals for appressorium formation

Differentiation of infection structures in phytopathogenic fungi can occur in response to a number of signals including surface hardness, hydrophobicity, surface topography and plant signals, including components of the host cuticle, such as wax or cutin, or the products of their degradation (Dean, 1997). Fungi may respond to such stimuli through either a change in direction of growth or by differentiation of an appressorium (Tucker and Talbot, 2001).

The rust fungus, *Uromyces appendiculatus*, is induced to differentiate appressoria through sensing surface topography alone. *U. appendiculatus* penetrates its host through stomatal openings, locating the stomata by recognition of a 0.5 μm ridge at the edges of stomatal guard cells. A replica of this 0.5 μm ridge is sufficient to induce maximum differentiation of appressoria (Terhune and Hoch, 1993). The most receptive surface for perception of signals for appressorium formation is

located within 10 μm of the germ tube apex. Mechano-sensitive ion channels have been identified which may have a role in detecting membrane stress on encounter with a stomatal ridge and thus causing a Ca^{2+} ion flux which acts as a cue for appressorium formation (Zhou *et al.*, 1991; Garrill *et al.*, 1993). Indeed, application of Ca^{2+} ions to *U. appendiculatus* uredospore germ tubes induces appressorium formation (Hoch *et al.*, 1987).

Contact with a solid surface and surface hydrophobicity appear to be important stimuli for appressorium development in *M. grisea* and *Colletotrichum* species (Hamer *et al.*, 1988, Xiao *et al.*, 1994b; Lee and Dean, 1994; Jelitto *et al.*, 1994). Contact with a solid surface alone is sufficient to induce differentiation in *C. trifolii* and *C. truncatum*, and is probably the single most important cue for appressorium formation in *M. grisea* (Xiao *et al.*, 1994a). In *C. gloeosporiodes*, specific hardness-induced gene expression occurs prior to appressorium formation (Kim and Kolattukudy, 1998).

In addition to physical surface stimuli, *M. grisea* appressorium formation can be induced by plant signals including cutin monomers, particularly *cis*-9, 10-epoxy-18-hydroxyoctadeca-noic acid and *cis*-9-octadecen-1-ol (Gilbert *et al.*, 1996). However, the chemical and physical signals appear to have redundant roles, as either one alone is sufficient to induce appressorial development (Gilbert *et al.*, 1996). *C. gloeosporiodes* is able to form appressoria on wax extracted from its host (Podila *et al.*, 1993), but will remain dormant after host penetration unless it receives a second signal, in the form of the plant-ripening hormone ethylene (Kolattukudy *et al.*, 1995).

In order to perceive physical surface features, fungi have to grow in close contact with the substratum. Talbot *et al.* (1993) identified a gene, *MPG1*, from *M. grisea*, which encodes an amphipathic class I hydrophobin protein capable of self-assembly at air-water interfaces or interfaces between hyphae and hydrophobic surfaces, thereby conferring hyphal adhesion (Wösten *et al.*, 1994). *MPG1* gene replacement mutants exhibited reduced adhesion to hydrophobic surfaces and

were significantly reduced in their ability to differentiate appressoria (Talbot *et al.*, 1996). In the presence of exogenous cAMP, Δ*mpg1* mutants could be induced to undergo appressorium formation, which is consistent with *MPG1* having a role in appressorial differentiation (Talbot *et al.*, 1996). Furthermore, Soanes *et al.* (2002), reported recently that *CPKA*, which encodes the catalytic subunit of PKA, is required for full expression of *MPG1* during appresorium formation and that the MAP kinase gene, *PMK1*, is required for full expression of *MPG1* in response to nitrogen starvation. Polymerisation of the MPG1 proteins is thought to initiate appressorium differentiation and might act as a sensor for the hydrophobic leaf surface, therefore contributing to surface recognition (Talbot *et al.*, 1996; Beckerman and Ebbole, 1996).

1.3.4 Perception of signals for appressorium differentiation

Until recently, little was known about the molecular mechanisms of signal perception in phytopathogenic fungi. However, the high level of conservation among eukaryotes of components of signalling pathways has led to an increasing interest in the mechanisms of perception of inductive signals by fungal plant pathogens. Indeed, the ability to clone and characterise genes based on homology to genes from *Sacharomyces cerevisiae* and other model fungi has allowed for tests of the involvement of given signal transduction pathways in infection-related development.

A putative transmembrane receptor, *PTH11*, has been identified in *M. grisea* that appears to respond to the presence of hydrophobic surfaces, transmitting a cue for appressorium formation (DeZwann *et al.*, 1999). *Pth11* mutants were able to initiate appressorium differentiation on inductive surfaces, but were not able to efficiently form functional appressoria. That is, *PTH11* is not essential for appressorium formation but since the mutant phenotype on inductive surfaces is comparable to the wild-type phenotype on hydrophilic non-inductive surfaces, the Pth11 protein is thought to act as an upstream effector of appressorium differentiation responding to inductive environmental cues (DeZwann *et al.*, 1999). Additionally, the *pth11* mutant could be complemented by the addition of

exogenous cAMP, thus PTH11 appears to operate upstream of, or convergent with, a signalling pathway leading to cAMP accumulation. Current speculation implicates the PTH11 receptor in a signalling pathway which acts via a GTP-binding protein mechanism (Tucker and Talbot, 2001), although no direct evidence for this has yet been found. However, *M. grisea* possesses at least three distinct G-protein α-subunit-encoding genes of which one, namely *MAGB*, affects appressorium formation and pathogenicity, although it is not clear how this interacts with other signalling cascades. Nevertheless, the *magB* mutant can be complemented by the addition of exogenous cAMP, which indicates that MAGB operates upstream of the generation of a cAMP signal for appressorium formation (Dean, 1997; Liu and Dean, 1997). G α-subunit proteins have been implicated in the pathogenicity of *Ustilago maydis* and *Cryphonectria parasitica* (Gao and Nuss, 1996; Regenfelder *et al.*, 1997).

1.3.5 Signal transduction

The cAMP signal transduction pathway has been shown to mediate many fundamental processes in filamentous fungi, including growth and morphological change (Bruno *et al.*, 1996; Bencina *et al.*, 1997), and to be important for virulence in phytopathogenic fungi including *Uromyces phaseoli* (Hoch and Staple, 1985), *U. maydis* (Gold *et al.*, 1994) and *C. parasitica* (Chen *et al.*, 1996; Kronstad, 1997). Additionally, cAMP has been shown to play an important role during the differentiation of appressorium in *M. grisea* (Lee and Dean, 1993), *C. trifolii* (Yang and Dickman, 1997) and, more recently, *B. graminis* f.sp. *hordei* (Hall *et al.*, 1999; Hall and Gurr, 2000; Bindslev *et al.*, 2001).

The major downstream effector of cAMP is cAMP-dependent protein kinase A (PKA), which has been extensively studied in mammalian systems and in yeast. PKA is a tetrameric protein. In mammals, PKA, in its inactive form, consists of an asymmetric tetramer comprised of two regulatory (R) and two catalytic (C) subunits (Taylor *et al.*, 1990). Activation is mediated by the binding of cAMP to the R subunits which alter the affinity of R for C, thus promoting the dissociation of the complex into a dimer of R subunits and two active monomeric C subunits

(Su *et al.*, 1995). The free enzymatically active C subunits then function by phosphorylating target substrate proteins.

In *M. grisea*, the addition of exogenous cAMP is sufficient to promote high levels of appressorium differentiation on an otherwise non-inductive surface (Lee and Dean, 1993). Furthermore, the importance of cAMP for appressorial formation was demonstrated by deletion of *MAC1*, a gene encoding adenylate cyclase, which catalyses generation of intracellular cAMP (Choi and Dean, 1997). *Mac1* mutants were unable to form appressoria, however, a bypass suppressor mutant, *sum1-99*, in the regulatory subunit of PKA was able to restore appressorium development. However, Δ*mac1* *sum1-99* mutants are still reduced in pathogenicity (Adachi and Hamer, 1998). PKA signalling may therefore be independently required for control of appressorium function in a manner that cannot be restored in Δ*mac1* *sum1-99* mutants (Thines *et al.*, 2000). Indeed, ablation of the gene encoding the catalytic subunit of PKA (*cpka*) resulted in the delayed formation of non-functional appressoria, which are not able to penetrate the host cuticle (Xu *et al.*, 1997). This phenotype is comparable to that obtained with the targeted deletion of a catalytic subunit of PKA in *C. trifolii* (Yang and Dickman, 1999). Mutants were able to produce appressoria, but were unable to penetrate the host cuticle and cause disease.

Nothing was known of the signal transduction events, or the role of protein kinases, occurring during the development of *Blumeria graminis* f.sp. *hordei* until the work of Hall *et al.* (1999) and Hall and Gurr (2000). In this work cAMP signalling and PKA were demonstrated to play important, but complex roles during the early development of *B. graminis* conidia. Hall *et al.* (1999) exploited the differential inductivities of various plant and artificial surfaces to show that on the fully-inductive barley leaf surface, application of 1 mM exogenous cAMP was inhibitory to appressorial formation. However, 1 mM cAMP stimulated appressorial differentiation of conidia on the semi-inductive surface of cellulose membrane, but was inhibitory when applied at a concentration of 100 mM. Additionally, Hall and Gurr (2000) showed that intracellular levels of cAMP rise

and fall during conidial differentiation on the barley leaf surface. Kinane *et al.* (2000) demonstrated that two peaks of endogenous cAMP occur during infection structure formation, that is, preceding emergence of the PGT, and preceding emergence of the second-formed germ tube destined to elongate into the AGT. These results are consistent with observations which show that PKA activity peaks prior to PGT and AGT emergence (Kinane *et al.*, 2000), with low levels of PKA activity required for appressorial hooking and differentiation of the apical appressorial lobe. RT-PCR analysis of *cpka* also substantiates a model where PKA is active during PGT and AGT emergence (Zhang *et al.*, 2001). Furthermore, it was recently demonstrated that the *cPKA* gene from *B. graminis* was able to functionally complement the Δ*cpka* mutant of *M. grisea* (Bindslev *et al.*, 2001).

Another signalling pathway that is potentially involved in infection structure differentiation of phytopathogenic fungi is the phospholipase C pathway. This pathway leads to the generation of inositol-1,4,5-triphosphate and diacylglycerol, and subsequently a Ca^{2+} signal, causing stimulation of calcium/calmodulin–dependent protein kinase signalling. Evidence for a calmodulin-mediated pathway in fungal differentiation has been described for *Colletotrichum gloeosporiodes* (Kim *et al.*, 1998) and *C. trifolli* (Buhr and Dickman, 1997) where calmodulin genes were found to be highly expressed in response to contact of conidia with hard surfaces. However, investigations into the role of calcium signalling in *B. graminis* f.sp. *hordei* were ambiguous, with no firm conclusions regarding the involvement of calcium during *B. graminis* development being drawn (Hall, 1999).

Protein kinase C (PKC) comprises a large family of serine/threonine kinases which are activated by extracellular signals and which play a pivotal role in many signal-transducing pathways in the cell. PKCs have been implicated in differentiation processes in several filamentous fungi including *Neurospora crassa* (Oved and Yarden, 1996; Arpaia *et al.*, 1999) and the phytopathogens *M.*

grisea (Thines *et al.*, 1997a,b) and *C. trifolli* (Dickman *et al.*, 1995). However, nothing is known about the role of PKC signalling in *B. graminis*.

Recently, mitogen-activated protein (MAP) kinases have been identified in several phytopathogenic fungi and found to be important for appressorium formation, as well as diverse growth and differentiation processes including conidiation, conidial germination and fertility (reviewed in Xu, 2000). MAP kinases, and their upstream regulatory kinases, comprise a functional unit that transmits input signals from the cell periphery to elicit gene expression (Herskowitz, 1995; Gustin *et al.*, 1998). MAP kinases involved in appressorium formation have been identified in *Claviceps purpurea* (Mey *et al.*, 2002a, b), *Pyrenophora teres* (Ruiz-Roldan *et al.*, 2001), *Botrytis cinerea* (Zheng *et al.*, 2000), *Fusarium oxysporum* (Di Pietro *et al.*, 2000), *Colletotrichum lagenarium* (Kojima *et al.*, 2002; Takano *et al.*, 2000), *Candida albicans* (Alonso-Monge *et al.*, 1999; Csank *et al.*, 1998; Navarro-Garcia *et al.*, 1995), *Pneumocystis carinii* (Fox and Smulian, 1999), *Cochliolobus heterotrophus* (Lev *et al.*, 1999), *M. grisea* (Xu and Hamer, 1996; Xu *et al.*, 1998), *U. maydis* (Mayorga and Gold, 1999; Muller *et al.*, 1999) and *Fusarium solani* f.sp. *pisi* (Li *et al.*, 1997). The MAP kinases found to be important for infection structure formation can be divided into two groups, that is, those that share homology with *S. cerevisiae* FUS3/KSS1 and/or *M. grisea* PMK1 (Xu and Hamer, 1996; Xu *et al.*, 1998) and those that share homology with *S. cerevisiae* SLT2 and/or *M. grisea* MPS1. Functional analysis of *PMK1* and *MPS1*, and some of their homologues, reveals that *PMK1* is essential for appressorium formation (Xu and Hamer, 1996), whereas MPS1 is not essential for appressorium formation, but is required for penetration of the host cuticle, sporulation and cell wall integrity (Xu *et al.*, 1998). Three MAP kinase genes, have been identified in *B. graminis* (Zhang and Gurr, 2001; unpublished). However, little is known about their role in infection structure differentiation.

1.4 OBJECTIVES

Infection structure differentiation in *B. graminis* is a highly regulated and complex process. It demands the coordinated perception of multiple external signals but little was known of how these signals are integrated and transduced within the fungus until the work of Hall *et al.* (1999) and Hall and Gurr (2000) who demonstrated that cAMP signalling and PKA play important, but complex roles, during early development. Signalling via cAMP alone, however, is not sufficient to promote progression through infection structure differentiation. Therefore, other signalling pathways must be required. Thus, the main objective of the work described in this thesis was to investigate the role of other signal transduction pathways in the regulation of early development and infection structure formation in *B. graminis* f.sp. *hordei.*

Preliminary experiments were performed, in Chapter 3, to define the parameters of development of *B. graminis* f.sp. *hordei* on host and artificial surfaces thereby providing a basis for experiments in subsequent chapters. Furthermore, the parameters of development of the rice blast fungus, *Magnaporthe grisea*, on barley and the artificial surface of cellulose membrane were investigated since *M. grisea* was to be employed as a "surrogate host" later in the thesis.

The remainder of the thesis focused on assessing the roles of PKC and MAP kinase signalling pathways in *B. graminis* infection structure differentiation. In Chapter 4 the aims were to:

- Characterise two recently-identified *pkc* genes, namely *pkc*1 and *pkc*-like
- Look for PKC activity in *B. graminis* protein extracts
- Assess the potential involvement of PKC in early development by observing the effects of PKC agonists and antagonists on germling differentiation
- Determine the transcript profiles of *pkc*1 and *pkc*-like at critical stages of *B. graminis* germling morphogenesis

In Chapter 5, the aims were to:

- Characterise two recently-identified MAP kinase genes, namely *mpk*1 and *mpk2*
- Look for MAP kinase activity in *B. graminis* protein extracts
- Assess the potential involvement of MAP kinase in early development by observing the effects of MAP kinase agonists and antagonists on germling differentiation
- Determine the transcript profiles of *mpk*1 and *mpk2* at critical stages of *B. graminis* germling morphogenesis

In Chapter 6, the aims were to:

- Complement the *M. grisea* MAP kinase mutant, Δ*pmk1*, with the *B. graminis mpk*1 gene
- Use Southern blot analysis to confirm transformants for subsequent phenotypic and expression analyses

CHAPTER 2
MATERIALS AND METHODS

2.1 PLANT AND FUNGAL MATERIAL

2.1.1 Plant material

Barley (*Hordeum vulgare* L.) cultivar Golden Promise was grown in a 50:50 (v/v) mixture of John Innes No. 3 compost and Astro peat-based compost (E. A. Goundrey & Sons Ltd., Oxfordshire, UK) in a glasshouse at 20°C. Natural light was supplemented by 400W high-pressure sodium lighting (700 $\mu Mol.m^{-2}.s^{-1}$) to extend the light period to 16 hours (h).

2.1.2 Fungal material: Isolate, maintenance and inoculation

2.1.2.1 Blumeria graminis f.sp. *hordei*

Blumeria graminis (DC.) Speer f.sp. *hordei* Marchal, derived from race IM82 (Newton, 1989), was maintained in a glasshouse by successive inoculations onto 10 day old Golden Promise plants. Inoculum for experiments was generated by shaking heavily-infected 8 to 10 day Golden Promise plants 24 h prior to use to remove old, non-viable conidia. Small-scale inoculation (for scoring experiments) was carried out using an inoculation turret constructed from a 16 x 52 cm plastic pipe, raised *ca.* 5 mm from the work surface, with a Perspex lid, and a 15 mm diameter plastic tube 70 mm from the top of the tower forming a spout into which infected leaves were placed. Surfaces to be inoculated were placed at the base of the tower, and conidia from infected Golden Promise leaves were dislodged using compressed air (Kenair air duster, Kenro Ltd., Swindon, UK) and allowed to settle for 5 min. Inoculation density was measured using a haemocytometer and adjusted to 50-60 $spores.mm^{-2}$.

Larger-scale inoculation (for collection of stage-specific material) was carried out using an inoculation frame constructed from a wooden frame 1.5 m wide, 2.5 m in length and 1.5 m deep, covered with polythene. Surfaces for inoculation were

placed at the bottom of the frame and infected Golden Promise plants were gently shaken at the top to dislodge conidia.

2.1.2.2 Magnaporthe grisea

Magnaporthe grisea strains were cultured on complete medium (CM) (Talbot *et al.*, 1993) in a 14 h light and 10 h dark cycle at 24°C for 10 to 12 days. Wild-type (Guy11) and mutant (Δ*pmk1*: nn95) strains were obtained from the laboratory of N. J. Talbot, University of Exeter. Conidia were harvested by scraping sporulating cultures with a glass rod in sterile distilled water (SDW). Inoculation density was measured using a haemocytometer and was adjusted to between 10^4 and 10^5 spores.mL^{-1}. For long-term storage, strains were grown through sterile Whatman 3 MM paper, followed by desiccation for 48 h and storage at -20°C.

2.1.3 Collection of fungal material

2.1.3.1 Ungerminated conidia

Conidia were collected directly from heavily sporulating 8 to 10 day infected plants using a hand-held computer vacuum cleaner (Office World, Oxford, UK) and stored at -80°C.

2.1.3.2 Stage-specific material

From the host

For extraction of *B. graminis* RNA, conidia were inoculated onto the abaxial surface of detached primary leaves kept moist by inserting the stem between layers of damp cotton wool, in square (12 cm x 12 cm) petri dishes. The infected leaf sections were incubated at 21°C in a cooled growth cabinet, in the dark, until the desired time post-inoculation. Material was collected by painting the leaf surface with a solution of 5% (w/v) cellulose acetate in absolute acetone. Following evaporation of the acetone, trapped conidia were lifted in the solidified cellulose acetate strips, immediately frozen in liquid nitrogen and stored at -80°C.

From agar

B. graminis mature primary germ tube (PGT) stage germlings were collected following inoculation onto 2% (w/v) water agar and incubation for 6 h at >95% relative humidity (RH), in the dark for protein extraction. Germlings were scraped from the agar surface into extraction buffer (COMPLETE™ Mini Protease Inhibitor Cocktail Tablets (Roche Diagnostics, Germany) in 50 mM Tris-HCl, pH 7.5) immediately frozen in liquid nitrogen and stored at -80°C.

From cellulose membrane

B. graminis and *M. grisea* germlings were inoculated onto sheets (250 mm x 250 mm) of cellulose membrane (Cuprophan Dialysis Membrane, 150pm, Medicell International Ltd., UK) and incubated for 20 h at >95% RH, in the dark to obtain tissue for RNA extractions. *M. grisea* was inoculated by submerging the cellulose membrane with a spore suspension of density 10^5 spores.mL^{-1}. Inoculated cellulose membrane was frozen in liquid nitrogen and stored at -80°C.

From cellophane

For tissue for genomic DNA extraction, *M. grisea* strains were cultured on complete media (CM) agar (see *2.1.2.2*) onto which autoclaved quarter sections of cellophane jampot covers (11 cm diameter, as supplied by Boswells, Oxford, UK) were laid. The strains were allowed to grow over the cellophane for 10 to 12 days before being frozen in liquid nitrogen and stored at -80°C.

2.2 CHEMICALS AND SOLUTIONS

Pharmacological agonists and antagonists referred to in Chapters 4 and 5 are detailed in Table 2.1. Solutions and media referred to in the text are detailed in Table 2.2. Chemicals were purchased either from Sigma Chemical (Sigma-Aldrich Co.) or BHD Laboratory Supplies unless otherwise stated.

Chemical name	**Abbreviated name**	**Supplier**	**Solvent**	**Stock conc.**
2-[1-(-Dimethylaminopropyl)-1H-indol-3-yl]-3-(1H-indol-3-yl)maleimide, HCl	Bisindolylmaleimide I, Hydrochloride	A	SDW	10 mM
UCN-1028c	Calphostin C	A	DMSO	10 mM
[1,2-Dimethoxy-N-methyl-[1,3]benzodioxolo[5,6-c]-phenanthridinium chloride]	Chelerythrine chloride	A	SDW	10 mM
1, 2-dioctanoyl-*sn*-glycerol	DOG	A	DMSO	50 mM
2-[1-(3-Dimethylaminopropyl)-5-methoxyindol-3-yl]-3-(1H-indol-3-yl) maleimide	Go6983	C	DMSO	10 mM
(5-Isoquinolinesulphonyl)piperazine, HCl]	HA 100, Dihydrochloride	A	SDW	10 mM
(±)-1-(5-isoquinolinesulfonyl)-2-methylpiperazine.2HCl	H7	A	SDW	10 mM
[N-[2-(p-Bromocinnamylamino)ethyl]-5-isoquinolinesulfonamide.2HCl]	H89	A	SDW	10 mM
2'-Amino-3'-methoxyflavone	PD98059	A	DMSO	50 mM
phorbol 12-myristate 13-acetate (12-O-Tetradecanoylphorbol 13-acetate)	PMA, TPA	A	DMSO	50 mM
antibiotic AM2282, from *Streptomyces* sp.	Staurosporine	A	DMSO	10 mM
1,4-Diamino-2,3-dicyano-1,4*bis*(2-aminophenylthio)-butadiene	U0126	A	SDW	10 mM

Table 2.1. Pharmacological agonists and antagonists referred to in Chapters 4 and 5. Chemicals were purchased from Alexis Corporation (A) and Calbiochem (C).

Table 2.2.

Solution	Composition
Bialophos-defined complex media (BDCM)	1.7 g yeast nitrogen base without amino acids and NH_4SO_4, 2 g ammonium nitrate, 1 g asparagine, 273.6 g sucrose. Make to 1 L in dH_20, adjust pH to 6.0 with Na_2HPO_4. Add 1.5% (w/v) agar. Autoclave.
Complete media (CM)	20x nitrate salts (see below) 1 mL trace elements (see below), 10 g D-glucose, 2 g peptone, 1 g yeast extract, 1 g casamino acids, 1 mL vitamin solution (see below). pH 6.5 with NaOH. Make to 1 L in dH_20. Autoclave.
Coomassie brilliant blue	0.24% (w/v) Coomassie Brilliant Blue in 90 mL of 1:1 (v/v) methanol:SDW and 10 mL glacial acetic acid, filtered through a Whatmann No. 1 filter.
Destain	1:1 (v/v) methanol:SDW and 10 mL of glacial acetic acid in 100 mL total volume.
6x DNA loading dye	0.25% (w/v) bromophenol blue, 40% (w/v) sucrose in SDW. Autoclave.
Low-salt Luria-Bertani (LB) medium	As for LB medium, but with 5 g NaCl.
Luria-Bertani (LB) agar	As for LB medium but with 1.5% (w/v) agar added before autoclaving.
Luria-Bertani (LB) medium	10 g NaCl, 10 g bacto-tryptone, 5 g yeast extract (Merck, Germany). Make to 1 L in dH_20, adjust pH to 7.0, autoclave.
Lysis buffer for Hela cells	1% (v/v) Triton X-100, 20 mM Tris-HCl (pH 7.5), 2 mM EDTA, 0.3% (v/v) β-mercaptoethanol, 10 mM benzamidine, and a protease inhibitor cocktail tablet (Sigma).
1x Maleic acid buffer	1 M maleic acid, 0.15 M NaCl (pH 7.5; adjust with concentrated or solid NaOH), autoclave.
20x Nitrate salts	120 g $NaNO_3$, 10.4 g KCl, 10.4 g $MgSO_4.7H_20$, 30.4 g KH_2PO_4. Make to 1 L in dH_20, adjust pH to 7.0, autoclave.
OM buffer	1.2 M $MgSO_4$, 10 mM $NaPO_4$ (pH 5.8) diluted from a 1.0 M stock of equimolar mono and dibasic. Filter sterilise.
Overlay medium	As for BDCM, but 10 g D-glucose instead of sucrose.
10% Polyacrylamide resolving gel	6.7 mL of 30% acrylamide mix (BioRad), 5.0 mL of 1.5 M Tris (pH 8.8), 0.2 mL of 10% (v/v) SDS, 7.9 mL of SDW, 0.2 mL of 10% (v/v) ammonium persulphate and 8 µL of N, N, N', N'-tetramethylethylenediamine (TEMED).
Phosphate-buffered saline (PBS)	0.137 M NaCl, 2.68 mM KCl, 1.64 mM Na_2HPO_4, 1.76 mM KH_2PO_4.
Phosphate-buffered saline with Tween 20 (PBST)	PBS + 0.05% (v/v) Tween 20.
Prehybridisation buffer	1x RNA blocking buffer, 5x SSC, 0.5% (w/v) SDS.
PTC buffer	60% PEG 4000, 10 mMTris-HCl (pH7.5), 10 mM $CaCl_2$.
Reaction buffer (Southern analysis)	0.1 M Tris-HCl, 0.1 M NaCl, pH 9.5.
Reaction buffer (Western)	100 mM NaCl, 5 mM $MgCl_2$ and 100 mM Tris (pH 9.5).
RNA blocking buffer	10% (w/v) blocking buffer (supplied) in 1x Maleic acid buffer from the DIG Wash and Block Buffer set (Roche).

continued overleaf

Table 2.2. continued

2x SDS gel loading buffer	100 mM Tris-Cl (pH 6.8), 200 mM dithiothreitol, 4% (w/v) SDS, 0.2% (w/v) bromophenol blue and 20% (v/v) glycerol.
20x SSC	3.0 M NaCl, 0.3 M sodium citrate, pH 7.0.
5% Stacking gel	0.83 mL of 30% acrylamide mix, 0.63 mL of 1.0 M Tris (pH 6.8), 0.05 mL of 10% (w/v) SDS, 3.4 mL of SDW, 0.05 mL of 10% ammonium persulphate and 5 µl of TEMED.
ST buffer	0.6 M sorbitol, 0.1 M Tris-HCl (pH 7.0). Autoclave.
STC buffer	1.2 M sorbitol, 10 mM Tris-HCl (pH 7.5), 10 mM $CaCl_2$. Autoclave.
1000x Trace elements	80 mL dH_20, 2.2 g $ZnSO_4.7H_20$, 1.1 g H_3BO_3, 0.5 g $MnCl_2.4H_20$, 0.5 g $FeSO_4.7H_20$, 0.17 g $CoCl_2.6H_20$, 0.16 g $CuSO_4.5H_20$, 0.15 g $Na_2MoO_4.2H_20$, 5 g NaEDTA. Add compounds in order. Boil and pH to 6.5 (with KOH) at 60°C. Adjust volume to 100 mL.
50x Tris acetate EDTA (TAE) buffer	2 M Tris-Acetate, 0.05 M EDTA, pH 8.3.
TFB1	10 mM morpholino ethane sulphonic acid (pH 6.2), 100 mM RbCl, 10 mM $CaCl.2H_20$, 50 mM $MnCl_2.4H_20$. Adjust to pH 5.8. Filter sterilise.
TFB2	100 mM MOPS, 100 mM $CaCl.2H_20$, 10 mM RbCl 15% (v/v) glycerol. Filter sterilise.
Tris-glycine electrophoresis buffer (pH 8.3)	25 mM Tris, 250 mM glycine (pH 8.3), 0.1% SDS.
Transfer buffer (Western)	39 mM glycine, 48 mM Tris base, 0.037% (w/v) SDS, and 20% (v/v) methanol.
Vitamin solution	0.01 g each of: biotin, pyridoxin, thiamine, riboflavin, *p*-aminobenzoic acid, nicotinic acid, in 100 mL SDW. Store in the dark at 4°C.

Table 2.2. Solutions referred to in the text. Autoclaving was performed at 121°C, 15 $lb.sq.in^{-1}$ for 20 min, unless otherwise stated.

2.3 LIGHT MICROSCOPY

Light microscopy was conducted using an Olympus BX50 microscope, using Normaski optics.

2.3.1 Preparation of surfaces for assay of *Blumeria graminis* f.sp. *hordei* and *Magnaporthe grisea* development

Conidial and germling development was assayed on barley epidermal peels, cellulose membrane and 2% (w/v) water agar for *B. graminis*, and barley epidermal peels and cellulose membrane for *M. grisea*. Surfaces inoculated with *B. graminis* were incubated at >95% RH, in a cooled incubator (BDH, Poole, UK), at 21°C, in the dark for a defined period of time. Surfaces inoculated with *M. grisea* were incubated at 24°C.

2.3.1.1 Barley epidermal peels

Epidermal peels were prepared from the abaxial leaf surface by "scoring" the barley leaf with a razor blade and peeling back the epidermal cells. Two methods were employed. Method 1 was used for *B. graminis* alone, and Method 2 was used for both *M. grisea* and *B. graminis*:

Method 1: Prior to inoculation, each epidermal peel was floated on 15 µL of either the chemical or the solvent control on 12-welled glass slides (C. A. Hendley Ltd., Loughton, UK). A further 15 µL was pipetted underneath the peel to ensure that the droplet contacted the underside of the epidermal leaf surface. Conidia were then inoculated directly onto the peels.

Method 2: Epidermal peels were placed on glass slides (BDH) coated with a thin layer (500 µL) of 2% (w/v) water agar. If chemicals were to be added, these were applied to the agar to give the final concentration required. *B. graminis* conidia were then inoculated directly onto the peels. *M. grisea* conidia were inoculated by pipetting a 20 µL droplet of spore suspension, of the required density, directly onto the peels and the peels inoculated.

2.3.1.2 Cellulose membrane

Cellulose membrane was washed and hydrated prior to use by boiling three times for 30 min in deionised water (dH_2O). For inoculation with *B. graminis*, the cellulose membrane was then placed on glass slides which had been covered with a thin layer (500 µL) of 2% water agar containing the chemical or solvent of interest. For inoculation with *M. grisea*, the cellulose membrane was submerged in a spore suspension of the required density.

2.3.1.3 Agar

Glass slides were covered with a thin layer (500 µL) of 2% (w/v) water agar. *B. graminis* conidia were inoculated directly onto the solidified water agar layer.

2.3.2 Determination of development

For *B. graminis* and *M. grisea*, following incubation, 6 replicates of 50 conidia were assessed for germination. Germination was defined as the production of at least one germ tube. In addition, either 6 replicates of 50 germinated conidia were assessed for the extent of their germ tube development, including germ tube elongation, swelling and appressorial differentiation. Statistical significance was determined using the General Linear Model (GLM) following an arcsine transformation.

2.3.3 Measurement of surface hydrophobicity

The relative hydrophobicities of surfaces were assessed using a goniometer to measure the contact angle between 0.6 µL droplets of SDW and the surface (Holloway, 1970). The goniometer was constructed from a modified microscope, that is, a microscope placed with the central barrel horizontal, with a protractor fixed perpendicular to the lens barrel. Wire was connected to an eyepiece, which possessed a single graticule, so as to lie parallel with the protractor, thus acting as a marker that rotated with the eyepiece. The surface to be measured was placed on a horizontal platform fixed onto the microscope stage, and the water droplet pipetted onto the edge of the surface closest to the objective lens. The eyepiece graticule was aligned with the surface on which the droplet was rested thus

causing the wire to be aligned at 0° on the protractor. The wire was then rotated against the protractor allowing contact angles of the water droplet to be measured.

2.5 ENZYME ASSAYS

2.5.1 Fungal protein extraction and purification

2.5.1.1 Protein extraction

B. graminis conidia, extraction buffer and sand (1:1:2, w/v/w) were ground in liquid nitrogen using a pre-cooled pestle and mortar. A further 0.25x volume of extraction buffer (Table 2.2) was added and the mixture was incubated on ice for 20 min and then centrifuged at 13 000 revolutions per minute (rpm) in a microcentrifuge, 4°C for 10 min. The supernatant was removed, divided into homogenous aliquots and stored at -80°C. PGT-stage protein was extracted by centrifuging the germling suspension at 13 000 rpm in a microcentrifuge, 4°C for 5 min and homogenising with sand. The suspension was then centrifuged for a further 5 min, aliquoted and stored at -80°C.

2.5.1.2 Protein purification

Ammonium sulphate precipitation

Ammonium sulphate precipitation was performed according to the method of Pears *et al.*, (1991). Hela cells (gift from Catherine Pears, University of Oxford) were used as a control. Hela cell protein was extracted by adding 1 mL of lysis buffer (Table 2.2). The cell suspension was centrifuged at 13 000 rpm in a microcentrifuge, 4°C for 5 min and the supernatant retained. Ammonium sulphate was added gradually to 18% (w/v) and spun at 13 000 rpm in a microcentrifuge, 4°C for 10 min. The supernatant, termed the 18% fraction, was retained and stored at -80°C. The pellet was resuspended in lysis buffer, without Triton X-100, and ammonium sulphate added to a total of 45% (w/v). This was centrifuged at 13 000 rpm in a microcentrifuge, 4°C for 10 min, the supernatant (45% fraction) was retained, the residual pellet resuspended and both stored at -80°C. Protein was extracted from conidia as previously mentioned. Ammonium sulphate

precipitation was performed as detailed for Hela cells. Antagonist experiments were performed using the 45% fraction.

Column purification

B. graminis conidial and germling protein extracts were concentrated and purified using a 50K Pall Filtotron Microsep™ microconcentrator (Flowgen, Ashby de la Zouch, UK) and centifuged for 5 min at 5 000 *g*, 4°C. The concentrated extract (>50 kDa) was removed and stored at -80°C.

2.5.1.3 Protein quantification

Protein concentrations were determined using a modified version of the Sigma Protein Determination assay (Sigma, Poole, UK). 100 µL of 1x phosphate-buffered saline (PBS: Table 2.2) was added to each of 12 wells of a 96-welled ELISA plate. 100 µL of the protein supernatant was added to the first well and a doubling serial dilution performed. Bradford reagent (Sigma) was added to each of the wells, and after leaving for 5 min, the plate, with replicates, was read spectophotometrically at 570 nm. Bovine serum albumin was used as a standard (Sigma).

2.5.2 Protein kinase C activity (PKC) assay

Protein kinase C (PKC) assays were performed using the PepTag® non-radioactive protein kinase C assay (Promega, Southampton, UK) following the manufacturer's protocol. Briefly, the PKC assay employs a fluorescently-tagged PKC-specific peptide substrate, Peptag C1 Peptide, with the amino-acid sequence P-L-S-R-T-L-S-V-A-A-K. Two µg of the PepTag® C1 peptide, phosphatidyl serine, diluted to a final concentration of 1 $mg.mL^{-1}$, and 1 µL peptide protection solution were prepared in PKC reaction buffer (supplied). The mixture was incubated at 30°C for 2 min and *B. graminis* protein extract was added to a final concentration of either 40 $\mu g.mL^{-1}$ of unpurified conidial protein, 700 $\mu g.mL^{-1}$ of 50 kDa column purified protein extract from ungerminated conidia, or 20 $\mu g.mL^{-1}$ of column purified protein extract from PGT-stage germlings, all in a total volume of 25 µL. Following incubation for a further 30 min at 30°C, the reaction was terminated by heating to 95°C for 10 min. One µL of 80% (v/v) glycerol was

added to each sample and phosphorylated and non-phosphorylated peptides were separated by agarose gel electrophoresis (0.8% agarose gel in 50 mM Tris-HCl, pH 8.0). The relative amounts of non-phosphorylated and phosphorylated peptide was determined by densitometry (Flur-S™ Multimager, Bio-Rad Laboratories Ltd., UK). For analysis of inhibitors and activators of PKC activity, the chemical under investigation was included in the initial reaction mixture prior to addition of protein extract.

2.5.2.1 Inhibitor IC_{50} value determination

A range of inhibitor concentrations was assayed to test the ability of inhibitors to block phosphorylation of the C1 peptide in the PKC assay and kemptide phosphorylation in the PKA assay. Average values were taken from independently replicated experiments and plotted as percentage inhibition against $\log_{10}$ concentration. The gradient of the linear portion of the sigmoidal activity curve was determined and used to determine the IC_{50}, *i.e.* the inhibitor concentration at which 50% inhibition of activity was predicted.

2.5.3 cAMP-dependent protein kinase (PKA) assay

The PepTag® cAMP-dependant protein kinase assay (Promega) was used for analysis of *B. graminis* (Protein Kinase A) PKA activity in which the PKA-specific peptide Kemptide, with amino acid sequence L-R-R-A-S-L-G, was the substrate. Two µg of the PepTag® A1 peptide (Kemptide with a dye molecule attached), cAMP to a final concentration of 1 µM and 1 µL peptide protection solution were prepared in PKA reaction buffer. The mixture was incubated at 30°C for 1 min and then the addition of *B. graminis* protein extract, incubation, termination of the reaction, separation of the A1 peptides on a gel, analysis by densitometry and IC_{50} determination were performed as for the PKC assay (section 2.5.2).

2.5.4 Mitogen-activated protein (MAP) kinase assay

2.5.4.1 SDS-polyacrylamide gel electrophoresis

A 10% polyacrylamide resolving gel (Table 2.2) was prepared and overlaid with

a 10 mm depth of 5% stacking gel (Table 2.2). Tris-glycine electrophoresis buffer (pH 8.3) was added to the gel apparatus. The protein samples were prepared by adding 15 µL of protein extract to 15 µL of 2x SDS gel loading buffer and denatured by heating at 100°C for 3 min. Non-denatured protein samples were prepared in the same way, except the gel loading buffer lacked dithiothreitol, and the samples were not heated. The gel electrophoresis wells were loaded in a predetermined order, beginning with 10 µl of a protein standard (High Molecular Weight standard from Sigma), and in duplicate, resulting in two halves of the gel being identical. 1 x SDS gel-loading buffer was added to unused wells. A voltage of approximately 8 $V.cm^{-1}$ was applied to the gel. After the dye front had moved into the resolving gel, the voltage was increased to 15 $V.cm^{-1}$ until the dye front reached the bottom of the stacking gel. The gel was removed from the apparatus and cut in half with a razor blade. One gel half was immersed in Coomassie Brilliant Blue stain (Sigma) for 6-8 h on a slowly rotating platform at room temperature, followed by approximately 4 h in destain. The gel was stored in water containing 20% (v/v) glycerol. The other (duplicate) gel half was used for western blot analysis.

2.5.4.2 Western blot analysis

Six pieces of Whatman 3MM paper and one piece of Immobilon™ Transfer membrane (Millipore, Watford, UK) were cut to the exact size of the gel half. The 3MM paper was soaked in transfer buffer, and the transfer membrane was soaked in methanol for 30 seconds followed by a wash in SDW. The blot apparatus was assembled, ensuring that there were no trapped air bubbles, and a current of 0.65 $mA.square.cm^{-1}$ was applied for 1.5 h. The apparatus was disassembled and the transfer membrane was air-dried. The membrane was subsequently rewetted and placed in 5% (w/v) Marvel (Premier Beverages, Stafford, UK) in PBS for 30 min. The membrane was washed three times for 5 min in PBS with Tris (PBST). Phospho-p44/42 MAP Kinase antibody (New England Biolabs, Hertfordshire, UK) was diluted 1/500 in PBST containing 5% Marvel and incubated, in a sealed plastic envelope, overnight at room temperature on a rotating platform. The membrane was washed as described previously and was incubated in a sealed

envelope with anti-rabbit IgG alkaline phosphatase conjugate (Sigma) diluted 1/500 in PBST containing 5% Marvel for 2 h. The membrane was washed, and then equilibrated in reaction buffer for 5 min. 1% (v/v) of disodium 3-(4-methoxyspiro{1,2-dioxetane-3,2'-(5'-chloro)tricyclodecan}-4-yl) phenyl phosphate (CSPD®) substrate in reaction buffer was applied directly and evenly to the membrane, which was placed in a clean, sealable polythene bag. Excess solution was driven out of the bag, the bag sealed and incubated at 37°C for 7 min. The membrane was exposed to Kodak BioMax MS film for 40 min in an X-ray cassette with intensifying screen.

2.6 DNA METHODS

2.6.1 Extraction of genomic DNA

Blumeria graminis and *Magnaporthe grisea* genomic DNA were extracted from 0.5 g fresh ungerminated conidia and 1.0 g mycelial tissue, respectively, using the Puregene™ DNA Isolation Kit (Gentra Systems, Minneapolis, USA) following the manufacturer's protocol. Briefly, fungal tissue was ground in liquid nitrogen with a pre-cooled pestle and mortar and transferred to eppendorfs with 500 µL of cell lysis solution. Following resuspension, samples were incubated at 80°C for 5 min to lyse the cells and then treated with an RNase solution. Proteins were precipitated with the supplied solutions and the samples centrifuged at 13 000 rpm in a microcentrifuge to pellet the precipitated protein. The supernatant containing the DNA was transferred to a clean eppendorf and precipitated using 100% (v/v) isopropanol, washed, resuspended in a DNA Hydration Solution (supplied) and stored at 4°C.

2.6.2 Restriction endonuclease digests

Restriction endonucleases were purchased from New England Biolabs. At least 1 unit (U) of enzyme was used per µg of DNA per hour. Genomic DNA for Southern analysis was incubated in volumes of 40 µL at 37°C for 15 h. All other reactions were incubated in volumes of 10 µL at 37°C for at least 2 h.

2.6.3 DNA agarose electrophoresis

Agarose gels were prepared by melting the desired quantity of agarose (0.6-1.2%, (w/v) as required) in 1x Tris acetate EDTA (TAE) buffer. Ethidium bromide was added to the cooled agarose (50°C) to give a final concentration of 0.2 $\mu g.mL^{-1}$. One quarter volume of DNA loading dye was added to the DNA samples prior to loading into the gel wells. The gel was immersed in 1x TAE in the appropriate gel unit. In addition, 0.5 µg of 1 kb pair DNA ladder (New England BioLabs) was loaded along with samples. Voltage of between 1 to 5 $V.cm^{-1}$ (taking the distance between electrodes) was applied across the gel. DNA was visualised using a UV transilluminator (λ= 245 nm).

2.6.4 Extraction and purification of DNA from agarose gels

DNA was excised from gels after electrophoresis using a scalpel and purified using a QIAquick gel extraction kit (Qiagen Ltd., Crawley, UK), following the manufacturer's protocol.

2.6.5 Transformation of *Escherichia coli*

2.6.5.1 Preparation of heat-shock competent cells

Heat-shock competent cells were made using an adaptation of the rubidium chloride protocol of Hanahan (1985). A single colony from an overnight culture of *E. coli* strain DH5α (*sup*E44 Δ*lac*U169 Φ80 *lac*ZΔ M15 *hsd*R17 *rec*A1 *end*A1 *gyr*A96 *thi*-1 *rel*A1), which had been freshly streaked onto LB agar, was used to inoculate 2.5 mL of low-salt LB medium. The culture was incubated overnight at 37°C with shaking at 225 rpm in a Lab-Line bench-top orbital shaker (Jencons (Scientific) Ltd, Bedfordshire, UK). The entire overnight culture was used to inoculate 250 mL of pre-warmed (37°C) low-salt LB medium. The cells were grown in a 1 L flask (which had been pre-rinsed three times with SDW and autoclaved for 30 min) at 37°C with shaking at 200 rpm in the bench-top shaker until the optical density at A_{600} reached 0.4-0.6 units. All subsequent steps were performed with ice-cold pipettes and tubes, with centrifuging being performed in a Beckman GS-6R centrifuge. The cells were collected into 50 mL polypropylene

tubes and placed on ice for 15 min. The culture was centrifuged at 2 500 rpm for 15 min at 4°C. After removing the supernatant, the pellet was gently resuspended in 15 mL TFB1 (Table 2.2) and left on ice for 15 min. The cells were centrifuged again at 2500 rpm for 15 min at 4°C, resuspended in 1.6 mL TFB2 (Table 2.2), and left on ice for 15 min. The cells were divided into 200 µL aliquots, frozen in liquid nitrogen and stored at -80°C.

2.6.5.2 DNA ligation

Following restriction endonuclease digestion, DNA was ligated into vector pCB1532 (5239 base pairs (bp)) (gift from N. Talbot, University of Exeter) containing the gene for sulphonyl urea selection, that is, acetolactate synthase, and ampicillin resistance. Ligations were performed in 6 µL volumes comprising 1x ligation buffer (supplied by the manufacturer (Invitrogen™ Life Technologies, Paisley, UK) as a 5x concentrate), molar ratio of 1:3 pmol ends/µL (vector to insert) DNA and 0.6 U of T4 ligase (Invitrogen™ Life Technologies). Ligation mixtures were placed in ice-cooled water at an initial temperature of 8°C overnight.

2.6.5.3 Heat-shock transformation method

Heat-shock competent *E. coli* cells were thawed on ice prior to use. 100-500 ng of ligated DNA was added to the cells and left to incubate on ice for 30 min, placed in a water bath at 42°C for 2 min and then incubated on ice for 5 min. 1 mL LB was added to each tube before incubation at 37°C for 60 min. Cells were then plated out on LB agar containing ampicillin.

2.6.5.4 Purification of plasmid DNA from Escherichia coli

Plasmids were purified from *E. coli* cells by alkaline lysis "miniprep". Overnight cultures of *E. coli* were grown in 10 mL LB medium containing ampicillin (100 $\mu g.mL^{-1}$), at 37°C and shaken at 175 rpm in an incubated shaker. Cultures were centrifuged at 5 000 rpm for 10 min to pellet the cells, the supernatant discarded and the plasmid DNA extracted using a QIAprep Miniprep Kit (Qiagen), following the manufacturer's instructions. Briefly, the pellet was resuspended,

bacterial cells were lysed and the resulting solution neutralised with the supplied buffers and centrifuged at 5 000 rpm to pellet the cell fractions. The supernatant was then centrifuged through the spin column, washed and finally eluted in 50 µL of 10 mM Tris-HCl (pH 8.5) and stored at -20°C.

2.6.6 Transformation of *Magnaporthe grisea*

2.6.6.1 Protoplast preparation and transformation

Protoplast isolation was carried out using a modification of the method by Talbot *et al.* (1993). Protoplasts were made from mutant strain Δ*pmk1* under sterile conditions. A 2.5 cm x 2.5 cm square of Δ*pmk1* mycelium was blended in 100 mL of CM and dispersed in 40 mL OM buffer containing 20 mg of Novozyme 234 (Novo Biolabs, Copenhagen, Denmark) followed by incubation with gentle shaking (75 rpm) at 30°C for 2-3 h. Protoplasts were transferred to clean 50 mL Falcon tubes and overlayed with an equal volume of ST buffer, followed by centrifugation in a swinging bucket rotor at 5 000 rpm, 4°C for 15 min. Protoplast were recovered from the OM/ST buffer interface and transferred to clean Falcon tubes which were filled with STC buffer. The protoplasts were pelleted by centrifuging at 3 000 rpm for 15 min, 4°C. The buffer was removed and the protoplasts washed three times by resuspending the pellet gently in 10 mL of fresh STC buffer, followed by centrifugation at 3 000 rpm for 15 min, 4°C. Protoplasts were resuspended in STC buffer and adjusted to a concentration of 5 x 10^6 per mL. Five µg of DNA were added to 150 µL of protoplasts in STC buffer and incubated at room temperature for 15 min. One mL of PTC buffer was added, gently mixed by inversion and incubated at room temperature for 15 min. Each aliquot of transformed protoplasts was added to 200 mL of cooled (not above 50°C) bialophos-defined complex media (BDCM: Table 2.2), plated into 5 petri dishes (9 cm diameter) and allowed to regenerate overnight at 24°C, in the dark.

2.6.6.2 Selection of transformants

Fifteen mL of overlay media, containing the fungal selection, chlorimuron ethyl (Greyhound Chromatography and Allied Chemicals, Birkenhead, UK), was overlaid onto the BDCM of each petri dish, resulting in an overall chlorimuron

ethyl concentration of 50 $\mu g.mL^{-1}$ per petri dish. Chlorimuron ethyl-resistant colonies were allowed to develop in a 14 h light and 10 h dark cycle at 24°C for 10 days. Emerging colonies were transferred to fresh BDCM plates containing chlorimuron ethyl, and, after a further 6 days, were subcultured onto CM.

2.6.7 Southern analysis

2.6.7.1 Southern blotting

5 µg of genomic DNA was used per sample for restriction endonuclease digestion followed by gel electrophoresis through 1% agarose. The gel was depurinated denatured and neutralised as described by Sambrook *et al.* (1989). Genomic DNA was then transferred from the agarose gel onto positively charged nylon membrane (Roche Diagnostics) as described by Sambrook *et al.* (1989). After blotting, the DNA was immobilised on the membrane by UV-crosslinking both sides of the membrane using the "optimal crosslink" setting of a Spectrolinker™ XL-100 UV crosslinker (Spectronics Corporation, Nebraska, USA).

2.6.7.2 Preparation of radiolabelled probes

Approximately 50 ng of plasmid-derived DNA was used to prepare random primed, radiolabelled probes using the Prime-It® II Random Primer Labeling Kit (Stratagene). The probe synthesis reaction mix consisted of 5 µL (50 ng) template DNA, 5 µL random 9-mer primers, 7 µL sterile distilled water (SDW). The mixture was heated to 100°C for 5 min, followed by incubation on ice for 1 min. Five µL 5x dCTP buffer, 0.5 µL exonuclease-free Klenow mix (5 $U.mL^{-1}$) and 2.5 µL [α-^{32}P]dCTP (NEN™ Life Science Products Inc, Boston USA) were added to the mixture and incubated at 37°C for 1 h. Unincorporated nucleotides were removed by spinning the mixture through a column of Sephacryl®S-400HR beads (Amersham Pharmacia Biotech., Amersham, UK) at 3 000 rpm for 1 min. Radiolabelled probe was either used immediately or stored at -20°C.

2.6.7.3 Hybridisation, washing, autoradiography and stripping of Southern blots

Membranes were washed twice for 15 min in 2x SSC and 0.1% (w/v) SCS prior to prehybridisation at 65°C for 3 h in pre-heated prehybridisation buffer. 0.2 mL of

prehybridisation buffer was used per square cm of membrane. Radiolabelled probe was added directly to the solution used for prehybridisation and incubated at 65°C for at least 12 h. Following hybridisation, membranes were washed twice in 2x SSC, 0.1% (w/v) SDS at room temperature for 15 min per wash, followed by two washes in 1x SSC, 0.1% (w/v) SDS at 60°C for 15 min per wash. Two final high stringency washes were performed in 0.1x SSC, 0.1% (w/v) SDS at 65°C for 15 min per wash prior to autoradiography. Kodak BioMax MS film was used for autoradiography of the hybridised membranes at -80°C in an X-ray cassette with an intensifying screen.

Removal of radiolabelled probes from membranes for rehybridisation was performed following the method of Sambrook *et al.* (1984). Briefly, 0.1% (w/v) SDS was added to a boiling solution of 0.05x SSC and 0.01 M EDTA (pH 8.0). The membrane was immersed in the solution for 15 min and the wash repeated with fresh solution for a further 15 min. The membrane was rinsed briefly in 0.01x SSC at room temperature and checked for radioactivity using a Geiger counter and overnight exposure to X-ray film.

2.6.8 Polymerase chain reaction (PCR) techniques

All oligonucleotide primers were synthesised by MWG Biotech (AG Ebersberg, Germany). Stock solutions were made to 100 pmol.μL^{-1} and stored at -20°C.

2.6.8.1 'Step-down' PCR

'Step-down' PCR was performed as detailed by Zhang and Gurr (2000). This is a PCR-based approach leading to the direct sequence analysis of unknown flanking genomic DNA. Template DNA for the first PCR reaction, derived from *B. graminis* genomic DNA, was prepared by Ziguo Zhang, University of Oxford, according to the method of Zhang and Gurr (2000). The PCR reaction mixture contained 1x Advantage cDNA PCR reaction buffer (BD Biosciences Clontech, Palo Alto, California, USA) (40 mM Tricine-potassium hydroxide (pH 9.2), 15 mM potassium acetate, 3.5 mM magnesium acetate, 3.75 $\mu g.mL^{-1}$ of BSA), 200 μM of each dATP, dCTP, dGTP and dTTP, 1x Advantage cDNA Polymerase Mix

(BD Biosciences Clontech), 10 pmol of each primer, 5 ng template DNA, in a total volume of 20 μL. The gene-specific walking primers designed for the *B. graminis mpk*1 promoter were named, for walk 1:

- MAP1-1: 5' GCATTAGGGGCACGGGTCGACAGCTTG 3'
- MAP1-2: 5' GTGCCTTTGACGATCTGAAAGCTGTATGAAAGC 3'

and for walk 2:

- MAP1-3: 5' GCAGTCCGGTACTCTAGTTCGATG 3'
- MAP1-4: 5' GGCTACCTCAACTCTTGAAGTGGATCTC 3'

Non-specific primers were:

- PP1: 5' GTAATACGACTCACTATAGGGC 3'
- PP2: 5' ACTATAGGGCACGCGTGGT 3'

The 'step-down' PCR reaction 1 carried primers PP1 and MAP1-1 for walk 1 and PP1 and MAP1-3 for walk 2. Thermal cycling conditions were:

- 94°C for 2 s and 72°C for 3 min, 3 cycles
- 94°C for 2 s and 70°C for 3 min, 3 cycles
- 94°C for 2 s and 68°C for 3 min, 3 cycles
- 94°C for 2 s, 66°C for 20 s, 68°C for 3 min, 26 cycles
- 68°C for 8 min
- 4°C to end

Five μL of the PCR products from reaction 1 were diluted with 200 μL of SDW, and 1 μL was used in PCR amplification reaction 2, essentially as PCR reaction 1, but using the primers PP2 and MAP1-2 for walk 1, and PP2 and MAP1-4 for walk 2. The PCR products were separated by gel electrophoresis and the dominant bands isolated and sequenced directly.

2.6.8.2 Amplification of DNA

Amplifications of fragments from genomic or plasmid DNA were carried out in 20 µL reaction mixtures containing 5 ng DNA template, 20 pmol of each primer, 1x Advantage cDNA PCR reaction buffer (BD Biosciences Clontech), 200 µM of each dATP, dCTP, dGTP and dTTP, 1 x Advantage cDNA Polymerase Mix (BD Biosciences Clontech), 10 pmol of each primer, in a total volume of 20 µL. Primers used for amplification were (designated A-F in Chaper 6, Figure 6.2; Appendices 1 and 2):

- PMK1 (F): 5' CCAAATACCTGCCGTACTGGC 3'
- PMK1 (R): 5' TTAATTGTGAGTGCCGGCG 3'
- MPK1 (F): 5' GAATAAGATGCTGCTCATGC 3'
- MPK1 (R): 5' GGGAATTAATCGGATCCAC 3'
- CONF (F): 5' TGTGCTGCAAGGCGATTAAGT 3'
- CONF (R): 5' AGAGCAGGCA CTACCTCC 3'

The thermal cycling conditions were:

- 94°C for 3 min, 1 cycle
- 94°C for 30 s, TM* for 60 s, 72°c for X[§] min, 25-35 cycles
- 72°C for 10 min
- 4°C to end

2.6.8.3 DNA sequencing

DNA sequencing was performed with Big Dye Terminator Chemistry from Perkin-Elmer Applied Biosystems (Foster City, California, USA) on an ABI 310 sequencer in the Department of Plant Sciences, University of Oxford.

---

* annealing temperature appropriate for particular primer pair

§ allow 30 s per 500 bp of DNA to be amplified

2.7 RNA METHODS

2.7.1 Maintenance of ribonuclease free environment

Every effort was made to minimise the activity of RNases during RNA work. Where possible, new, disposable plasticware was used. Otherwise, re-used plasticware and solutions were treated by overnight immersion in 0.2% (v/v) diethylpyrocarbonate (DEPC), followed by autoclaving at 121°C for 30 min to remove residual DEPC. Pestles and mortars were baked for at least 6 h at 200°C. Electrophoresis tanks, gel casts and combs were washed with 0.1% SDS and rinsed with DEPC-treated SDW prior to use.

2.7.2 Isolation of total RNA

Total RNA was isolated from ungerminated conidia and stage-specific material using a modification of the SV Total RNA isolation kit system (Promega). Fungal material was ground in liquid nitrogen with a pre-cooled pestle and mortar and transferred to 1.5 mL eppendorf tubes with 1 mL of SV RNA Lysis Buffer. Samples were homogenised with a small tissue homogeniser and 350 µL of the mixture transferred to a clean eppendorf. The remaining mixture was stored at -80°C. 700 µL of SV RNA Dilution Buffer was added to the samples and mixed by gentle inversion, followed by incubation at 70°C for 3 min. Samples were subsequently centrifuged at 13 000 rpm for 10 min to pellet cellular debris and precipitated protein, and the RNA-containing supernatant was transferred to a new eppendorf tube containing 200 µL 95% ethanol per 500 µL of supernatant. Samples were mixed gently by inversion, transferred to the Spin Basket Assembly and centrifuged at 13 000 rpm for 1 min to bind nucleic acids to the basket silica membrane. The eluate was discarded and the basket membrane was washed with 600 µL SV RNA Wash Solution, followed by centrifugation at 13 000 rpm for 1 min. Nucleic acids bound to the basket membrane were treated with 50 µL DNase incubation mix for 15 min at room temperature. The reaction was stopped by addition of 200 µL DNase Stop Solution, and washed with 600 µL SV RNA Wash Solution by centrifuging at 13 000 rpm for 1 min, followed by a final wash with 200 µL SV RNA Wash Solution by centrifuging at 13 000 rpm for 2 min. RNA

was eluted with 100 µL RNase-free water by centrifuging at 13 000 rpm for 1 min.

The resulting RNA solution was concentrated by ethanol co-precipitation with GlycoBlue™ (Ambion, Huntingdon, UK) and quantified by visualisation of 1 µL of the sample under UV light after gel electrophoresis and staining with ethidium bromide (at a concentration of 0.5 $\mu g.mL^{-1}$).

2.7.3 cDNA synthesis

First strand cDNA was synthesised from total RNA using the RETROscript™ First Stand Synthesis Kit (Ambion), following the manufacturer's instructions. Briefly, total RNA was heat denatured in a reaction mix containing 1-2 µg total RNA and 2 µL of a 50 µM stock solution of Oligo(dT) primers in a total volume of 12 µL by heating to 75°C for 5 min. Subsequently, the remaining RT components were added to give a final volume of 20 µL: 1x RT buffer, 33 µM of each dNTP, 1 U RNase inhibitor, 100 U Reverse Transcriptase. No template controls and minus reverse transcriptase controls were included. The thermal cycling conditions were:

- 42°C for 60 min, 1 cycle
- 55°C for 12 min, 1 cycle
- 92°C for 10 min, 1 cycle
- 4°C to end

2.7.4 Reverse transcriptase PCR

First strand cDNA (5ng), from ungerminated conidia and germlings, was used for semi-quantitative RT-PCR quantification in a 10 µL reaction mix containing 10 nM Tris-HCl (pH 9.0), 1.5 mM $MgCl_2$, 50 mM KCl, 0.1% (v/v) Triton X-100, 0.01% (w/v) gelatin, 200 mM each dNTP, 5 mM Dig-UTP, 200 nM forward and reverse primers, 1 unit of SuperTaq (HT Biotechnology Ltd., Cambridge, UK). Considerable care was taken to "equilibrate" the starting cDNA templates from the different tissues (Zhang *et al.*, 2000). The forward (F) and reverse (R) primers

for *B. graminis* β-*tubulin* (Sherwood and Somerville, 1990), *B. graminis mpk*1, *M. grisea* β-*tubulin* and *M. grisea PMK1* genes were:

- *B. graminis* β-*tubulin*:(F) 5' TCTGCCATT TTCCGCGGTAA 3'
  (R) 5' CGTTGCTAACTTCCTCTGGA 3'
- *B. graminis mpk*1: (F) 5' GTTTACTTGATTCAGGAGCTTATG 3'
  (R) 5' GTTAATTGGTGATGGTAATCTTTTCC 3'
- *M. grisea* β-*tubulin*: (F) 5' CTGCCATCTTCCGTGGAA 3'
  (R) 5' GTGAACTCCATCTCGTCC 3'
- *M. grisea PMK1*: (F) 5' CTTATGGAGTCGTTTGCTCTG 3'
  (R) 5' AGCTGGTGGT GGTAGTCCT 3'

Considerable care was taken in the design of the primers so as to span the introns of the genes to ensure that RT-PCR amplification products were not due to spurious amplification of genomic DNA. The thermal cycling conditions were:

- 94°C for 60 s, 60°C for 6 s, 68°C for 60 s, 1 cycle
- 94°C for 60 s, 59°C for 6 s, 68°c for 60 s, 1 cycle
- 94°C for 60 s, 58°C for 6 s, 68°c for 60 s, 1 cycle
- 94°C for 60 s, 57°C for 6 s, 68°c for 60 s, 1 cycle
- 94°C for 60 s, 56°C for 6 s, 68°c for 60 s, for 14 or 16 cycles

The samples were subjected to 1% agarose gel electrophoresis, blotted onto Hybond N (Amersham) membrane and the PCR products were detected using the DIG Luminescent Detection Kit (Roche Diagnostics).

2.7.5 Real-time PCR

Real-time PCR was performed on first strand cDNAs, prepared as above, using the Qiagen QuantiTect SYBR Green RT-PCR kit (Qiagen) according to the manufacturer's instructions. Primers were designed to amplify *ca.* 100 bp fragments and to span introns to eliminate spurious amplification of genomic DNA. The real-time forward and reverse primers were:

- β-*tubulin*: (F) 5' TTCCGCGGTAAGGTATCT 3'
  (R) 5' GCAGTTTGAACATTATTTGGA 3'
- *pkc*1: (F) 5' CCGAGATTTTACTGGACAAGA 3'
  (R) 5' GATCTCATCTTCATCTTCACC 3'
- *pkc*-like: (F) 5' GTGCATATACAACAAAAGACCGT 3'
  (R) 5' TGAGCTAATAGCGTGCATACA 3'
- *mpk*1: (F) 5' GGGAAAAGATTACCATCACCA 3'
  (R) 5' TTCTTGAATGGAAGGGATCGA 3'
- *mpk2*: (F) 5' TACCAAAGCCATCGATGTTTG 3'
  (R) 5' GGGCTAGTGTCTCTTCATTC 3'

Real-time quantification was performed using the Rotorgene 2000 real-time PCR machine (Corbett Research, Australia) following the steps:

- Denaturation: 95°C for 15 min,
- Amplification: 94°C for 30 s, 52°C for 30 s, 72°C for 30 s, 35 cycles with a fluorescence measurement
- Hold: 72°C for 20 s
- Melt: 72°C to 95°C with a heating rate of 0.2°C per second.

Primer efficiencies were calculated by ascertaining the "crossing point" values (the point at which fluorescence rises appreciably above background fluorescence) of a two-fold dilution series of cDNA, determining the slope of these values, and then an efficiency value being calculated according to the equation $E=10^{[-1/slope]}$. These were used to calculate values of expression of *pkc*1, *pkc*-like, *mpk*1 and *mpk2* transcripts relative to those of the endogenous, constituitively expressed control gene, β-*tubulin*, using the method described by Pfaffl (2001). No template controls (NTCs) were included to monitor the presence of primer dimers or contamination.

2.8 SUPPLIERS

Alexis Corporation (UK) Ltd., 3 Moorbridge Court, Moorbridge Road East, Bingham, Nottingham, NG13 8QG.

Ambion (Europe) Ltd., Ermine Business Park, Spitfire Close, Huntingdon, Cambridgeshire, PE29 6XY.

Amersham Biosciences UK Ltd., Amersham Place, Little Chalfont, Buckinghamshire, HP7 9NA.

BD Biosciences Clontech, 1020 East Meadow Circle, Palo Alto, CA 94303, USA.

BDH, VWR International Ltd., Merck House, Poole, Dorset, BH15 ITD.

Bio-Rad Laboratories Ltd., Bio-Rad House, Maylands Avenue, Hemel Hempstead, Hertfordshire, HP2 7TD.

C. A. Hendley Ltd., Oakwood Hill Industrial Estate, Loughton, Essex, IG10 3TZ.

Corbett Research, 1/14 Hilly Street, Mortlake, NSW 2137, Sydney, Australia

E. A. Goundrey & Sons, Duns Tew, Oxfordshire, OX6 4JR.

Flowgen, Findel House, Excelsior Rd., Ashby Park, Ashby de la Zouch, Leicestershire, LE65 1NG.

Greyhound Chromatography and Allied Chemicals, 88 Grange Road West, Birkenhead, Wirral, CH43 4XF.

Gentra Systems Inc., 13355 10th Avenue, N Suite 120, Minneapolis, MN 55441 USA.

HT Biotechnology Ltd., Unit 4, 61 Ditton Walk, Cambridge, Cambridgeshire, CB5 8QD

Invitrogen Ltd., 3 Fountain Drive, Inchinnan Business Park, Paisley.

Jencons (Scientific) Ltd., Cherrycourt Way, Stanbridge Road, Leighton Buzzard, Bedfordshire, LU7 4UA.

Kenro Ltd., Greenbridge Road, Swindon, SN3 3LH.

Medicell International Ltd., 239 Liverpool Road, London, NI ILX.

Merck, Merck KgaA, 64271, Darmtadt, Germany.

Millipore (UK) Ltd., Units 3&5 The Courtyards, Hatters Lane, Watford, WD18 8YH.

MWG-Biotech AG, Anzinger Str. 7, D-85560, Ebersberg, Germany.

NEN™ Life Science Products Inc., Boston, MA 02118, USA.

New England Biolabs (UK) Ltd., 73 Knowl Piece, Wilbury Way, Hitchin, Hertfordshire, SG4 0TY.

Novo Biolabs, Novo Industri A/S, DK 2880 bagsvaerd, Denmark.

Office World, 14-16 Park End Street, Oxford, Oxfordshire, OX1 1HH.

Perkin-Elmer Applied Biosystems, 850 Lincoln Centre Drive, Foster City, CA, 94404.

Premier Beverages, Knighton, Adbaston, Stafford, ST20 0QL.

Promega, Delta House, Chilworth Science Park, Southampton, SO16 7NS.

Qiagen Ltd., Boundary Court, Gatwick Road, Crawley, West Sussex, RH10 9AX.

Roche Diagnostics GmbH, Sandhoferstrasse 116, 68305 Mannheim, Germany.

Sigma Chemical Co., Fancy Lane, Poole, Dorset, BH17 7BR.

Spectronics Corporation, 956 Brush Hollow Road, PO Box 483, Westbury, NY 11590, USA.

CHAPTER 3
BLUMERIA GRAMINIS F.SP. *HORDEI* AND *MAGNAPORTHE GRISEA* DEVELOPMENT ON BARLEY AND ARTIFICIAL SURFACES

3.1 INTRODUCTION

3.1.1 *Blumeria graminis* f.sp. *hordei* infection structure differentiation

Blumeria graminis f.sp. *hordei* infection structure differentiation is a highly complex process requiring that multiple leaf-derived signals are perceived by germinated conidia in order to drive the differentiation process (Carver *et al.*, 1996). *B. graminis* development can be promoted by both physical properties of the leaf surface, such as hydrophobicity (Carver *et al.*, 1996; Carver *et al.*, 1999), as well as chemical signals such as the presence of cellulose and cutin monomers (Kobayashi *et al.*, 1991; Carver *et al.*, 1996; Francis *et al.*, 1996; Suzuki *et al.*, 1999). However, no single signal alone appears to promote the same degree of appressorial differentiation as that observed on the leaf surface.

3.1.2 *Magnaporthe grisea* infection structure differentiation

Magnaporthe grisea infection structure development is also promoted by physical and chemical properties of the leaf surface. Surface hardness is probably the single most important cue for appressorium formation in *M. grisea* (Xiao *et al.*, 1994b), however differentiation is contingent on substrate hydrophobicity and the solute composition of the surrounding environment. In contrast to *B. graminis*, either hydrophobicity or cutin monomers alone are sufficient to induce appressorium differentiation (DeZwaan *et al.*, 1999). Additionally, *M. grisea* will differentiate appressoria in response to starvation (Jelitto *et al.*, 1994).

3.1.3 The study of infection structure development

In order to study infection structure differentiation in *B. graminis*, *M. grisea* will be employed within this thesis as a "surrogate host". Indeed, appressorium formation in *M. grisea* has been well-characterised thanks to the experimental

tractability of the fungus. Various studies have described, in detail, the morphologic changes that take place during appressorium development (Heath *et al.*, 1992; Howard and Valent, 1996), and mutants can be generated to test the roles of specific genes in infection structure formation.

Studies into infection structure differentiation in *B. graminis* have frequently employed artificial surfaces, as well as plant surfaces, in order to test conditions that might modulate fungal development. Barley epidermal peels are used as a fully-inductive surface for *B. graminis* appressorium studies, whereas the artificial surfaces of cellulose membrane and water agar provide surfaces that are semi-inductive and non-inductive to *B. graminis*, respectively (Carver and Ingerson, 1987; Kobayashi *et al.*, 1991; Pryce-Jones *et al.*, 1999; Hall *et al.*, 1999; Hall, 1999). Specifically, cellulose membrane has been found to induce high levels of *B. graminis* conidial differentiation (Kobayashi *et al.*, 1991; Pryce-Jones *et al.*, 1999), however, it is uncertain whether the inductiveness of cellulose membrane is the result of physical properties of the membrane or a chemical signal from cellulose or its breakdown products. On water agar, the majority of *B. graminis* conidia form short germ tubes (Carver and Ingerson, 1987; Hall, 1999).

The barley leaf surface is used extensively in experiments with *M. grisea* (Sweigard *et al.*, 1998) and artificial surfaces have also been used in order to follow infection structure differentiation. For example, *M. grisea* forms appressoria efficiently on hydrophobic surfaces such as polytetra-fluoroethylene (Teflon®) membranes but on hydrophilic, chemically inert surfaces, germlings fail to proceed beyond the early recognition phase of appressorium differentiation (Lee and Dean, 1994; Gilbert *et al.*, 1996). In the same way, such surfaces have been used to characterize *M. grisea* mutants, including the mitogen-activated (MAP) protein kinase mutant Δ*pmk1* (Xu and Hamer, 1996). However, cellulose membrane has not been employed for the study of *M. grisea* infection structure differentiation, even though this surface has properties, other than its partial inductivity to *B. graminis* appressorium formation, that are experimentally useful.

For instance, it is cheap, easy to use and can be used to harvest tissue for molecular analysis.

3.1.4 Objectives

The aim of the work described in this Chapter was to define the parameters of *B. graminis* f.sp. *hordei*, *M. grisea* strain Guy11 and *M. grisea* MAP kinase mutant Δ*pmk1* development on a range of surfaces to be employed in experiments in subsequent Chapters. To this end, time-courses of *B. graminis* germination and appressorial differentiation were performed on a host-derived (full-inductive) surface, that is, barley epidermis, and the artificial surfaces of cellulose membrane (semi-inductive) and water agar (non-inductive). Similarly, *M. grisea* time-courses were performed on barley epidermis and cellulose membrane.

3.2 RESULTS

3.2.1 Time-courses of *Blumeria graminis* f.sp. *hordei* and *Magnaporthe grisea* development on host and artificial surfaces

Blumeria graminis f.sp. *hordei* and *Magnaporthe grisea* were tested for their abilities to germinate and differentiate on the barley (*Hordeum vulgare* L.) epidermal surface of cultivar Golden Promise and on artificial surfaces, that is, hydrated cellulose membrane overlying 2% (w/v) water agar for both *B. graminis* and *M. grisea* and 2% water agar alone for just *B. graminis*. Conidia were inoculated onto the prepared surfaces and incubated at >95% relative humidity (RH), in the dark at 20°C for *B. graminis* and 25°C for *M. grisea*. Time-courses of development were performed with conidia being scored for germination (6 replicates of 50 conidia) and differentiation (6 replicates of 50 germinated conidia) at 0, 2, 4, 8, 12, 16, 20 and 24 hours post inoculation (hpi). For differentiation studies, *B. graminis* germlings were classed as either having a primary germ tube (PGT), an elongated germ tube (EGT), a swollen germ tube (SwGT) or a hooked appressorial germ tube (AGT). However, germ tubes on 2% water agar were classed as "short germ tubes" (SGTs) because "true" PGTs fail to form on such non-inductive surfaces. *M. grisea* germlings were classed as either having elaborated a germ tube (GT), an EGT, SwGT or an appressorium. Statistical significance was determined using the General Linear Model (GLM) following an arcsine transformation.

Time-courses of germination for *B. graminis* and *M. grisea* are given in Figures 3.1 and 3.4, respectively. Time-courses of differentiation of *B. graminis* are given in Figure 3.2, with light micrographs shown in Figure 3.3. Time-courses of differentiation of *M. grisea* are given in Figure 3.5, with light micrographs in Figures 3.6 and 3.7.

3.2.1.1 Germination and differentiation of Blumeria graminis f.sp. hordei on barley epidermis, 2% (w/v) water agar and cellulose membrane

Figure 3.1 shows the germination of *B. graminis* f.sp. *hordei* conidia over a time-course of 24 hours on barley epidermal peels, cellulose membrane and 2% water agar. Table 3.1 gives the P-values comparing the significance of differences in germination between each of the three surfaces over the 24 h time-course. By 2 hpi, the conidial population on barley epidermal peels had germinated significantly (Table 3.1) more than those on cellulose membrane and 2% water agar (60% of conidia had germinated on epidermal peels, 50% on 2% water agar and 42% on cellulose membrane). However, there was no significant difference in germination level between cellulose membrane and agar. By 4 hpi, the difference in level of germination between *B. graminis* conidia on barley epidermal peels and the artificial surfaces had increased, whereas there was still no significant difference in germination level between populations on agar or cellulose membrane. By 12 hpi, the level of germination for conidia on barley epidermal peels began to plateau, with a mean of 82% of conidia having germinated by 24 hpi. Germination levels for conidia on cellulose also began to plateau at 12 hpi, with a mean of 60% of conidia having germinated by 24 hpi. Germination levels for conidia on 2% water agar began to plateau at the earlier time point of 8 hpi, with a mean of 52% of conidia having germinated by 24 hpi.

Figure 3.2(a) shows a graph of the extent of differentiation of *B. graminis* on epidermal peels over a 24 h time-course. Figure 3.3 shows micrographs of *B. graminis* on barley epidermal peels at 2, 4, 8 and 24 hpi. By 2 hpi, germlings had differentiated PGTs alone. By 4 hpi, whereas the majority of germlings, *i.e.* 57%, had not differentiated beyond the PGT-stage, 16% of the germling population had elaborated swollen, appressorial germ tubes, with the remaining germlings having differentiated EGTs. By 8 hpi the majority (70%) of the *B. graminis* germling population had differentiated AGTs, with 20% still having not differentiated beyond the PGT-stage. By 12 hpi, 92% of germlings had differentiated AGTs, with this level staying constant over the remainder of the time-course.

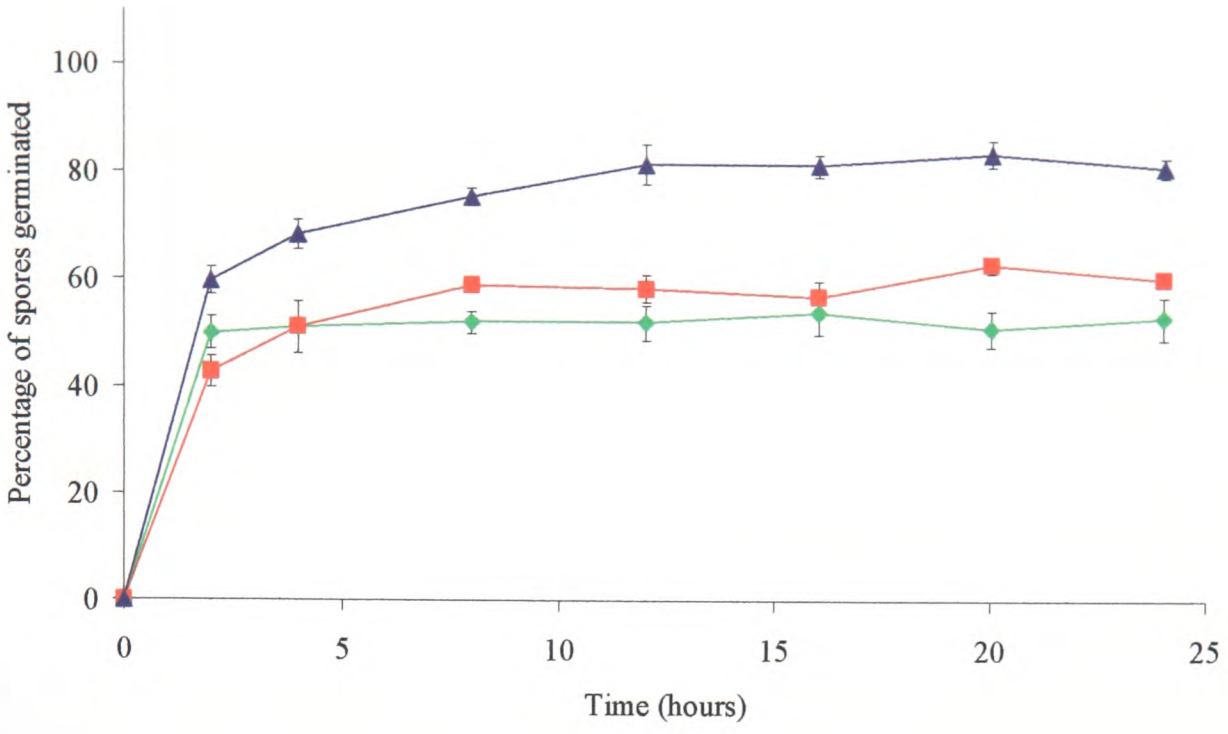


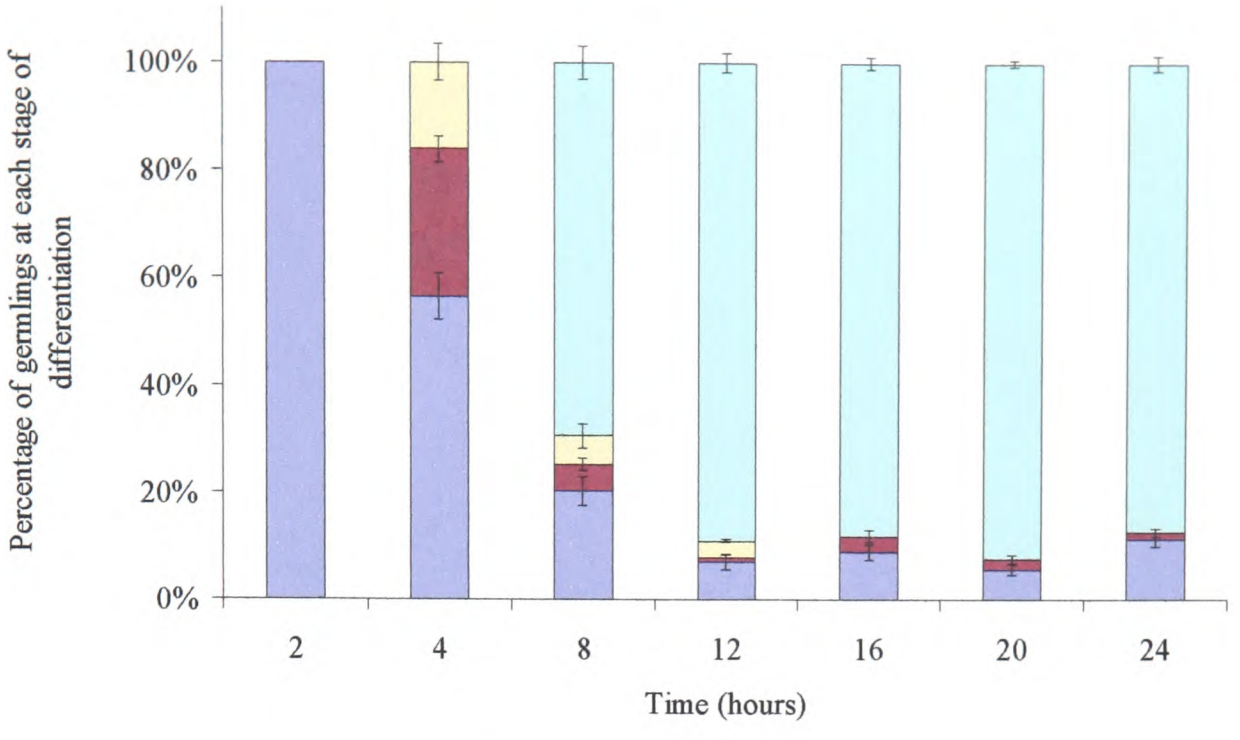
Figure 3.1. Time-course of germination of *Blumeria graminis* f.sp. *hordei* on barley epidermal peels (▲), hydrated cellulose membrane (■) and 2% (w/v) water agar (◆) For each time point, 6 x 50 conidia were scored for germination. The mean ± standard error is shown.

	Time (hpi)						
	2	4	8	12	16	20	24
Ep v. Cm	0.002**	0.000***	0.000***	0.000***	0.000***	0.000***	0.000***
Ep v. Agar	0.036*	0.010**	0.000***	0.000***	0.000***	0.000***	0.000***
Cm v. Agar	0.113	0.997	0.019*	0.149	0.567	0.011*	0.119

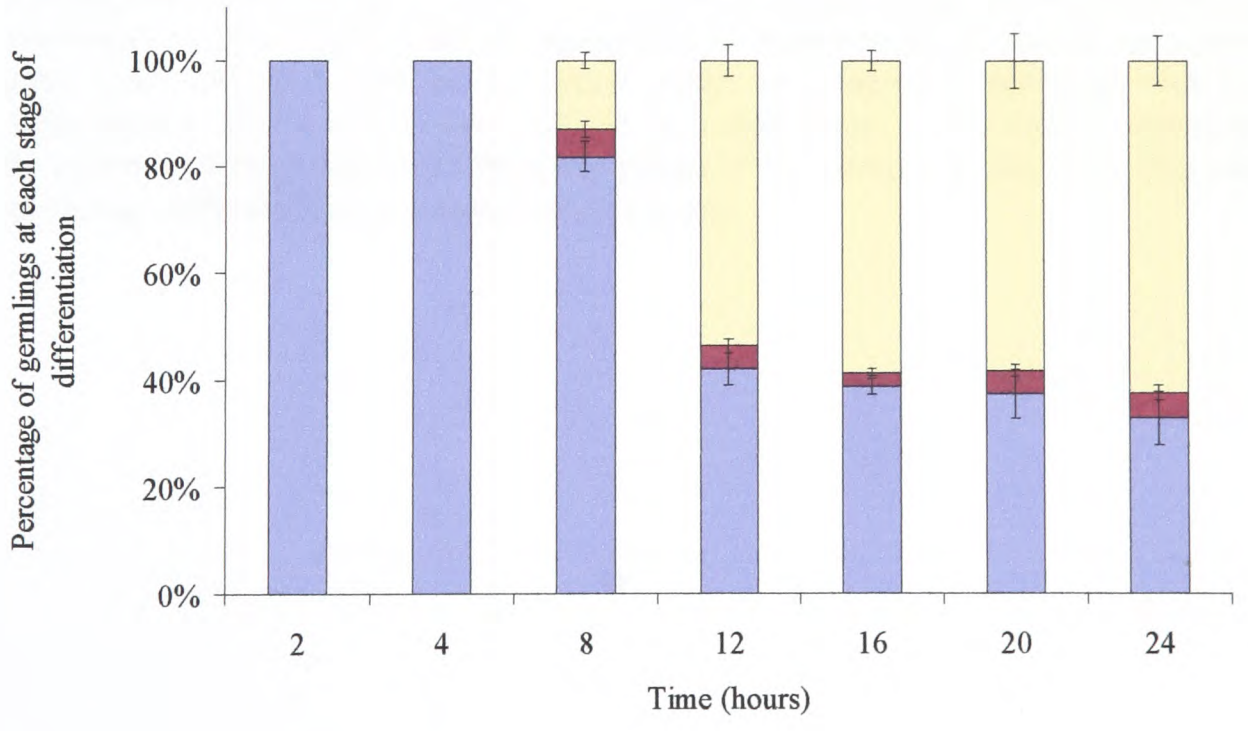
Table 3.1. P-values comparing the significance of differences in germination of *Blumeria graminis* f.sp. *hordei* between epidermal peels (Ep), hydrated cellulose membrane (Cm) and 2% (w/v) water agar (Agar) over a 24 h time-course. For each time point and surface, 6 x 50 conidia were scored for germination. * indicates $P \leq 0.05$, ** indicates $P \leq 0.01$ and *** indicates $P \leq 0.000$.

Figure 3.2.

a)


Percentage of germlings at each stage of differentiation
100%
80%
60%
40%
20%
0%
2
4
8
12
16
20
24
Time (hours)

b)


Percentage of germlings at each stage of differentiation
100%
80%
60%
40%
20%
0%
2
4
8
12
16
20
24
Time (hours)

c)

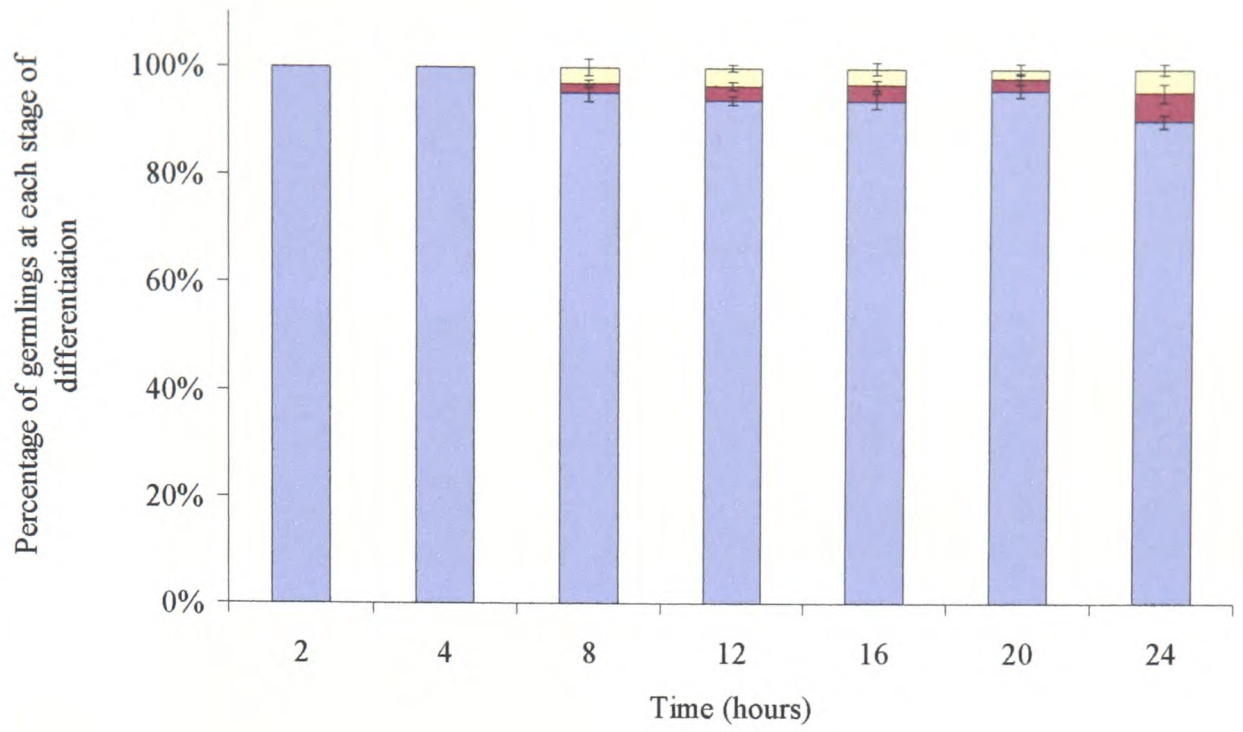


Figure 3.2. Time-courses of differentiation of *Blumeria graminis* f.sp. *hordei* on (a) barley epidermal peels (b) hydrated cellulose membrane and (c) 2% (w/v) water agar. ■ corresponds to germlings with primary germ tubes, ■ corresponds to germlings having differentiated elongated germ tubes, ■ corresponds to germlings having differentiated swollen germ tubes (SwGT) and ■ corresponds to differentiation of hooked appressorial germ tubes (AGT), except in (b) where yellow bars represent germlings that have differentiated either a SwGT or an AGT. In each experiment, 6 x 50 conidia were scored for extent of differentiation and the mean values of 50 conidia are illustrated. The mean percentage differentiation ± standard error is shown.

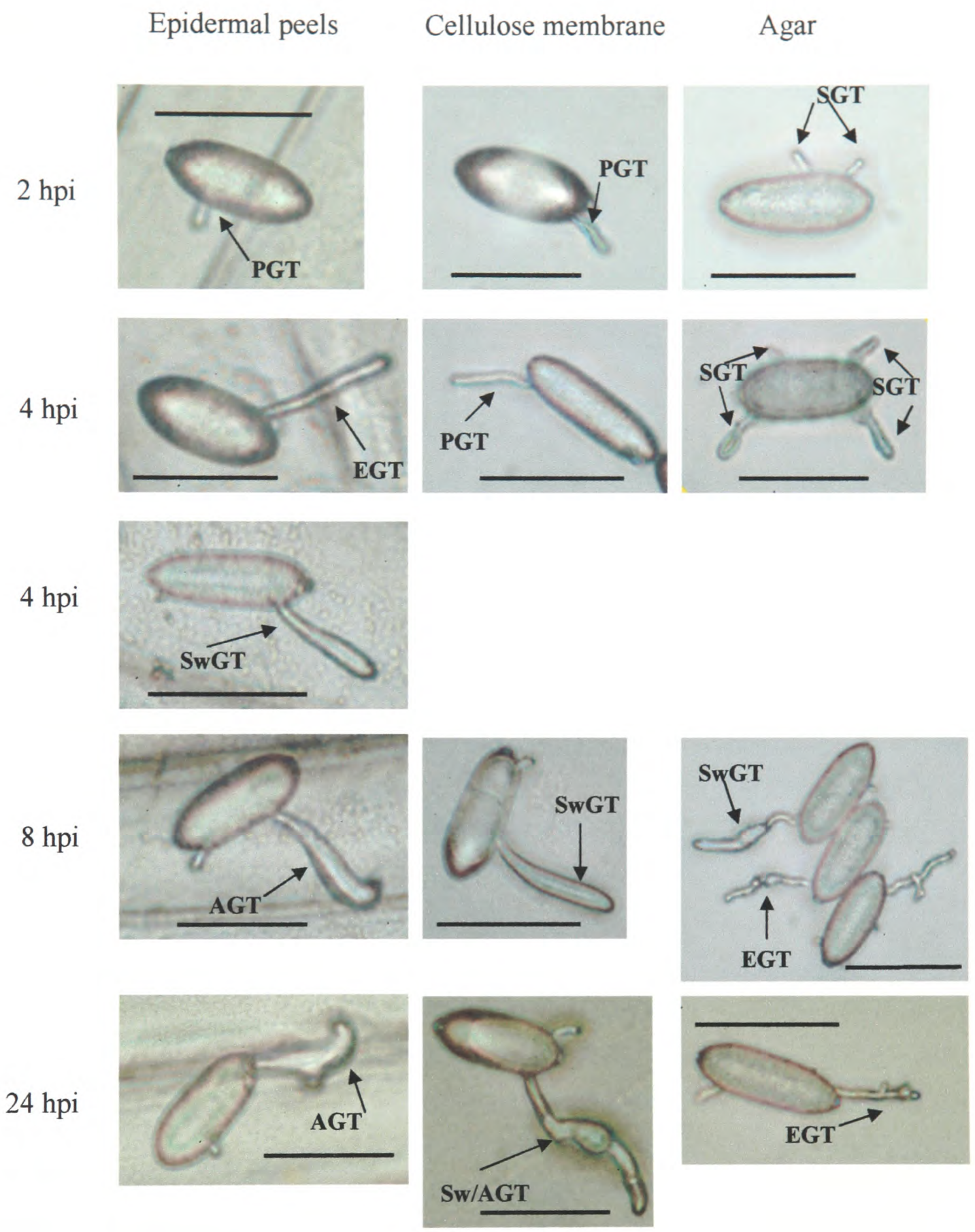


Figure 3.3. Light micrographs of *Blumeria graminis* f.sp. *hordei* on barley epidermal peels, hydrated cellulose membrane and 2% (w/v) water agar at 2, 4, 8 and 24 hours post inoculation (hpi). Arrows indicate short germ tubes (SGT), primary germ tubes (PGT), elongated germ tubes (EGT), swollen germ tubes (SwGT) and appressorial germ tubes (AGT). The bar indicates a length of 28 μm. Magnification x400.

Figure 3.2(b) shows a graph of the extent of differentiation of *B. graminis* on hydrated cellulose membrane over a 24 h time-course. Figures 3.2(b) and 3.3 show that by 8 hpi, the majority (84%) of germlings had not differentiated beyond the PGT stage. By 12 hpi, however, most germlings had differentiated SwGTs/AGTs, with 42% of the population still not having differentiated beyond the PGT stage. The proportion of the population having differentiated SwGTs/AGTs gradually increased over the next 12 h of the time-course, with 62% of the population having differentiated SwGTs/AGTs and 33% having not differentiated beyond the PGT-stage by 24 hpi. Figure 3.3 shows a micrograph of an abnormal *B. graminis* germling that, by 24 hpi, has swollen, hooked but continued to elongate.

Figure 3.2(c) shows a graph of the extent of differentiation of *B. graminis* on 2% water agar over a 24 h time-course. Over the 24 h the majority of germlings had not differentiated beyond producing a SGT. By 24 hpi, 90% of the germling population had SGTs, with 6% having elaborated EGTs and 4% SwGTs. Figure 3.3 shows germlings at 2 and 4 hpi which had produced multiple PGTs. By 8 hpi, abnormal EGTs and SwGTs could be seen (Figure 3.3).

3.2.1.2 Germination and differentiation of Magnaporthe grisea Guy11 and Δpmk1 on barley epidermis and cellulose membrane

Figure 3.4 shows the germination profiles of *M. grisea* isolate Guy11 and MAP kinase mutant Δ*pmk1* on barley epidermal peels and cellulose membrane over a 24 h time-course. Table 3.2 gives the P-values comparing the significance of differences in germination between Guy11 and Δ*pmk1* on barley epidermal peels and Guy11 on barley epidermal peels and Guy11 on cellulose membrane. Figure 3.4 and Table 3.2 show that there was little difference in the levels of germination of Guy11 and Δ*pmk1* on barley epidermal peels over the 24 h. However, Table 3.2 shows that the differences in level of germination are different for the two populations at 2 and 12 hpi. The germination profiles of *M. grisea* isolate Guy11 and MAP kinase mutant Δ*pmk1* on barley epidermal peels over the first 12 hours of the time-course are considerably different to the profiles on cellulose

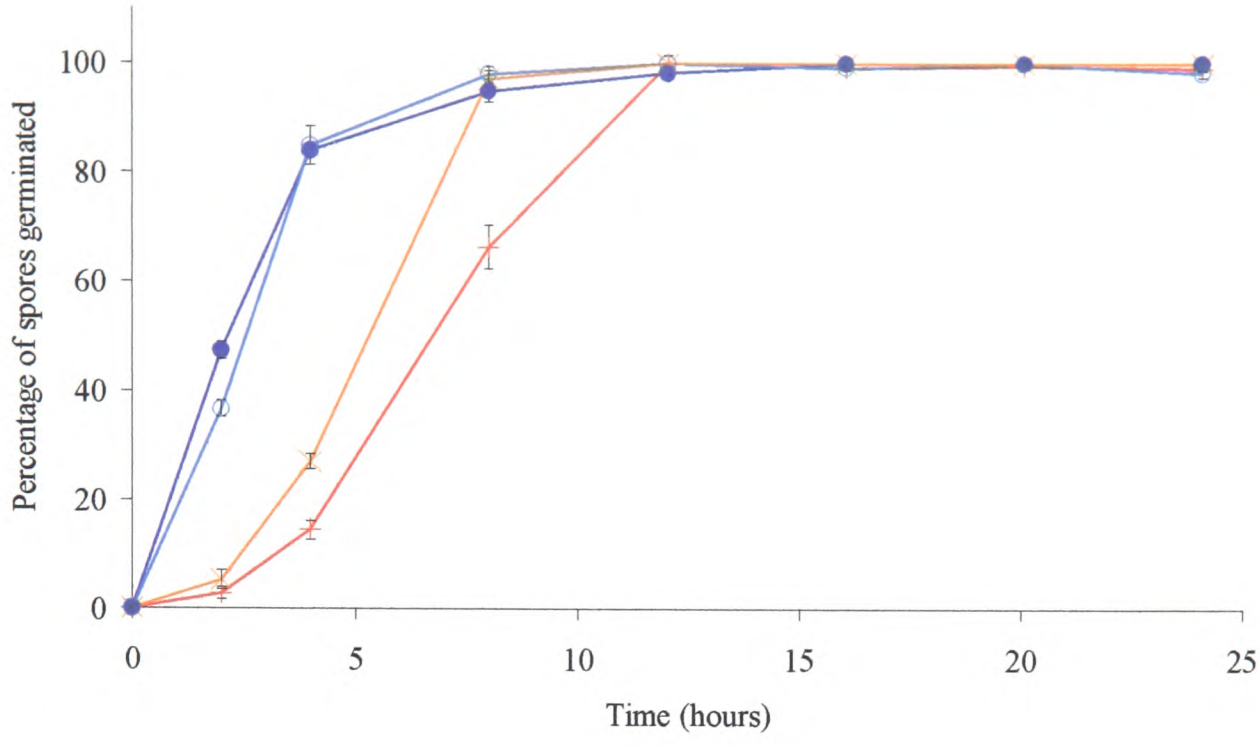


Figure 3.4. Time-course of germination of *Magnaporthe grisea* wild-type strain Guy11 and mitogen-activated protein (MAP) kinase mutant Δ*pmk1* on barley epidermal peels and hydrated cellulose membrane. ● corresponds to Guy11 and ○ corresponds to Δ*pmk1* on epidermal peels, + corresponds to Guy11 and × to Δ*pmk1* on cellulose membrane. For each time point, 6 x 50 conidia were scored for germination. The mean ± standard error is shown.

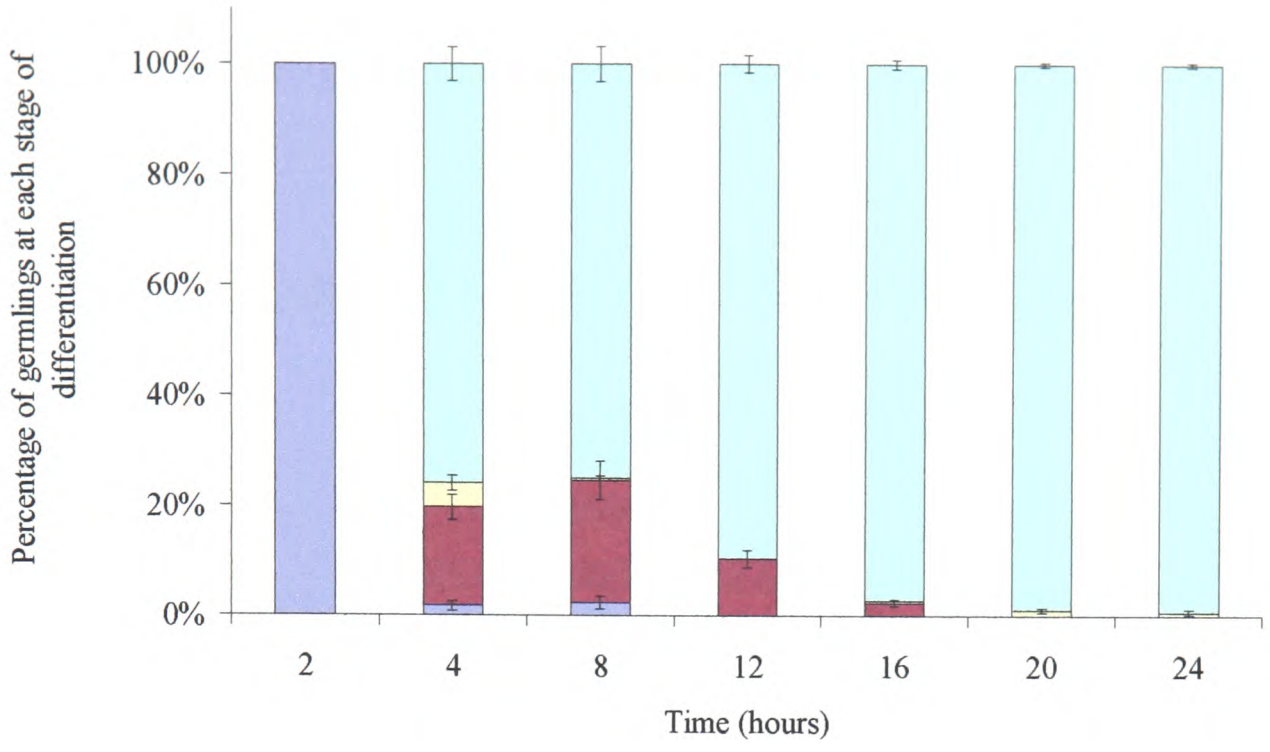
	Time (hpi) 2	4	8	12	16	20	24
Guy11 on Ep v. Δ*pmk1* on Ep	0.001**	0.851	0.133	0.012*	1.000	1.000	0.153
Guy11 on Cm v. Δ*pmk1* on Cm	0.406	0.000***	0.000***	1.000	1.000	0.314	0.713
Guy11 on Ep v. Guy11 on Cm	0.000***	0.000***	0.000***	0.022*	0.145	0.341	0.145

Table 3.2. P-values comparing the significance of differences in germination between *Magnaporthe grisea* wild-type Guy11 and mitogen-activated protein (MAP) kinase mutant Δ*pmk1* on barley epidermal peels (Ep), Guy11 and Δ*pmk1* on cellulose membrane (Cm), and Guy11 on barley epidermal peels and Guy11 on cellulose membrane. For each time point and surface, 6 x 50 conidia were scored for germination. * indicates P≤0.05, ** indicates P≤0.01 and *** indicates P≤0.000.

membrane. Table 3.2 shows that the differences in germination levels between Guy11 on epidermal peels and Guy11 on cellulose membrane were significant up to 12 hpi, but non-significant for the rest of the time-course. Specifically, by 2 hpi, only a mean of 2% of Guy11 and 6% of Δ*pmk1* conidia had germinated on cellulose membrane, respectively, compared to means of 47% and 37% for Guy11 and Δ*pmk1* on barley epidermal peels, respectively. By 4 hpi, the difference in germination levels between Guy11 and Δ*pmk1* on the two surfaces was even larger, with means of 14% and 28% of Guy11 and Δ*pmk1* conidia germinating on cellulose membrane, respectively, compared to a mean of 82% for Guy11 and Δ*pmk1* conidia on epidermal peels. However, by 8 hpi, Guy11 conidia on barley epidermal peels and Δ*pmk1* conidia on epidermal peels and cellulose membrane had almost 100% germination, whereas Guy11 conidia on cellulose membrane had a germination level of only 55%. By 12 hpi, all populations had almost 100% germination on both surfaces.

Figure 3.5 shows graphs of the extent of differentiation of *M. grisea* isolate Guy11 (Figure 3.5(a)) and, mutant Δ*pmk1* (Figure 3.5(b)) on epidermal peels over the 24 h time-course. Figure 3.6 shows micrographs of Guy11 and Δ*pmk1* on barley epidermal peels at 2, 4, 8, 12 and 24 hpi. At 2 hpi, both Guy11 and Δ*pmk1* germlings had not differentiated beyond the GT stage. By 4 hpi, however, 76% of the Guy11 population had differentiated AGTs, with 18% having differentiated EGTs. In contrast, by 4 hpi, the majority, that is 55%, of the Δ*pmk1* population had only differentiated EGTs, with 38% having differentiated SwGTs. By 12 hpi, all Guy11 germlings had differentiated either an EGT or an AGT with around 99% of the germling population having differentiated AGTs by 20 hpi. Additionally, Figure 3.6 shows that at 12 hpi, Guy11 germlings had produced infection hyphae within the barley epidermal cells, whereas Δ*pmk1* germlings had produced highly elongated, but swollen germ tubes. By 20 hpi, 99% of the Δ*pmk1* germling population had differentiated SwGTs. Figure 3.6 shows that at 24 hpi, Guy11 had produced branching hyphae within the barley epidermal cells, whereas Δ*pmk1* had not penetrated the epidermal cells, but had produced elongating hyphae across the surface of the plant tissue.

a)



b)

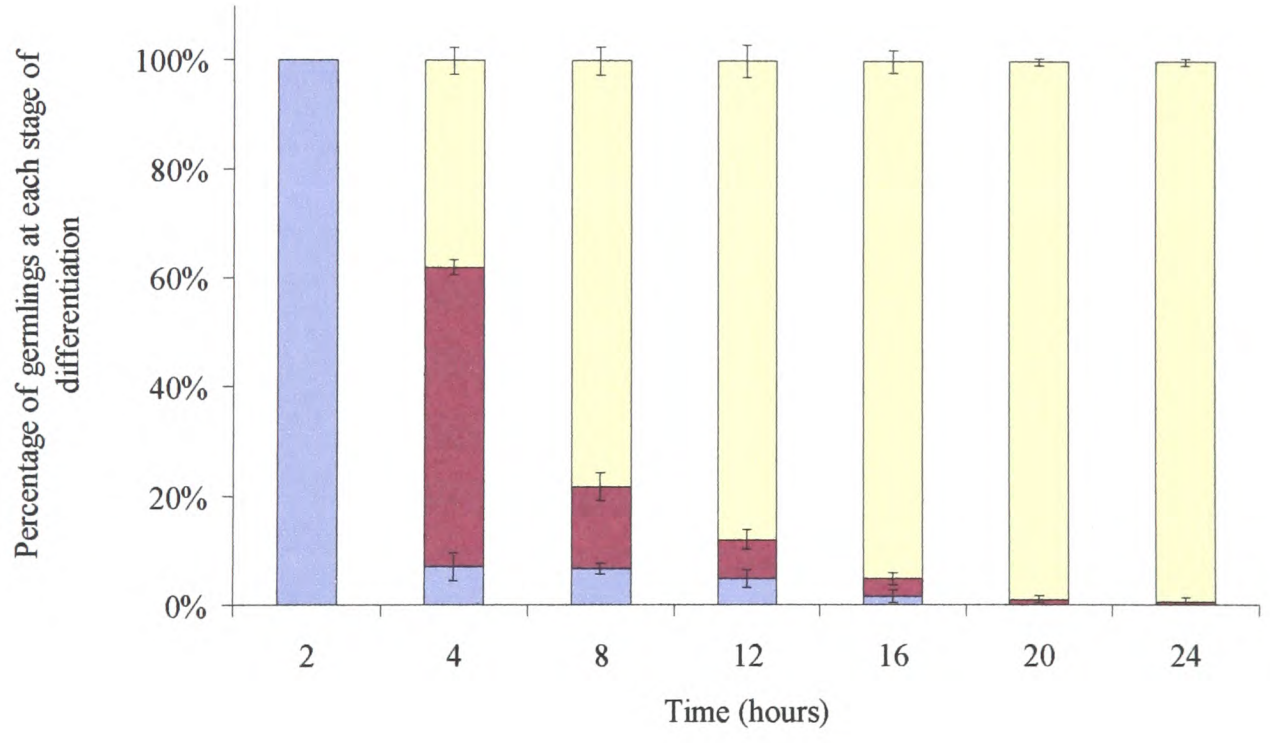


Figure 3.5. Time-courses of differentiation of *Magnaporthe grisea* (a) wild-type Guy11 and (b) mitogen-activated protein (MAP) kinase mutant Δ*pmk1* on barley epidermal peels. ■ corresponds to germlings with germ tubes, ■ corresponds to germlings having differentiated elongated germ tubes, corresponds to germlings having differentiated swollen germ tubes and corresponds to differentiation of an appressorium. In each experiment, 6 x 50 conidia were scored for extent of differentiation and the mean values of 50 conidia are illustrated. The mean percentage differentiation ± standard error is shown.

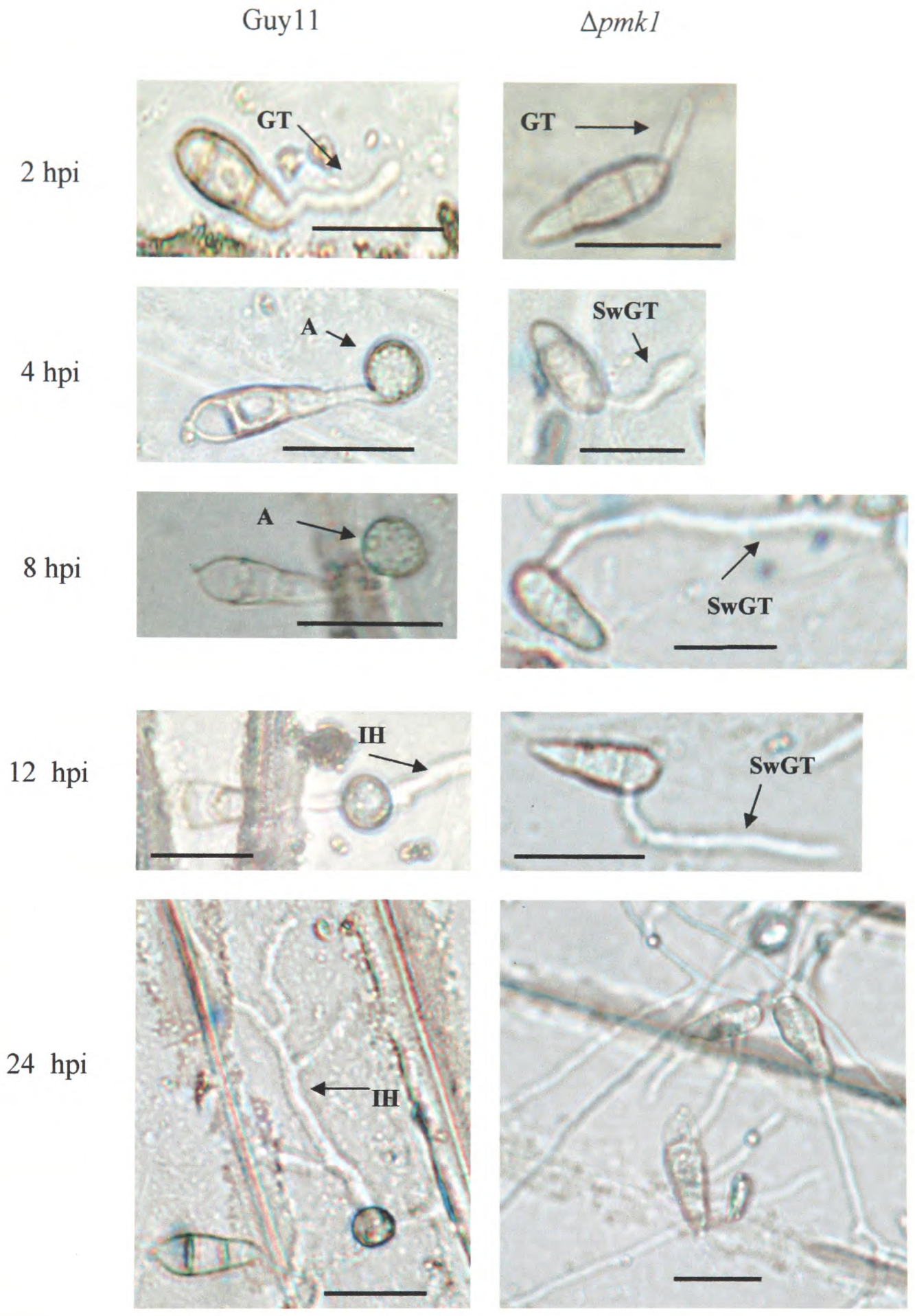


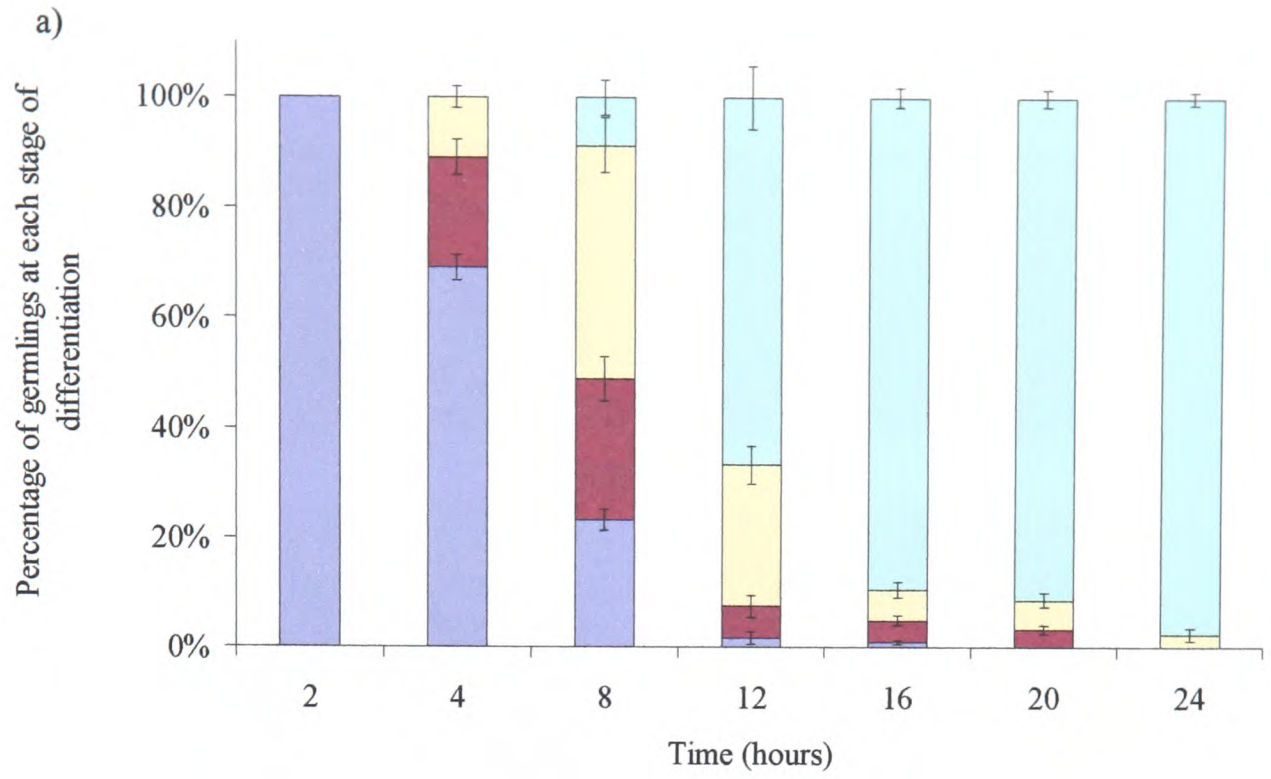
Figure 3.6. Light micrographs of *Magnaporthe grisea* wild-type Guy11 and mitogen-activated protein (MAP) kinase mutant Δ*pmk1* on barley epidermal peels 2, 4, 8, 12 and 24 hours post inoculation (hpi). Arrows indicate germ tubes (GT), elongated germ tubes (EGT), swollen germ tubes (SwGT), appressoria (A) and infection hypha (IH). The bars indicates a length of 20 μm. Magnification x400.

Figure 3.7 shows graphs of the extent of differentiation of *M. grisea* isolate Guy11 (Figure 3.7(a)) and, mutant Δ*pmk1* (Figure 3.7(b)) on hydrated cellulose membrane over a 24 h time-course. Figure 3.8 shows micrographs of Guy11 and Δ*pmk1* on cellulose membrane at 4, 8 and 12 hpi. By 2 hpi, the Guy11 and Δ*pmk1* populations had not differentiated beyond the GT stage. However, by 4 hpi, the Guy11 population had elaborated some (5%) SwGTs (Figure 3.8) and 19% of the Δ*pmk1* population had differentiated EGTs. By 8 hpi, within the Guy11 population, AGTs had begun to develop, with the majority of the population (43%) having elaborated SwGTs. By 8 hpi, 97% of the Δ*pmk1* population had differentiated EGTs, with 99% having EGTs by 12 hpi. Beyond 12 hpi the Guy11 population was still differentiating AGTs with 97% of the population having differentiated AGTs. Figure 3.8 shows a Guy11 germling at 12 hpi that had elaborated an appressoria typical of those seen on cellulose membrane. Compared to the typical round, dome-shaped appressoria produced on barley epidermal peels (Figure 3.6), the appressoria produced on cellulose membrane were distorted.

3.2.2 Surface hydrophobicity

Infection structure differentiation in *B. graminis* and *M. grisea* is promoted by several features, one of which is surface hydrophobicity (Carver *et al.*, 1996; Lee and Dean, 1994). A method for determining the relative hydrophobicity of a surface is to measure the contact angle a droplet of water makes with the surface. If the surface is hydrophobic, then a high contact angle will be obtained, conversely, if the contact angle is low, then the surface is hydrophilic.

To determine the hydrophobicities of the surfaces used herein, a goniometer was employed (see section *2.3.1.4*) to measure the contact angles of 0.6 µl droplets of sterile distilled water (SDW) applied to barley epidermal peels, hydrated cellulose membrane and 2% water agar (Holloway, 1970). Ten replicate measurements were made per surface.



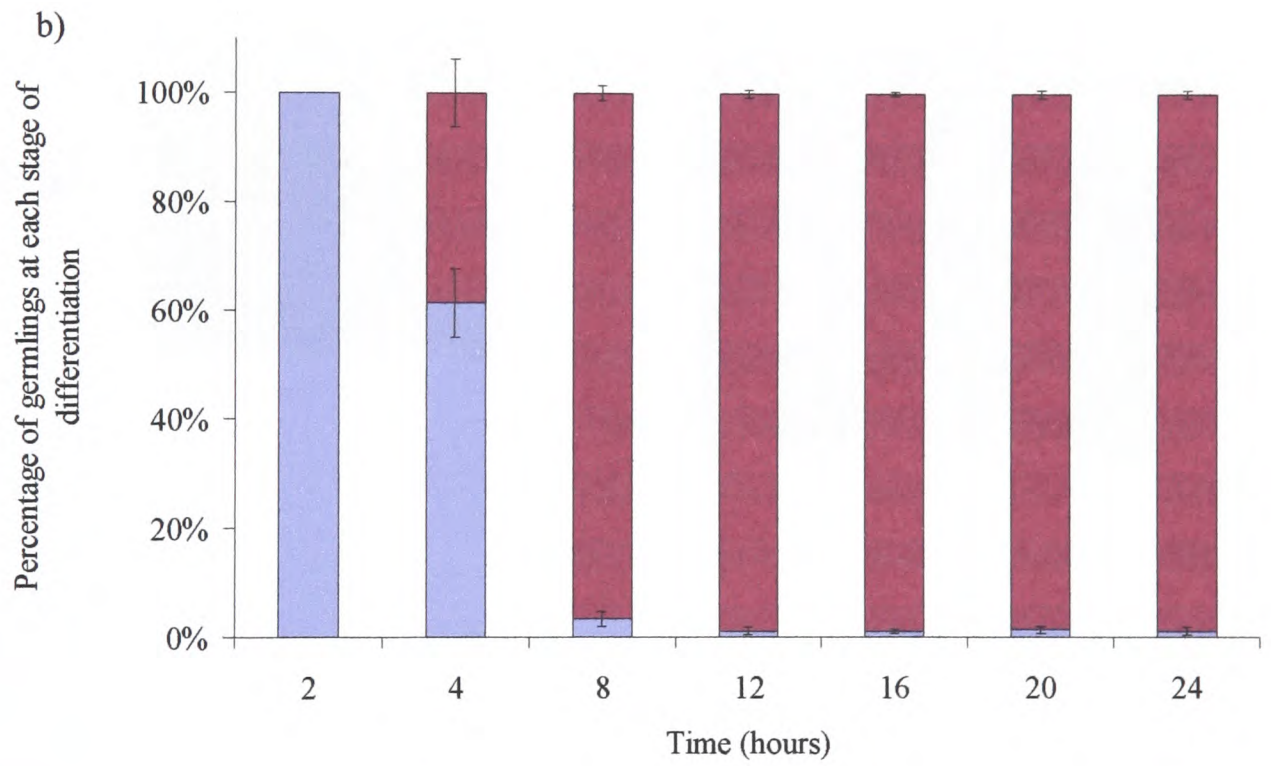


Figure 3.7. Time-courses of differentiation of *Magnaporthe grisea* (a) wild-type Guy11 and (b) mitogen-activated protein (MAP) kinase mutant Δ*pmk1* on hydrated cellulose membrane. ■ corresponds to germlings with germ tubes, ■ corresponds to germlings having differentiated elongated germ tubes, ■ corresponds to germlings having differentiated swollen germ tubes and ■ corresponds to differentiation of an appressorium. In each experiment, 6 x 50 conidia were scored for extent of differentiation and the mean values of 50 conidia are illustrated. The mean percentage differentiation ± standard error is shown.

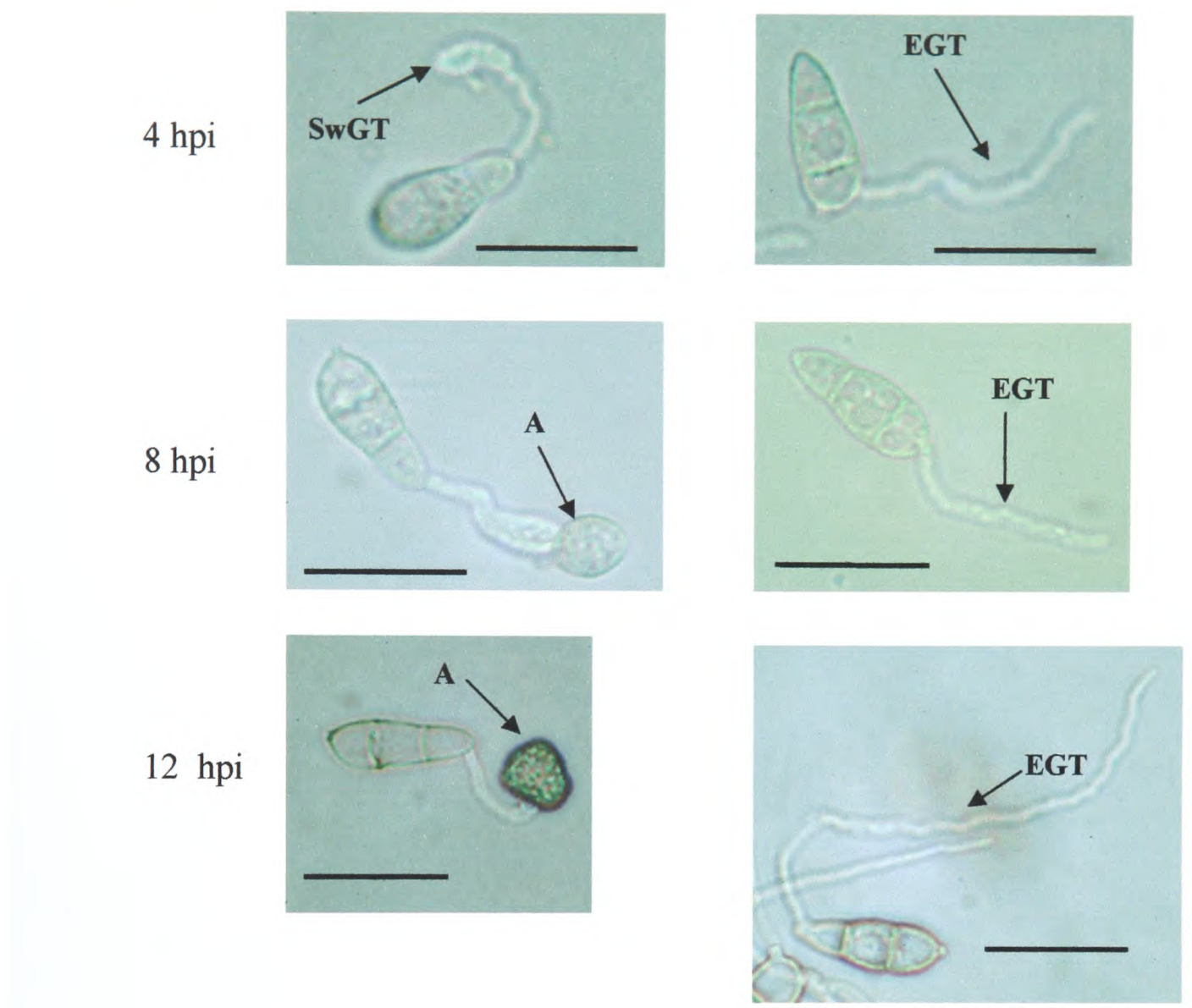


Figure 3.8. Light micrographs of *Magnaporthe grisea* wild-type Guy11 and mitogen-activated protein (MAP) kinase mutant Δ*pmk1* on hydrated cellulose membrane 4, 8 and 12 hours post inoculation (hpi). Arrows indicate elongated germ tubes (EGT), swollen germ tubes (SwGT) and appressoria (A). The bars indicate a length of 20 μm. Magnification x400.

Barley epidermal peels gave the largest contact angle of 141°± a standard error of 10, followed by cellulose membrane with a contact angle of 14°±1 and 2% water agar with an angle of 11°±1 meaning that barley epidermal peels are hydrophobic, whereas cellulose membrane is hydrophilic, with water agar being slightly more hydrophilic than cellulose membrane.

3.3 DISCUSSION

This chapter has described the germination and differentiation of *B. graminis* f.sp. *hordei* and *Magnaporthe grisea* on the barley epidermal surface and artificial surfaces, including cellulose membrane and 2% (w/v) water agar. *B. graminis* development on these surfaces has been described previously (Carver and Ingerson, 1987; Carver *et al.*, 1996; Hall, 1999; Hall *et al.*, 1999). However, this work was undertaken in order to define the parameters of germling development on the surfaces for later work.

3.3.1 *Blumeria graminis* f.sp. *hordei* development on host barley epidermis and on the artificial surfaces of cellulose membrane and 2% water agar

3.3.1.1 Stages of infection structure development

Previous work (Carver and Ingerson, 1987; Carver *et al.*, 1996; Hall, 1999) has demonstrated that *B. graminis* f.sp. *hordei* infection structure differentiation can be broken down into several key stages, each requiring signal perception: 1) conidial germination, 2) PGT differentiation 3) elongation of a subsequent-formed germ tube, 4) swelling of the appressorium and 5) hooking of the appressorium. In this study, these key stages were used to classify the extent of differentiation of *B. graminis* thoughout time-courses on barley epidermal peels, hydrated cellulose membrane and 2% (w/v) water agar. Thus, conidia were classed as having germinated on the emergence of a germ tube from the conidium. Subsequent stages of differentiation were classed as the "elongated germ tube" (EGT) stage, the "swollen germ tube" (SwGT) stage and the "appressorial germ tube" (AGT) stage. However, first-formed germ tubes on water agar were classed as "short germ tubes" (SGTs). It is the SGT that differentiates into the PGT following contact with an inductive surface, such as leaf epidermis, a hydrophobic surface, or cellulose membrane, but not following contact with non-inductive surfaces such as glass or agar (Carver *et al.*, 1996; Hall, 1999). If the first formed tube fails to contact an inductive surface, or if it fails to recognize contact, the germ tube becomes redundant and remains short (Carver and Ingerson, 1987; Carver *et al.*, 1999).

3.3.1.2 Germination

In agreement with Hall (1999), germination of *B. graminis* was highest on the barley epidermal surface, compared to cellulose membrane and 2% water agar. However, levels of germination in this study were higher than those obtained by Hall (1999) on all three surfaces by 24 hpi. This may be accounted for by differences in the method of preparation of the surfaces and the incubation conditions of *B. graminis*. Carver and Ingerson (1987) reported that surface contact is not required for a minority of the *B. graminis* conidial population to germinate, as demonstrated through observations of conidia germinating on spiders' threads. Carver and Ingerson (1987) hypothesised that the release from the conidiophore could be a signal to the conidia to germinate. However, although this may be sufficient to allow germination in about 20% of the conidia, additional signals promote germination in a larger proportion of the population. Multiple germ tubes were observed on the water agar surface. Indeed, conidia may form several subsidiary germ tubes until one makes contact with an inductive surface and triggers differentiation of a PGT (Green *et al.*, 1999).

3.3.1.3 Differentiation

As expected from Carver and Ingerson's work (1987) and that of Hall (1999) barley epidermal peels promoted high levels of infection structure differentiation whereas 2% water agar was non-inductive to *B. graminis* development, with 96% of the population having not progressed beyond the SGT stage after 24 hpi. Indeed, contact of the PGT with an inductive surface, such as leaf epidermis or a hydrophobic surface, is required to promote elongation of the second-formed germ tube (Carver and Ingerson, 1987).

In *B. graminis*, elongation of the second-formed germ tube is a pre-requisite to the differentiation of appressorial lobes, with elongation being dependent upon PGT contact. However, if water agar does not induce PGT formation, then why were EGTs and SwGTs observed on water agar in the time-courses in this work? This could be explained by using a "threshold-theory" of signal perception, put forward by Hall (1999). Specifically, a population of conidia is heterogeneous (Gay *et al.*,

1985) so that at one extreme a sub-population may require little additional stimulus to differentiate, whereas at the other extreme, a sub-population may require a more extensive set of signals. Each signal, *i.e.* physical or chemical properties, may nudge the germling closer to the threshold, but each signal alone may be sufficient to trigger differentiation in only a sub-population of germlings. Thus, the signals could act to reinforce one another, and the summation of the signals may push the majority of the germlings beyond the threshold. On the leaf surface, the full set of signals required for differentiation would be available and so the majority of the population differentiate, whereas on artificial surfaces only a sub-set of the signals is present, so lower levels of differentiation are observed.

Also in agreement with Hall (1999), differentiation occurs over a longer period on cellulose membrane as compared to epidermal peels. However, higher levels of differentiation were identified on cellulose membrane and 2% water agar than those reported by Hall (1999). Although levels of differentiation were lower on cellulose membrane than those reported by Kobayashi *et al.* (1991). Such variations may be accounted for by differences in the method of preparation of the surfaces and the incubation conditions of *B. graminis*.

In the course of this work, it was noted that true, hooked AGTs are often difficult to distinguish from SwGTs on cellulose membrane. The majority of germlings with swollen germ tubes appear not to be hooked, but close inspection of a few apparent SwGT germlings revealed that they could also be classed as AGT-stage germlings, but they do not appear as distinct as on epidermal peels. Thus, for subsequent chapters, germlings that have differentiated SwGTs and/or AGTs on cellulose membrane will be counted together in a SwGT/AGT category.

3.3.2 *Magnaporthe grisea* development on host barley epidermis and on the artificial surface of cellulose membrane

Whereas *B. graminis* f.sp. *hordei* is only able to infect barley, *M. grisea* causes disease of over 50 species of the grass (Poaceae) family including barley, wheat, rice and millet (Valent, 1990). Thus, barley has been adopted in this work to study

the development of *M. grisea.* Indeed, barley is often used as an experimental host for *M. grisea* when testing strains for pathogenicity to leaves (Sweigard *et al.*, 1998). In addition, a number of artificial surfaces which induce appressorium formation have been used in studies of *M. grisea* (Lee and Dean, 1994).

3.3.2.1 Stages of infection structure development

In this study, as with *B. graminis*, prominent stages of *M. grisea* infection structure development were identified in order to classify the extent of differentiation on the barley epidermal surface and cellulose membrane. In *M. grisea* differentiation, the first stage after the adherence of a spore to a surface is the production of a germ tube (GT), which normally emerges from one of the terminal cells of the three-celled spore (Talbot, 1995). Production of a germ tube is a non-contact-mediated process as conidia will also germinate in suspension (Xiao *et al.*, 1994b). Following germination, the germ tube elongates through apical extension. In this study, an "elongated germ tube" (EGT) was taken as being a germ tube that had not swollen, but was longer than a "typical" GT. After around 4 h, the germ tube stops growing at the tip and a terminal "hooking" of the hypha appears, which marks the beginning of cellular differentiation and thus appressorial development (Talbot, 1995). The initial steps in appressorial formation are the swelling of the tip of the germ tube, denoted in this study as the "swollen germ tube" (SwGT) stage. Following the formation of a septum, the cell wall of the nascent appressorium begins to thicken through the addition of a melanin layer, producing the appressorium.

3.3.2.2 Germination

In *M. grisea*, conidial germination appears to be independent of the nature of the surface inoculated, as high levels of germination are observed on both solid and liquid surfaces (Xiao *et al.*, 1994b) and germination is independent of surface hydrophobicity (Lee and Dean, 1994). In corroboration of this, the highly hydrophobic barley epidermal surface and the hydrophilic surface of hydrated cellulose membrane promoted high levels of germination in this study. However,

germination levels on cellulose membrane were lower than those on barley epidermal peels in the first 8 h of the time-course.

The *M. grisea* MAP kinase mutant, Δ*pmk1*, produces normal mycelia and conidia, but fails to form appressoria and cannot grow invasively in rice plants, even through wound sites (Xu and Hamer, 1996). The results herein show that there is no difference in germination of Δ*pmk1* on barley epidermis when compared to the wild-type, Guy11. Moreover, germination levels of Δ*pmk1* on cellulose membrane were initially higher than those of Guy11. Indeed, Xu and Hamer (1996) revealed that Δ*pmk1* mutants germinate on artificial surfaces as efficiently as wild-type conidia since *M. grisea PMK1* is not involved in the regulation of germination (Xu and Hamer, 1996).

3.3.2.3 Differentiation

In contrast to germination in *M. grisea*, appressorium formation requires prior surface recognition (Talbot, 1995). In general, recognition of the host surface occurs through perception of physical and/or chemical signals (Hoch and Staples, 1991), where physical features include surface hardness, surface hydrophobicity and specific recognition of topographical features. Chemical signals include components of the host cuticle such as wax or cutin, or the products of their degradation. However, the physical and chemical stimuli appear to have redundant roles, as either one alone is sufficient to induce appressorial differentiation (Gilbert, 1996). Indeed, Lee and Dean (1993) showed that hydrophobic surfaces are sufficient for the induction of appressorium in *M. grisea*, with appressorium formation being strongly correlated to the degree of surface hydrophobicity, and with wax paper being the most inductive surface. In the absence of additional signals, the default developmental pathway of germinated *M. grisea* conidia is germ tube elongation (Lee and Dean, 1993; Gilbert *et al.*, 1996). Once appressorial differentiation is initiated in the elongating germ tube, no further signals appear to be necessary for the differentiation programme to reach completion.

In this study, the barley epidermal surface promoted *M. grisea* Guy11 appressorium formation, and Δ*pmk1* SwGT formation, within 4 h. Hydrophobicity studies revealed that the barley epidermal surface has a high hydrophobicity, but lower than that of rice (Talbot, 1995), which has one of the most hydrophobic surfaces of all plants, with a water contact angle of up to 170°. Nevertheless, barley epidermis has a high hydrophobicity when compared to other plant surfaces, such as broad-bean leaves, the contact angles of which are 29-60° (Talbot, 1995). Moreover, Teflon®, an artificial surface widely used to study the infection structure development of *M. grisea*, has a contact angle of between 90-130°, compared with the barley epidermal surface, which has a contact angle of 140° (Talbot, 1995).

In comparison to the barley epidermal surface, cellulose membrane did not invoke *M. grisea* Guy11 appressorium differentiation as rapidly, with a small proportion of appressoria appearing after only 8 h, and the majority appearing after 12 h. Even so, the ability of this artificial surface to invoke appressorium differentiation, even though hydrophilic, indicates that it will be a useful tool in later experiments. However, the appressoria produced on cellulose membrane appeared distorted and were not typical of the round, dome-shaped appressoria produce on epidermal peels. On rice leaves, *M. grisea* appressoria stick using a thick layer of adhesive material that partially infiltrates the underlying rice cuticle. The appressoria then inflate to full size (Talbot, 1995). An explanation for the distorted appressoria on cellulose membrane could be that the hydrophilicity of this surface does not allow proper adherence of the appressoria to the surface, so that on inflation, its round shape cannot be maintained.

Whereas the barley epidermal surface was able to invoke SwGTs in the Δ*pmk1* mutant germlings, germlings on cellulose membrane were only able to elaborate undifferentiated hyphae, that is, EGTs. Xu and Hamer (1996) established that Δ*pmk1* mutants are able to recognise hydrophobic surfaces and form subapical swollen bodies, but fail to arrest the germ tube tip growth and form appressoria on Teflon® membranes or onion epidermal cells. Moreover, whereas the majority of

both Guy11 and Δ*pmk1* germlings form undifferentiated hyphae on hydrophilic surfaces, Xu and Hamer (1996) reported that on the addition of exogenous cAMP, Guy11 germlings were able to form appressoria and in Δ*pmk1* mutants the level of germ tube hooking and swelling was elevated. Therefore, Δ*pmk1* mutants can respond to both thigmotrophic surface signals and a cAMP inducible signal (Xu and Hamer, 1996). However, in this study, the hydrophilic surface of cellulose membrane did not appear to impart the signals for germ tube differentiation in Δ*pmk1*.

3.3.3 *Blumeria graminis* f.sp. *hordei* infection structure development versus *Magnaporthe grisea* infection structure development

Comparison of infection structure development of *B. graminis* and *M. grisea* reveals a number of differences in their infection strategies. Consideration of germination reveals that both fungi reach peak levels of germination by around 12 hpi. However, on epidermal peels, *B. graminis* did not reach a germination level of higher than 80%, and levels were even lower on cellulose membrane and water agar. In contrast, regardless of the surface, *M. grisea* reached germination levels of almost 100%.

Comparison of differentiation processes reveals that *M. grisea* was able to form appressoria much faster than *B. graminis*, that is, appressoria were formed by 4 hpi and 8 hpi, respectively. Moreover, by 24 hpi on barley epidermal peels, only 87% of *B. graminis* germlings had differentiated appressoria compared to almost 100% of *M. grisea* germlings. Additionally, by 12 hpi, *M. grisea* infection hyphae could be seen in barley epidermal cells, whereas *B. graminis*, being an obligate biotroph, cannot penetrate the dead barley epidermal cells of the epidermal strips.

3.3.4 Summary

The work in this Chapter has defined the parameters of *B. graminis* f.sp. *hordei*, *M. grisea* strain Guy11 and *M. grisea* MAP kinase mutant Δ*pmk1* development on a range of surfaces to be employed in experiments in subsequent chapters. Cellulose membrane provides a surface that is inductive to *M. grisea* appressoria,

but only semi-inductive to *B. graminis*. Time-courses have shown that barley epidermal peels provide a good experimental surface for the study of infection structure differentiation in *B. graminis* and *M. grisea*, with both elaborating appressoria.

CHAPTER 4
THE ROLE OF PROTEIN KINASE C IN THE EARLY DEVELOPMENT OF *BLUMERIA GRAMINIS* F.SP. *HORDEI*

4.1 INTRODUCTION

4.1.1 Protein kinase C

The discovery of protein kinase C (PKC) by Nishizuka and co-workers in 1977 represented a major breakthrough in the understanding of signal transduction in mammals (Takai *et al.*, 1977). PKC comprises a large family of serine-threonine kinases activated by extracellular signals which play a pivotal role in a wide variety of signal transduction events. In mammalian systems, PKC has been found in all cells and tissues examined and, to date, 12 distinct isoforms have been identified. Several non-mammalian isoforms have been described (Nishizuka, 1995; Mellor and Parker, 1998; Toker, 1998). The PKC isoforms have been grouped into three subclasses according to their primary sequence similarities and regulatory properties, which are conferred by specific domains in the protein (Ron and Kazanietz, 1999). Initially, PKC was defined as a calcium and phospholipid activated protein kinase and it is this description that defines the "classical" PKCs (cPKCs), which include the alpha, beta, beta-variant and gamma isozymes. In addition, cPKCs bind to, and are activated by the endogenous PKC activator, diacylglycerol (DAG), which increases the specificity of the enzyme for phosphatidylserine and also increases the affinity of the enzyme for calcium (Ca^{2+}). The "novel" PKCs (nPKCs: delta, epsilon, eta and theta) respond to DAG and are Ca^{2+} independent. The "atypical" PKCs (aPKCs: zeta, iota and lambda) are related to the others by sequence, but are not readily activated by DAG or Ca^{2+}, though still require phosphatidylserine (PS) as a cofactor. In addition, PKCmu (Johannes *et al.*, 1994; Valvarde *et al.*, 1994) and the more distantly related PKC-related kinases, PKN, have been described.

4.1.2 PKC structure

PKCs are multi-domain proteins which have, in common, a conserved catalytic region carboxy terminal to a regulatory domain, connected by a labile "hinge" region. In the absence of activating cofactors (Ca^{2+}, phospholipids, DAG, phorbol esters) the regulatory domain inhibits the kinase activity of the catalytic domain. This inhibition is exerted by the "pseudosubstrate domain", a moderately conserved sequence motif which resembles a consensus phosphorylation site in PKC substrates, but which has an alanine residue in place of the phosphorylatable serine/threonine residue (Hardie, 1988; Gschwendt *et al.*, 1991; Kemp and Pearson, 1991). The pseudosubstrate domain serves as an allosteric autoinhibitor, binding to the substrate-binding cavity in the catalytic domain. Activation of the enzyme occurs on the release of the pseudosubstrate from the kinase core (Orr *et al.*, 1992).

Common to all PKC isozymes is the C1 domain located within the regulatory region. This is a cysteine-rich region of approximately 50 residues that forms a ligand (DAG and phorbol ester) binding pocket. In cPKCs and nPKCs C1 is present as a tandem repeat, and as a single domain in aPKCs (Hurley *et al.*, 1997). However, in aPKCs, one face of the ligand-binding pocket is compromised and consequently the module cannot bind either phorbol esters or DAG (Mott *et al.*, 1996). Ligand binding does not result in conformational change in the domain, rather the ligands cap the hydrophilic ligand-binding pocket creating a hydrophobic surface to recruit PKC to membranes (Zhang *et al.*, 1995).

The C2 domain is an independent membrane-targeting module found in cPKCs, nPKCs, and in a large number of proteins unrelated to PKC (reviewed in Nalefski and Falke, 1996). In cPKCs it is found immediately carboxy-terminal to the C1 domain and is the binding site for Ca^{2+}; however, nPKC C2 domains do not bind Ca^{2+} due to a lack of a key aspartic acid residue that is required to coordinate Ca^{2+} binding (Pappa *et al.*, 1998). Ca^{2+} bound to the cPKC C2 domain interacts allosterically with phospholipids, dramatically increasing the affinity of PKC for

membranes. In nPKCs, however, the function of the C2 domain remains elusive. One hypothesis is that it controls the spatial distribution of PKC via protein-protein interactions (reviewed in Newton, 2001).

The C3 and C4 domains together comprise the catalytic domain. The C3 domain possesses a highly conserved binding site for ATP, the phosphate donor for phosphotransferase activity. The C4 domain contains the site for substrate binding. In addition, it is within the catalytic site that a series of ordered phosphorylations are required so that the enzyme gains catalytic competence and correct intracellular localisation (Keranen *et al.*, 1995; Tsutakawa *et al*, 1995).

Another prerequisite for PKC activation is the binding of cofactors of which there are three "classical" activators: phosphatidylserine (PS), Ca^{2+} and DAG. The activity of all isozymes of PKC is regulated by PS, an aminophospholipid found exclusively on the cytoplasmic leaflet of membranes (Newton, 1993). However, in the absence of DAG, PS displays little selectivity for PKC. In the presence of DAG, PKC binds to PS with an order of magnitude higher affinity than membranes composed of other anionic lipids (reviewed in Newton, 2001).

Phorbol esters and DAG cause a dramatic increase in the affinity of PKCs for membranes by binding to a hydrophilic site in the C1 domain. This allows the formation of a contiguous hydrophobic region that promotes insertion of the domain into the lipid bilayer (Zhang *et al.*, 1995), thus enhancing the activity of the enzyme.

4.1.3 PKC and fungi

Signal transduction pathways in higher eukaryotic systems rely on an array of PKC isozymes for a wide range of growth and differentiation processes. In contrast, fungal systems appear to generally be equipped with one or a few members of the PKC family. For example, within the yeasts, *Saccharomyces cerevisiae* possesses only one member of the PKC family, encoded by *PKC1* (Levin *et al.*, 1990); *Schizosaccharomyces pombe* carries two PKC-encoding

sequences (Toda *et al.*, 1993); and one PKC gene has been described in *Candida albicans* (Paravicini *et al.*, 1996).

PKC genes have been identified in the Euoascomycete fungi *Neurospora crassa* (Oved and Yarden, 1996), *Trichoderma reesei* and *Aspergillus niger* (Morawetz *et al.*, 1996), *C. albicans* (Paravicini *et al.*, 1996), *Cochliobolus heterotrophus* (Oeser, 1998), *Tuber borchii* and *Tuber magnatum* (Ambra and Macino, 2000), *Magnaporthe grisea* (EMBL accession AAD33693), *Sporothrix schenckii* (Aquino-Pinero and Rodriguez-del Valle, 2002), *Botryotina fuckeliana* (CAB59301) and *Colletotrichum trifolii* (Dickman *et al.*, 1995). All Euoascomycete PKC genes, which have been sequenced to date, align most closely with the mammalian nPKC family. Little is known about the function of the PKCs identified in pathogenic fungi, however, deletion of both endogenous copies of *PKC1* in the diploid *C. albicans* resulted in a cell lysis phenotype suppressed by high osmolarity growth conditions (Paravicini *et al.*, 1996), with PKC1 being implicated in a cellular integrity role. In the alfalfa pathogen, *C. trifolii*, PKC is thought to be involved in spore germination (Dickman *et al.*, 1995). The function of *C. heterotrophus PKC1* is unknown (Oeser, 1998).

4.1.4 Objectives

This chapter describes the identification and characterisation of two *Blumeria graminis* f.sp *hordei pkc* genes, named *pkc*1 and *pkc*-like, and the subsequent detection of PKC activity in *B. graminis* protein extracts. The potential involvement of PKC in the early development of *B. graminis* was investigated by observing the effects of PKC agonists and antagonists on germling differentiation. Furthermore, the transcript profiles of *pkc*1 and *pkc*-like at critical stages of *B. graminis* germling morphogenesis were determined using real-time PCR.

4.2 RESULTS

4.2.1 Identification of *pkc*1 and *pkc*-like genes in *Blumeria graminis* f.sp. *hordei*

Two partial *B. graminis* f.sp. *hordei* PKC gene sequences were obtained by Ziguo Zhang (University of Oxford) by designing degenerate primers to conserved domains (ATP-binding and kinase domains) of 27 aligned eukaryotic 'PKC' peptide sequences. Fragments derived from PCR amplification of cDNA species from the AGT stage of germling morphogenesis were subcloned and sequenced, and the full-length genomic sequences of two genes, designated *pkc*1 (Accession number AF247001) and *pkc*-like (AF283107), were obtained using 'Step down' PCR (all performed by Z. Zhang), a walking technique described by Zhang and Gurr (2000). Southern analysis revealed both *pkc*1 and *pkc*-like genes to be present as single copies within *B. graminis* (performed by Z. Zhang).

*B. graminis pkc*1 has an open reading frame of 3471 base pairs (bp), six introns of 47-51 bp length with consensus 5'GT/3'AG splice sites and a putative splice sequence ($TG_{/T}CTA_{/T}AT_{/A}$) within 8-13 bp of the 3' end (Gurr *et al.*, 1987). The amino acid sequence of *B. graminis pkc*1 (Figure 4.1) was deduced from the full-length genomic clone and subjected to BLAST (Altschul *et al.*, 1997) and 'Prosite ProfileScan' (Bioinformatics Group of Swiss Institute for Experimental Cancer Research, Switzerland) searches. The *B. graminis* PKC1 protein has both regulatory and catalytic domains, separated by a hinge region. The regulatory region contains a pseudosubstrate binding site and two cysteine rich repeats, while the catalytic domain contains an ATP binding motif. The carboxy terminus carries a PKC terminal domain whilst the extended amino terminus has two rho-binding domains.

The *B. graminis pkc*-like gene has an open reading frame of 1101 bp with six introns varying in length between 43 and 66 bp. Not all of the introns show the consensus 5'GT/AG splice sequence, this being replaced by a 5'GC/AG sequence. BLAST searches of 800 bp of sequence 5'-to the putative translation start codon

```
MNNDDEALSLVFKKIERERALLNAANQMRQQTQNEQVKARLDTQMREGRRNIQYLEERMQ 60
   rho-binding repeat (3-62)
ELQMRKMGQDMENMNLSPVGTGPGRRASEGYDGRSGPSTPLAKSPRTHIDAGQGTGYGMQ 120
ETGGSQGELMPSRHPFAPPGPSSSLPKRPNYTKLDLIKYDTPFLGPRIQLMLSQIEFKLN 180
                                    * intron1
VEKQYLKGIEKMVQLYAIEGDRKSRADAAGRRIESTQKIQILKQALKRYEDLHIDMESSA 240
rho-binding repeat (167-229)
DAPDDDSINTPNLRKPLTGQLSIRILAVKDVDHATTSRFARGPETFVTIRVEDNVVARTK 300
    * intron2
ISRNDKWEAEYHNITVDQANEIELIVYDKPTDHPLPMGLLWIRLSDIVEEMRRKRIEAEI 360
NNSGWVSADRMGSGSLPSSAPPQFPLSPSHATFTANPGSVVVAENPALSGSMVASQPIDA 420
WFALEPTGAVQLSINFTKQIKEKRGFDAGLNRKGAIRQRKEEVHEMYGHKFVSQQFYNIM 480

RCALCGDFLKYAGGMQCEDCKYTCHTKCYTSVVTKCISKSNAETDPDEEKINHRIPHRFE 540
    PKC-C1 domain (468-516)                          ←--------WR4
KFSNMSANWCCHCGYILPFGKKNCRKCSECNLTCHAQCVHLIPDFCGMSMAVANVIIDGI 600
       PKC-C1 domain (536-586)
          ←--------WR3     * intron3
RNQKRRQTAQVPSVGQSKQNQSGIPTASLVESFGPGSRASFSQEPHRSTQSGSYGSASSS 660
TGAAEAAKVMYNQGHPSQKRLSAPNPALPSSATAAAAAAMSGTKIPNTRESFSTPPTEYS 720
QAGRSSATNYTGHPSPRTDNNLYNASSVPQSPSQVSYNPAAYAQVSGYPTQPLSPAYVQQ 780
HPLPSKNLYSSEAQNKAPISEPSSSQTPAMTRKAAPQANEPGTGRRIGLDHFNFLAVLGK 840
                                                          DF--
GNFGKVMLAETKSTKKLYAIKVLKKEFIIENDEVESTRSEKRVFLIANKERHPFLTNLHA 900
ATP-binding domain (838-861)
----→  ----------→WF1      --------→WF2
CFQTETRVYFVMEYVSGGDLMLHIQRGQFGTKRAQFYAAEVCLALKYFHENGVIYRDLKL 960
                                  QF------→          ←-------
                                      * intron4
DNILLTLDGHIKMADYGLCKEDMWYGSTTSTFCGTPEFMAPE*ILLDKKYGRSVDWWAFGV
1020
-WR2        ←----------WR1                    intron5     ←------DR
LIYQMLLQQSPFRGEDEDEIYDAILADEPLYPIHMPRDSVSILQKLLTREPEQRLGSGPT 1080
  protein kinase domain (832-1091)
DAQEIMSQPFFSNNNWDDIYHKRIPTPFKPSIKDETDTSNFDSEFTSVTPVLTPVQSVLT 1140
                                                          *

intron5
QAMQEEFRGFSYSTDAI
```

Figure 4.1. Amino acid sequence of *Blumeria graminis* f.sp. *hordei* PKC1 (EMBL accession no. AF247001). The degenerate primers for the initial cDNA and genomic isolation of *pkc*1 are DF (forwards) and DR (reverse). The walking primers used in 'step down' PCR are WF1 & 2 and WR 1 & 2, 3 & 4. The positions of the six introns are denoted * and by underlining the relevant interrupted amino acid; intron 1, G*AT codon D; intron 2, G*AT codon D; intron 3, G*AA codon E; intron 4, CA*A codon Q; intron 5, between codons E and I; intron 6, G*TA codon V. The protein signature motifs are boxed and named beneath the amino acid sequence

failed to reveal sequence homology to any named genes but did reveal the presence of a pyrimidine-rich area upstream of ATG (Gurr *et al.*, 1987). The 367 amino acids (aa) were subjected to BLAST and profile-scan searches, revealing a putative ATP binding motif and kinase domain (Figure 4.2).

The structure of classical, atypical and novel PKCs, consensus fungal PKC and *B. graminis* PKC1 and PKC-like are shown in Figure 4.3.

4.2.2 *pkc*1 and *pkc*-like phylogeny

The *B. graminis* PKC1 amino acid sequence was compared with 47 eukaryotic PKC amino acid sequences. A partial phylogenetic tree, obtained for this analysis, is shown as a neighbour-joining tree (Thompson *et al.*, 1997) in Figure 4.4(a) revealing *B. graminis* PKC1 to be closest to PKC of *Botryotina fuckeliana* (anamorph *Botrytis cinerea*), with which it shares 68% identity. The 367 amino acids of PKC-like reveals it to lie equidistantly between serine threonine kinase and the PKC (zeta and iota) sequences of *Homo sapiens* (Figure 4.4(b)).

4.2.3 *In vivo* detection of PKC activity in ungerminated *Blumeria graminis* f.sp. *hordei* conidia

Identification of *PKC*1 and *PKC*-like in *B. graminis* led to experiments to look for PKC activity in *B. graminis* protein extracts. The most common method for assaying kinases involves measuring the transfer of radioactive phosphate to a substrate protein or peptide. However, a non-radioactive PepTag® method has been developed (Promega, UK) to detect cAMP-dependent protein kinase (PKA) and PKC activity. This method utilises fluorescent peptide substrates that are highly specific for the kinases in question. In the PKA assay, the PKA-specific substrate is a fluorescent-tagged version of kemptide, with amino acid sequence L-R-R-A-S-L-G, and in the PKC assay the PKC-specific substrate is C1 Peptide, with amino acid sequence P-L-S-R-T-L-S-V-A-A-K.

PKC activity was detected in protein extracted from ungerminated conidia and from primary germ tube (PGT)-stage germlings, using the PKC PepTag® assay.

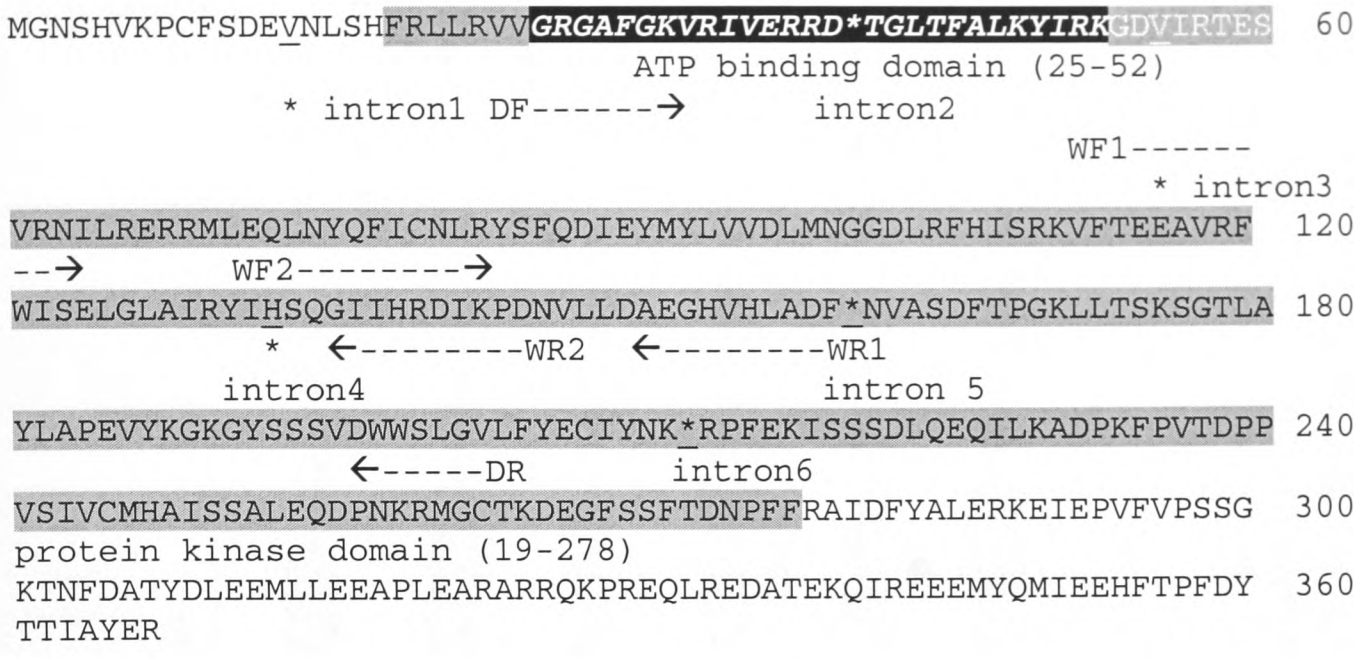


Figure 4.2. Amino acid sequence of *Blumeria graminis* f.sp. hordei PKC-like (EMBL accession no. AF283107). The degenerate primers for the initial cDNA and genomic isolation of *pkc*-like are DF (forwards) and DR (reverse). The walking primers used in 'step down' PCR are WF1 & 2 and WR 1 & 2. The six intron positions are: intron 1, G*TA codon V; intron 2, between codons D and T; intron 3, G*TC codes V; intron 4, CA*C codon H, intron 5, between codons F and N; intron 6, between codons K and R. The protein signature motifs are boxed and named beneath the amino acid sequence.

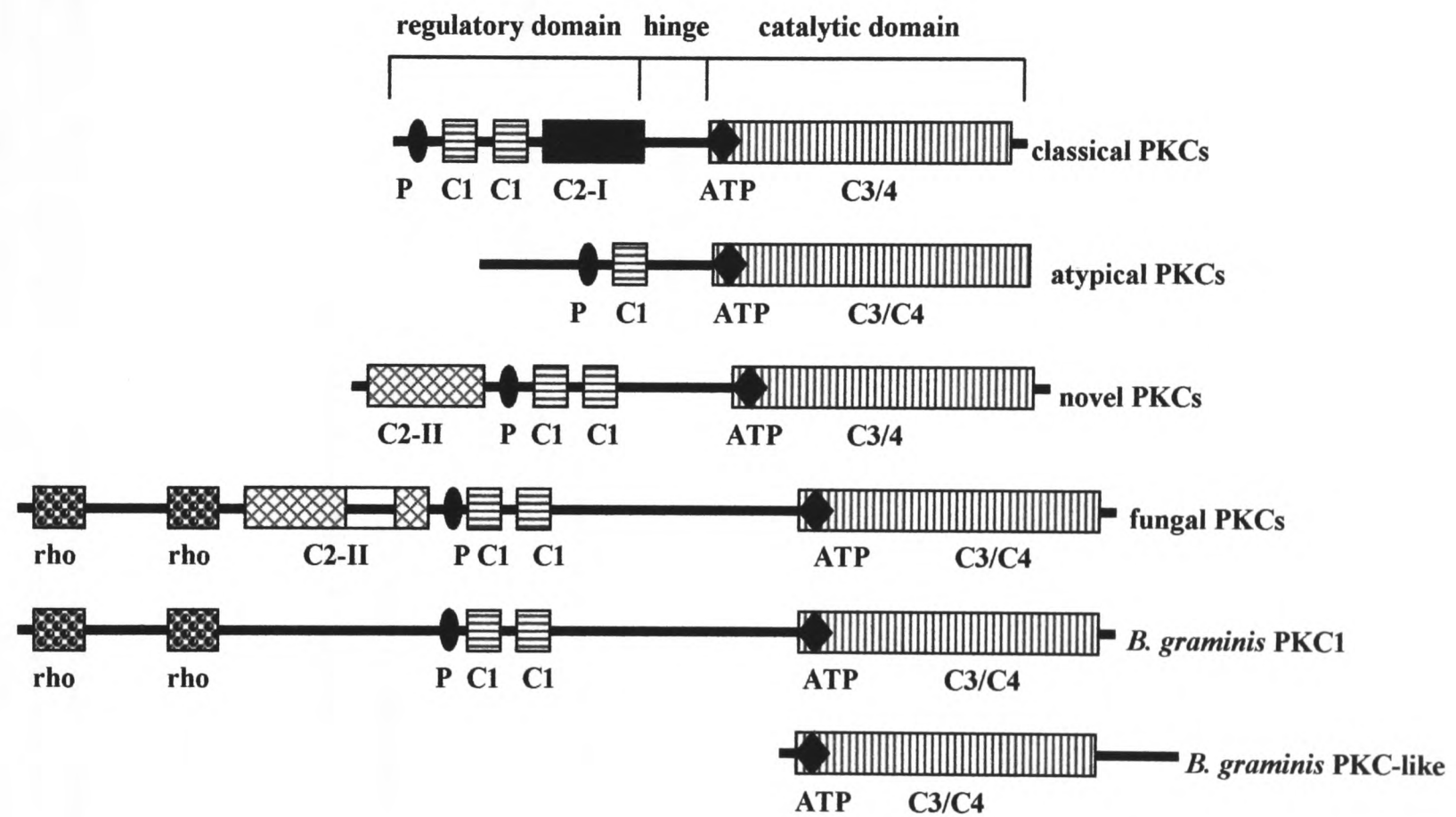
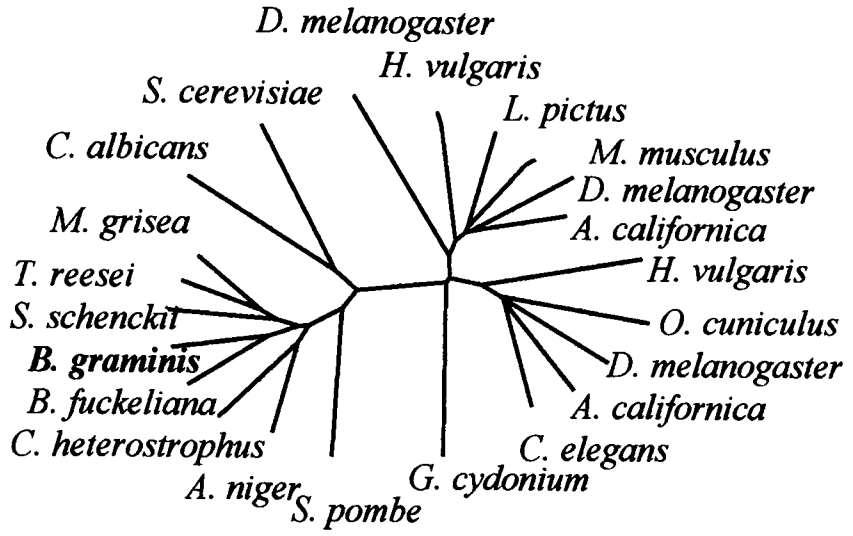


Figure 4.3. Structure of classical, atypical, novel and fungal PKCs and *Blumeria graminis* f.sp. *hordei* PKC1 and PKC-like. The schematic representation of fungal PKCs is adapted from Oeser (1998). The signature motifs are rho, rhotekin-rho / phorbol-esters binding domain: P, pseudosubstrate site; C1, cysteine rich domain; C2-I, calcium regulated C2 domain; C2-II, not calcium regulated C2 domain; C3 / 4, catalytic domain; (diamond), ATP binding site.

(a)



(b)

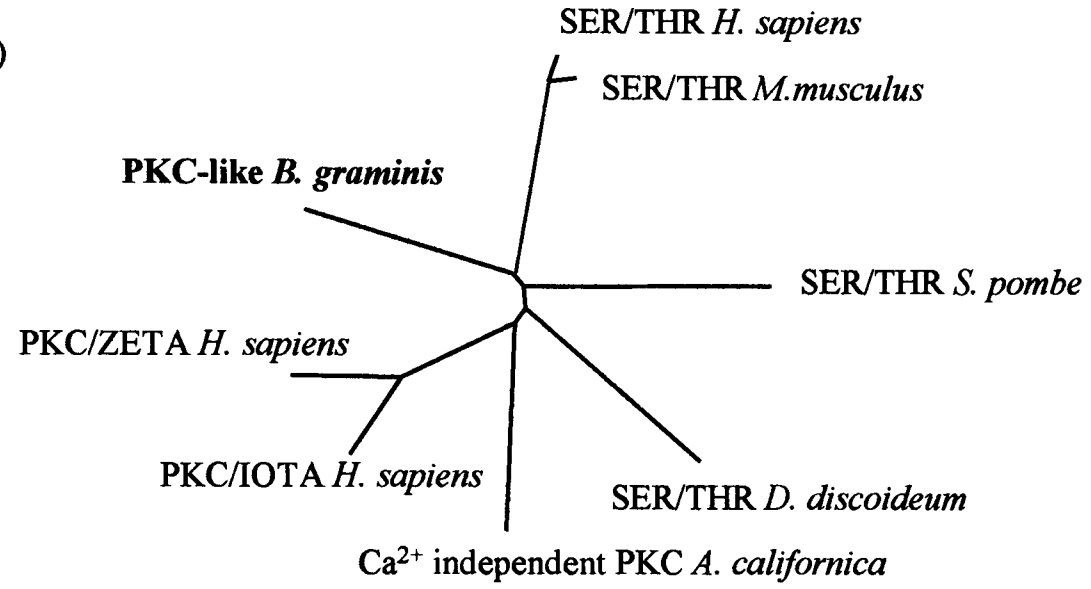


Figure 4.4. Amino acid sequence relationships of *Blumeria graminis* f.sp. *hordei* (a) PKC1 and (b) PKC-like, determined by neighbour-joining analysis, to PKCs from (a) *B. fuckeliana* (EMBL accession: CAB59301), *Cochliolobus heterostrophus* (O42632), *Magnaporthe grisea* (AAD33693), *Sporothrix schenckii* (AAD22633), *Aspergillus niger* (U10549-1), *Trichoderma reesei* (Q99014), *Schizosaccharomyces pombe* (NP_595950), *Candida albicans* (CAA57048), *Saccharomyces cerevisiae* (NP_009445), *Drosophila melanogaster* (NP_524545; NP_476863; A32545), *Mus musculus* (CAA36907), *Oryctolagus cuniculus* (P10830), *Aplysia californica* (Q16974; Q16975), *Hydra vulgaris* (CAA73363; CAA73362), *Geodia cydonium* (CAA76911), *Caenorhabditis elegans* (P34885), *Lytechinus pictus* (Q25378) and (b) *Homo sapiens* (AAH38238; AAH22016; CAA78813), *M. musculus* (AAH26457), *Dictyostelium discoideum* (AAM43765), *A. californica* (Q16975), *S. pombe* (NP_588234). Scale bar indicates 0.1 nucleotide substitutions per site. The tree was prepared using the Clustal W alignment programme (http://www.ddbj.nig.ac.jp/E-mail/homology.html) and TreeView (Page, 1996).

PGT-stage germlings were collected 6 hpi from 2% (w/v) water agar. However, *B. graminis* does not fully differentiate on agar and insufficient protein, derived from AGT-stage extracts prepared from tissue developing on the semi-inductive surface of hydrated cellulose membrane, precluded a complete time-course analysis of PKC activity during germling morphogenesis.

In order to determine the sensitivity limits of the PKC PepTag® assay a dilution series of *B. graminis* protein extract was assessed for its ability to promote C1 peptide phosphorylation. This demonstrated that 2 μg (8 μL of protein extract at 0.25 $mg.mL^{-1}$ in a total volume of 25 μL), 1 μg, 0.5 μg, 0.2 μg and 0.1 μg total protein yielded measurable C1 peptide phosphorylation, but lower concentrations (0.05 μg) did not. In addition, the sensitivity of the PKA PepTag® assay was also determined as this assay would be used in subsequent experiments to establish the specificity of agonists and antagonists towards PKC. With the PKA assay, 2 μg, 1 μg, 0.5 μg and 0.2 μg total protein yielded measurable kemptide phosphorylation, but lower concentrations (0.05 to 0.1 μg) did not.

4.2.4 Investigation of the effects of inhibitors on *Blumeria graminis* f.sp. *hordei* PKC activity

Having identified PKC activity in *B. graminis* f.sp. *hordei*, a range of inhibitors, characterized in mammalian systems as serine/threonine kinase inhibitors, were screened for their ability to inhibit *B. graminis* PKC activity by exploiting the activity detected using the PKC Peptag® assay. Inhibitors were chosen on the basis of their target sites, that is, those characterised in mammals as either catalytic-domain targeting or regulatory-domain targeting. The inhibition spectrum of the compounds tested has not previously been determined in fungal systems. In mammalian systems, however, H7 and HA-100 are active against a wide range of Ser/Thr protein kinases (Hidaka *et al.*, 1984; Tamaoki *et al.*, 1986; Kase *et al.*, 1987; Chijiwa *et al.*, 1990; Engh *et al.*, 1996; Hagiwara *et al.*, 1987) whereas bisindolylmaleimide I-HCl, Go6983, calphostin C and chelerythrine chloride are reported to be relatively specific inhibitors of PKC (Toullec *et al.*,

1991; Herbert *et al.*, 1990; Bruns *et al.*, 1991; Gschwendt *et al.*, 1996). H89 is a relatively specific inhibitor of PKA (Engh *et al.*, 1996).

Each putative inhibitor was assayed over a concentration range of 10 nM to 2 mM and, in each case, the assay was repeated three times. *B. graminis* protein extract was added to a final concentration of 40 $\mu g.mL^{-1}$ of unpurified conidial protein. The results are shown in Figure 4.5. The inhibitor concentration predicted to give 50% inhibition of PKC activity (IC_{50}) was determined from the linear region of log inhibitor concentration against percentage inhibition of PKC. Each potential inhibitor was also assayed using the PKA PepTag® assay to determine the inhibition spectrum of these compounds and thus the specificity of the inhibitors for PKC. Table 4.1 gives the IC_{50} values for both *B. graminis* PKC and PKA.

None of the inhibitors showed specificity for *B. graminis* PKC. Inhibitors either had no effect on PKC activity (HA-100 and H7), or gave high IC_{50} values, that is, mM concentrations (bisindolylmaleimide I-HCl, calphostin C, staurosporine) and μM concentrations, but were not notably different to IC_{50} values for PKA (Go6983 and chelerythrine chloride).

4.2.4.1 Purification of Blumeria graminis f.sp. hordei protein extracts

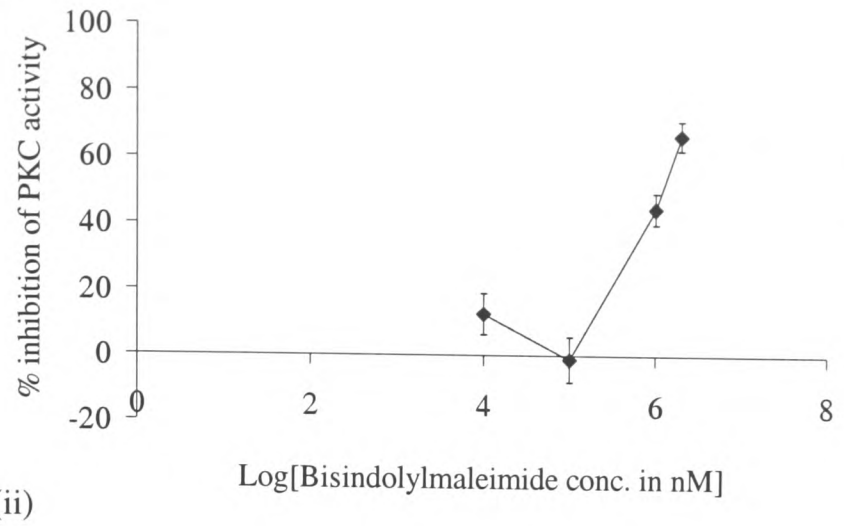
Ammonium sulphate precipitation

Having observed no effect of the PKC inhibitors on *B. graminis* PKC activity, ammonium sulphate precipitation was performed in order to fractionate the crude protein extract. This method separates the protein extract into a fraction of 18% (w/v) ammonium sulphate in which activity is attributed to "novel" PKCs, a second fraction of 45% (w/v) ammonium sulphate where activity is ascribed to "classical" PKCs and a third fraction of "residual" PKC activity. The HeLa (Henrietta Lacks) cells (a human tumour cell line) (a gift from Catherine Pears, University of Oxford) were used as a control (Figure 4.6(a)).

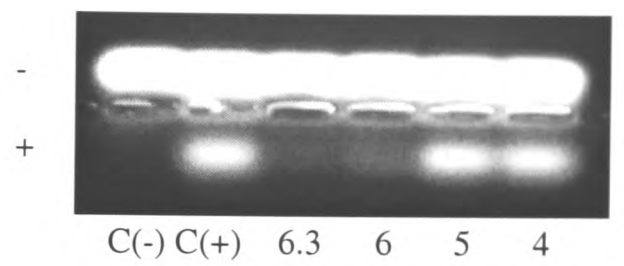
Fractionation of *B. graminis* conidial protein revealed that most PKC activity is present in the 45% ammonium sulphate fraction, *i.e.* that attributed to the classical

Figure 4.5

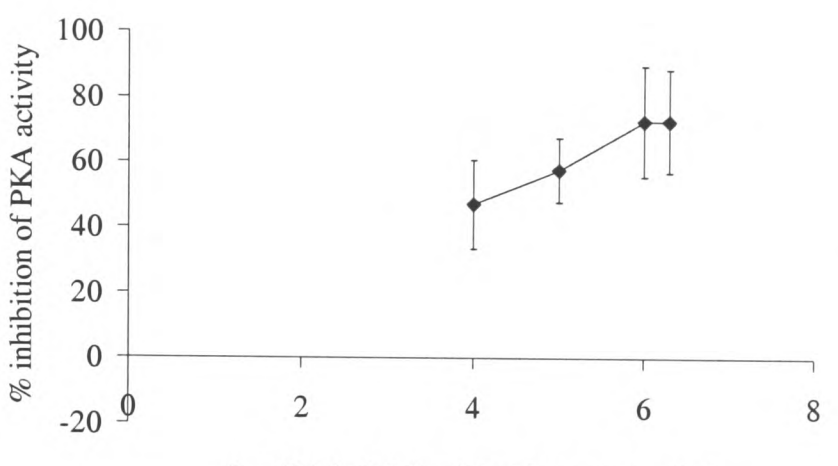
a(i)



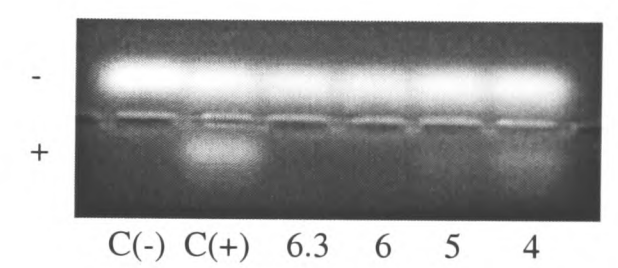
a(iii)



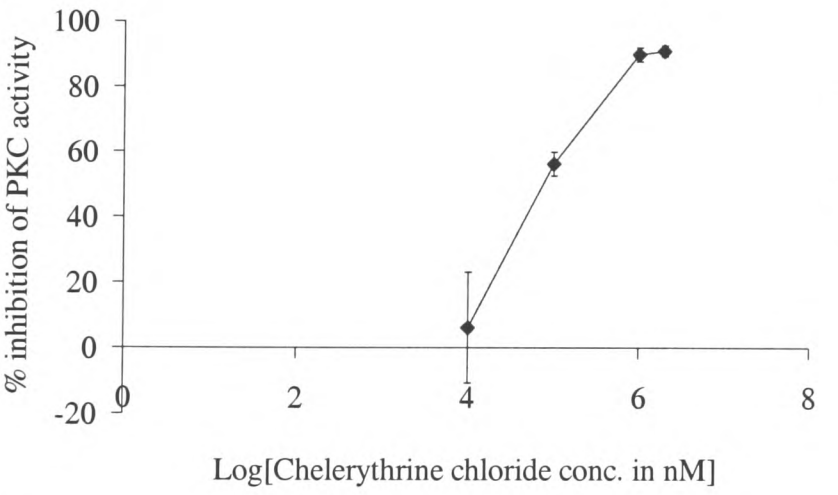
a(ii)



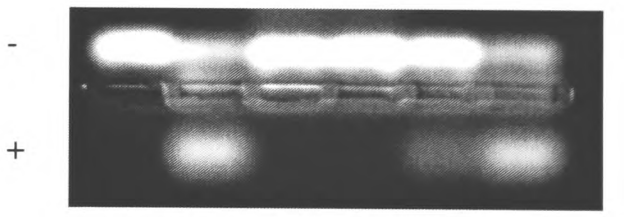
a(iv)



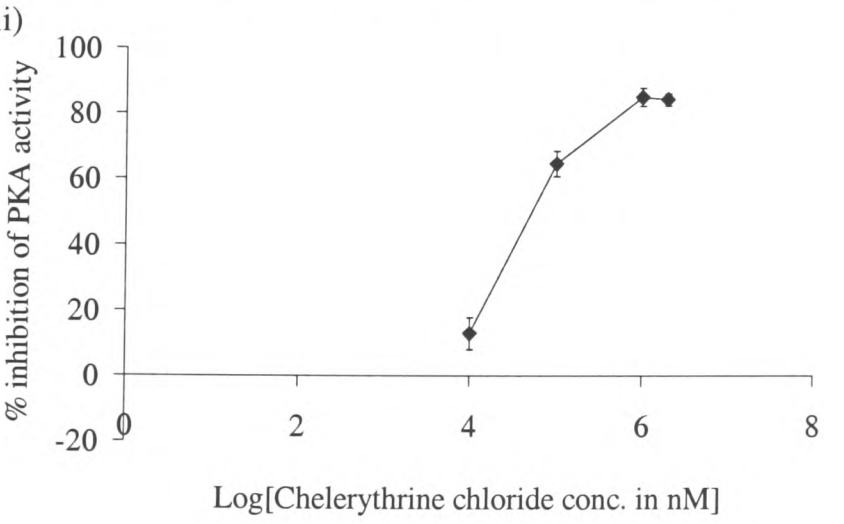
b(i)



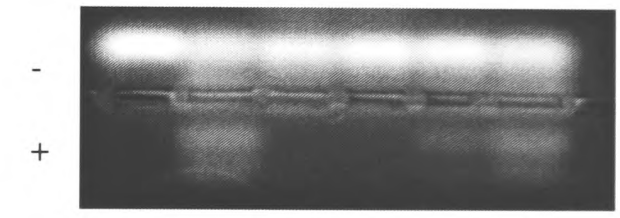
b(iii)



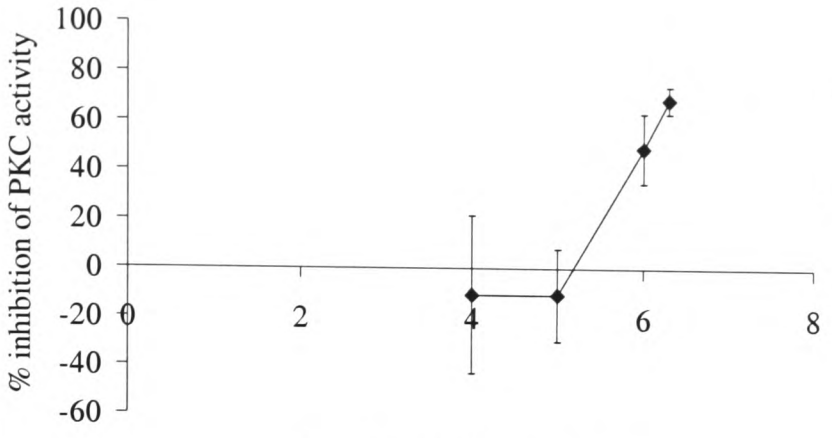
b(ii)



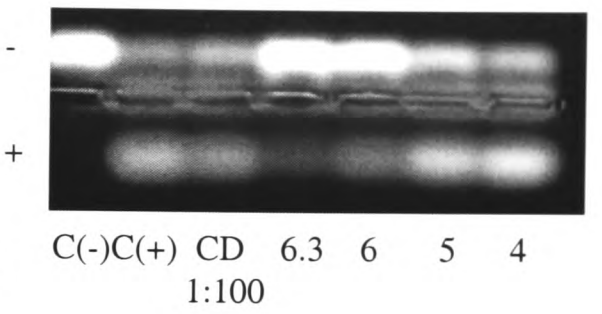
b(iv)



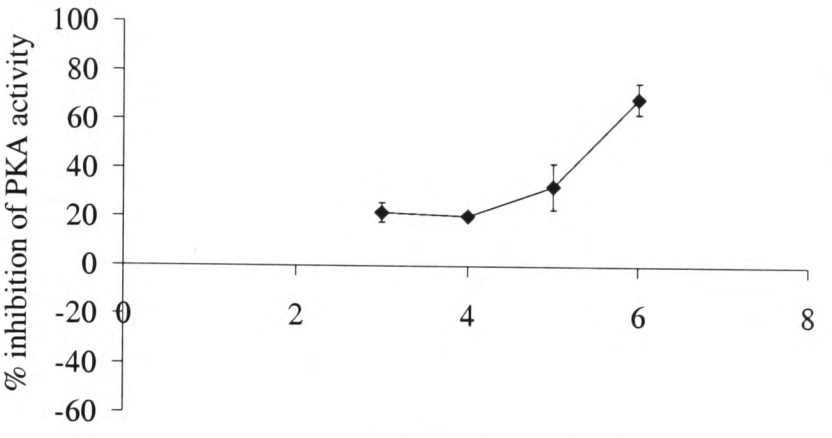
c(i)



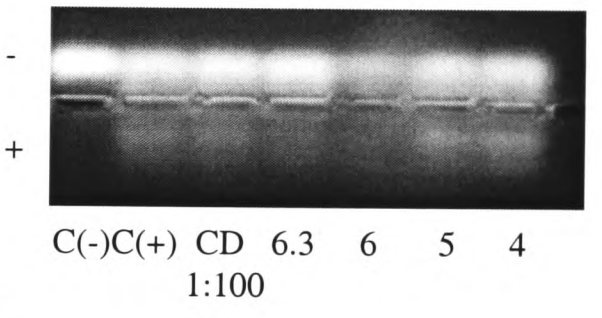
c(iii)



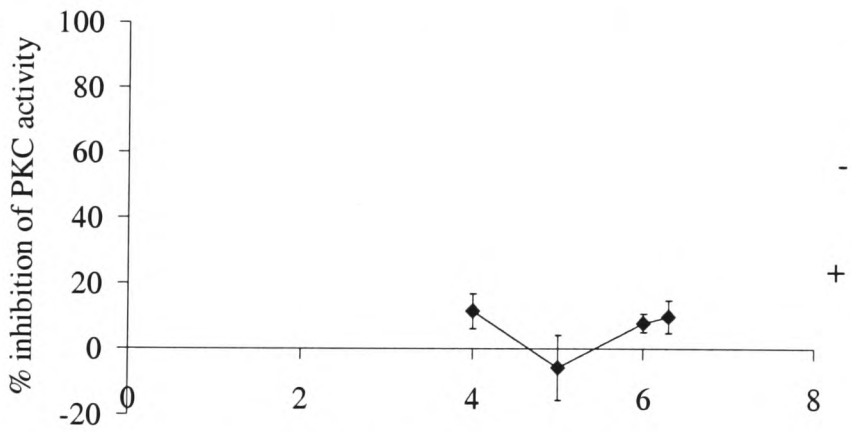
c(ii)



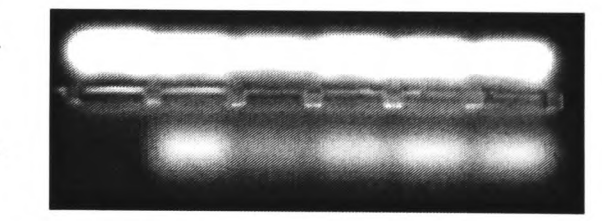
c(iv)



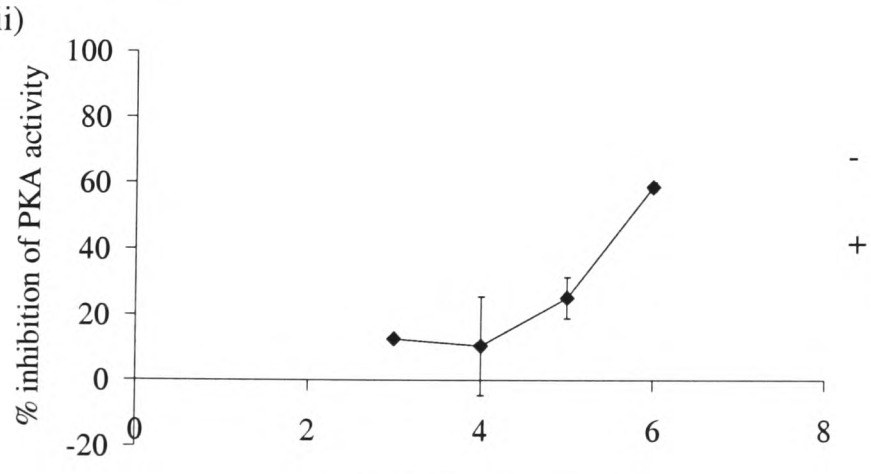
d(i)



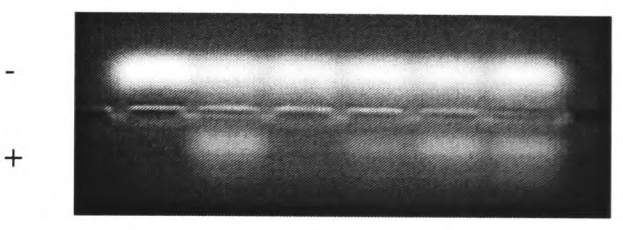
d(ii)



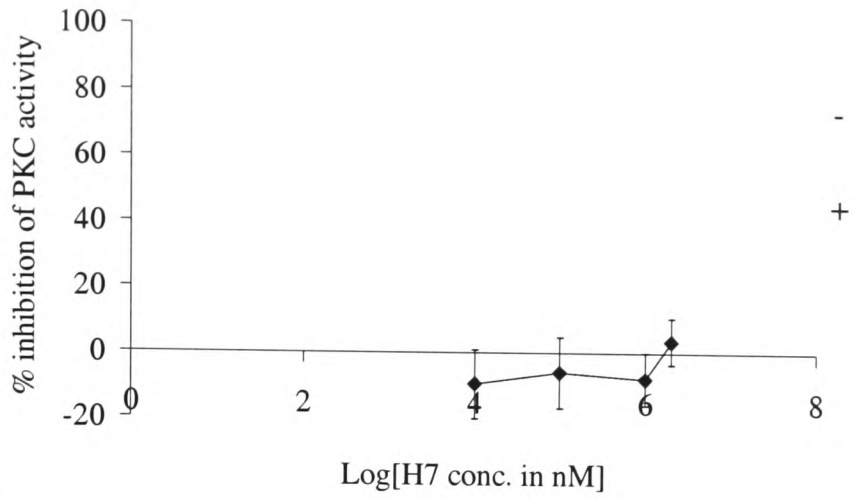
d(iii)



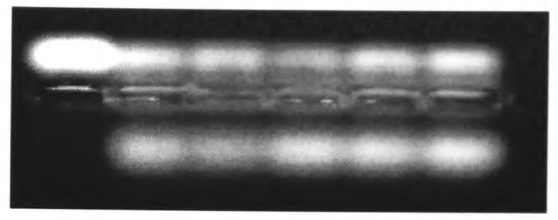
d(iii)



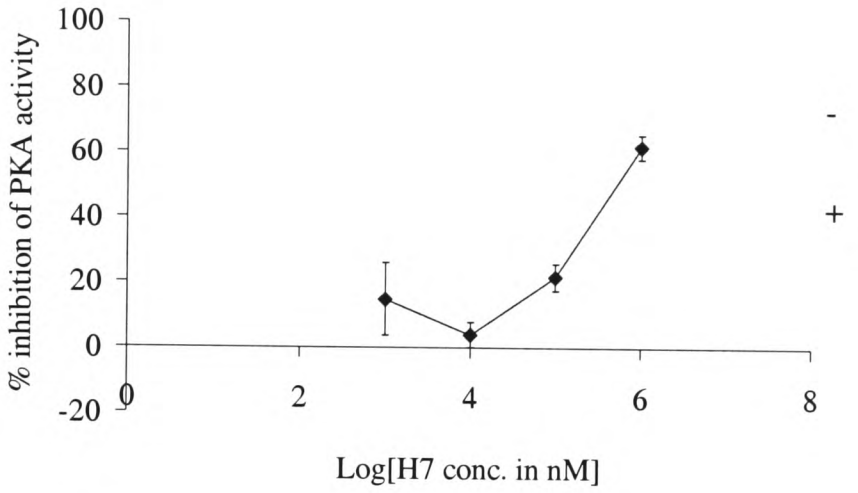
e(i)



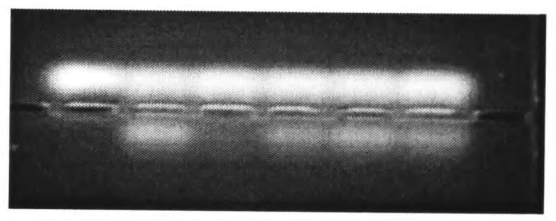
e(iii)



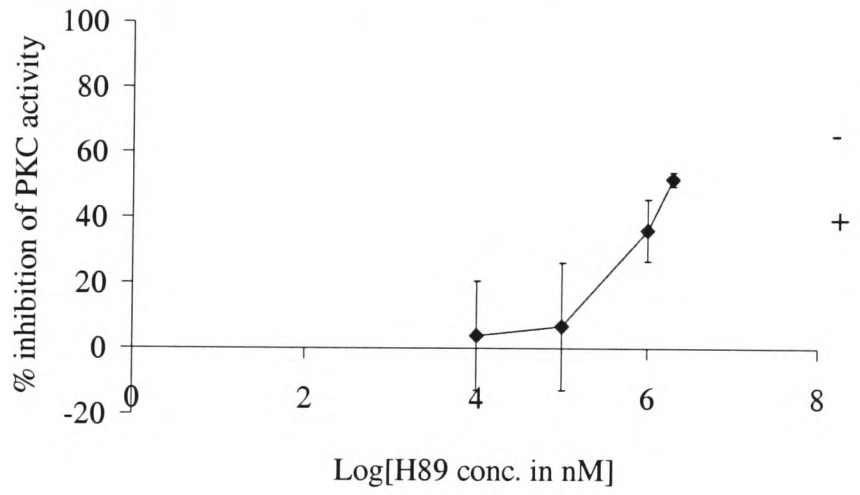
e(ii)



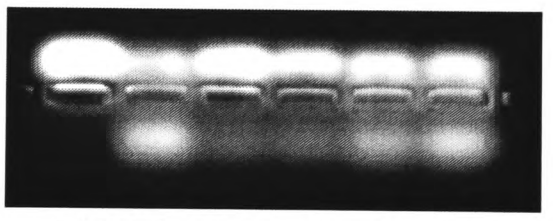
e(iv)



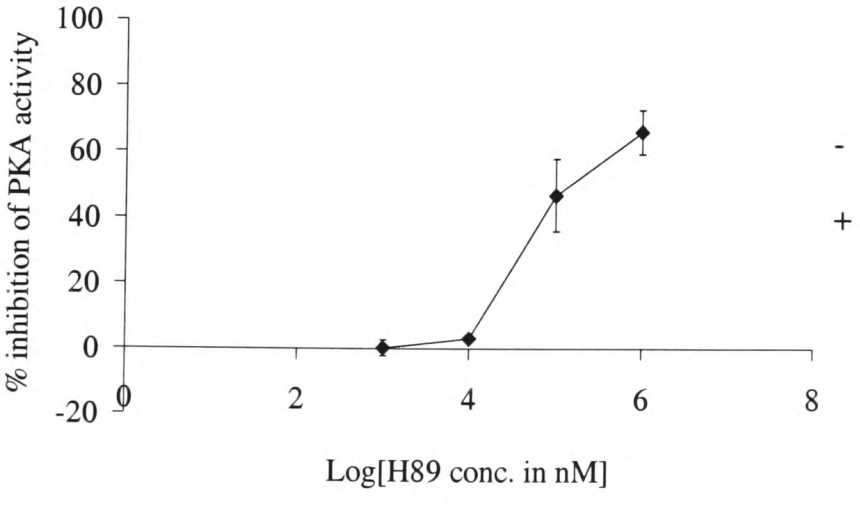
f(i)



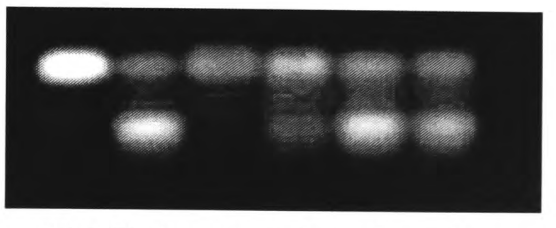
f(iii)



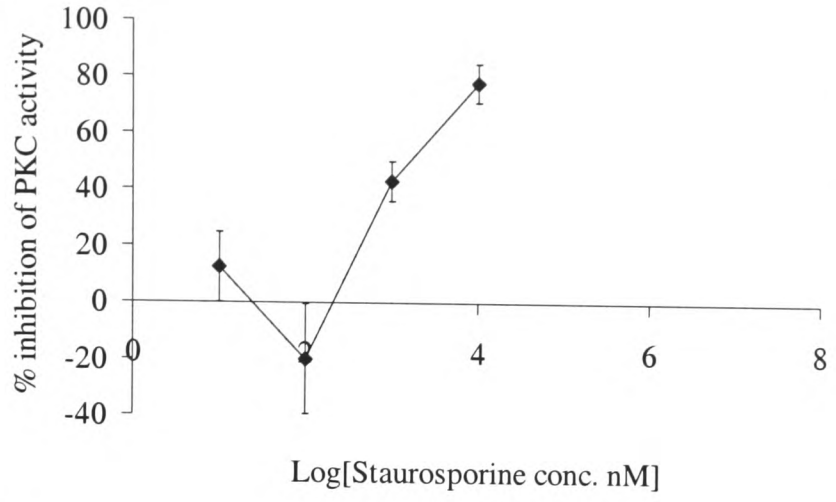
f(ii)



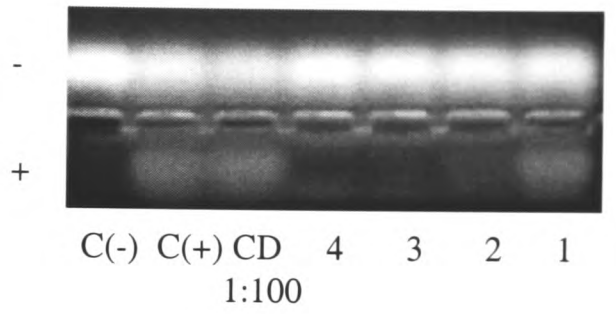
f(iv)



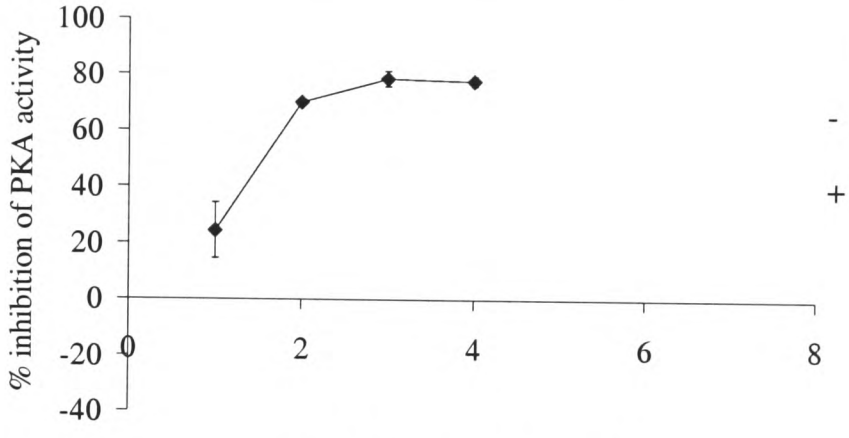
g(i)



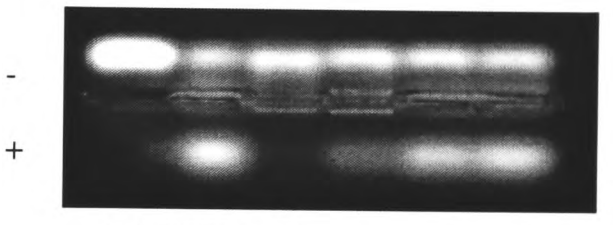
g(iii)



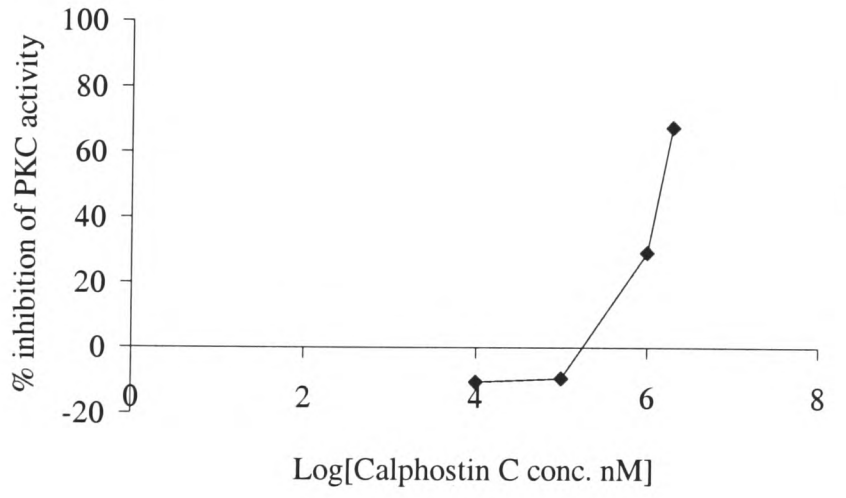
g(ii)



g(iv)



h(i)



h(ii)

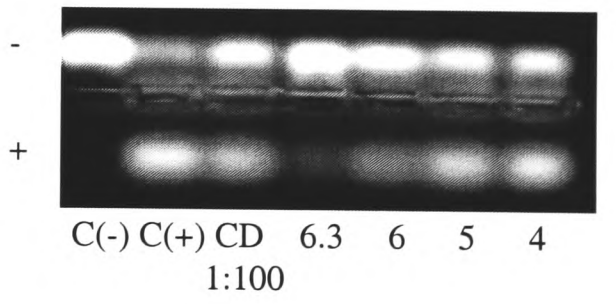


Figure 4.5. Inhibition of *Blumeria graminis* f.sp. *hordei* PKC (i) and cAMP-dependent PKA (ii) activity by (a) bisindolylmaleimide I-HCl, (b) chelerythrine chloride, (c) Go6983, (d) HA-100, (e) H7, (f) H89, (g) staurosporine and (h) calphostin C. (a-h.i and ii.) illustrate the percentage inhibition of PKC and PKA activity (mean of three experiments) ± SE. (a-g.iii and iv; h.ii) show the migration of phosphorylated (+) and non-phosphorylated (-) C1 peptide (iii, ii for h) (for PKC) and kemptide (iv) (for PKA) in the PepTag® assays. C(-) represents the negative control (no protein added), C(+) the positive control (protein added, but no inhibitor) and CD represents the positive control with DMSO. Inhibitor concentration is given in nM. NB: Only one PKC assay was performed for calphostin C, and no PKA assays.

Inhibitor	PKC IC_{50} (mM)	PKA IC_{50} (mM)
Bisindolylmaleimide I, HCl	1.2	0.035
Calphostin C	1.6	-
Chelerythrine chloride	0.076	0.052
Go6983	0.63	0.30
HA-100	No effect	0.54
H7	No effect	0.53
H89	1.9	0.16
Staurosporine	$1.7x10^{-3}$	$3.6x10^{-5}$

Table 4.1. IC_{50} values (inhibitor concentration predicted to give 50% inhibition of enzyme activity) for *Blumeria graminis* f.sp. *hordei* spore protein kinase C (PKC) and cAMP-dependent protein kinase (PKA) activities (calculated from 3 independently repeated experiments) given to 2 significant figures.

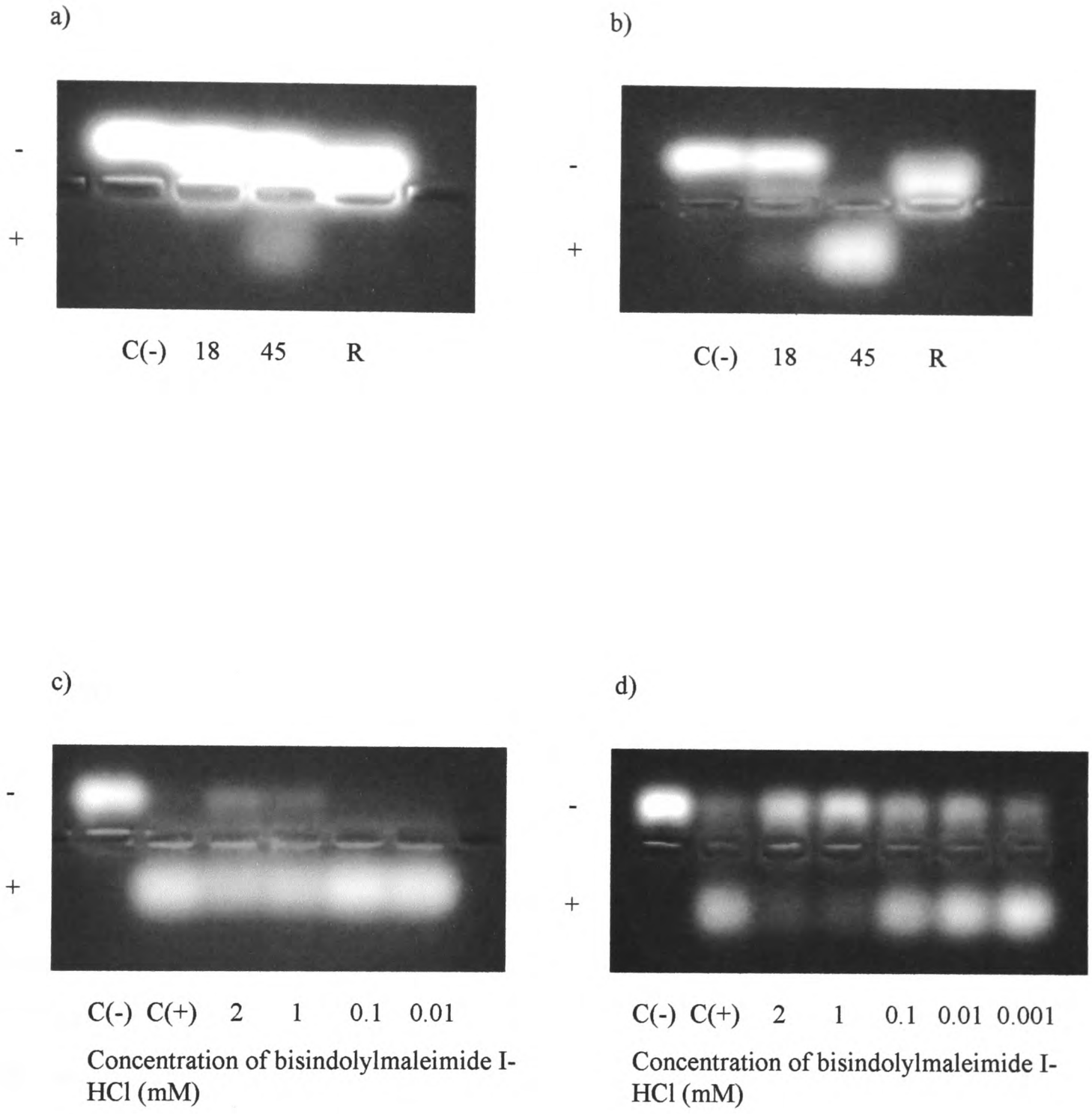


Figure 4.6. Migration of C1 peptide in the Peptag® protein kinase C assay after ammonium sulphate precipitation of HeLa cell extract (a) and *Blumeria graminis* f.sp. *hordei* spore extract (b). (a)-(d) nonphosphorylated substrate migrates to the cathode (-), while phosphorylated substrate migrates to the anode (+). C(-) represents negative control (no protein added), C(+) represents the positive control (protein added, but no inhibitor). 18 and 45 represent the percentage of ammonium sulphate in the fraction, R represents the residual fraction in (a) and (b). c) Inhibition by bisindolylmaleimide I-HCl of PKC activity in the 45% ammonium sulphate fraction from *B. graminis* f.sp. *hordei* spores. d) Inhibition by bisindolylmaleimide I-HCl of PKC activity in 50 kDa column-filtered *B. graminis* f.sp. *hordei* spore extract.

PKCs, with some activity corresponding to the "novel" PKCs also being evident in the 18% ammonium sulphate fraction (Figure 4.6(b)). Application of the PKC-specific inhibitor bisindolylmaleimide I-HCl to the 45% fraction yielded no differences in inhibition when compared to the crude protein extract (Figure 4.6(c)).

Column purification

Having observed no effect of bisindolylmaleimide I-HCl on PKC activity in fractionated PKC extracts, conidial protein extracts were purified using a column to remove all particles/impurities of less than 50 kDa. Subsequently, bisindolylmaleimide I-HCl was applied to the column-purified protein in the Peptag® PKC assay. No differences in inhibition were observed when compared with the crude protein extract or the fractionated protein extract (Figure 4.6(d)).

4.2.5 Investigation of the effects of agonists on *Blumeria graminis* f.sp. *hordei* PKC activity

Phorbol esters and diacylglycerol (DAG) are well known modulators of PKC activity in mammalian systems. Both ligands regulate PKC by the same mechanism, but have very different biological effects. In mammals it is known that membrane recruitment and PKC activation initiated by DAG is short-lived due to its rapid metabolism, whereas phorbol esters are not readily metabolised and thus result in the constitutive activation PKC (reviewed in Newton, 2001). In the phytopathogenic fungi DAG is known to affect infection structure differentiation in *Uromyces appendiculatus* (Staples and Hoch, 1987) and *M. grisea* (Thines *et al.*, 1997a, b).

4.2.5.1 Phorbol 12-myristate 13-acetate

The phorbol ester, phorbol 12-myristate 13-acetate (PMA), was applied to protein extracts in the Peptag® PKC assay that had first been purified using a column to remove all proteins of less than 50 kDa. The effect of PMA (0.1 pM to 1 μM) on phosphorylation of the PKC-specific substrate was determined for conidial (Figure 4.7(a)) and PGT-stage extracts (Figure 4.7(b)), and revealed that 1 nM

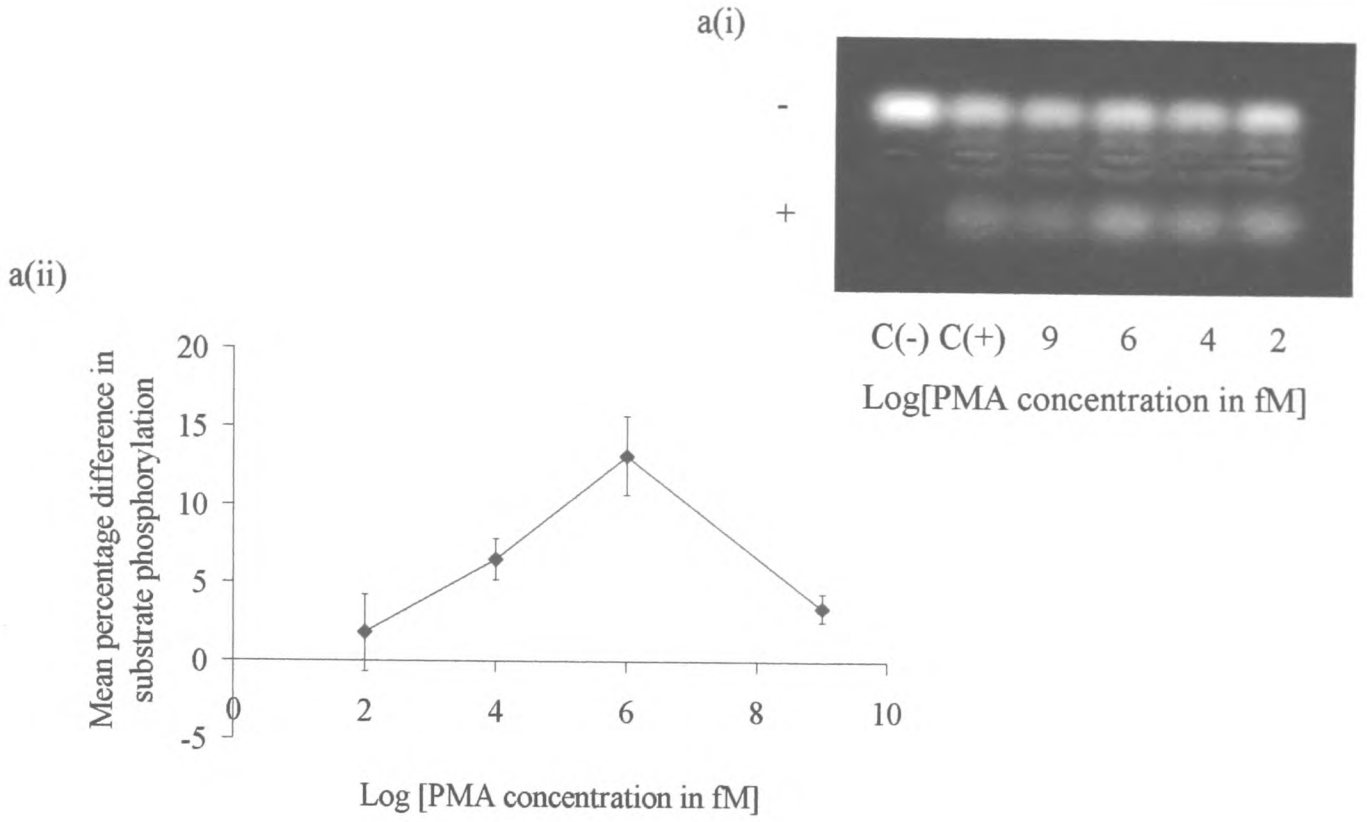


Figure 4.7. The effect of phorbol 12-myristate 13-acetate (PMA) on *Blumeria graminis* f.sp. *hordei* spore (a) and primary germ tube (PGT)-stage protein kinase C (PKC) activity. a(i) and b(i) show representative assays. Non-phosphorylated substrate migrates to the cathode (-), while phosphorylated substrate migrates to the anode (+). C(-) represents negative control (no added protein), C(+) the positive control (protein added, but no PMA). The effect of phosphorylation on the PKC-specific substrate in the PKC assays was determined for PMA concentrations between 10^2 and 10^9 fM. a(ii) and b(ii) show the mean percentage difference in substrate phosphorylation on DOG addition. The experiments were repeated three times and the mean ± standard error is shown. Using the Kruskal-Wallace test, the null hypothesis that the points have the same mean can be rejected (P=0.043, H=8.13 for a(ii); P=0.047, H=7.99 for b(ii)).

PMA gave the greatest increase in substrate phosphorylation. The experiments were repeated three times. Using the Kruskal-Wallace test, the null hypothesis that the points have the same mean can be rejected (for conidial extracts P=0.043, H=8.13; for PGT-stage extracts P=0.047, H=7.99). In eight independently replicated experiments, with conidial extracts and PGT-stage extracts, the increase in phosphorylation caused by the addition of 1 nM PMA was significant with P=0.006 for conidial extracts and P=0.023 for PGT-stage extracts, using a paired *t*-test analysis.

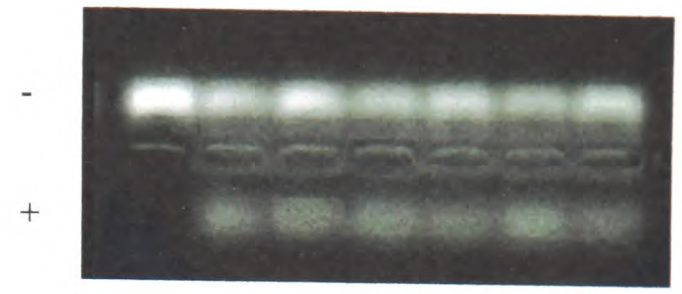
4.2.5.2 Dioctanoyl 1, 2-sn-glycerol

Application of between 0.1 pM and 100 μM DOG to unpurified (Figure 4.8(a)) and column purified (Figure 4.8(b)) protein extracts in the Peptag® PKC assay failed to show enhanced PKC substrate phosphorylation in three independently conducted experiments. Using the Kruskal-Wallace test, the null hypothesis that the points have the same mean cannot be rejected for column purified conidial extracts (P=0.384, H=4.7). For the unpurified extracts, the null hypothesis that the points have the same mean can be rejected (P=0.018, H=11.88). However, Figure 4.8(a.ii) shows there is no positive correlation between the DOG concentration and mean percentage difference in substrate phosphorylation. Thus, an explanation for the value of $P<0.05$ could be due to the small number of data points and the inherent inaccuracy of the technique. That is, error that may be introduced through lack of sensitivity in measuring fluorescence, and through the limits of the sensitivity of the assay itself.

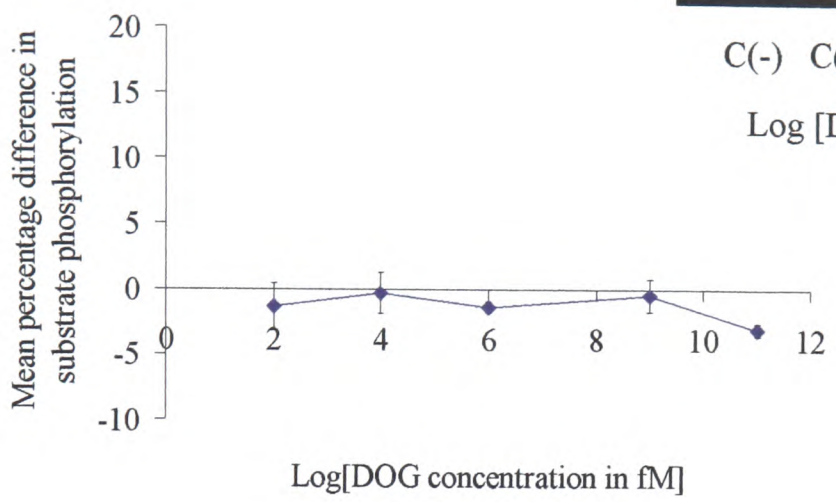
4.2.6 Investigation into the effects of PKC agonists on *Blumeria graminis* f.sp. *hordei* germling development

Having established the effect of PMA and DOG on PKC activity *in vitro*, the effect of these agonists on *B. graminis* f.sp. *hordei* differentiation was investigated *in vivo*. Either PMA or DOG was applied exogenously to conidia, *i.e.* to agar beneath hydrated cellulose membrane. Conidia were scored for germination (6 replicates of 50 conidia) and differentiation (6 replicates of 50 germinated

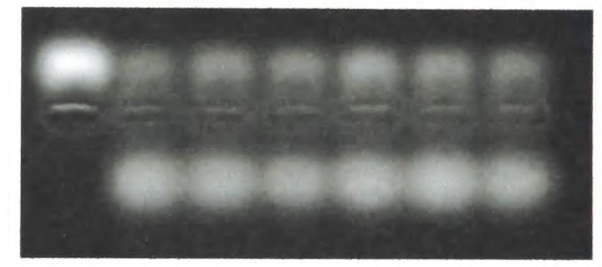
a(i)



a(ii)



b(i)



b(ii)

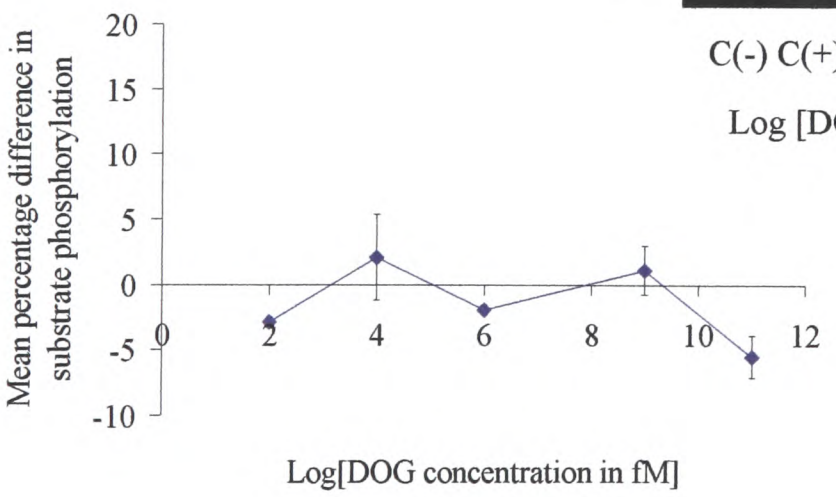


Figure 4.8. The effect of dioctanoyl 1,2-*sn*-glycerol (DOG) on protein kinase C (PKC) activity in crude *Blumeria graminis* f.sp. *hordei* protein extract (a) and 50 kDa column purified spore extract (b). a(i) and b(i) are representative assays. Non-phosphorylated substrate migrates to the cathode (-), while phosphorylated substrate migrates to the anode (+). C(-) represents negative control (no added protein), C(+) the positive control (protein added, but no DOG). The effect of phosphorylation on the PKC-specific substrate in the PKC assays was determined for DOG concentrations between 10^2 and 10^{11} fM. a(ii) and b(ii) show the mean percentage difference in substrate phosphorylation on DOG addition. The experiments were repeated three times and the mean ± standard error is shown. Using the Kruskal-Wallace test, the null hypothesis that the points have the same mean can be rejected (P=0.018, H=11.88 for a(ii); P=0.384, H=4.7 for b(ii)).

conidia) at 24 hpi. Statistical significance was determined using the General Linear Model (GLM) following an arcsine transformation.

4.2.6.1 Phorbol 12-myristate 13-acetate

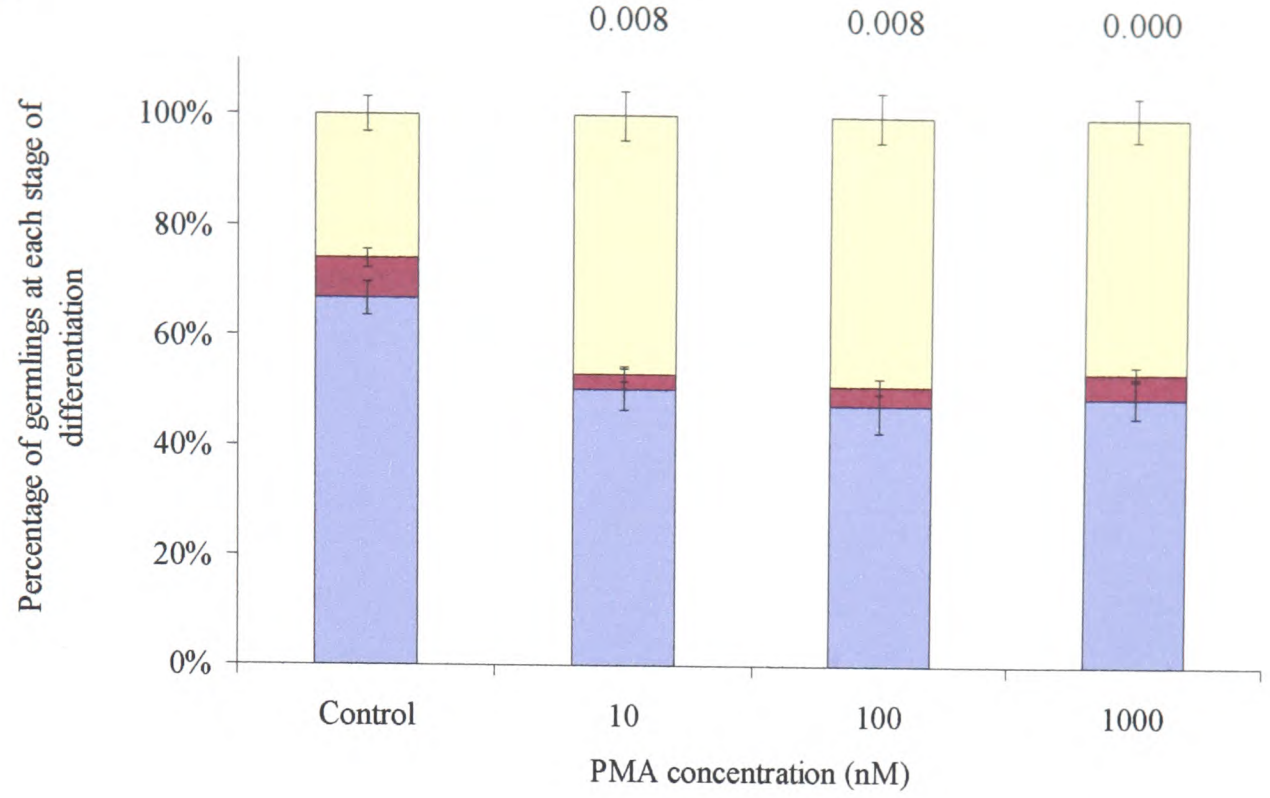
PMA was applied beneath cellulose membrane at concentrations of between 0.001 nM and 1 μM. However, PMA had no significant effect on germination (Table 4.2). PMA between 0.1 nM and 1 μM, though, resulted in an increased number of germlings differentiating secondary elongated (EGT), swollen (SwGT) or appressorial germ tubes (AGT) as compared with the controls on cellulose membrane alone. Figure 4.9 shows the percentage increase in differentiation of germlings upon PMA application. Three independently-repeated experiments were performed. P-values for all 3 independent repeat experiments are shown in Table 4.2.

A time-course of *B. graminis* f.sp. *hordei* development on cellulose membrane overlying agar containing 1 nM and 1000 nM PMA was performed. Conidia were scored for differentiation (6 replicates of 50 germinated conidia) at 0, 2, 4, 8, 12, 16, 20 and 24 hpi where differentiation was defined as the production of an EGT, a SwGT or an AGT. Figure 4.10 shows that up until 8 hpi, the PMA-treated populations have similar rates of differentiation to the control population. However, at 12 hpi, twice as many germlings have differentiated in the PMA-treated populations as for the control, (mean differentiation of 20% and 22% for 1 nM PMA and 1000 nM PMA-treated populations respectively, compared to 10% for the control population). This trend continues at 16 hpi, while at 20 hpi, the reduction in rate of differentiation becomes apparent in all populations. By 24 hpi, a mean of 24% of germlings have differentiated in the control population, whereas in the PMA-treated populations, a mean of 38% and 34% of germlings have differentiated in the 1 nM PMA and 1000 nM PMA-treated populations respectively.

Repeat	Concentration of PMA (nM)	Germination	Differentiation
1	1000	0.913	0.000***
	100	0.468	0.008**
	10	0.550	0.008**
2	1000	0.388	0.000***
	100	0.641	0.224
	10	0.334	0.001***
3	1000	0.653	0.000***
	100	0.064	0.000***
	10	0.030	0.000***
1	10	0.552	0.001**
	1	0.729	0.000***
	0.1	0.626	0.007**
2	10	0.183	0.032*
	1	0.766	0.002**
	0.1	0.151	0.010**
3	10	0.126	0.044*
	1	0.495	0.047*
	0.1	0.201	0.034*
1	0.1	0.477	0.047*
	0.01	0.658	0.296
	0.001	0.065	0.112
2	0.1	0.298	0.217
	0.01	0.377	0.663
	0.001	0.351	0.991
3	0.1	0.870	0.333
	0.01	0.704	0.267
	0.001	0.160	0.335

Table 4.2. P-values to show the significance between treatment of *Blumeria graminis* f.sp. *hordei* with phorbol 12-myristate, 13-acetate (PMA) and the control (no PMA) for germination and differentiation on cellulose membrane. The controls were 0.01% (v/v) DMSO in experiments with PMA concentrations of 10 to 1000 nM, 0.0001% (v/v) DMSO in experiments with PMA concentrations of 0.1 to 10 nM and 0.000 001% (v/v) DMSO in experiments with PMA concentrations of 0.001 to 0.1 nM. For each repeat experiment, 6 x 50 conidia were scored for germination and 6 x 50 germlings were scored for differentiation, meaning the production of either an elongated germ tube, a swollen germ tube or an appressorial germ tube. The results of nine independent experiments are shown. * indicates $P \leq 0.05$, ** indicates $P \leq 0.01$ and *** indicates $P \leq 0.000$.

a)



b)

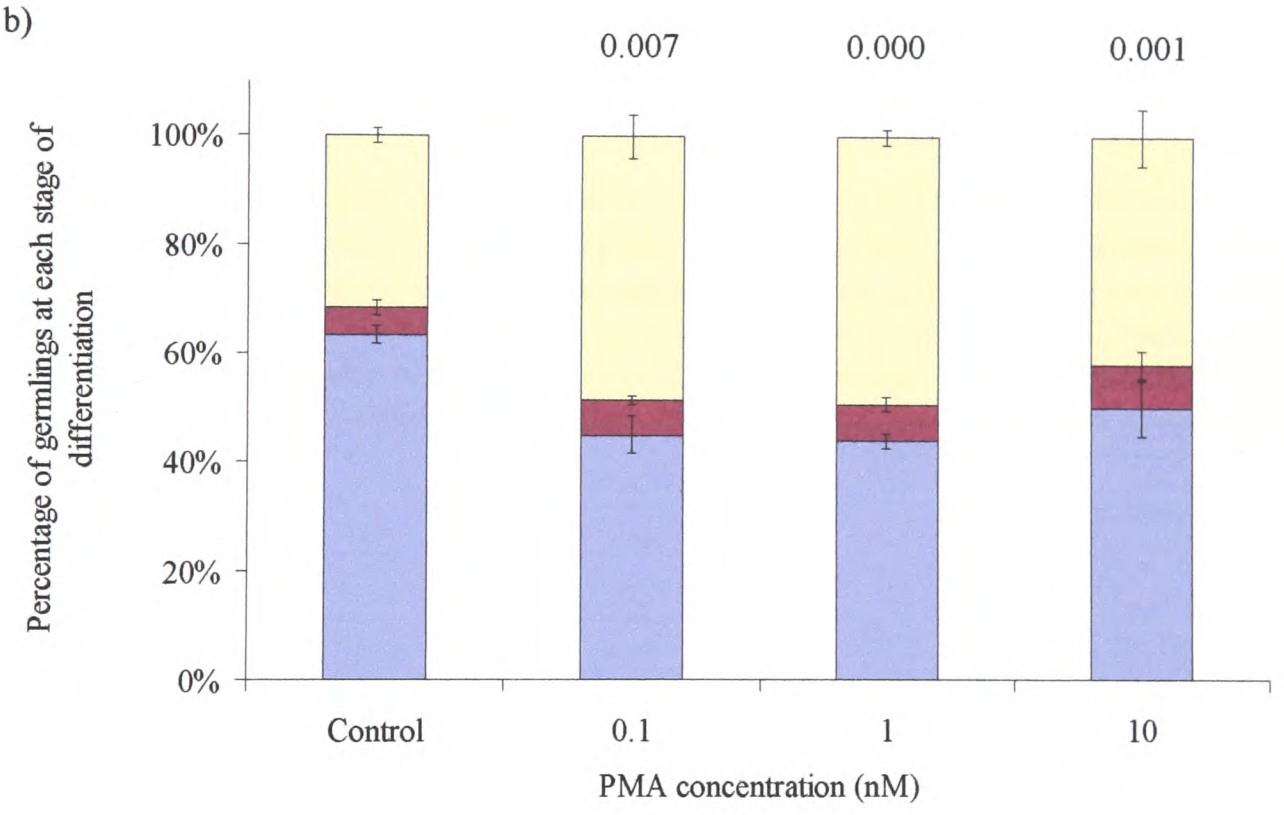


Figure 4.9. Differentiation of *Blumeria graminis* f.sp. *hordei* conidia on cellulose membrane overlying phorbol 12-myristate 13-acetate (PMA), 24 hours post inoculation. ■ corresponds to conidia with short germ tubes, ■ corresponds to conidia having differentiated elongated germ tubes and ■ corresponds to conidia having differentiated either a swollen germ tube, or an appressorial germ tube. The results shown are representative of 3 independent experiments. In each experiment, 6 x 50 conidia were scored and the mean values of 50 conidia are illustrated. The controls are 0.01% (v/v) DMSO for graph (a) and 0.0001% (v/v) DMSO for graph (b). P-values showing the significant differences in differentiation (that is, germlings that have differentiated elongated, swollen or appressorial germ tubes) compared to the control are given above each corresponding bar.

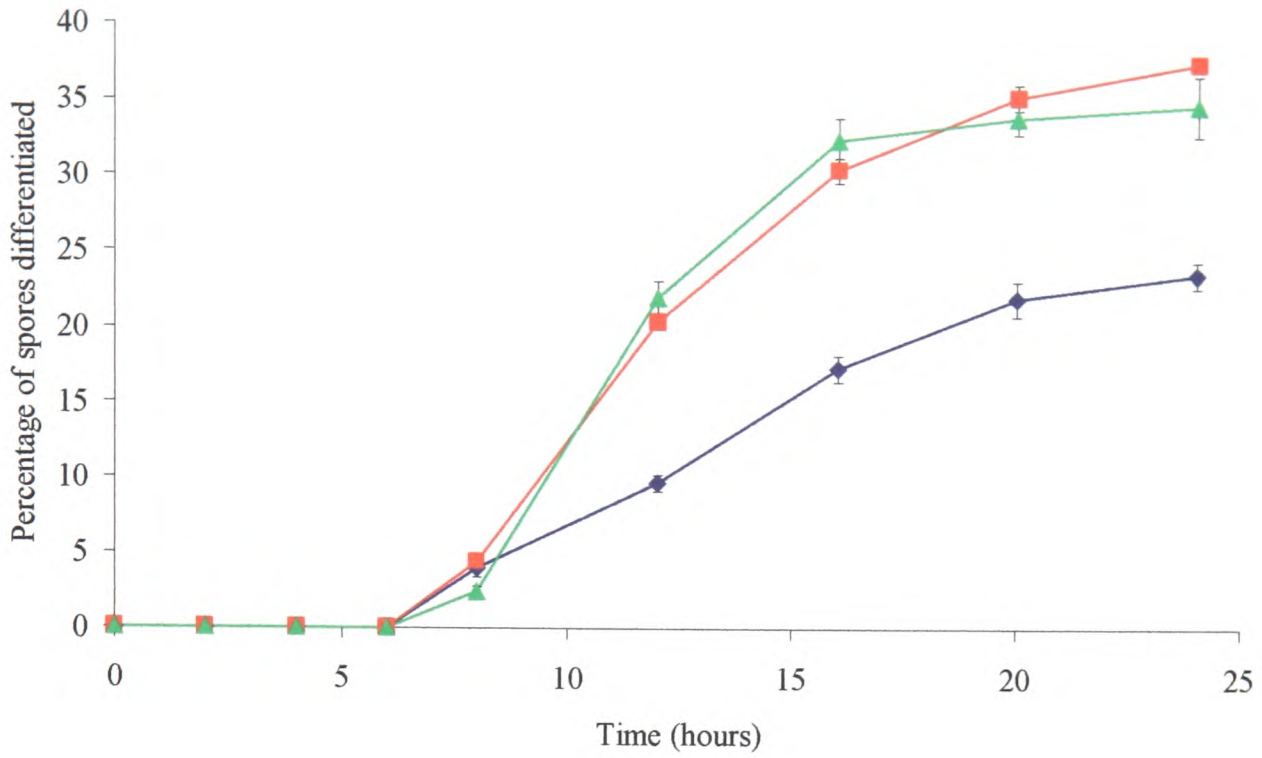


Figure 4.10. Time course of differentiation of *Blumeria graminis* f.sp. *hordei* conidia on cellulose membrane overlying phorbol 12-myristate 13-acetate (PMA). ◆ corresponds to the control (0.01% (v/v) DMSO), ■ correspond to 1 nM PMA and ▲ correspond to 1000 nM PMA. The results shown are representative of 3 independent experiments. For each time point, 6 x 50 germlings were scored for differentiation, meaning the production of either an elongated germ tube, a swollen germ tube or an appressorial germ. The mean ± standard error is shown.

4.2.6.2 Dioctanoyl 1, 2-sn-glycerol

Application of 0.01 μM to 100 μM DOG beneath cellulose membrane did not enhance *B. graminis* germination or appressorial differentiation. Figure 4.11 shows the differentiation of germlings upon DOG application. Three independently-repeated experiments were performed. P-values for germination and differentiation for all 3 independent repeat experiments are shown in Table 4.3.

4.2.7 Expression of *pkc*1 and *pkc*-like gene during germling morphogenesis

Transcript abundance of the *B. graminis pkc*1 and *pkc*-like genes in ungerminated conidia (0 hpi), mature primary germ tube stage germlings (4 hpi) and appressorial germ tube stage germlings (12 hpi) has previously been described (Zhang *et al.*, 2001). This work exploited the RT-PCR method as described by Zhang *et al.* (2000) which employs end-point (competitive) analysis of amplification products. To verify and provide a more extensive time-course of expression, transcript abundance of the *B. graminis pkc*1 and *pkc*-like genes was determined using a real-time PCR approach. This technique uses data from the exponential phase of amplification where there is a quantitative relationship between the amount of starting target DNA and the amount of amplification product (Rotorgene 2000 Real-Time PCR machine user manual, Corbett Research, Australia).

For real-time PCR, stage-specific, 1st strand cDNA was synthesised from total RNA extracted from ungerminated conidia, and germlings harvested from the barley leaf surface at 0.5, 3, 8, 12 and 20 hpi. These time points were selected to correspond with significant stages in the differentiation of *B. graminis*, that is, the ungerminated state (0 h), just prior to the emergence of the PGT (0.5 h), during PGT differentiation (3 h), during AGT elongation and swelling (8 h), at the mature AGT stage (12 h) and beyond (20 h). The *B. graminis* β-*tubulin* gene transcript was used as an endogenous, consititutively expressed control (Sherwood and Somerville, 1990). PCR was undertaken with primers designed

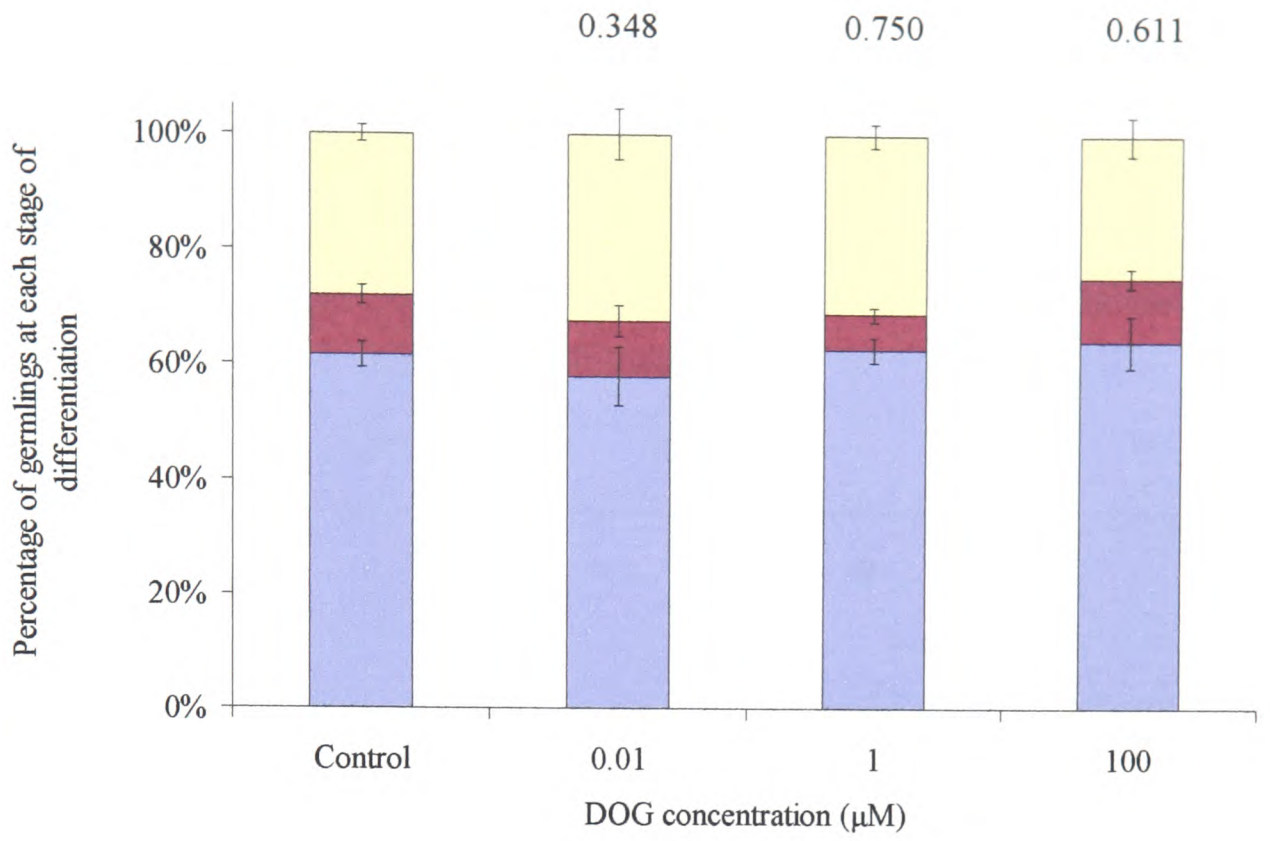


Figure 4.11. Differentiation of *Blumeria graminis* f.sp. *hordei* conidia on cellulose membrane overlying dioctanoyl-*sn*-glycerol (DOG), 24 hours post inoculation. ■ corresponds to conidia with short germ tubes, ■ corresponds to conidia having differentiated elongated germ tubes and ■ corresponds to conidia having differentiated either a swollen germ tube, or an appressorial germ tube. The results shown are representative of 3 independent experiments. In each experiment, 6 x 50 conidia were scored and the mean values of 50 conidia are illustrated. The control is 0.1% (v/v) DMSO. P-values showing the significance of differences in differentiation (that is, germlings that have differentiated elongated, swollen or appressorial germ tubes) compared to the control are given above each corresponding bar.

No. of replica	Concentration of DOG (μM)	P-values for germination	P-values for differentiation
1	100	0.211	0.611
	1	0.457	0.750
	0.01	0.375	0.348
2	100	0.023*	0.171
	1	0.865	0.102
	0.01	0.844	0.078
3	100	0.256	0.335
	1	0.936	0.281
	0.01	0.198	0.267

Table 4.3. P-values to show the significance between treatment of *Blumeria graminis* f.sp. *hordei* with dioctanoyl 1, 2-*sn*-glycerol (DOG) and the control (no DOG) for germination and differentiation on cellulose membrane. Controls were 0.1% (v/v) DMSO. For each repeat experiment, 6 x 50 conidia were scored for germination and 6 x 50 germlings were scored for differentiation, meaning the production of either an elongated germ tube or a swollen or appressorial germ tube. The results of three independent experiments are shown. * indicates $P \leq 0.05$, ** indicates $P \leq 0.01$ and *** indicates $P \leq 0.000$.

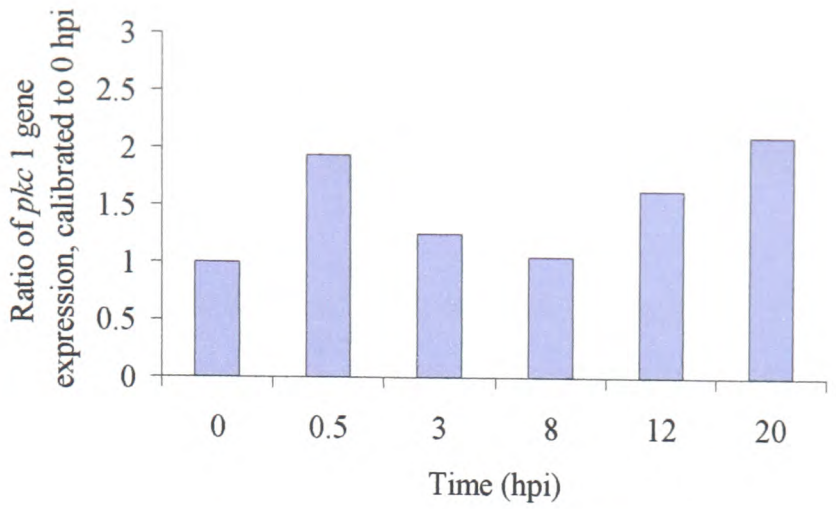
either side of a predicted intron to eliminate amplification of spurious genomic DNA.

Primer efficiencies were calculated by i) establishing the "crossing point" (CP) value (the point at which fluorescence rises appreciably above background fluorescence) of a two-fold dilution series of cDNA, ii) determining the gradient of the slope of the CP values and iii) calculating the efficiency value (*E*) using the equation $E=10^{[-1/\text{slope}]}$. The *E* values were used to calculate expression levels of *pkc*1 and *pkc*-like relative to the β-*tubulin* gene using the method described by Pfaffl *et al.* (2001).

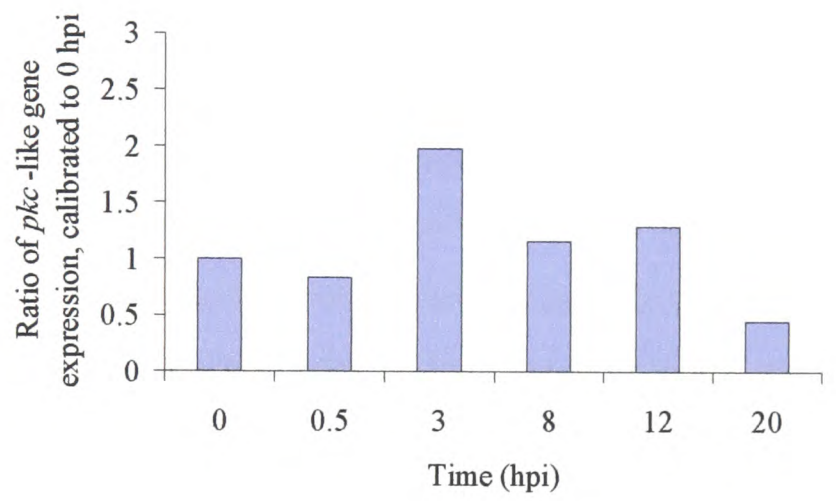
Real-time transcript profiles are shown in Figure 4.12(a). All values are relative to 0 h. For comparison, Figure 4.12(b) shows the end-point RT-PCR analysis of *pkc*1 and *pkc*-like as designed and performed by Ziguo Zhang (Zhang *et al.*, 2000; Zhang and Gurr, 2001). Here again, the *B. graminis* β-*tubulin* gene transcript was followed as an internal control for the equivalence of stage-specific 1st strand cDNA and equal amplification.

Figure 4.12(a.i) shows peaks in the *pkc*1 transcript profile at 0.5 hpi and 20 hpi, with a trough in transcript levels at 8 hpi. However, the real-time profile does not follow the same trend as the end-point RT-PCR profile in Figure 4.12(b). Specifically, the end-point RT-PCR profile shows that *pkc*1 transcripts are more abundant in the mature PGT-stage tissue (4 hpi) than in the mature AGT-stage (12 hpi) tissue, whereas at 3 hpi, *pkc*1 transcript levels were lower than those at 12 hpi in the real-time profile. Both profiles show that transcript levels of *pkc*1 are lowest in ungerminated conidia. For *pkc*-like, the real-time (Figure 4.12(a.ii) and end-point RT-PCR (Figure 4.12(b)) transcript levels are greatest in the mature PGT-stage tissue. However, again, the profiles do not correlate because the end-point RT-PCR shows no *pkc*-like transcripts in the ungerminated conidial tissue and AGT-stage tissue, whereas transcripts were detected in all stages tested in the real-time profile.

a(i)



a(ii)



b)

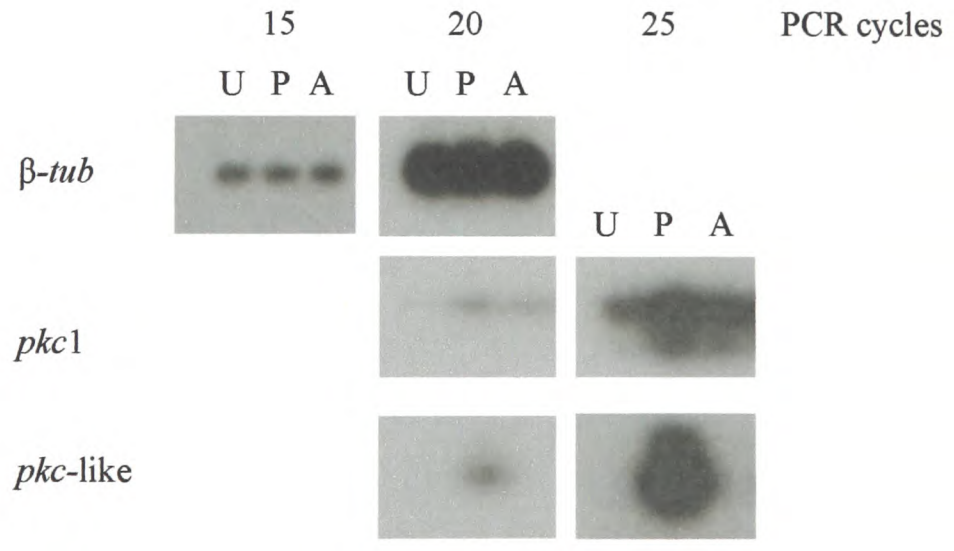


Figure 4.12. a(i) and a(ii) show transcript profiles of *Blumeria graminis* f.sp. *hordei pkc*1 and *pkc*-like on barley leaves at 0, 0.5, 3, 8, 12 and 20 hpi, elucidated using real-time RT-PCR. Expression levels are calibrated to β-*tubulin*. All values are expressed as ratios compared to 0 hpi. (b) End-point RT-PCR quantification of *B. graminis* β-*tubulin*, *pkc*1and *pkc*-like in ungerminated conidia (U); mature primary germ tube (P) and mature appressorial germ tube stage germlings (A), collected at 0, 4 and 12 hpi, respectively (Zhang *et al.*, 2001).

4.3 DISCUSSION

4.3.1 Identification of *pkc*1 and *pkc*-like genes in *Blumeria graminis* f.sp. *hordei*

PKC sequences from the filamentous fungi *N. crassa*, *T. reesei* (syn. *H. jecorina*), *A. niger*, *C. heterostrophus*, *M. grisea*, *S. schenckii*, *B. fuckeliana* and the truffle fungi *T. borchii* and *T. magnatum* carry the regulatory and catalytic domains separated by an elongate hinge region and with an extended amino terminus. None of them contain a calcium-regulated site motif but some authors argue that this region is substituted with a poorly conserved stretch of glutamine, proline and alanine residues ≈ 200 amino acids in length (designated C2-II) and which may be involved in binding other regulatory proteins (Courey and Tjian, 1988). In common with the mammalian PKC structure and with fungal PKCs generally, *B. graminis* PKC1 contains two conserved cysteine rich motifs and a pseudosubstrate site (Figure 4.1). The evidence for a Q/A/P region the *B. graminis* PKC1 sequence is tenuous, with this region carrying only 10% glutamine residues, 10% proline and 9.5% alanine residues. Within the extended *B. graminis* PKC1 amino-terminus lie conserved subdomains, designated CN1 and CN2, described in *T. borchii* and *T. magnatum* by Ambra and Macino (2000). Secondary structure predictions of the two subdomains CN1 and CN2 reveal two hydrophobic helices which may interact with cellular membranes (Ambra and Macino, 2000). In *B. graminis* regions close to, or indeed overlapping, putative CN1 and CN2 motifs reveal two rho-binding sites.

All Euoascomycete fungal PKC sequences determined to date reveal that they carry putative rho motifs (Figure 4.2). Rho belongs to the small G protein superfamily, which consists of the Rho, Rac and Cdc42 families (Hall, 1994; Takai *et al.*, 1995), and cycles between the GDP-bound inactive state, and the GTP-bound active form. In *S. pombe*, GTP-bound Rho1p and Rho2p interact with Pck1p and Pck2p by binding to two N-terminal HR1 motifs, resulting in an increase in stability of both kinases (Arellano *et al.*, 1999; Sayers *et al.*, 2000). In *S. cerevisiae*, Rho1p is required for the dynamic spatial and temporal localisation

of Pkc1p to sites of polarised growth and cell wall damage. Thus, Rho GTPases are required for PKC activation in yeasts although the precise mechanism has yet to be elucidated (reviewed by Perez and Calonge, 2002). However, activation results in the maintenance of cell wall integrity and regulation of the actin cytoskeleton polarity by controlling signalling through a MAP kinase cascasde (Nonaka *et al.*, 1995; Zhao *et al.*, 1998). Nothing is currently known about rho proteins in *B. graminis*. However, the role of the MAP kinase signalling pathway in early differentiation events in *B. graminis* will be discussed in detail in Chapter 5.

The *B. graminis* PKC-like sequence represents a truncated PKC-like gene, comprising a protein kinase domain within which lies an ATP-binding signature motif and serine-threonine protein kinase active site signature sequence. A short *pkc*-like gene has also been revealed in *Colletotrichum trifolii* (Dickman *et al.*, 1995) and shows increased expression levels upon germination. However, its function remains to be determined.

4.3.2 *pkc*1 and *pkc*-like phylogeny

Phylogenetic analysis places *B. graminis* PKC1 closest to *Botryotina fuckeliana* PKC. Furthermore, all structural features described herein place the *B. graminis* PKC1 between the "classical" and "novel" classes of mammalian PKCs. The closest neighbours to PKC-like, in a phylogenetic sense, are serine/threonine kinases of *Homo sapiens*, *Mus musculus* and *Schizosaccharomyces pombe* and the kinase domains of the mammalian PKC zeta and iota sequences.

4.3.3 The effect of inhibitors on *Blumeria graminis* f.sp. *hordei*

In order to investigate the potential role of PKC during the early development of *B. graminis* f.sp. *hordei*, various compounds were assessed for their ability to influence *B. graminis* activity *in vitro*. Inhibitors screened for their ability to inhibit *B. graminis* PKC activity were chosen on the basis of their target sites. That is, the catalytic domain-targeting inhibitors (including bisindolylmaleimide I-HCl, the bisindolylmaleimide-related inhibitor Go6983, chelerythrine chloride,

HA-100, H7 and staurosporine) and the regulatory (C1 domain) domain-targetting PKC inhibitors (including calphostin C). Indeed, a pharmacological approach has been used to study PKC in both *N. crassa* and *C. trifolli* (Dickman *et al.*, 1995; Arpaia *et al.*, 1999). Specifically, H7 inhibited spore germination in *C. trifolli* (Dickman *et al.*, 1995) and use of calphostin C and chelerythrine chloride implicated PKC as a component of the light transduction machinery in *N. crassa* (Arpaia *et al.*, 1999). Nevertheless, none of the mammalian inhibitors assayed showed specificity to *B. graminis* PKC.

Due to a high level of conservation of the PKC catalytic site (Bosemeyer, 1995), inhibitors targeted to this are usually highly toxic (Herbert *et al.*, 1990; Tamaoki *et al.*, 1986; Toullec *et al.*, 1991). However, a high level of conservation of the PKC catalytic domain means that the specificity of inhibitors targeting this domain may be poor. Specifically, staurosporine, balanol analogues, phenylaminopyrimidines and rotterlin inhibit protein kinases non-specifically (Brose and Rosenmund, 2002). Although, there are some, including the bisindolylmaleimides and their derivatives, that are rather PKC specific, some even showing preference for certain isozymes (Brose and Rosenmund, 2002). In contrast to the catalytic domain-targetting PKC inhibitors, regulatory domain-targetting inhibitors of PKC were thought to be highly selective for PKC compared to other kinases since the regulatory domain is not as highly conserved as the PKC catalytic domain. However, inhibitors such as the C1 domain-targetting calphostin C, which was once one of the most widely used PKC inhibitors (reviewed in Barry and Kazanietz, 2001) may bind with comparable affinity to other C1 domain proteins (Brose and Rosenmund, 2002).

Although the PKC activity identified in this work cannot be attributed to any specific PKC within *B. graminis*, the structures of the *B. graminis* PKCs described herein may give some indication for the lack of specific inhibition by the mammalian inhibitors. Specifically, PKC1 and PKC-like represent novel forms when compared to the mammalian PKCs (discussed above) which may impose a

conformation in the tertiary structure of these proteins which causes the mammalian PKC-targetting inhibitors to not gain access to their target sites.

4.3.4 The effect of PKC agonists on *Blumeria graminis* f.sp. *hordei* PKC activity and germling development

Two PKC agonists were used in this study, the diacylglycerol, dioctanoyl 1,2-*sn*-glycerol (DOG), and the phorbol ester, phorbol 12, 13-myristate acetate (PMA). Diacylglycerols are glycerol derivatives in which two hydroxyl groups are substituted by fatty acids through ester bond formation (Brose and Rosenmund, 2002). Most of the work on DAGs to-date has been in mammalian systems where, under equilibrium conditions, biological membranes contain very little DAGs. However, their production is stimulated upon activation of a multitude of cellular signalling cascades, and DAGs produced by these mechanisms act as key second messengers to modulate the function of at least six different types of target protein, the most prominent of which belongs to the PKC family (Wakelam, 1998; Hodkin *et al.*, 1998; Goni and Alonso, 1999). Phorbol esters are functionally analogous to DAGs, and are natural diterpene secondary metabolites of *Euphorbiaceae* and *Thymelaceae* (Brose and Rosenmund, 2002). In comparison with phorbol esters, efficacy and specificity of alternative PKC activators are much lower (Way *et al.*, 2000).

Exogenous application of the phorbol ester, PMA, invoked PKC activity when assayed with protein extracts of conidia or germlings. Furthermore, PMA enhanced the number of germlings able to differentiate AGTs on cellulose membrane. Interestingly, higher PMA concentrations (1 μM) did not enhance PKC substrate phosphorylation as much as lower concentrations (1 nM and 10 pM). This could be due to the use of relatively crude protein extracts in which activation of phosphatases or proteases may occur.

The importance of the diacylglycerols in PKC signal transduction in *B. graminis* could not be demonstrated, perhaps because unlike diacylglycerols, phorbol esters are not as rapidly metabolised and treatment of cells with phorbol ester results in

prolonged activation of PKC (Asaoka *et al.*, 1992; Nishizuka, 1992). However, Staples and Hoch (1987) induced infection structure development in *Uromyces appendiculatus* by the exogenous application of diacylglycerols, including 1, 2-dipalmitoyl-*sn*-glycerol. More recently, Thines *et al.* (1997a, b) invoked the activation of PKC in *M. grisea* appressorum differentiation by the addition of the diacylglycerol 1, 2-dioctanoyl-glycerol (DOG). Moreover, they found that glisoprenin A, a fungal metabolite of *Gliocladium roseum*, blocks appressorial differentiation in *M. grisea* of hydrophobic surfaces, and that DOG reversed this inhibition in a competitive manner. Glisoprenin A does not, however, inhibit induction by cAMP (Thines *et al.*, 1997a), suggesting that more than one signal transduction pathway is involved in appressorium differentiation.

Until recently, phorbol ester and DAG were thought to compete directly for a common binding site on PKC (Sharkey *et al.*, 1984; Sharkey and Blumberg, 1985). However, Slater *et al.*, (1996) proposed that DAG and phorbol ester have discrete low and high affinity binding sites on PKC indicating that natural regulators of PKC activity can potentially bind simultaneously, raising the possibility that PKC may function as an "integrator" of independent signalling pathways.

Modulation of cellular processes by DAG and phorbol esters has often been attributed exclusively to activation of PKCs. However, this reasoning has recently been called into question because most eukaryotic cells contain five alternative types of DAG targets including chimaerins, protein kinase D1 (PKD1), RasGRPs, Munc13s and DAG kinase γ (reviewed in Brose and Rosenmund, 2002). Brose and Rosenmund (2002) indicate that the relevance of non-PKC DAG receptors in the DAG second messenger pathway is appreciated only by a rather small circle of experts in DAG signalling, but is otherwise ignored. Also, they argue that the pharmacological tools that are used to study PKC function are not sufficiently specific to exclude the involvement of other DAG targets in cellular processes that are thought to be mediated by modulatory effects of DAG or phorbol esters on

PKCs. Moreover, the alternative DAG target proteins are also able to bind phorbol esters with PKC-like affinity (Brose and Rosenmund, 2002).

Thus, the most frequently used pharmacological tools for PKC activation and inhibition are not sufficiently specific alone to define PKC-mediated physiological effects unequivocally – particularly the separation of PKC-mediated effects from those caused by other C1 domain proteins or by other kinases. PKC-isozyme-specific inhibitor and activator peptides and antisense oligonucleotides are the most promising tools to overcome the problems of non-specific inhibitors and activators (Brose and Rosenmund, 2002).

4.3.5 *pkc*1 and *pkc*-like gene expression profiles

End-point RT-PCR transcript profiles have previously shown that *pkc*1 and *pkc*-like are differentially regulated during germling morphogenesis (Zhang *et al.*, 2001). In this study, a real-time PCR approach was used to assess the relative abundance of transcripts at six time points throughout germling differentiation. Real-time PCR revealed elevated *pkc*1 transcript levels upon conidial germination. The real-time profile shows a peak in transcript levels just prior to PGT emergence (0.5 hpi), and later in morphogenesis (*i.e.* 20 hpi) to similar levels of expression. The elevation in transcript levels upon germination correlates with the pattern of expression of a *Neurospora crassa PKC* gene which shows low transcriptional activity in dormant spores but elevated transcript levels during germination (Oved and Yarden, 1996).

For *pkc*-like, the real-time transcript levels are greatest in the PGT-stage tissue. This agrees with expression data from *C. trifolii*, which reveals high levels of transcript abundance during germination for a PKC-like gene (Dickman *et al.*, 1995). In addition, the *B. graminis pkc*-like transcript profile appears to follow the same trend as the catalytic subunit of PKA (*cpka*) (Zhang *et al.*, 2001), which has the greatest abundance of transcripts in the mature PGT tissue, but basal levels in the ungerminated conidia and in the mature AGT tissue. cAMP signalling and protein kinase A (PKA) have been demonstrated to play a role in *B. graminis*

conidial differentiation (Hall *et al.*, 1999). Kinane *et al.* (2000) revealed peaks in cAMP levels and PKA activity just prior to the emergence of the PGT and AGT. Hall and Gurr (2000) showed that cAMP signalling must be active to trigger AGT development but inactive during subsequent appressorial germ tube hooking. Taken collectively, these data reveal not only the presence of cAMP-dependent protein kinase activity in *B. graminis* but also support the role for protein phosphorylation, possibly modulated by PKA, and its involvement in conidial morphogenesis. However, the work also highlights that cAMP alone is not able to trigger the complete programme of differentiation in this obligate biotroph. Additional signal transduction pathways, such as signalling via PKC or a MAP kinase cascade (Zhang and Gurr, 2001) may be required.

4.3.6 Summary

In conclusion, two genes, *pkc*1 and *pkc*-like, have been characterized from *B. graminis* f.sp. *hordei*. PKC activity has been detected in conidia and PGT stage tissue of *B. graminis*. However, no inhibitor was found that was specific or potent enough to *B. graminis* PKC to warrant further investigations of the potential role of PKC on germling morphogenesis using antagonists. However, it has been shown that the PKC agonist PMA can invoke both germling morphogenesis and boost PKC activity in spore and PGT stage extracts. In addition, real-time PCR confirms the differentially regulated transcript profiles of both *pkc*1 and *pkc*-like, and reveals a peak in transcript levels just prior to PGT emergence (0.5 hpi) in *pkc*1, with transcript abundance gradually falling to a low during AGT elongation and swelling (8 hpi), and subsequently rising thereafter. Transcripts of *pkc*-like, however, show a peak during PGT differentiation (3 hpi).

CHAPTER 5
THE ROLE OF MITOGEN-ACTIVATED PROTEIN KINASES IN THE EARLY DEVELOPMENT OF *BLUMERIA GRAMINIS* F.SP. *HORDEI*

5.1 INTRODUCTION

5.1.1 Mitogen-activated protein kinase

Mitogen-activated protein (MAP) kinase cascades are among the most thoroughly studied of signal transduction systems. Evolutionarily conserved in all eukaryotes, MAP kinase cascades are known to participate in a diverse array of cellular processes, including differentiation, development, division and death, playing a key rôle in the regulation of gene expression as well as cytoplasmic activities (Schaeffer and Webber, 1999). MAP kinases are a group of serine/threonine kinases that are activated by a diversity of extracellular stimuli, mediating signal transduction from the cell surface to the nucleus through a series of phosphorylation events. They are typically organized in a three-kinase cascade module consisting of a MAP kinase (MAPK), a MAP kinase activator (MEK, MKK, or MAPK kinase), and a MEK activator (MEK kinase [MEKK] or MAPK kinase kinase). Classification of the MAP kinases in mammals and yeasts is according to the pathways in which they participate and also by the identity of the amino acid between tyrosine (Tyr) and threonine (Thr) residues in the activation loop of the enzyme: Glu, Pro, or Gly in mammals, and Glu, Gly, or Asn in yeast (Gustin *et al.*, 1998).

5.1.2 MAP kinase activation and structure

MAP kinases exist in an inactive, dephosphorylated form in quiescent cells. Activation of the MAP kinase cascade occurs upon reception of extracellular signals such as pheromones, mitogens, osmotic stress, UV stress, and cytokines (Caffrey *et al.*, 1999). The signal that leads to activation of the MAP kinase cascade is perceived by a variety of receptors: G-protein coupled receptors, seven-transmembrane receptors, receptor-tyrosine kinases, and integral membrane

proteins (reviewed in Herskowitz, 1995). MAP kinase itself is activated by phosphorylation of two closely-spaced tyrosine and threonine residues (Thr-X-Tyr) found in the catalytic domain (Banuett, 1998).

The components of the MAP kinase module are related to other kinases by virtue of their catalytic domains, which consist of approximately 250 to 300 amino acid residues (Hanks and Hunter, 1995). As with all kinases, the catalytic domain of MAP kinases can be subdivided into 12 conserved domains within which 12 residues are invariant or highly conserved, indicating that these may be critical for activation. The Thr-X-Tyr activation domain is located in catalytic subdomain VIII. The three-dimensional structures of both inactive (Zhang *et al.*, 1994) and active forms of the mammalian MAP kinase, ERK2, have been solved by X-ray crystallography and reveal that upon activation by dual phosphorylation on Thr183 and Tyr185, the activation lip of ERK2 undergoes a conformational change, thereby creating a surface pocket that is specific for proline. MAP kinases are proline-directed and recognize a proline of a potential substrate (Schaeffer and Weber, 1999). Interestingly, this proline-specific pocket is occupied by the side chain of Arg192 when ERK2 is in an inactive state. Therefore, access of proline to the catalytic specificity pocket is blocked when the enzyme is not activated, and a productive enzyme-substrate interaction cannot take place (Canagarajah, 1997).

Once the MAP kinase has been activated in the cytoplasm, the MAP kinase may translocate into the nucleus where the target of activation of the MAP kinase is, in most instances, a transcription factor (Banuett, 1998). Phosphorylation of transcription factors is thought to increase their binding affinity, activation ability or cellular location, resulting in an increase in transcriptional activation of target genes. An example of MAP kinase transcriptional activation is the regulation of the *S. cerevisiae* transcription factor STE12 by both FUS3 and KSS1 to induce genes specific to mating or filamentous growth (Schaeffer and Weber, 1999). Alternatively, the MAP kinase may translocate to other cytoplasmic sites to phosphorylate specific enzymes or cytoskeletal components or other signalling components (Lewis *et al.*, 1998).

Inappropriate cross-talk between the different MAP kinase modules is prevented by two mechanisms. First, scaffold proteins create multi-enzyme complexes that bring together components of a single kinase cascade (reviewed in Whitmarsh and Davis, 1998). These complexes insulate the module from activation by irrelevant stimuli and favour the rapid transmission of the signal through the cascade. Second, specific docking sites on MAP kinases, which serve for the binding of substrates, activators and regulators, increase the fidelity and the efficiency of the enzymatic reactions.

5.1.3 ERKS, JNKs and p38 MAP kinases

In multicellular organisms, there are three well-characterized subfamilies of MAP kinases (reviewed in Johnson and Lapadat, 2002). These MAP kinases include the extracellular signal-regulated kinases (p42/p44 MAP kinases), ERK1 and ERK2; the c-Jun NH_2-terminal kinases, JNK1, JNK2, and JNK3; and the four p38 enzymes, p38α, p38β, p38γ and p38δ. ERK1 and ERK2 are widely expressed and are involved in the regulation of meiosis, mitosis, and postmitotic functions in differentiated cells. The JNKs were isolated and characterized as stress-activated protein kinases on the basis of their activation in response to inhibition of protein synthesis (Kyriakis, *et al.*, 1994). The p38 MAP kinases regulate the expression of many cytokines and are activated by many stimuli, including hormones, ligands for G protein-coupled receptors, and stresses such as osmotic shock and heat shock (Johnson and Lapadat, 2002).

5.1.4 MAP kinase inhibitors

The ERK, JNK, and p38 pathways have all been implicated as having roles in tumour development and have been found to be switches for genes that control a variety of diseases (Johnson and Lapadat, 2002). This knowledge has led to an intense effort over the last decade to develop potent, small molecule MAP kinase inhibitors for the investigation of MAP kinase pathways and for the development of drugs (English and Cobb, 2002). In particular, MAP kinase kinases (MEKs) are attractive targets for therapeutic intervention because of their unusually restricted substrate specificities in that they phosphorylate and regulate only a very small

number of downstream MAP kinases (English and Cobb, 2002). Due to the complex nature of MAP kinase pathways and the multiplicity of the various enzymes that undergo simultaneous alterations of their structure or functions, it is important to develop biochemical reagents that are highly specific and highly selective to individual enzymes in the signalling pathway. For example, PD98059 and U0126 represent highly selective MAP kinase signal cascade inhibitors that are proving to be invaluable tools in elucidating the roles of the MAP kinase cascades in a variety of biological contexts (Dudley *et al.*, 1995; Favata *et al.*, 1998).

5.1.5 MAP kinases and fungi

Due to extensive genetic and biochemical research, our knowledge of the *S. cerevisiae* MAP kinase pathways is more complete than that of MAP kinase pathways in other organisms (Gustin *et al.*, 1998). Five functionally distinct cascades have been identified in *S. cerevisiae*: the mating pathway, the filamentation-invasion pathway, the cell integrity pathway, the high-osmolarity growth pathway and the spore wall assembly pathway (reviewed in Banuett, 1998; Gustin *et al.*, 1998; Herskowitz, 1995). *Schizosaccharomyces pombe* carries a set of MAP kinase cascades that have some similarity to those in *S. cerevisiae* (Gustin *et al.*, 1998).

Knowledge of the yeast MAP kinases has been instrumental in our understanding of MAP kinases in other eukaryotes, particularly other fungi (reviewed in Xu, 2000). Indeed, MAP kinases have recently been shown to be important for pathogenesis in several fungal pathogens including *Claviceps purpurea* (Mey *et al.*, 2002a, b), *Pyrenophora teres* (Ruiz-Roldan *et al.*, 2001), *Botrytis cinerea* (Zheng *et al.*, 2000), *Fusarium oxysporum* (Di Pietro *et al.*, 2000), *Colletotrichum lagenarium* (Kojima *et al.*, 2002; Takano *et al.*, 2000), *Candida albicans* (Alonso-Monge *et al.*, 1999; Csank *et al.*, 1998; Navarro-Garcia *et al.*, 1995), *Pneumocystis carinii* (Fox and Smulian, 1999), *Cochliolobus heterotrophus* (Lev *et al.*, 1999), *Magnaporthe grisea* (Xu and Hamer, 1996; Xu *et al.*, 1998),

Ustilago maydis (Mayorga and Gold, 1999; Muller *et al.*, 1999) and *Fusarium solani* f.sp. *pisi* (Li *et al.*, 1997).

Three MAP kinase genes have been characterised in the "model" pathogenic fungus *M. grisea* so far: *PMK1* (Pathogenicity MAP Kinase), *MPS1* (MAP Kinase for Penetration and Sporulation) and *OSM1* (Osmotic Sensitivity MAP kinase). PMK1, which is homologous to *S. cerevisiae FUS2/KSS1* (Xu and Hamer, 1996), is not essential for vegetative growth, or sexual and asexual reproduction. It is, however, essential for appressorial formation and thus pathogenesis. *MPS1*, a homologue of *S. cerevisiae SLT2*, is not essential for appressorial formation, but is required for penetration of the host cuticle, sporulation and cell wall integrity (Xu *et al.*, 1998). *OSM1*, a homologue of *S. cerevisiae HOG1* regulates growth under high osmolarity conditions but is dispensable for pathogenesis (Dixon *et al.*, 1999).

PMK1/FUS3 homologues have been isolated and functionally analysed in several phytopathogenic fungi: *U. maydis UB3/KPP2* (Mayorga and Gold, 1999; Muller *et al.*, 1999), *C. heterostrophus CHK1* (Lev *et al.*, 1999), *Colletotrichum lagenarium CMK1* (Takano *et al.*, 2000), *B. cinerea BMP1* (Zheng *et al.*, 2000), *Fusarium oxysporum* f.sp. *lycopersici FMK1* (Di Pietro *et al.*, 2001), *P. teres PTK1* (Ruiz-Roldan *et al.*, 2001) and *Claviceps purpurea CPMK1* (Mey *et al.*, 2002a). *C. lagenarium CMK1*, *C. heterotrophus CHK1* and *P. teres PTK1* are essential for appressorial formation, and, in the non-appressorial-producing fungi, *B. cinerea BMP1* and *F. oxysporum FMK1* are essential for pathogenicity (Lev *et al*, 1999; Takano *et al*, 2000; Ruiz-Roldan *et al.*, 2001; Zheng *et al.*, 2001; Di Pietro *et al.*, 2000).

In contrast, few *MPS1/SLT2* homologues have been isolated from phytopathogenic fungi. *C. lagenarium MAF1* is essential for conidiation, appressorial formation and pathogenicity (Kojima, 2002). *C. purpurea CPMK2* is essential for conidiation, however, deletion mutants retain a limited ability to colonize host tissue (Mey *et al.*, 2002b). *Fusarium graminearum MGV1* is

required for female fertility, heterokaryon formation, and plant infection (Hou *et al.*, 2002).

Analysis of signalling pathways in fungi has revealed that interactions frequently exist between MAP kinase pathways and other signalling pathways (reviewed in Kronstad, 1997; Kronstad *et al.*, 1998; Madhani and Fink, 1998; Xu, 2000). In particular, interactions are thought to occur between MAP kinase pathways and cAMP signalling pathways in mating, morphogenesis, virulence and stress response. Of the phytopathogenic fungi, such interactions have been best studied in *U. maydis* and *M. grisea*. For instance, in *M. grisea*, addition of exogenous cAMP to the MAP kinase mutant, Δ*pmk1*, which are unable to form appressoria, restores the early stages of appressorium formation, indicating a connection between the two pathways (Xu and Hamer, 1996). In addition, the *M. grisea MPS1* MAP kinase is thought to act downstream of a *PKC* to regulate appressorial wall synthesis and deposition (Xu *et al.*, 1998).

5.1.6 *Magnaporthe grisea* as a "surrogate host"

In studies of infection processes in phytopathogenic fungi performed to date, *M. grisea* has proved to be a very useful tool. Appressorium formation in *M. grisea* has been extensively studied thanks to the experimental tractability of the fungus. Furthermore, the process can be followed *in vitro* using artificial and plant surfaces, and various studies have described, in detail, the morphogenetic changes that take place during appressorium development (Howard and Valent, 1996). Thus, appressorium-defective mutants can be characterised and their defects can be assigned to a particular stage of the formation or function of the appressorium (Hamer and Talbot, 1998). Such knowledge has helped to characterise the MAP kinases of various phytopathogenic fungi, where *M. grisea* has served as a "surrogate host" for, in particular, complementation experiments. *M. grisea* will prove especially useful in subsequent experiments in this thesis for the study of infection structure development in *B. graminis*, being employed for *in vivo* experiments (this Chapter) and functional complementation experiments (Chapter 6).

5.1.6 Objectives

This chapter describes the identification and characterisation of two *Blumeria graminis* f.sp *hordei* MAP kinase genes, named *mpk*1 and *mpk2*, and the subsequent detection of MAP kinase activity in *B. graminis* spore protein extracts. The putative involvement of MAP kinase in the early development of *B. graminis* was investigated by observing the effects of MAP kinase antagonists on germling differentiation. Furthermore, the transcript profiles of *mpk*1 and *mpk2* at critical stages of *B. graminis* germling morphogenesis were determined using real-time PCR.

5.2 RESULTS

5.2.1 Identification of *mpk*1 and *mpk*2 genes in *Blumeria graminis* f.sp. *hordei*

Three partial *B. graminis* f.sp. *hordei* MAP kinase gene sequences were obtained by Ziguo Zhang (University of Oxford) by designing degenerate primers to four conserved domains (HRDLKP; CDFGLAR; WYRAPE; WSVGCI) of 24 fungal MAP kinase sequences deposited in the NCBI database (Zhang and Gurr, 2001). Fragments derived from PCR amplification of cDNA species from the ungerminated conidial, PGT and AGT stages of germling morphogenesis were directly sequenced, and the full-length genomic sequences of two genes, designated *mpk*1 and *mpk*2 obtained using 'Step down' PCR (all performed by Z. Zhang), a walking technique described by Zhang and Gurr (2000). Southern analysis revealed both genes to be present as single copies within the *B. graminis* genome (performed by Z. Zhang).

*B. graminis mpk*1 (Accession number AF301165) has an open reading frame of 1068 bp, with three introns of 64-142 bp in length. The predicted amino acid sequence, deduced from the full-length genomic clone, is of 356 amino acid residues with a molecular weight of 41 kDa. Analysis of *B. graminis mpk*2 (AF301166) revealed a 1230 bp ORF, with four short introns of 49-53 bp, encoding a predicted protein of 410 amino acids with a molecular weight of 46.6 kDa. All introns from the two MAP kinases carry the consensus 5'GT/3'AG splice sites (Gurr *et al.*, 1987).

The two *B. graminis* MAP kinase amino acid sequences were subjected to BLAST (Altschul *et al.*, 1997) and 'Prosite ProfileScan' (Bioinformatics Group of Swiss Institute for Experimental Cancer Research) searches. Figure 5.1 shows an alignment of MPK1 and MPK2 alongside the amino acid sequences of *Botrytis cinerea* BMP1 (AAG23132), *Magnaporthe grisea* PMK1 (AAC49521) and MPS1 (AAC63682), *Colletotrichum lagenarium* CMK1 (AAD50496), *Claviceps purpurea* CPMK1 (CAC47939), *Saccharomyces cerevisiae* KSS1 (P14681) and SLT2 (AAB26249), and *Homo sapiens* ERK1 (AAK52329). The amino acid sequences of *B. graminis* MPK1 and MPK2 contain all the invariant kinase consensus sequences characteristic of the 11 conserved serine/threonine protein

```
                                                
```

```
                                                                XI
MgPMK1   268 FKKKVPFRTLFPKTSD--LALDLLEKLLAFNPVKRITVEEALKHPYLEPYHDPDDEPTAP
ClCMK1   267 FKKKVPFRTLFPKTSD--LALDLLEKLLAFNPVKRITVEDALKHPYLEPYHDPDDEPTAP
CpCPMK1  267 FKKKVPPRVLFPKTSD--LALDLLEKLLAFNPVKRITVEEALKHPYLEPYHDPDDEPTAP
BcBMP1   267 FKKKVPFKTMFPKTSD--LALDLLEKLLAFNPVKRITVEEALKHPYLEPYHDPEDEPTAN
BgMPK1   268 SRRRFPSNKCFPKTSD--LALDLLEKLLAFNPVKRITVDEALQHPYLEPYHDPEDEPTAD
ScKSS1   267 MRPPLPWETVWSKTDLNPDMIDLLDKMLQFNPDKRISAAEALRHPYLAMYHDPSDEPEYP
HsERK1   286 SKTKVAWAKLFPKSDS--KALDLLDRMLTFNPNKRITVEEALAHPYLEQYYDPTDEPVAE
BgMPK2   270 FMAKRPFAQIFPNANP--DALDLLNRMLAFDPASRISVEEALEHPFLQIWHDVSDEPCCP
MgMPS1   270 FMAKKPFPTLFPNANP--DALDLLDRMLAFDPSSRISVEQALEHPYLHIWHDASDEPDCP
ScSLT2   274 FIPKVPFVNLYPNANS--QALDLLEQMLAFDPQKRITVDEALEHPYLSIWHDPADEPVCS

MgPMK1   326 --PIPEEFFDFD------KHKDNLSKEQLKQFIYQEIMR--------------------
ClCMK1   325 --PIPEEFFDFD------KHKDNLSKEQLKQLIYQEIMR--------------------
CpCPMK1  325 --PIPEAFFDFD------KHKDNLSKEQLKLLIYEEIMR--------------------
BcBMP1   325 --PIPEEFFDFD------KNKDNLTKEQLKKLIYDEIMR--------------------
BgMPK1   326 --PIPEEFFDFD------KNKDNLSKEQLKELIFQEIMR--------------------
ScKSS1   327 PLNLDDEFWKLDNKIMRPEEEEEVPIEMLKDMLYDELMKTME------------------
HsERK1   344 ------EPFTFA------MELDDLPKERLKELIFQETARFQPGVLEAP------------
BgMPK2   328 ------TTFNFD-------FEVTDDVGEMRKMILDEVARFRHHVRVQPGMQSP-------
MgMPS1   328 ------TTFNFD-------FEVVEDVGEMRKMILDEVYRFRQLVRTAPGAGGHGAPH---
ScSLT2   332 ------EKFEFS-------FESVNDMEDLKQMVIQEVQDFRLFVRQPLLEEQRQLQLQQQ

MgPMK1       ------------------------------------------------------------
ClCMK1       ------------------------------------------------------------
CpCPMK1      ------------------------------------------------------------
BcBMP1       ------------------------------------------------------------
BgMPK1       ------------------------------------------------------------
ScKSS1       ------------------------------------------------------------
HsERK1       ------------------------------------------------------------
BgMPK2   368 ------------------------------------------------------------
MgMPS1   372 ------------------------------------------------------------
ScSLT2   379 QQQQQQQQQQQQQPSDVDNGNAAASEENYPKQMATSNSVAPQQESFGIHSQNLPRHDADF

MgPMK1       ------------------------------------------
ClCMK1       ------------------------------------------
CpCPMK1      ------------------------------------------
BcBMP1       ------------------------------------------
BgMPK1       ------------------------------------------
ScKSS1       ------------------------------------------
HsERK1       ------------------------------------------
BgMPK2   368 SNDPSVPTLQTSVAWGSEDPRPQENNDQEITGLERDLTVGLDR---
MgMPS1   372 APQVPIPAGAGQGQWKAEDPRPQEYVG-QMNDLEAELAGGLDQRR-
ScSLT2   439 PPRPQESMMEMRPATGNTADIPPQNDNGTLLDLEKELEFGLDRKYF
```

Figure 5.1. Amino acid sequence data of *Blumeria graminis* f.sp. *hordei* MPK1 (AAG53654) and MPK2 (AAG53655). The relatedness of MPK1 and MPK2 to other fungal MAP kinases with aligned sequences of *Botrytis cinerea* BMP1 (AAG23132), *Magnaporthe grisea* PMK1 (AAC49521) and MPS1 (AAC63682), *Colletotrichum lagenarium* CMK1 (AAD50496), *Claviceps purpurea* CPMK1 (CAC47939), *Saccharomyces cerevisiae* KSS1 (P14681) and SLT2 (AAB26249), and *Homo sapiens* ERK1 (AAK52329). Black boxes indicate identical residues, shaded boxes indicate similar residue. The 11 protein kinase domains are labeled with Roman numerals.

kinase subdomains (Hanks *et al.*, 1998) (Figure 5.1). Specifically, the MPK1 and MPK2 polypeptides contain the DLxxxN motif in subdomain VI (DLKPSN in MPK1 and DLKPGN in MPK2) and, in subdomain VIII, TEYVATRWYRAPE and TEYVATRWYRAPE in MPK1 and MPK2, respectively, that is, a variation on the TxYxxTxxYxAxE motif. Both these subdomains are characteristic of the ERK family of serine/threonine kinases. The tripeptide TEY, within subdomain VIII of both MPK1 and MPK2, may represent the putative target for stimulatory threonine and tyrosine phosphorylation in the MPK by the upstream MAPK kinase. The consensus catalytic subdomain XI, carrying nine residues DLxxxxLxxxPxKRxxxxxxLxHP, is highly conserved amongst tyrosine-autophosphorylating protein kinases, and appears exactly in *B. graminis* MPK1 and a near copy in MPK2, where S substitutes the K residues at position 13. Furthermore, the deduced amino acid sequence of *B. graminis* MPK2 carries all of the 11 conserved tyrosines and prolines found in the MAP kinase homologues of yeast, rats and *Xenopus* and in filamentous fungi (Li *et al.*, 1997).

5.2.2 *mpk*1 and *mpk*2 phylogeny

The *B. graminis* MPK1 and MPK2 amino acid sequences were compared with other MAP kinase amino acid sequences from yeast, filamentous fungi and other pathogenic fungi. Also included in the comparison was *B. graminis* HOG1 (Ziguo Zhang, unpublished), a homologue of the *S. cerevisiae* HOG1, and *M. grisea* OSM1. *S. cerevisiae* HOG1 is essential for maintaining the osmotic gradient across the plasma membrane of yeast cells grown under hypertonic conditions (Nevoigt and Stahl, 1997), and *M. grisea* OSM1, a functional homologue of *S. cerevisiae HOG1*, controls the accumulation of the compatible solute arabitol in mycelia, (Dixon *et al.*, 1999). Figure 5.2 shows a neighbour-joining phylogenetic tree (Thompson *et al.*, 1997) which reveals distinct lineages that separate the MAP kinases into three clades. *B. graminis* MPK1 is shown to be most closely related to *Botryotina cinerea* (teleomorph *Botrytis fuckeliana*) BMP1, sharing an identity of 90%, and lies within the clade that also carries *Colletotrichum lagenarium* CMK1 (Takano *et al.*, 2000) and *Pyrenophora teres* PTK1 (Ruiz-Rolan *et al.*, 2001) which also share 90% identity with MPK1; *Magnaporthe grisea* PMK1 (Xu and Hamer, 1996), *Colletotrichum gloeosporioides* CGK1 (BAB21569) and *Fusarium oxysporum* FMK1 (AF286533) which all share 89%

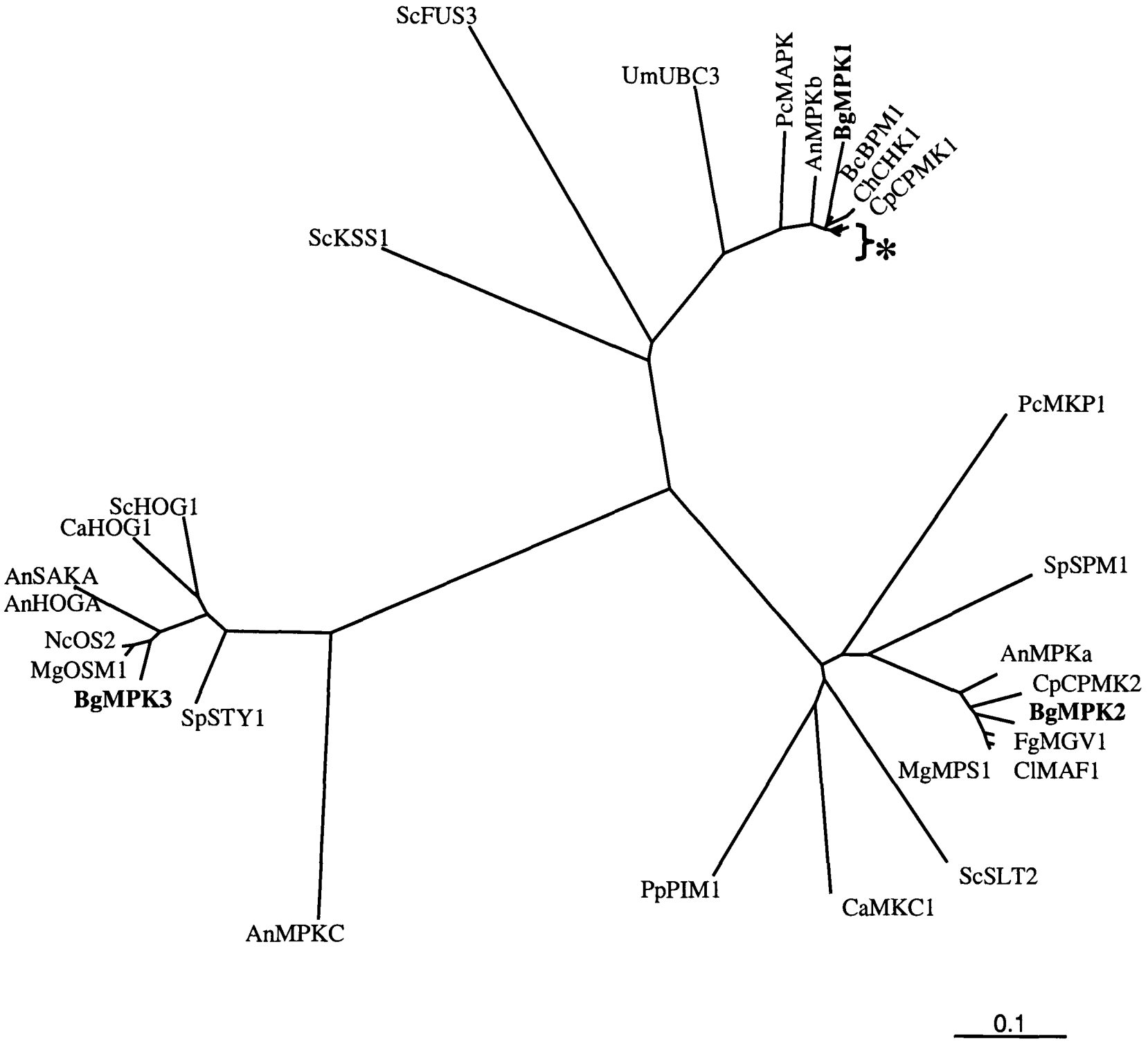


Figure 5.2. Relatedness of *Blumeria graminis* f.sp. *hordei* (Bg) MPK1, MPK2 and HOG1 to MAP kinases from *Botrytis cinerea* (Bc: BPM1, AAG23132), *Aspergillus nidulans* (An: MPKa, AAD24428; MPKb, AAF12815; HOGA, AAF81523; MPKC, AAG28463; SAKA, AAF97243), *Magnaporthe grisea* (Mg: PMK1, AAC49521; MPS1, AAC63682; OSM1, AAF09475), *Pneumocystis carinii* (Pc: MAPK, AAC98088; MKP1, AF077677), *Claviceps purpurea* (Cp: CPMK1, CAC47939; CPMK2, CAC87145), *Colletotrichum lagenarium* (Cl: CMK1, AAD50496; MAF1, AAL50116), *Pyrenophora teres* (Pt: PTK1, AAK52840), *Cochliobolus heterostrophus* (Ch: CHK1, AAF05913), *Ustilago maydis* (Um: UBC3, AAF09452), *Colletotrichum gloeosporioides* (Cg: CGK1, BAB21569), *Fusarium graminearum* (Fg: MGV1, AAM13670), *Fusarium oxysporum* (Fo: FMK1, AAG01162), *Fusarium solani* (Fs: MAPK, AAB72017), *Gaeumannomyces graminis* (Gg: GMK1, AAG44657), *Pichia pastoris* (Pp: PIM1, CAB93665), *Neurospora crassa* (Nc: OS2, AAK83124), *Saccharomyces cerevisiae* (Sc: FUS3, AAA34613; KSS1, NP_011554; SLT2, Q00772; HOG, AAB67558), *Schizosaccharomyces pombe* (Sp: SPM1, Q92398; STY1, Q09892), *Candida albicans* (Ca: MKC1, P43068; HOG1, Q92207). * indicates CgCGK1, ClCMK, MgPMK, PtPTK1, GgGMK1, FoFMK and FsMAPK. Bar indicates 0.1 nucleotide substitutions per site. The tree was prepared using the Clustal W alignment programme (http://www.ddbj.nig.ac.jp/E-mail/homology.html) and TreeView (Page, 1996).

identity with MPK1; *Claviceps purpurea* CPMK1 (Mey *et al.*, 2002a), *Cochliolobus heterotrophus* CHK1 (Lev *et al.*, 1999) and *Gaeumannomyces graminis* GMK1 (AAG44657) which share 88% identity with MPK1 and *Fusarium solani* FsMAPK (Li *et al.*, 1997) which shares 85% identity.

MPK2 is most closely related to *C. purpurea* CPMK2, with which is shares 81% identity (Mey *et al.*, 2002b), and lies within the clade that also includes *M. grisea* MPS1 (Xu *et al.*, 1998) and *Fusarium graminearum* MGV1 (Hou *et al.*, 2002) with which it shares 84% identity; *C. lagenarium* MAF1 with which it shares 83% identity (AAL50116) and *Aspergillus nidulans* MPKA (Bussink and Osamani, 1999) with which it shares 82% identity.

5.2.3 *In vivo* detection of MAP kinase activity in *Blumeria graminis* f.sp *hordei* protein extracts

With three MAP kinase genes having been identified in *B. graminis* f.sp. *hordei*, Western analysis was used in order to look for MAP kinase activity in *B. graminis* protein extracts. For detection of activated MAP kinases, a polyclonal antibody was obtained from New England Biolabs (Hertfordshire, UK) which was raised by immunizing rabbits with a synthetic phospho-peptide corresponding to residues around Thr202/Tyr204 of human p44 MAP kinase. The resulting antibody, named phospho-p44/42 MAP Kinase (Thr202/Tyr204), detects endogenous levels of p42 and p44 MAP kinase (ERK1 and ERK2) only when catalytically activated by phosphorylation at Thr202 and Tyr204 of human ERK, or Thr183 and Tyr185 of rat Erk2. The antibody does not cross-react with the corresponding phosphorylated residues of either JNK/SAPK or p38 MAP kinase (detailed in manufacturer's protocol). However, a high level of conservation of the TEY domain (Figure 5.1) indicates that this antibody should be useful for detection of *B. graminis* MAP kinase activity.

Protein extracts used in detection experiments were purified using a Pall Filtron Nanosep™ Microconcentrator (Pall Gelman Laboratories, Hampshire, UK) to remove all particles and impurities of less than 10 kDa. For Western analysis, protein extracts were separated by SDS-PAGE electrophoresis and blotted onto nylon membrane. Following incubation with phospho-p44/42 MAP Kinase

antibody, and then with anti-rabbit IgG alkaline phosphatase conjugate (Sigma), the chemiluminescent substrate, disodium 3-(4-methoxyspiro{1,2-dioxetane-3,2'-(5'-chloro)tricyclodecan}-4-yl) phenyl phosphate (CSPD®), was applied.

MAP kinase activity was detected in protein extracted from ungerminated conidia in denatured extracts (addition of dithiothreitol with heating to 100°C for 3 min), but not natured extracts (Figure 5.3). The faint band corresponding to MAP kinase activity is between 29 and 45 kDa. No MAP kinase activity was detected in protein extracted from PGT-stage germlings collected 6 hpi from water-agar in either natured or denatured extracts. Figure 5.3(b) shows the control experiment, that is, C3H10T½ murine fibroblast whole cell extracts (gift from Louis Mahadevan, University of Oxford) with no added MAP kinase activator (i), and fibroblasts activated with 100 nM 12-O-Tetradecanoylphorbol 13-acetate (TPA) (ii) and 50 $ng.ml^{-1}$ epidermal growth factor (EGF) (iii). The bands correspond to between 29 and 45 kDa.

5.3.4 Investigation into the effects of MAP kinase signalling pathway antagonists on *Blumeria graminis* f.sp. *hordei* germling differentiation

Having identified MAP kinase activity in *B. graminis* f.sp. *hordei in vitro*, two inhibitors, characterized in mammalian systems as inhibitors of the MAP kinase signalling pathway were chosen for *in vivo* investigations into the effects of these antagonists on *B. graminis* differentiation.

PD98059 is a synthetic inhibitor of the MAP kinase pathway, which selectively inhibits the MAP kinase-activating enzyme, that is, MAP kinase/ERK1 kinase (MEK1) in mammalian systems (Dudley *et al.*, 1995). U0126 (1,4-diamino-2,3-dicyano-1, 4-bis[2-aminophenylthio]butadiene) directly inhibits MEK1 and MEK2. The mode of inhibition for both U0126 and PD98058 is noncompetitive with respect to ATP and ERK (Favata *et al.*, 1998).

Either U0126 or PD98059 was applied exogenously to conidia, *i.e.* in solution beneath epidermal peels. U0126 was assayed over a concentration range of 0.01 to 100 μM, with a control of 0.1% (v/v) DMSO. Two repeat experiments were performed. PD98059 was assayed over a concentration range of 1 to 100 μM, with

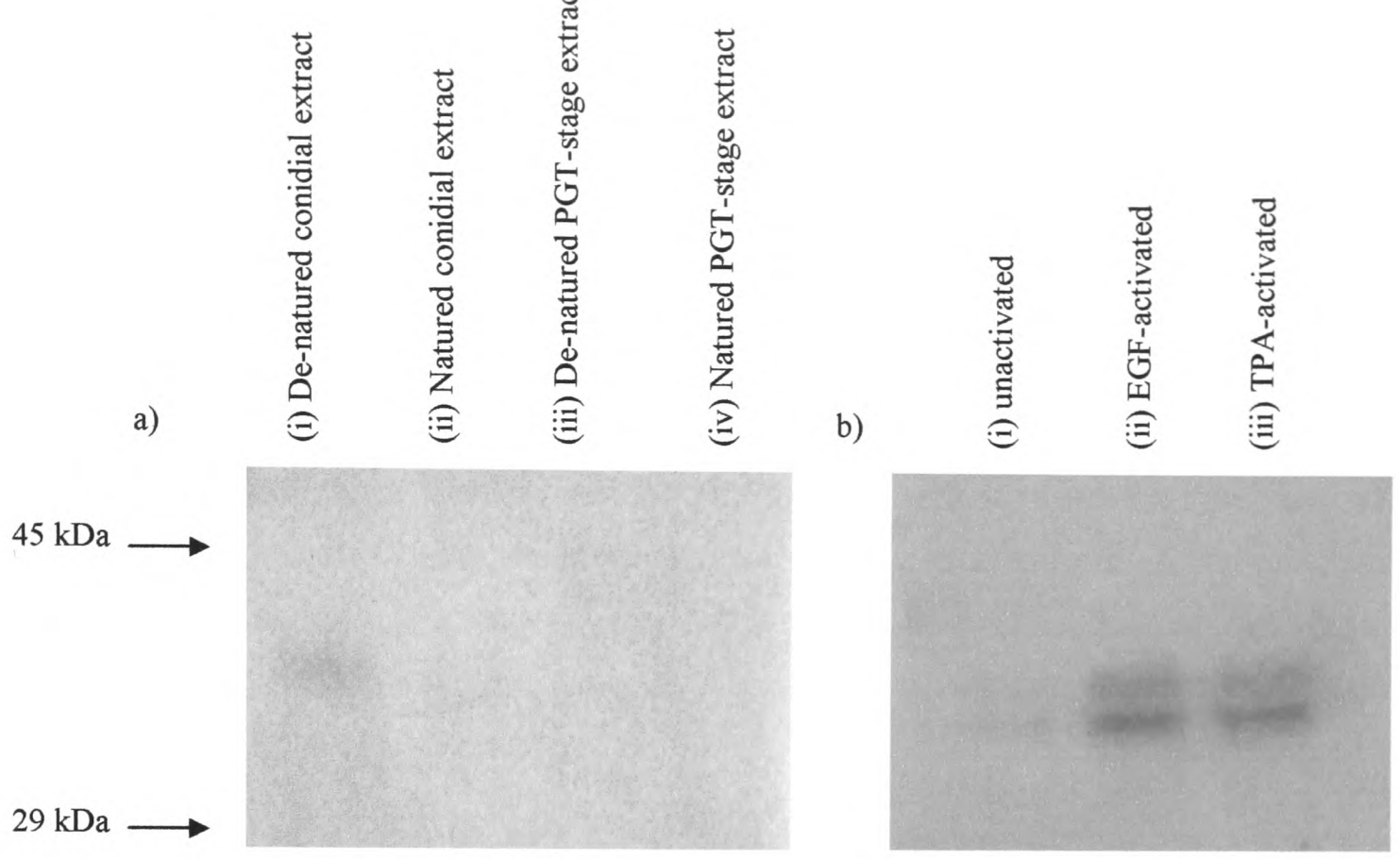


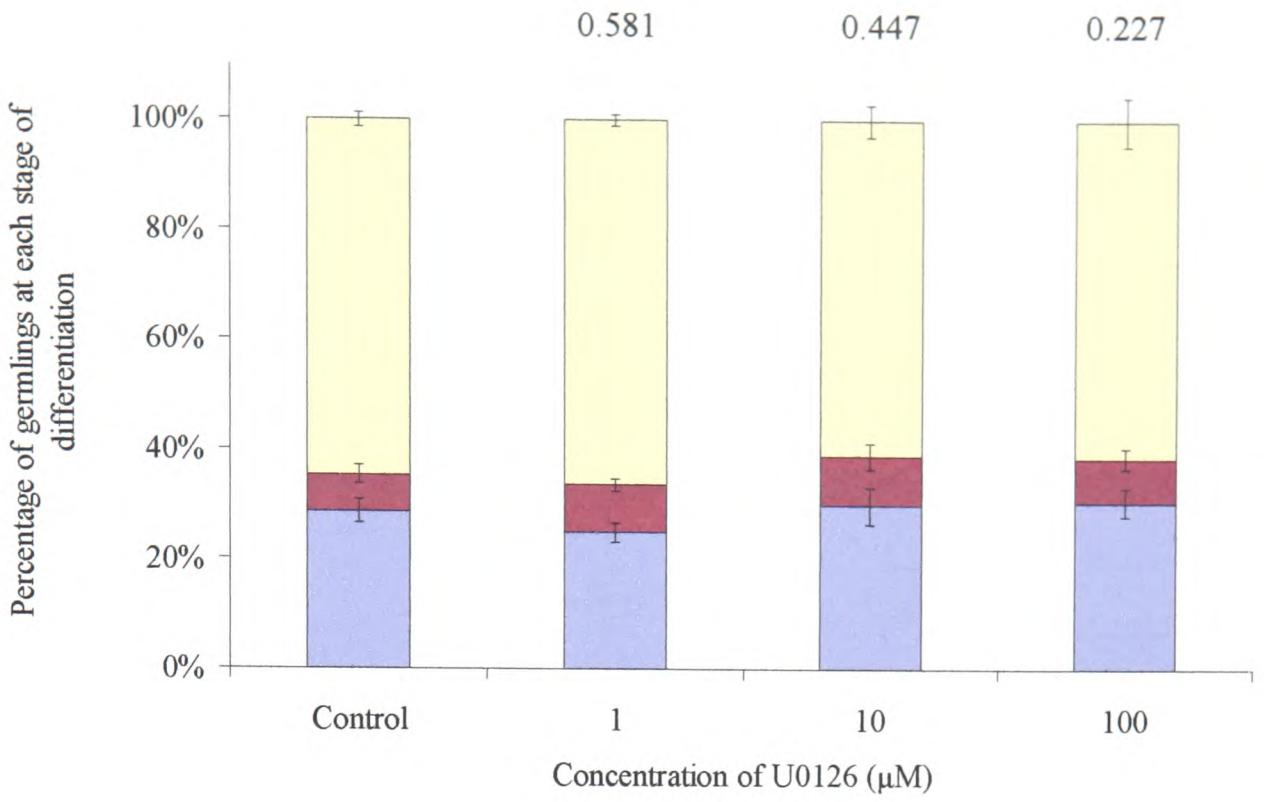
Figure 5.3. Western analysis showing mitogen-activated protein (MAP) kinase activity in (a) protein extracted from ungerminated *Blumeria graminis* f.sp. *hordei* conidia (a.i-ii), and protein extracted from PGT-stage germlings collected 6 hpi from water agar (a.iii-iv); (b) C3H10T½ murine fibroblast whole cell extracts (gift from Louis Mahadevan, University of Oxford) with no added MAP kinase activator (i), with 100 nM 12-O-tetradecanoylphorbol 13-acetate (TPA) (ii), and with 50 $ng.ml^{-1}$ epidermal growth factor (EGF) (iii). Activity was detected using phospho-p44/42 MAP Kinase antibody. Arrows indicate molecular weights.

a control of epidermal peels overlying 6.6 mg.ml^{-1} Bovine Serum Albumin (BSA) (Sigma) and 0.5% (v/v) DMSO. Three repeat experiments were performed. For each inhibitor, conidia were scored for both germination (6 replicates of 50 conidia) and differentiation (6 replicates of 50 germinated conidia), that is, for differentiation, scoring for the production of either a primary germ tube (PGT), an elongated germ tube (EGT) or a swollen/appressorial germ tube (SwGT/AGT), at 16 hpi. Statistical significance was determined using the General Linear Model (GLM) following an arcsine transformation.

Application of 0.01 μM to 100 μM U0126 beneath epidermal peels had no significant effect on *B. graminis* germination or appressorial differentiation. Figure 5.4 shows the differentiation of germlings upon U0126 application. P-values for all 3 independently repeated experiments are shown in Table 5.1.

Application of 1 μM to 100 μM PD98059 beneath epidermal peels had no significant effect on *B. graminis* germination. However, application of 10 μM and 100 μM PD98059 resulted in a decrease in the number of germlings differentiating SwGTs or AGTs as compared with the control in all independently replicated experiments. One of three experiments showed a significant reduction in SwGT/AGT differentiation with an application of 1 μM PD98059. Figure 5.5 shows the percentage decrease in differentiation of germlings upon PD98059 application. P-values for all 3 independently repeated experiments are shown in Table 5.2.

A time-course of *B. graminis* development on epidermal peels overlying 100 μM PD98059 was performed. Conidia were scored for differentiation (6 replicates of 50 germinated conidia) at 0, 2, 4, 8, 12, 16, 20 and 24 hpi. Figure 5.6 shows that at 4 hpi, there was no significant difference in differentiation between the control and PD98059-treated populations (P=0.233). By 8 hpi, however, there was a significant reduction in the number of germlings that had differentiated EGTs or Sw/AGTs on PD98059 application when compared to the control (P=0.038), with a mean of 82% of germlings having differentiated beyond the PGT-stage in the control population, compared to a mean of 76% in the PD98059-treated population. By 16 hpi, a mean of 92% of germlings had differentiated in the



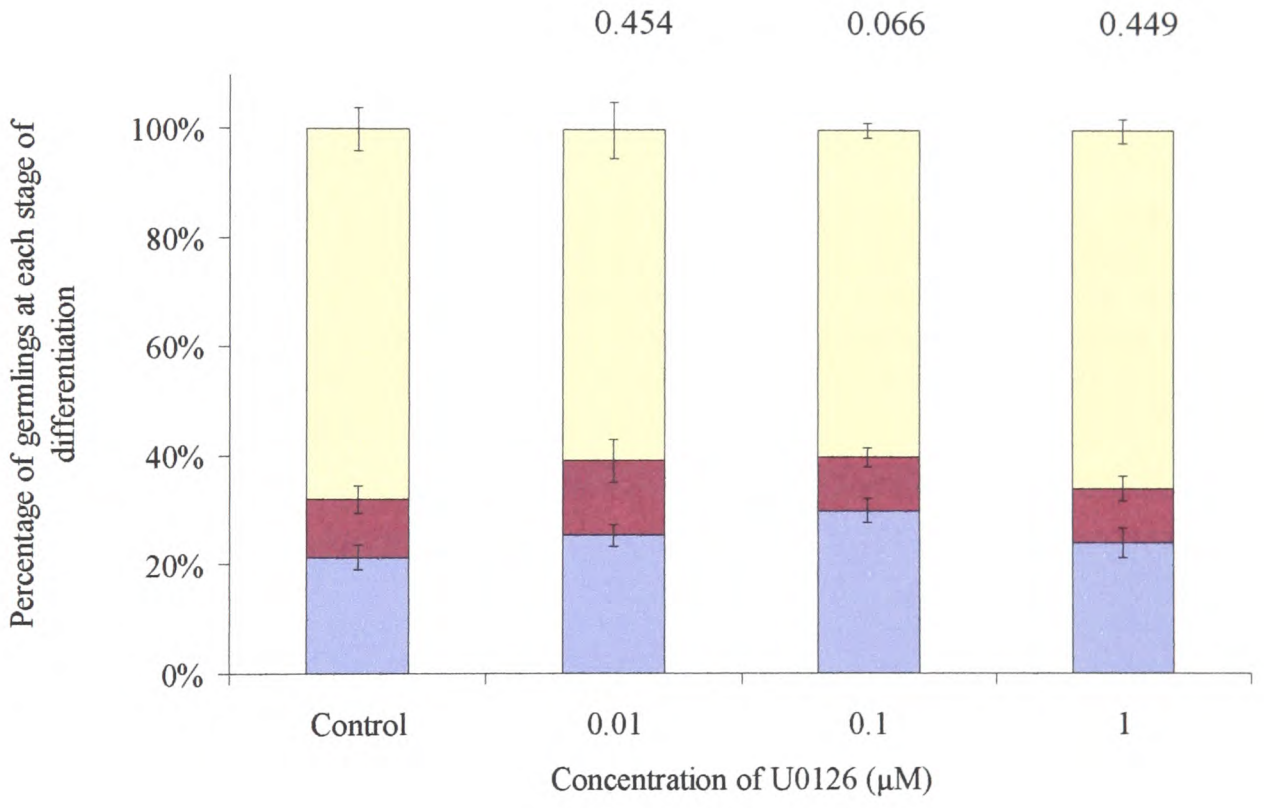


Figure 5.4. Differentiation of *Blumeria graminis* f.sp. *hordei* conidia on barley epidermal peels overlying U0126, 16 hours post inoculation (hpi). ■ corresponds to conidia with short germ tubes, ■ corresponds to conidia having differentiated elongated germ tubes and ■ corresponds to conidia having differentiated either a swollen germ tube, or an appressorial germ tube. The results shown are representative of 3 independent experiments. In each experiment, 6 x 50 conidia were scored and the mean percentage values of 50 conidia are illustrated. The mean ± standard error is shown. The control was 0.1% (v/v) DMSO. P-values showing the significance of differences in differentiation (that is, germlings that have differentiated swollen or appressorial germ tubes) compared to the control are given above each corresponding bar.

No. of replica	Concentration of U0126 (μM)	P-values for germination	P-values for differentiation
1	100	0.271	0.227
	10	0.869	0.447
	1	0.479	0.581
2	100	0.642	0.730
	10	0.582	0.483
	1	0.641	0.469
1	1	0.985	0.449
	0.1	0.118	0.066
	0.01	0.589	0.454
2	1	0.734	0.476
	0.1	0.582	0.777
	0.01	0.717	0.719

Table 5.1. P-values to show the significance between treatment of *Blumeria graminis* f.sp. *hordei* with U0126 and the control (0.5% (v/v) DMSO, 6.6 $mg.ml^{-1}$ BSA) for germination and differentiation on barley epidermis. For each repeat experiment, 6 x 50 conidia were scored for germination and 6 x 50 germlings were scored for differentiation (meaning the production of either an elongated germ tube, a swollen germ tube or an appressorial germ tube). The results of two independent experiments are shown. * indicates $p \leq 0.05$, ** indicates $p \leq 0.01$ and *** indicates $p \leq 0.000$.

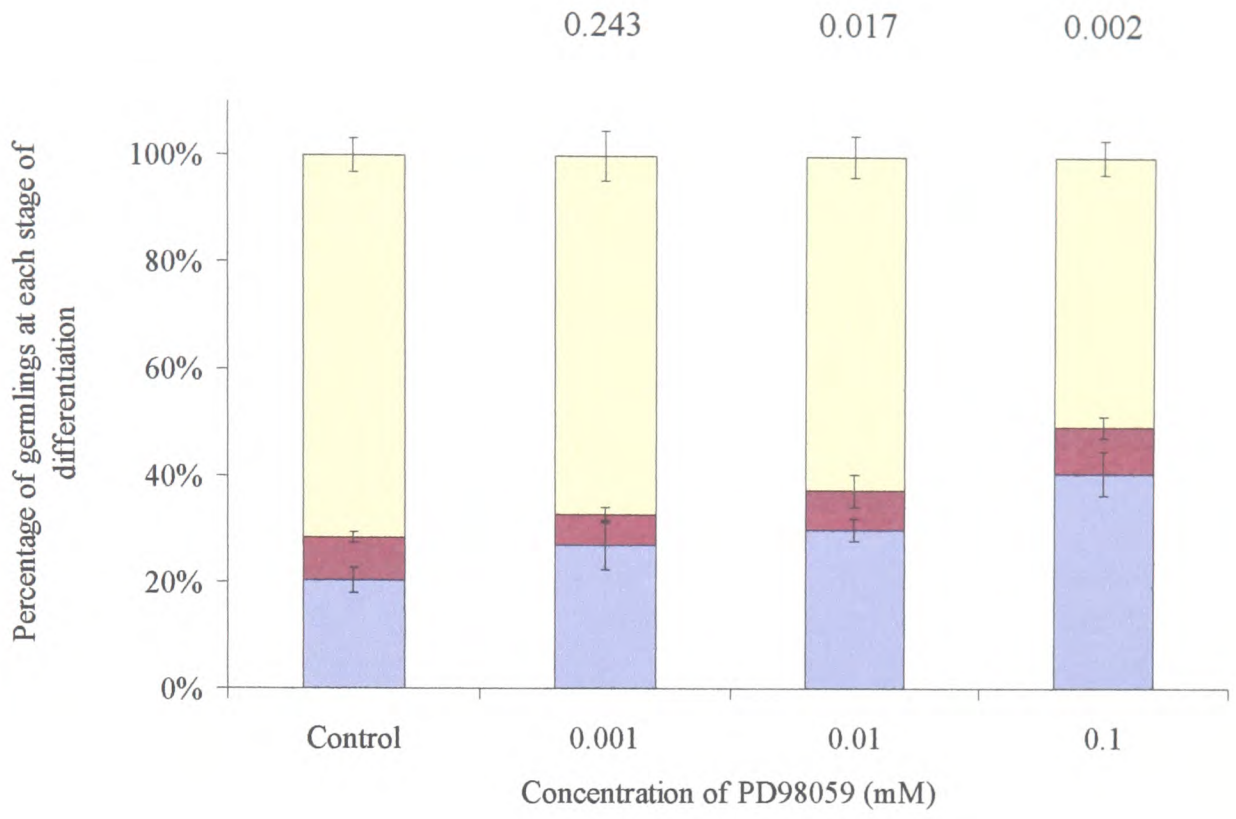
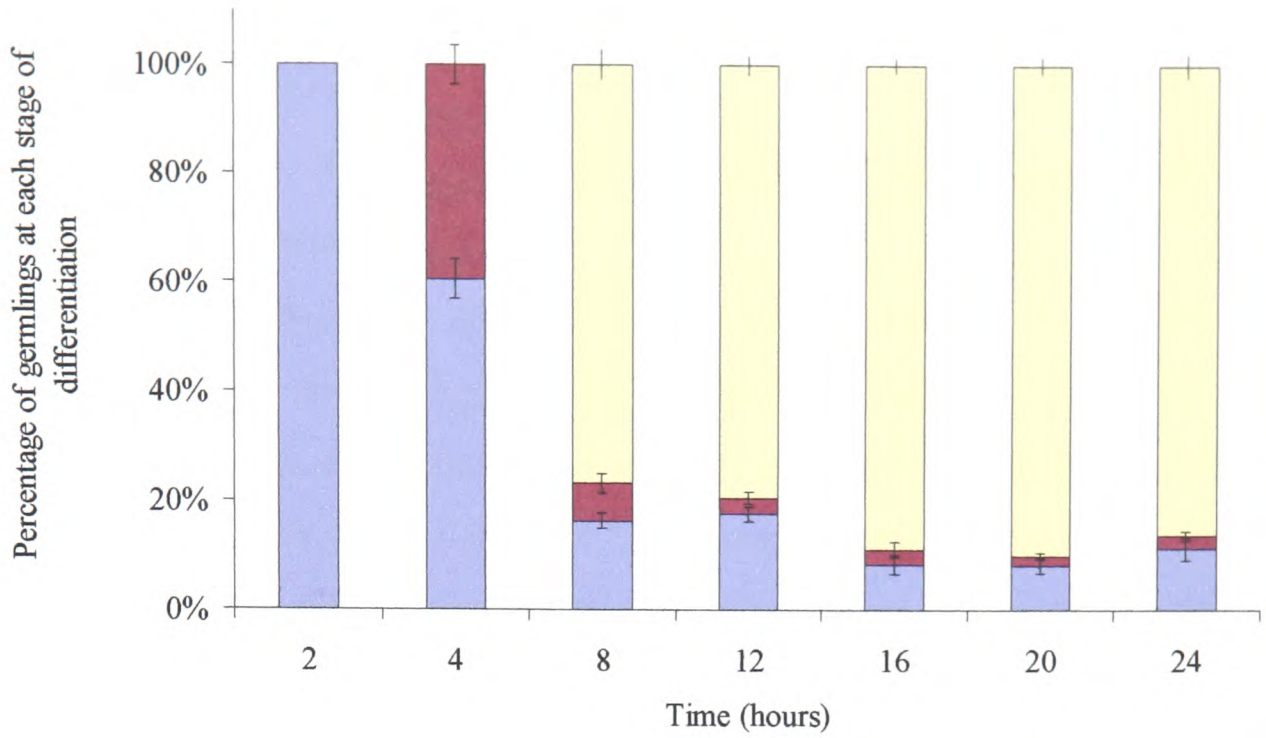


Figure 5.5. Differentiation of *Blumeria graminis* f.sp. *hordei* conidia on barley epidermal peels overlying PD98059, 16 hours post inoculation. ■ corresponds to conidia with short germ tubes, ■ corresponds to conidia having differentiated elongated germ tubes and ■ corresponds to conidia having differentiated either a swollen germ tube, or an appressorial germ tube. The results shown are representative of 3 independent experiments. In each experiment, 6 x 50 conidia were scored and the mean values of 50 conidia are illustrated. The mean ± standard error is shown. The control is 6.6 $mg.ml^{-1}$ BSA and 0.5% (v/v) DMSO. P-values showing the significant differences in differentiation (that is, germlings that have differentiated elongated, swollen or appressorial germ tubes) compared to the control are given above each corresponding bar.

No. of replica	Concentration of PD98059 (μM)	P-values for germination	P-values for differentiation
1	100	0.042*	0.002**
	10	0.873	0.017*
	1	0.750	0.243
2	100	0.153	0.001**
	10	0.249	0.004**
	1	0.455	0.007**
3	100	0.550	0.004**
	10	0.271	0.022*
	1	0.539	0.653

Table 5.2. P-values to show the significance between treatment of *Blumeria graminis* f.sp. *hordei* with PD98059 and the control (0.5% (v/v) DMSO, 6.6 $mg.ml^{-1}$ BSA) for germination and differentiation on barley epidermis. For each repeat experiment, 6 x 50 conidia were scored for germination and 6 x 50 germlings were scored for differentiation (meaning the production of either an elongated germ tube, a swollen germ tube or an appressorial germ tube). The results of three independent experiments are shown. * indicates $p \leq 0.05$, ** indicates $p \leq 0.01$ and *** indicates $p \leq 0.000$.

a)



b)

1.000 0.233 0.038 0.141 0.004 0.002 0.007

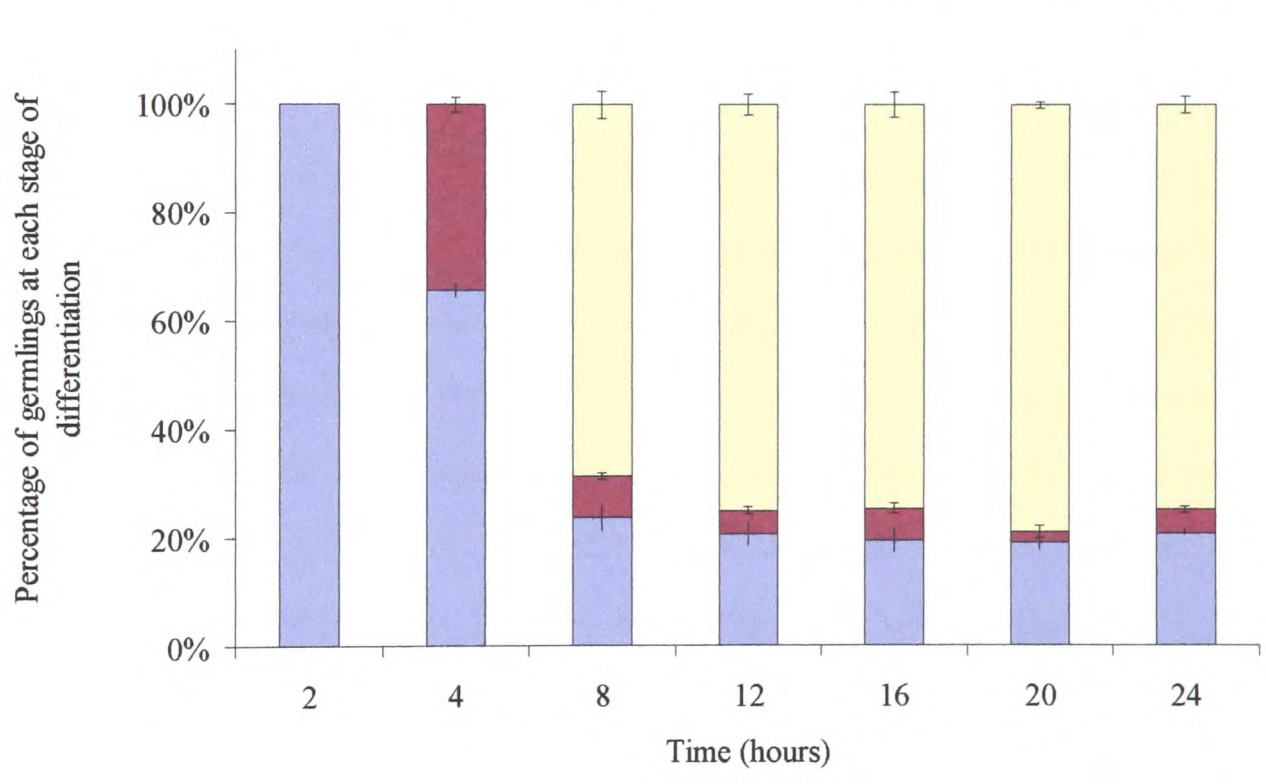


Figure 5.6. Time-course of differentiation of *Blumeria graminis* f.sp. *hordei* conidia on epidermal peels overlying (a) the control (6.6 mg.ml^{-1} BSA and 0.5% (v/v) DMSO) and (b) 100 μM PD98059. ■ corresponds to conidia with short germ tubes, ■ corresponds to conidia having differentiated elongated germ tubes and ■ corresponds to conidia having differentiated either a swollen germ tube, or an appressorial germ tube. In each experiment, 6 x 50 conidia were scored and the mean values of 50 conidia are illustrated. The mean ± standard error is shown. P-values showing the significant differences in differentiation (that is, germlings that have differentiated elongated, swollen or appressorial germ tubes) compared to the control are given above each corresponding bar in (b).

control population, compared to 80% for the PD98059-treated population (P=0.004), with similar differences at 20 hpi (P=0.002) and 24 hpi (P=0.007).

5.2.5 Investigation into the effects of PD98059 on *Magnaporthe grisea* germling differentiation

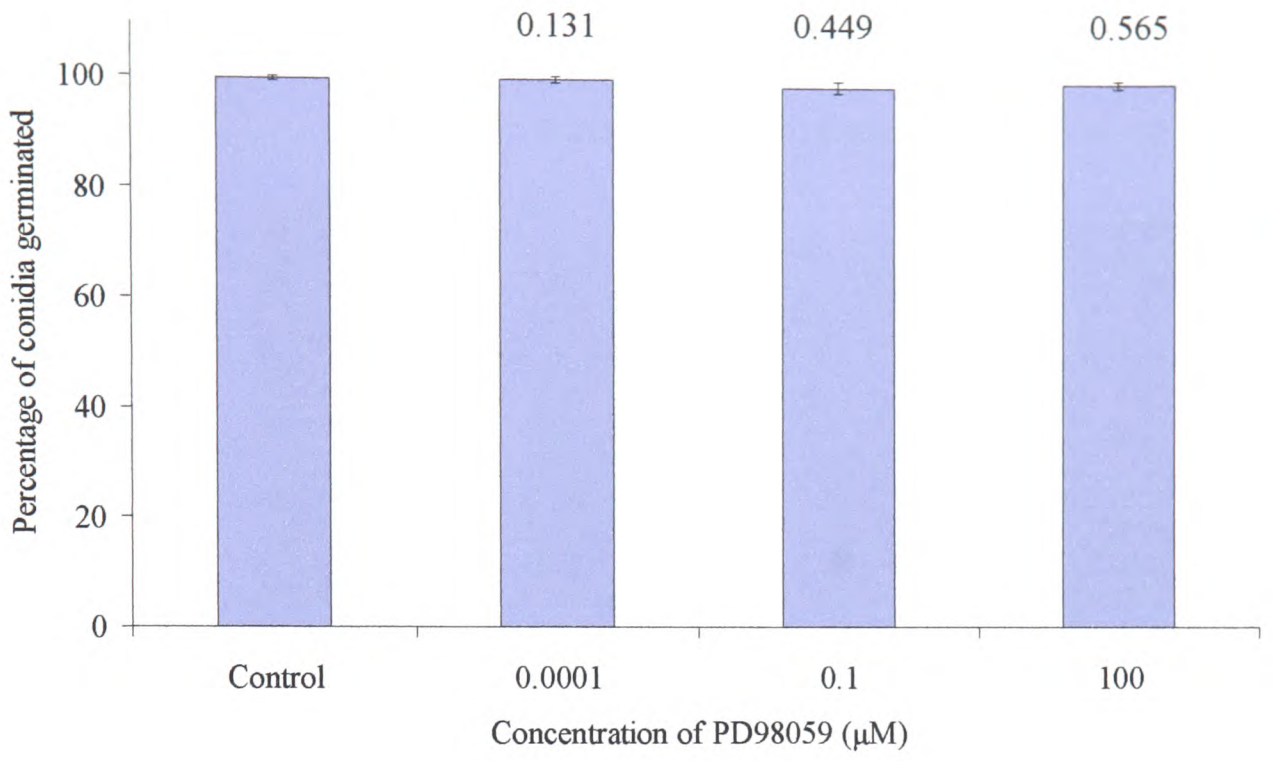
It is impossible to elucidate, from the data available, which *B. graminis* MAP kinase pathway is being targeted by PD98059. Therefore, to obtain more information, *Magnaporthe grisea* was used in an attempt to further characterise the effects of this inhibitor. All three *M. grisea* MAP kinases identified to date have been characterised and the phenotypes of the deletion mutants described (Xu and Hamer, 1996; Xu *et al.*, 1998; Dixon *et al.*, 1999). If PD98059 is able to inhibit *M. grisea* germling differentiation as it does *B. graminis*, and if the target of PD98059 is one of the characterised MAP kinase pathways, then the phenotype of the inhibited germlings might give some indication as to the target pathway of PD98059 since Δ*pmk1*, Δ*mps1* and Δ*hog1* have distinct phenotypes.

PD98059 was applied to *M. grisea* conidia in suspension ($1x10^4$ conidia mL^{-1}), with 6.6 $mg.mL^{-1}$ BSA over a concentration range of between 0.0001 μM to 100 μM PD98050. The control was 6.6 $mg.ml^{-1}$ BSA in 0.5% (v/v) DMSO. Spore suspensions were inoculated onto barley epidermal peels. For each concentration, conidia were scored for germination (6 replicates of 50 conidia) and differentiation (6 replicates of 50 germinated conidia), that is, scoring for the production of either a germ tube (GT), an elongated germ tube (EGT), a swollen germ tube (SwGT) or production of an appressoria. In addition, at each concentration, germlings with appressoria were scored for penetration by scoring for the production of infection hyphae (6 replicates of 50 germlings with appressoria). All scoring was done at 12 hpi. Statistical significance was determined using the General Linear Model (GLM) following an arcsine transformation.

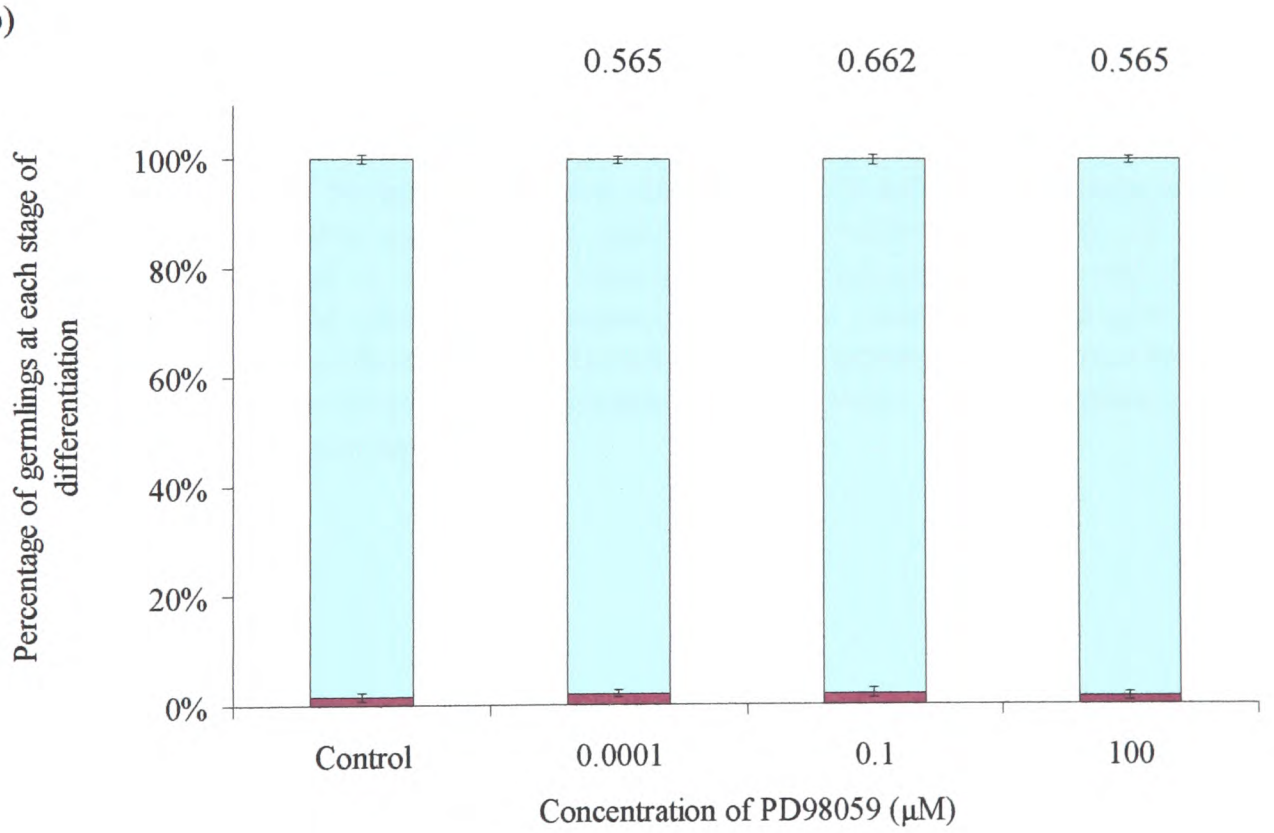
Figure 5.7 shows the germination, differentiation and penetration levels of *M. grisea* conidia upon PD98059 application. P-values are also given to compare the treated populations with the control population. Application of 0.001 μM to 100 μM PD98059 to *M. grisea* spore suspensions inoculated onto epidermal peels had

Figure 5.7.

a)


0.131
0.449
0.565
100
80
60
40
20
0
Percentage of conidia germinated
Control
0.0001
0.1
100
Concentration of PD98059 (μM)

b)


0.565
0.662
0.565
100%
80%
60%
40%
20%
0%
Percentage of germlings at each stage of differentiation
Control
0.0001
0.1
100
Concentration of PD98059 (μM)

c)

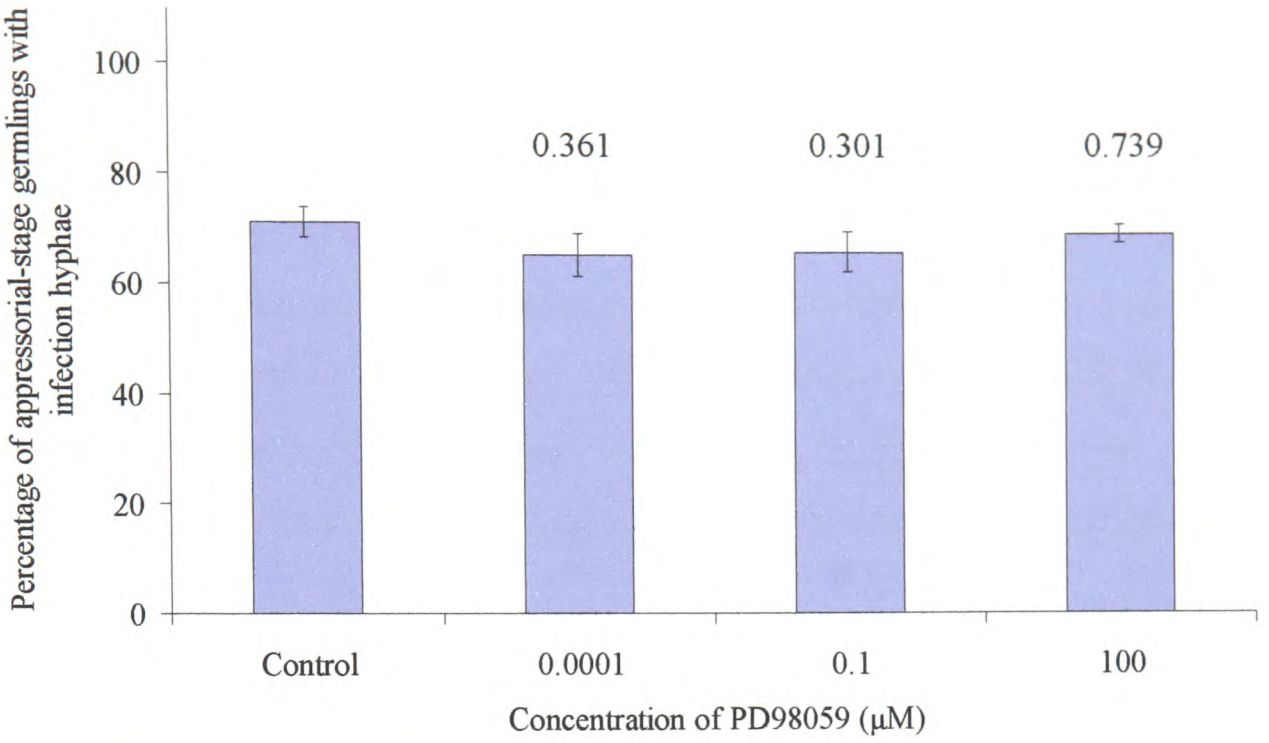


Figure 5.7. Germination (a), differentiation (b) and penetration (c) of *Magnaporthe grisea* on barley epidermal peels overlying PD98059, 12 hours post inoculation. In (b) ■ corresponds to conidia having differentiated elongated germ tubes and ■ corresponds to conidia having differentiated appressoria. The control is 0.5% (v/v) DMSO, 6.6 mg.ml^{-1} BSA. 6 x 50 conidia were scored for germination, 6 x 50 germlings were scored for differentiation, meaning the production of either an elongated germ tube, a swollen germ tube or an appressorium, and 6 x 50 appressorial-stage germlings were scored for penetration, *i.e.* the production infection hyphae. The mean ± standard error is shown. P-values to show the significance between treatment of *M. grisea* with PD98059 and the control for germination, differentiation and penetration are given above each corresponding bar.

no significant effect on germination, appressorial differentiation or penetration of the plant tissues.

5.2.6 Investigation into the effects of MAP kinase agonists on *Blumeria graminis* f.sp. *hordei*

Having identified that the mammalian MEK inhibitor PD98059 inhibits *B. graminis* differentiation, an activator of mammalian MAP kinase was tested for its effect on *B. graminis* germination and differentiation. N-Hexanoyl-D-*erythro*-sphingosine (Alexis Corporation, Nottingham, UK), otherwise named C_6 ceramide, is known to induce p42 phosphorylation in HL-60 cells (Raines *et al.*, 1993).

Application of between 0.01 μM to 100 μM N-Hexanoyl-D-*erythro*-sphingosine beneath cellulose membrane did not enhance *B. graminis* germination or appressorial differentiation. Figure 5.8 shows the differentiation of germlings upon N-Hexanoyl-D-*erythro*-sphingosine application. P-values for all 3 independent repeat experiments are shown in Table 5.3.

5.2.7 Expression of *mpk*1 and *mpk*2 during germling morphogenesis

Transcript abundance of the *B. graminis mpk*1 and *mpk*2 genes in ungerminated conidia (0 hpi), mature primary germ tube stage germlings (4 hpi) and appressorial germ tube stage germlings (12 hpi) has previously been described (Zhang and Gurr, 2000). This work implemented the RT-PCR method as described by Zhang *et al.* (2000) which employs end-point (competitive) analysis of amplification products. To verify and provide a more extensive time-course of expression, transcript abundance of the *B. graminis mpk*1 and *mpk*2 genes was determined using a real-time PCR approach.

For real-time PCR, stage-specific, 1st strand cDNA was synthesised from total RNA extracted from ungerminated conidia, and germlings harvested from the barley leaf surface at 0.5, 3, 8, 12 and 20 hpi. These time points were selected to correspond with significant stages in the differentiation of *B. graminis*, that is, the ungerminated state (0 h), just prior to the emergence of the PGT (0.5 h), during PGT differentiation (3 h), during AGT elongation and swelling (8 h), at the

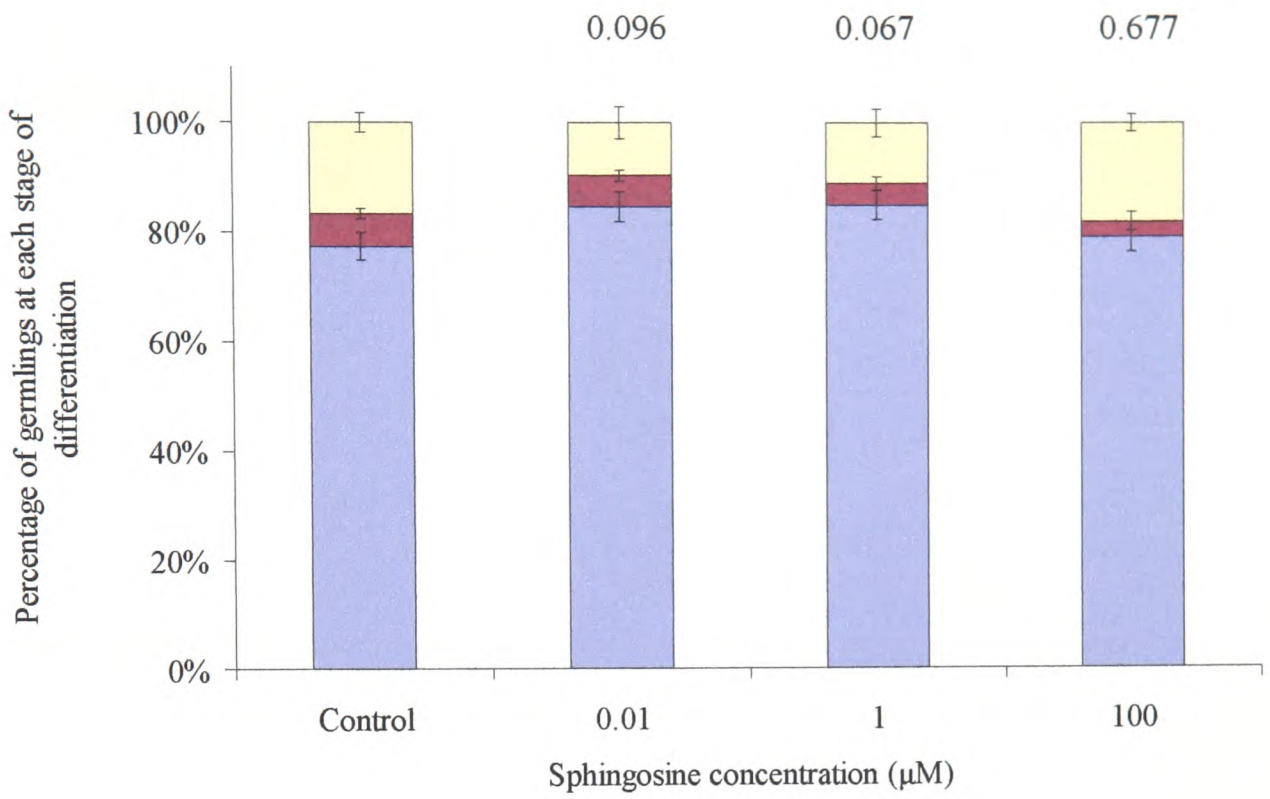


Figure 5.8. Differentiation of *Blumeria graminis* f.sp. *hordei* conidia on cellulose membrane overlying N-Hexanoyl-D-*erythro*-sphingosine (sphingosine), 24 hours post inoculation (hpi). ■ corresponds to conidia with short germ tubes, ■ corresponds to conidia having differentiated elongated germ tubes and ■ corresponds to conidia having differentiated either a swollen germ tube, or an appressorial germ tube. The results shown are representative of 3 independent experiments. In each experiment, 6 x 50 conidia were scored and the mean values of 50 conidia are illustrated. The mean ± standard error is shown. The control was 0.1% (v/v) DMSO. P-values showing the significance of differences in differentiation (that is, germlings that have differentiated swollen or appressorial germ tubes) compared to the control are given above each corresponding bar.

No. of replica	Concentration of sphingosine (μM)	P-values for germination	P-values for differentiation
1	100	0.048*	0.677
	1	0.378	0.067
	0.01	0.220	0.096
2	100	0.336	0.923
	1	0.163	0.838
	0.01	0.527	0.111
3	100	0.295	0.129
	1	0.114	0.225
	0.01	0.294	0.056

Table 5.3. P-values to show the significance between treatment of *Blumeria graminis* f.sp. *hordei* with N-hexanoyl D-*erythro*-sphingosine (sphingosine) and the control (DMSO) for germination and differentiation on cellulose membrane. For each repeat experiment, 6 x 50 conidia were scored for germination and 6 x 50 germlings were scored for differentiation, meaning the production of either an elongated germ tube, a swollen germ tube or an appressorial germ tube. The results of three independent experiments are shown. * indicates $p \leq 0.05$, ** indicates $p \leq 0.01$ and *** indicates $p \leq 0.000$.

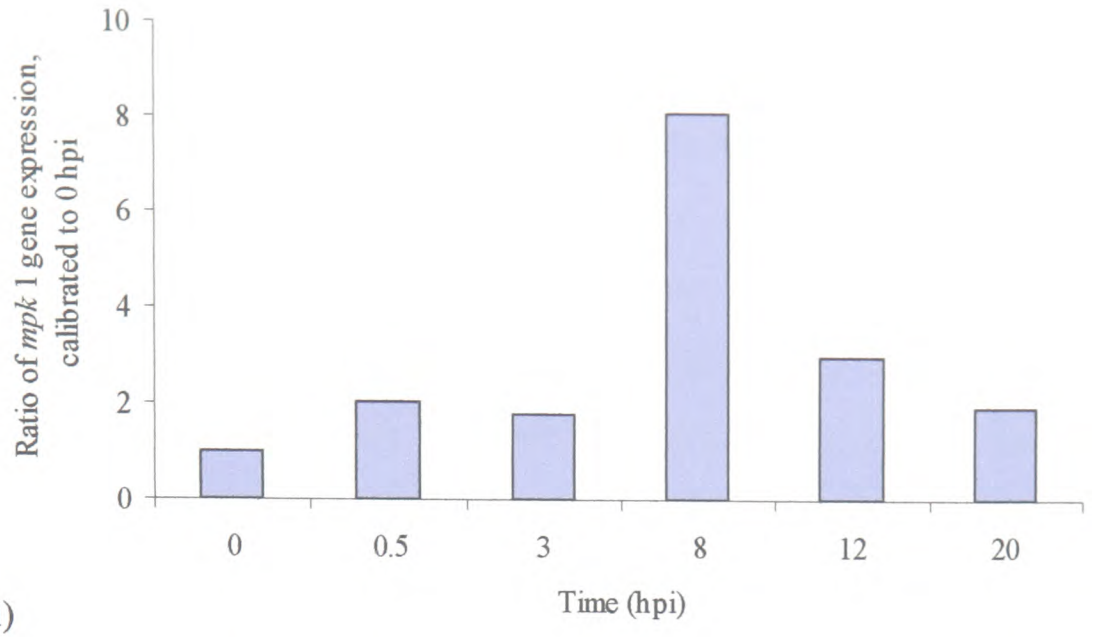
mature AGT stage (12 h) and beyond (20 h). The *B. graminis* β-*tubulin* gene transcript was used as an endogenous, consititutively expressed control (Sherwood and Somerville, 1990).

Primer efficiencies were calculated by i) establishing the "crossing point" (CP) value (the point at which fluorescence rises appreciably above background fluorescence) of a two-fold dilution series of cDNA, ii) determining the gradient of the slope of the CP values and iii) calculating the efficiency value (*E*) using the equation $E=10^{[-1/\text{slope}]}$. The *E* values were used to calculate expression levels of *mpk*1 and *mpk*2 relative to the β-*tubulin* gene using the method described by Pfaffl (2001).

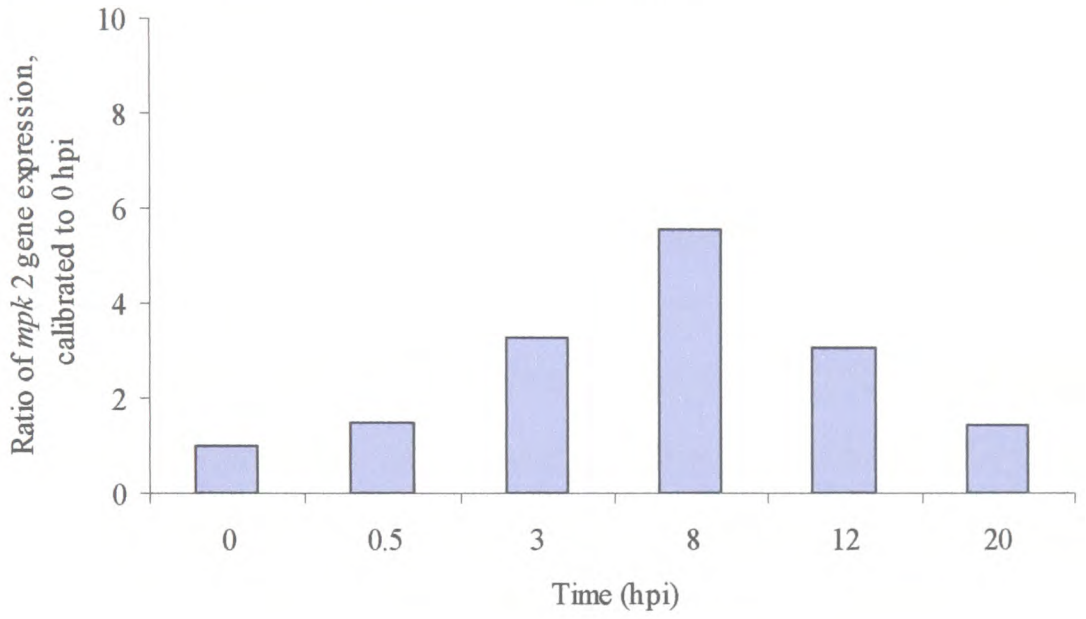
Real-time transcript profiles are shown in Figure 5.9(a). All values are relative to 0 h. For comparison, Figure 5.9(b) shows a time-course of expression using end-point RT-PCR analysis performed with Catherine Henderson (University of Oxford) using the method of Zhang *et al.*, (2000). In this study, germlings were harvested from the barley leaf surface at 0.5, 3, 8, 12 and 20 hpi, that is, to correspond with the time-points used in the real-time study. Again, the *B. graminis* β-*tubulin* gene transcript was followed as an internal control for the equivalence of stage-specific 1st strand cDNA and equal amplification.

Figure 5.9(a.i) shows a slight increase in *mpk*1 transcript abundance upon germination (0.5 hpi and 3 hpi) in comparison to transcript levels in ungerminated conidia (0 hpi). However, at 8 hpi, that is, during AGT elongation and swelling, there is a peak in *mpk*1 of almost eight times that of *mpk*1 levels at 0 hpi. Subsequently, *mpk*1 transcripts fall to levels seen earlier in germling differentiation. The profile follows the same trend as the end-point RT-PCR profile in Figure 5.9(b), which shows a distinct increase in *mpk*1 transcript abundance at 8 hpi. Figure 5.9(a.ii) shows that the transcript profile for *mpk*2 follows the same trend as that of *mpk*1. However, the rise in *mpk*2 transcript levels at 3 hpi is more pronounced than that of *mpk*1, but the peak in transcripts at 8 hpi in *mpk*2 is not as pronounced as *mpk*1. Figure 5.9(b) shows that the end-point RT-PCR verifies the transcript profile of *mpk*2 obtained using real-time RT-PCR and reveals that *mpk*2 transcripts at 0, 0.5, 3 and 20 hpi are very low in abundance.

a(i)



a(ii)



b)

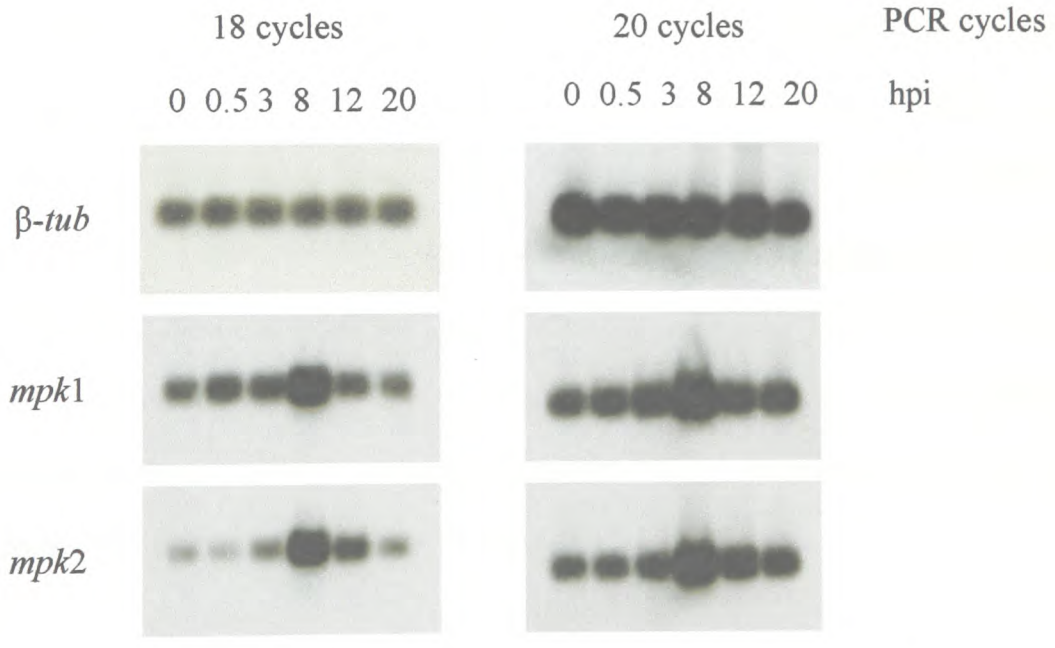


Figure 5.9. a(i) and a(ii) show transcript profiles of *Blumeria graminis* f.sp. *hordei mpk*1 and *mpk2* on barley leaves at 0, 0.5, 3, 8, 12 and 20 hours post inoculation (hpi), elucidated using real time PCR. Expression levels are calibrated to β-*tubulin*. All values are expressed as ratios compared to 0 hpi. (b) End-point RT-PCR quantification of *B. graminis* β-*tubulin*, *mpk*1and *mpk2* on barley leaves at 0, 0.5, 3, 8, 12 and 20 hpi.

5.3 DISCUSSION

5.3.1 Identification of *mpk*1 and *mpk*2 genes in *Blumeria graminis* f.sp. *hordei*

Two MAP kinases, *mpk*1 and *mpk*2, have previously been isolated from *B. graminis* (Zhang and Gurr, 2001), and, more recently, a third, *hog*1, has been identified (Ziguo Zhang, unpublished). Phylogenetic analysis reveals that the predicted protein sequences of MPK1, MPK2 and HOG1 cluster into three different clades (Figure 5.2). That is, MPK1 clusters with *S. cerevisiae* KSS1/FUS3 and its homologues, MPK2 clusters with *S. cerevisiae* SLT2 and its homologues and HOG1 clusters with *S. cerevisiae* HOG1 and its homologues. Caffrey *et al.* (1999) constructed a MAP kinase family tree based on 52 sequences rooted on human CDK2 (SP P24941). Their findings showed a tree with two broad groups, one including the HOG fungi alongside the animal groups for p38 and JNK (stress stimuli and pro-inflammatory cytokines) and a second grouping of "everything else". Intercollating the *B. graminis* MPK1 and MPK2 data places MPK1 in the filamentous, pheromone, classical cluster of MAP kinases whilst MPK2 would reside with the hypo-osmolarity grouping. That is, both fall broadly within the Caffrey *et al.* (1999), category of "everything else".

Interestingly, like *B. graminis*, only three MAP kinase homologues have been identified in each of *M. grisea*, *S. pombe* and *C. albicans*. There has been speculation that most higher fungi may only have these three MAP kinase pathways (Xu, 2000). Even though there are five MAP kinases in *S. cerevisiae*, two of them (*FUS3/KSS1*) are closely related and partially redundant (Xu, 2000). In addition, *S. cerevisiae* Smk1 is phylogenetically distinct from other fungal MAP kinases and it has a TNY phosphorylation motif that has not been found in any other known MAP kinases (Kultz, 1998).

5.3.2 MPK1 and MPK2 phylogeny

Phylogenetic analysis places *B. graminis* MPK1 closest to *Botryotina cinerea* BMP1 (Zheng *et al.*, 2000). Other pathogenic fungal MAP kinases cluster with *B. graminis* MPK1 (Figure 5.2) including *Fusarium oxysporum* FMK1 (AF286533), *Fusarium solani* FsMAPK (Li *et al.*, 1997), *Gaeumannomyces graminis* GMK1 (AAG44657), *Magnaporthe grisea* PMK1 (Xu and Hamer, 1996), *Colletotrichum*

lagenarium CMK1 (Takano *et al.*, 2000) *Colletotrichum gloeosporioides* CGK1 (BAB21569).

We can speculate as to the function of *B. graminis* MPK1 by considering the MAP kinase homologues that have already been characterized (Table 5.4). *Magnaporthe grisea*, PMK1 (Xu and Hamer, 1996), *Cochliobolus heterotrophus*, *CHK1* (Lev et al., 1999), *Colletotrichum lagenarium* CMK1 (Takano *et al.*, 2000), *Fusarium oxysporum* FMK1 (Di Pietro *et al.*, 2001) and *Pyrenophora teres* PTK1 (Ruiz-Rolan *et al.*, 2001) are required for appressorium formation, suggesting conserved rôles for the formation of infection structures by plant pathogens. "Knockout" mutants of each of the listed fungi show different phenotypes in growth, conidiation and germination, which suggests diverse roles of FUS3/KSS1-related MAP kinases in phytopathogenic fungi. It is interesting to note that a MAP kinase from *B. cinerea*, a necrotrophic fungus which has a wide host range, is so closely-related to the MPK1 from an obligately biotrophic, host-specific fungus, *i.e. B. graminis* f.sp. *hordei*. It has been widely assumed that *B. cinerea* is not a true appressorium-forming fungus. However, Zheng *et al.* (2000) highlight that to infect the plant, *B. cinerea* germ tubes swell slightly and form appressorium-like infection structures. Indeed, BMP1 is 94% identical to *M. grisea* PMK1, and it has been noted that *B. cinerea* and *M. grisea* clearly share related MAP kinase pathways for plant infection, even though they cause different diseases and have different infection mechanisms (reviewed in Tucker and Talbot, 2001). Additionally, in the non-appressorial producing biotroph *C. purpurea*, Δ*cpmk1* mutants are almost identical in phenotype to *M. grisea* Δ*pmk1* mutants, indicating that the basic penetration mechanism could be related in spite of the lack of morphological differentiation (Mey *et al.*, 2002a). Alternatively, MAP kinase cascades may represent evolutionary old signalling pathways involved in sensing the host surface, thus initiating penetration programs that have divergently adapted to the different host/organs involved (Mey *et al.*, 2002a).

Analysis of the predicted amino acid sequences of MPK2 reveals that it is a MAP kinase homologue with a closer relationship to *C. purpurea* CPMK2 (Mey *et al.*, 2002b) than to other pathogenic and filamentous fungi or yeast (Figure 5.2). Other pathogenic fungal MAP kinases clustering with *B. graminis* MPK1 include *M.*

Organism	Gene	Function	Reference
Botrytis cinerea	*BMP1*	Growth and pathogenicity on different plant species	Zheng *et al.*, 2000
Claviceps purpurea	*CPMK1*	Pathogenicity and cuticle-penetration on rye	Mey *et al.*, 2002
Cochliobolus heterotrophus	*CHK1*	Hyphal integrity, conidiation, appressorial formation and pathogenicity on corn	Lev *et al.*, 1999
Colletotrichum lagenarium	*CMK1*	Pathogenicity, germination of conidia, appressorium formation, invasive growth on cucumber	Takano *et al.*, 2000
Fusarium oxysporum	*FMK1*	Penetration of root and pathogenesis	Di Pietro *et al.*, 2001
Fusarium solani	*FsMAPK*	Unknown	Li *et al.*, 1997
Magnaporthe grisea	*PMK1*	Appresorium formation and pathogenicity on rice	Xu and Hamer, 1996
Pyrenophora teres	*PTK1*	Conidiation appressorum formation, and pathogenicity on barley	Ruiz-Rolan *et al.*, 2001

Table 5.4. Function of *Saccharomyces cerevisiae KSS/FUS3* mitogen activated protein (MAP) kinase homologues in phytopathogenic fungi.

grisea MPS1 (Xu *et al.*, 1998), *Fusarium graminearum* MGV1 (Hou *et al.*, 2002) and *Colletotrichum lagenarium* MAF1 (Kojima *et al.*, 2002). Phenotypic analysis of *M. grisea*, Δ*mps1* mutants reveals that *MPS1* is dispensible for appressorium formation, but is required for penetration of the plant cuticle (Xu *et al.*, 1998). Furthermore, Δ*mps1* mutants are hypersensitive to cell-wall digesting enzymes, suggesting that *MPS1* is involved in cell-wall integrity (Xu *et al.*, 1998). Indeed, *MPS1* is a homologue of *S. cerevisiae SLT2* which is known to be involved in the PKC-mediated cell wall integrity signalling pathway (Lee *et al.*, 1993) as are *S. pombe* PMK1 (Toda *et al.*, 1996) and *C. albicans MKC1* (Navarro-Garcia *et al.*, 1995).

It is interesting that *C. purpurea* CPMK2 should be so closely related to *B. graminis* MPK1. Both are biotrophic pathogens, however, *C. purpurea* does not produce appressoria. Like Δ*mps1* mutants, though, Δ*cpmk2* mutants are hypersensitive to lytic enzymes, indicating the composition of the cell wall is affected, and Δ*cpmk2* mutants are not able to penetrate stigmatic hair tissue in rye (Mey *et al.*, 2002b). In contrast to *M. grisea MPS1*, *C. lagenarium MAF1* is essential for appressorium formation (Kojima *et al.*, 2002). Moreover, Δ*maf1* mutants remained insensitive to cell wall degrading enzymes, indicating that either *MAF1* redundantly regulates the maintenance of cell wall integrity, or is not involved in the maintenance of cell wall integrity (Kojima *et al.*, 2002). Additionally, Kojima *et al.* (2002) revealed that rearrangement of the actin cytoskeleton plays an important role in appressorial formation by *C. lagenarium*, and they hypothesised that the inability of Δ*maf1* mutants to form appressoria might be due to a failure of the actin organisation required for appressoria formation.

5.3.3 MAP kinase activity

MAP kinase activity was detected in *B. graminis* spore protein extracts using Western analysis. A single band corresponding to activated MAP kinase was obtained at a molecular weight similar to the murine control. However, MAP kinase activity could not be detected in *B. graminis* PGT-stage protein extracts. The most likely explanation for this result is that there was insufficient protein for the analysis.

The inability to obtain a strong MAP kinase signal of activity even for conidial protein extracts precluded any further studies using this technique, including a complete time-course analysis of MAP kinase activity during germling morphogenesis and *in vitro* characterisation of MAP kinase antagonists and agonists.

5.3.4 The effect of MAP kinase antagonists on *Blumeria graminis* f.sp. *hordei* germling development

In order to investigate the potential role of MAP kinase during the early development of *B. graminis* f.sp. *hordei*, two MEK-targeting compounds, U0126 and PD98059, were assessed for their ability to influence *B. graminis* germling morphogenesis. PD98059, applied exogenously to conidia, was inhibitory to *B. graminis* germling differentiation, but not germination, at concentrations of 10 and 100 μM. In mammalian systems, the high degree of specificity of PD98059 to MEK has been demonstrated by its failure to inhibit 18 mammalian protein Ser/Thr kinases (Xu and Hamer, 1996; Xu *et al.*, 1998; Dixon *et al.*, 1999). However, it is unclear to which of the *B. graminis* MAP kinase pathways PD98059 is targeted. Indeed, attempts at elucidating the target MAP kinase pathway by applying PD98059 to *M. grisea*, in which three MAP kinases identified to date have been well-characterised (Xu and Hamer, 1996; Xu *et al.*, 1998; Dixon *et al.*, 1999), were unsuccessful.

U0126 is inhibitory to MEK1 and MEK2 in mammalian systems, with an IC_{50} of 0.07 μM for MEK1 and 0.06 μM for MEK2 (Duncia *et al.*, 1998), in comparison to PD98059 which has an IC_{50} of 10 μM for MEK1 alone (Alessi *et al.*, 1995). Thus, U0126 represents a much more potent inhibitor of MEK1 than PD98059 (Favata *et al.*, 1998). However, exogenous application of between 0.01 and 100 μM U0126 had no effect on *B. graminis* germination or differentiation. A reason for this lack of effect could be one of selectivity. U0126 is known to be highly selective for MEK1 and MEK2 in 3T3 fibroblasts, as U0126 shows little, if any, effect on the kinase activities of PKC, Abl, Raf, MEKK, ERK, JNK, MKK-3, MKK-4/SEK, MKK-6, Cdk2, or Cdk4 (Favata *et al.*, 1998). Thus, perhaps this high level of selectivity in mammalian cells means that the inhibitor is not likely

to affect *B. graminis* MAP kinase signalling. Alternatively, the inhibitor might not be taken up by the fungus due to the presence of the cell wall.

5.3.5 The effect of MAP kinase agonists on *Blumeria graminis* f.sp. *hordei* germling development

Having identified that the mammalian MEK inhibitor PD98059 inhibits *B. graminis* differentiation, attempts were made to further characterise the putative effects of MAP kinase signalling on *B. graminis* germling development by applying N-Hexanoyl-D-*erythro*-sphingosine (C_6 ceramide), characterised in mammalian systems as a MAP kinase activator, to *B. graminis* germlings. However, exogenous application of between 0.01 μM and 100 μM N-Hexanoyl-D-*erythro*-sphingosine had no effect on *B. graminis* germination or differentiation. N-Hexanoyl-D-*erythro*-sphingosine is a cell-permeable ceramide analogue known to induce p42 phosphorylation in HL-60 cells (Raines *et al.*, 1993). In this system, maximal phosphorylation was detected on sphingosine addition after 10-30 seconds (Raines *et al.*, 1993). However, dephosphorylation back to basal levels occurred after just five minutes. It is impractical in the *B. graminis* system to work on such short time-scales, due to the inability to collect sufficient material for analysis, so this must be considered among the reasons as to why there was no evident effect of this agonist on *B. graminis* differentiation. Nevertheless, Thines *et al.* (1997a) observed an increase in appressorial formation from 1% to 15% in *M. grisea* on application of N-Hexanoyl-D-*erythro*-sphingosine. Additionally, Thines *et al.* (1997a) indicated that sphingosine may target PKC pathways since diacylglycerol (DAG) and ceramide are interlinked through the reactions of sphingomyelin synthase. Specifically, transfer of a choline phosphate from phosphatidylcholine to sphingosine yields DAG and sphingomyelin. This reveals that results obtained through the use of such compounds must be analysed with care.

5.3.6 *mpk*1 and *mpk*2 gene expression profiles

Semi-quantitative (end-point) RT-PCR transcript profiles have previously shown that *mpk*1 and *mpk*2 are differentially regulated during germling morphogenesis (Zhang and Gurr, 2001). In this study, a real-time PCR approach was used to assess the relative abundance of transcripts at six time points throughout germling

differentiation. This technique uses data from the exponential phase of amplification where there is a quantitative relationship between the amount of starting target DNA and the amount of amplification product (Rotorgene 2000 real-time PCR machine user manual, Corbett Research, Australia). PCR was undertaken with primers designed either side of a predicted intron to eliminate amplification of spurious genomic DNA.

Real-time PCR revealed elevated *mpk*1 transcript levels upon conidial germination, which correlates well with the results of Zhang and Gurr (2001). The real-time profile shows a peak in transcript levels during AGT elongation and swelling (8 hpi), with a decline in transcript abundance subsequent to this. This profile corresponds to that of the end-point RT-PCR and also correlates with the *PMK1* expression profile in *M. grisea*. Specifically, *M. grisea* transformants expressing GFP-PMK1 fusion proteins (under the control of the native *PMK1* promoter) revealed that GFP-PMK1 was present at low levels in mycelia, conidia and germ tubes, and that it became highly concentrated in appressoria (Tenjo *et al.*, 1999), indicating that *PMK1* is constitutively expressed at low levels in *M. grisea*, but that appressoria formation may require high levels of *PMK1*. In contrast, *P. teres PTK1* (Ruiz-Rolan *et al.*, 2001) is constitutively expressed. However, little else is known about the transcriptional regulation of the *PMK1*-like genes (Mey *et al.*, 2002b).

Little is known about the transcripts profiles of the *MPS1* homologues in phytopathogenic fungi. Indeed, *MPS1*, or its homologue, could not be detected in *B. cinerea* or *F. graminearum* by Northern analysis (Xu, Pers. Comm.). However, this study used a real-time PCR approach to show that the *mpk*2 expression profile follows the same trend as the *mpk*1 profile in *B. graminis*. End-point RT-PCR reveals that transcripts at 0, 0.5, 3 and 20 hpi are low in abundance. This correlates with the end-point analysis of Zhang and Gurr (2001) who observed no *mpk*2 transcripts in ungerminated conidia, however, there was a rise in transcript levels as morphogenesis progressed towards the mature appressorium, which indicates that *mpk*1 appears to be upregulated earlier than *mpk*2.

Taken together with the inhibitor, amino acid alignment and phylogenetic analyses, these results may hint at a rôle for *B. graminis mpk*1 and *mpk*2 in appressorium formation and plant penetration respectively. Interestingly, other genes implicated in appressorial formation and plant penetration processes are also upregulated in *B. graminis* at the same time as *mpk*1 and *mpk*2, that is, at 8 hpi, during AGT elongation and swelling. Such genes include those implicated in protection against host-derived stress including catalase B (*cat*B: Accession no. AAL56982), alternative oxidase (*aox*: AAL56983) and glutathione peroxidase (*gpx*1), and enzymes implicated in penetration including an extracellular alkaline protease (AAK84436) and extracellular 1, 3-β glucanase (AAL26904) (Z. Zhang and C. Henderson, *pers. comm.*)

5.3.7 Summary

In conclusion, two genes, *mpk*1 and *mpk*2, have been characterized from *B. graminis* f.sp. *hordei*. MAP kinase activity has been detected in conidia of *B. graminis*. However, insufficient material for experiments precluded detection of MAP kinase activity in PGT-stage germlings. Of two MEK inhibitors investigated, one, namely PD98059, inhibited *B. graminis* germling morphogenesis. However, a MAP kinase agonist failed to show any effect on germling differentiation. In addition, real-time PCR confirmed the differentially regulated transcript profiles of both *mpk*1 and *mpk*2, and revealed a peak in transcript levels during AGT elongation and swelling (8 hpi). *Mpk*2 follows a similar pattern of expression as *mpk*1, but with lower transcript levels prior to AGT elongation and swelling.

CHAPTER 6
COMPLEMENTATION OF THE *MAGNAPORTHE GRISEA* MITOGEN-ACTIVATED PROTEIN KINASE MUTANT Δ*pmk1* WITH *BLUMERIA GRAMINIS* F.SP. *HORDEI mpk*1

6.1 INTRODUCTION

6.1.1 Mitogen-activated protein kinases and *Saccharomyces cerevisiae*

Mitogen-activated protein (MAP) kinases are known to mediate the adjustment of intracellular activities of eukaryotic cells to environmental changes. They are activated by a MAP kinase cascade that has been shown to be highly conserved in a wide variety of eukaryotic organisms (Schaeffer and Weber, 1999). Within *Saccharomyces cerevisiae*, five MAP kinase signal transduction pathways have been extensively studied (reviewed in Banuett, 1998; Gustin *et al.*, 1998; Herskowitz, 1995) and knowledge of these has been instrumental for our understanding of MAP kinases in other eukaryotes, particularly other fungi (Xu, 2000). Specifically, the *S. cerevisiae* pheromone response pathway has been intensively studied for many years and is one of the best-understood pathways in eukaryotes (Banuett, 1998).

The *S. cerevisiae* pheromone response pathway mediates cell-cell interactions via two partially-redundant MAP kinases, FUS3 and KSS1, which regulate yeast mating processes including the expression of mating-specific genes, G1 arrest, schmoo formation and cell fusion (reviewed in Xu, 2000). In addition, elements of the pheromone response pathway, including KSS1, are involved in invasive growth in haploid cells and pseudohyphal development in diploid cells (Madhani and Fink, 1998).

6.1.2 *Magnaporthe grisea PMK1*

Whereas *S. cerevisiae* has served as a good model organism for the study of MAP kinases in eukaryotes generally, the rice blast fungus, *Magnaporthe grisea*, has served as an important model organism for the study of MAP kinases in

phytopathogenic fungi. Indeed, little was known about the role of MAP kinases in filamentous fungi, and certainly, phytopathogenic fungi, until the identification of *M. grisea PMK1* (Pathogenicity MAP Kinase 1) by Xu and Hamer (1996).

The *M. grisea* PMK1 coding region contains all 11 conserved protein kinase subdomains and characteristic MAP kinase phosphorylation sites, including the "TEY" residues at position 174-176 (Xu and Hamer, 1996). The PMK1 amino acid sequence has 60.5% identity and 77.9% similarity with *S. cerevisiae* FUS3 and 63.7% identity and 79.4% similarity with *S. cerevisiae* KSS1 (Xu and Hamer, 1996). The high degree of relatedness of *PMK1* to the yeast *FUS3/KSS1* genes prompted Xu and Hamer (1996) to test whether *PMK1* could function in the yeast pheromone signalling pathway as a MAP kinase. Therefore, the *PMK1* coding region, under the control of the yeast *GAL1* promoter, was introduced into yeast strain yDM300, which had been deleted for the *FUS3/KSS1* kinases. *PMK1* was capable of rescuing the phenotype of the *fus3/kss1* double mutants in mating assays.

Experimentally, *M. grisea* is a highly tractable fungus and so molecular genetic techniques can be used to introduce recombinant DNA molecules into it, by both homologous and ectopic integration (Talbot *et al.*, 1993). Consequently, *M. grisea* has become an important model system for the functional analysis of genes. Thus, Xu and Hamer (1996) were able to construct a gene replacement vector (pSSE3, Figure 6.1) to delete *PMK1* precisely from *M. grisea* and replace it with a gene encoding hygromycin phosphotransferase (HPH). They found that the *PMK1* mutants fail to form appressoria and do not grow invasively. However, *PMK1* is nonessential for vegetative growth and sexual and asexual reproduction (Xu and Hamer, 1996).

6.1.3 *Magnaporthe grisea* and complementation experiments

In addition to providing a good system for gene replacement experiments, *M. grisea* serves as an ideal system in which to test the function of genes from less tractable phytopathogenic fungi. Complementation of *M. grisea* mutants,

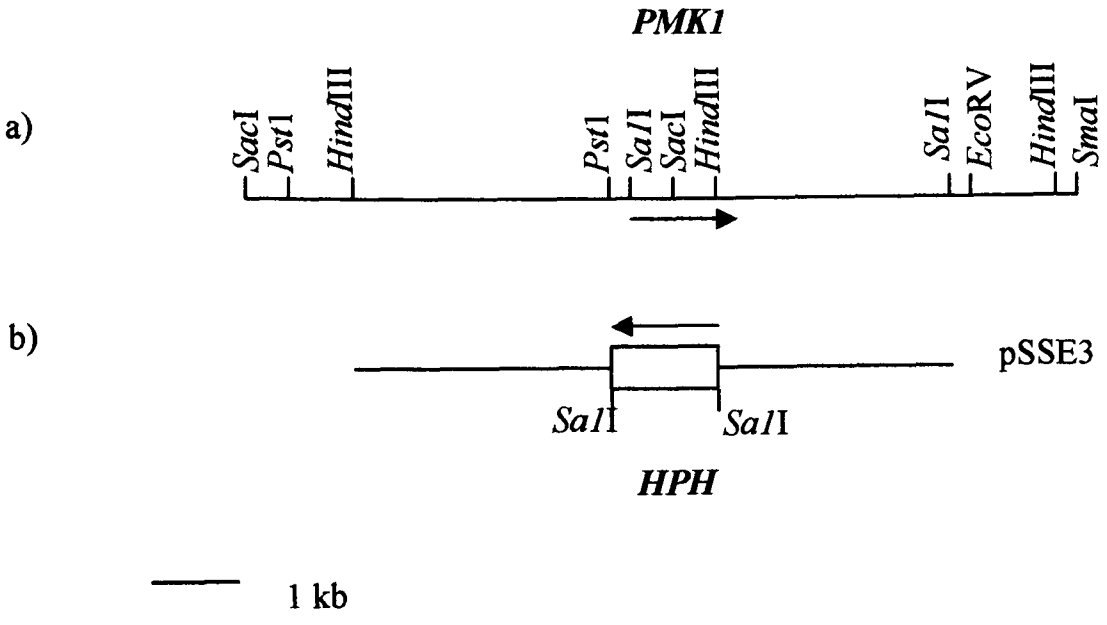


Figure 6.1. *PMK1* gene replacement vector. (a) Physical map of the PMK1 genomic region and (b) the gene replacement vector pSSE3. The arrows indicate the directions of PMK1 and hygromycin phosphotransferase (HPH) genes. Modified from Xu and Hamer (1996).

including the MAP kinase mutants Δ*pmk1* and Δ*mps1*, have been performed to functionally analyse genes from other phytopathogenic fungi. Specifically, *M. grisea* Δ*pmk1* has been used to examine the function of *Claviceps purpurea CPMK1* (Mey *et al.*, 2002a) and *Colletotrichum lagenarium CMK1* (Takano *et al.*, 2000) and *M. grisea* Δ*mps1* has been used to examine the function of *C. purpurea CPMK2* (Mey *et al.*, 2002b). In addition, complementation of a *M. grisea* Δ*cpka* mutant with *B. graminis BKA1* represented the first functional genetic analysis of pathogenicity in, not only *B. graminis* f.sp. *hordei*, but in a true obligate pathogen (Bindslev *et al.*, 2001).

Chapter 5 described the characterisation of *B. graminis mpk*1, a MAP kinase gene speculated as having a role in appressorium formation. With the availability of the *M. grisea* transformation system, it is possible to test the functions of *mpk*1 further by performing complementation experiments using the *M. grisea* Δ*pmk1*.

6.1.4 Objectives

This chapter describes attempts to complement the *Magnaporthe grisea* MAP kinase mutant, Δ*pmk1*, with the *Blumeria graminis* f.sp *hordei* MAP kinase gene, *mpk*1. To do this, the *B. graminis mpk*1 promoter was sequenced and a plasmid construct made comprising the *B. graminis mpk*1 gene under the control of the *B. graminis mpk*1 promoter. A control construct, that is, the *M. grisea PMK1* gene under the control of the *PMK1* promoter, was also made. Both constructs were transformed into *M. grisea* Δ*pmk1*. Putative transformants were selected using sulphonyl urea selection and were confirmed by Southern blot analysis, which allowed identification of transformants for subsequent phenotypic studies and expression analysis.

6.2 RESULTS

6.2.1 The *mpk*1 promoter

The full-length gene sequence of *mpk*1 has previously been determined by Zhang and Gurr (2001) who used a 'step down' PCR-based technique, for the direct sequencing of the gene (Zhang and Gurr, 2000). Similarly, this same method was used to directly sequence the *mpk*1 promoter region. Two walks were required to gain 888 bp of *mpk*1 promoter. The gene-specific primers for walk 1 and walk 2 are labeled in Figure 6.2.

6.2.2 Transformation vector construction: *mpk*1 and *PMK1*

In order to determine whether the *B. graminis* MAP kinase, *mpk*1, can restore the functions of its homologue, Δ*pmk1*, in *M. grisea*, two vectors were constructed for transformation into *M. grisea* Δ*pmk1* mutant strain nn78 (gift from M. Kershaw, University of Exeter). Specifically, a control construct, containing the *M. grisea PMK1* gene (Figure 6.3(a); Appendix 1), and the test construct, containing the *B. graminis mpk*1 gene (Figure 6.3(b); Appendix 2), were made in pCB1532 (gift from M. Kershaw) (Figure 6.4), containing the fungal selectable marker that confers resistance to chlorimuron ethyl, a sulfonylurea herbicide (Sweigard *et al.*, 1997). Both genes were under the control of their respective promoters and terminators.

The *M. grisea PMK1* promoter and gene, within vector pFL1, were obtained from J-R Xu (Purdue University, USA) and were isolated using primers A and B (Figure 6.3(a); Appendix 1). The *B. graminis mpk*1 promoter and gene were isolated from *B. graminis* genomic DNA using primers C and D (Figure 6.3(b); Appendix 2).

6.2.3 Transformation

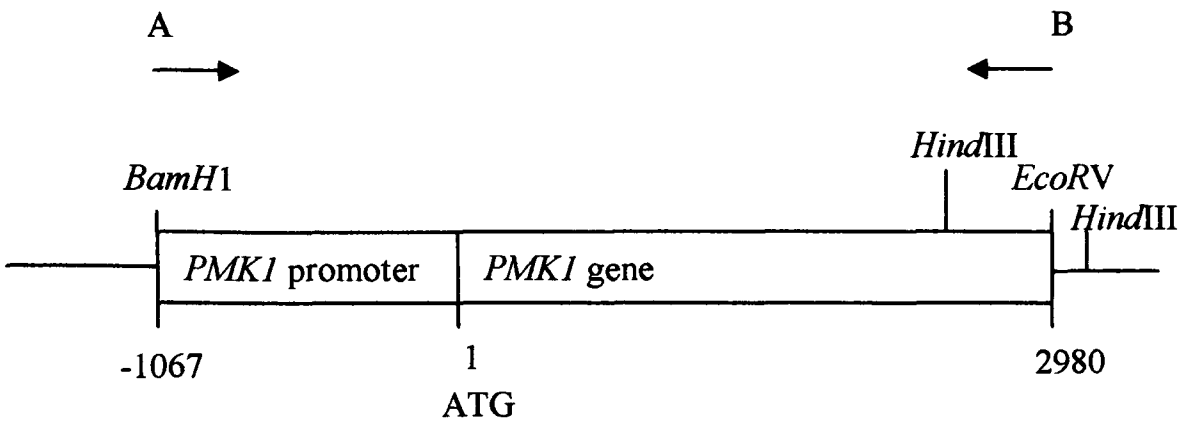
Protoplast-mediated transformation experiments were performed using 5 μg of circular vector DNA with 150 μl Δ*pmk*1 protoplasts at $1x10^6$ mL^{-1} for each construct. After 6 days, chlorimuron ethyl-resistant regenerated protoplasts

```
1       GAATAAGATG CTGCTCATGC CTCAGGCTCG GTCCTCATGG CATAACCTAA AGGCCAGCAT
                                                          MAP1-4 <------
61      TGTCTGTCTC ATATACCAGC TTTCCCTTGA TTGCCCCGCG TATCAGATTA GGCGAGATCC
        ----------------------  <---------------------------- MAP1-5
121     ACTTCAAGAG TTGAGGTAGC CTTCATCGAA GTTCTAGAGT ACCGGACGTC AATTGAGCTT

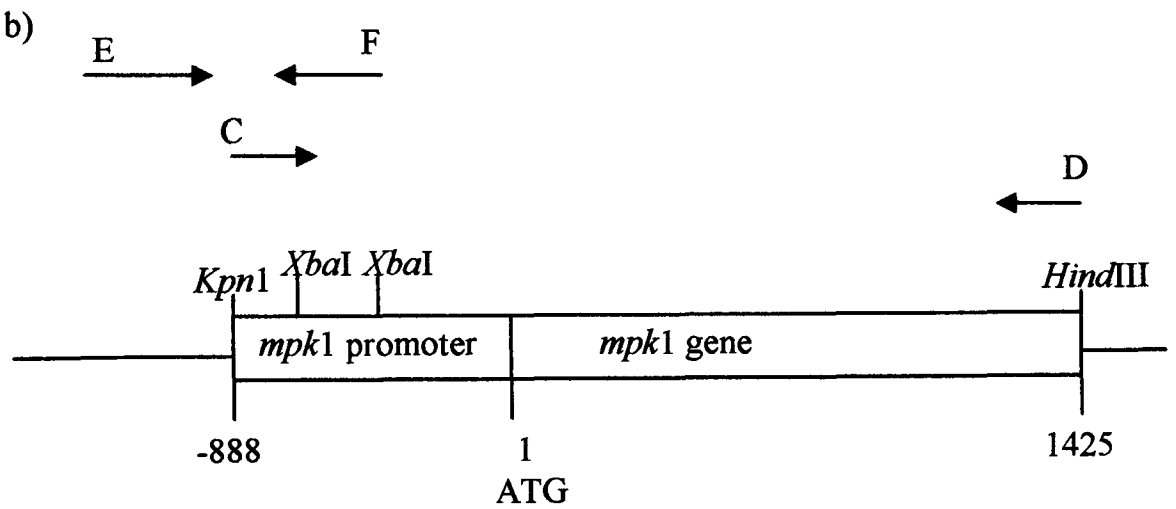
181     CACAGCGAGC CAAGGCCTCG CAGCTCTTGT TTAGCAGTAT CCTTTGAAAA TATTTTGATA
241     TCACGTCTCC ATTCATTTCG TACATCTTTA ATCTAACTGG CCTCAGCTTT GTTTGAGGTC
301     TGGTTTACCC AAGCGTTGAC CAGACTAGTC CATCAGATTC GGAACGCGAC TACGGAAGTT
361     GCAGCTTAGT GGAGGTAGTG CCTGCTCTGC TACTACAAAT GCTCGAGGGA CCGAGCGCAA
421     TTGCTGCAGG TAGCTGACAG GCGAAACTTG GACTCTAGGG GTATAAGCTG AGGACAACAA
481     CGACAATCCA TAACAGCAAA GTTCAATCTA GAATAGCTGC AAACTACATC GACTTGAGCT
541     ATTCCTTTAA CTTCCGCACC CTTTGCTCGT AGGCTGCTTG TGAGAGACGA AACATCTCGC
601     GCTTTCATTG CTATTGCTGC AACTGTCTGC TGTCCACATC TCTCGCCACT CTTCTCTGCT
661     YTGACATCTC CTACCCTGAG ACCTTGCTCA TTCAATAGTA ATAGCTCATC TTTTACAACA
721     TCCCCTTACT ACTACCGGTC ATCTGTCAGC TTTCAAGCTG CATCTATCTA ATATTCAAGA
781     CTTGCAAGCG AACACCAGAG TTGTCTTTTT CCTAATTTCA CCAACCCCTC CTCTTTAGAT
                      MAP1-2 <------------------------  <----------------
841     AGGAACAGCT TTCATACACG CTTTCAGATC GTCAAAGGCA CTTTCAAGAT GTCGACCCGT
        ------------ MAP1-1
901     GCCCCTAATG CTACGACAGG ATCGCGTAAG ATCTCATTCA ACGTAAGTGA GCAGTATGAT
961     ATTCAAGATG TTGTGGGAGA GGGTGCCTAT GGTGTTGTCT GGTGAGTCTC ACTCAGCCTG
```

Figure 6.2. Gene-specific primers (MAP1-1, MAP1-2, MAP1-3 and MAP1-4) used to obtain 888 bp of the *Blumeria graminis* f.sp. *hordei mpk*1 promoter using the 'step down' PCR-based technique described by Zhang and Gurr (2000). The start codon (ATG) is indicated (red).

a)



b)



c)

Primer sequences

A 5' CCAAATACCTGCCGTACTGGC 3'

B 5' AGTCTGCAGTTAATTGTGAGTGCCGGCG 3'

C 5' GAATAAGATGCTGCTCATGC 3'

D 5' GGGAATTAATCGGATCCAC 3'

E 5' TGTGCTGCAAGGCGATTAAGT 3'

F 5' AGAGCAGGCACTACCTCC 3'

Figure 6.3. Constructs used for transformation of *Magnaporthe grisea* Δ*pmk1*. (a) Plasmid pCB1532 with genomic *Magnaporthe grisea PMK1* controlled by the *PMK1* promoter; (b) Plasmid pCB1532 with genomic *Blumeria graminis* f.sp. *hordei mpk*1 controlled by the *mpk*1 promoter; c) Primer sequences shown in (a) and (b), indictated by arrows A to F. Primer E lies Primer E lies 5' to the *B. graminis mpk*1 promoter region in the vector pCB1532.

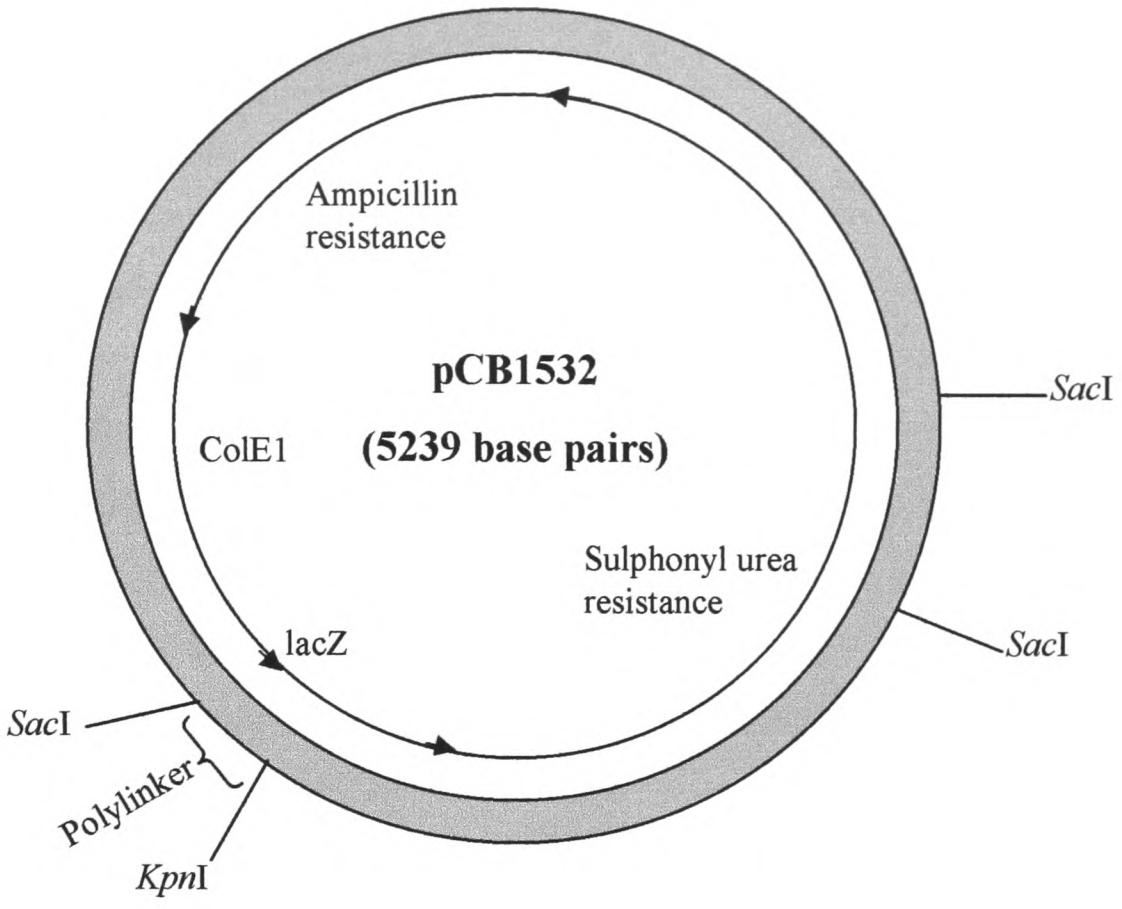


Figure 6.4. Vector for transformation, pCB1532 (gift from M. Kershaw, University of Exeter). The vector is based on pBSSKII- and has the polylinker: *Sst*I, *Not*I, *Xba*I, *Spe*I, *Bam*HI, *Sma*I, *Pst*I, *Eco*RI, *Eco*RV, *Hind*III, *Cla*I, *Sal*I, *Xho*I, *Apa*I, *Kpn*I.

(Figure 6.5) were transferred to fresh chlorimuron ethyl-containing plates, and, after a further 6 days, were subcultured onto Complete Media (CM). Of the 10 *PMK1* and 38 *mpk*1 putative transformants recovered, 5 putative *PMK1* transformants (designated P1 to P5) and 16 putative *mpk*1 transformants (designated Bg1 to Bg5, Bg7, Bg11, Bg18, M1, M3, M7, M8, M13, M17, M18 and M23) were taken for further analysis. Genomic DNA obtained from 10 day-old plate cultures of Bg1, Bg2, Bg3, Bg4, Bg5, Bg7, Bg11, Bg18, M1, M3, M7, M8, M13, M17, M18 and M23 was used for polymerase chain reaction (PCR) analysis to screen for the presence of the *mpk*1 construct (data not shown). Primers used for this analysis are shown in Figure 6.3(b) and are designated "E" and "F". The genomic DNA samples were then used for Southern analysis.

6.2.4 Southern blot analysis

Southern blot analyses were performed on the *PMK1* transformants, P1 to P5, and the *MPK1* transformants, Bg1 to Bg5, Bg7, Bg11, Bg18, M1, M3, M7, M8, M13, M17, M18 and M23. Genomic DNA from P1 to P5, including Guy11 and Δ*pmk1* controls, were restriction endonuclease-digested with *Hind*III and fractionated by gel electrophoresis and blotted onto nylon membrane. The single *Hind*III restriction endonuclease site in *PMK1* is shown in Appendix 1. Another *Hind*III site lies at the 3' end of the sequence within the polylinker region of the vector for transformation (pCB1532) (see Figure 6.3). Together, these sites yield a restriction endonuclease fragment of 730 bp. Blots were hybridised with either radiolabelled *PMK1* insert DNA or pCB1532 vector DNA (Figure 6.6). Genomic DNA from Bg1 to Bg5, Bg7, Bg11, Bg18, M1, M3, M7, M8, M13, M17, M18 and M23, including Guy11 and Δ*pmk1* controls, were restriction endonuclease-digested with *Xba*1. The two *Xba*I restriction endonuclease sites in *mpk*1 are shown in Appendix 2 and yield a fragment of 354 bp. Following blotting onto nylon membrane, the blots were hybridised with either radiolabelled *mpk*1 insert DNA or pCB1532 vector DNA (Figure 6.7).

Figure 6.6(a) shows that *Hind*III-digested, *PMK1*-hybridised P2 has the ~730 bp fragment expected with the presence of the *PMK1* construct and an additional

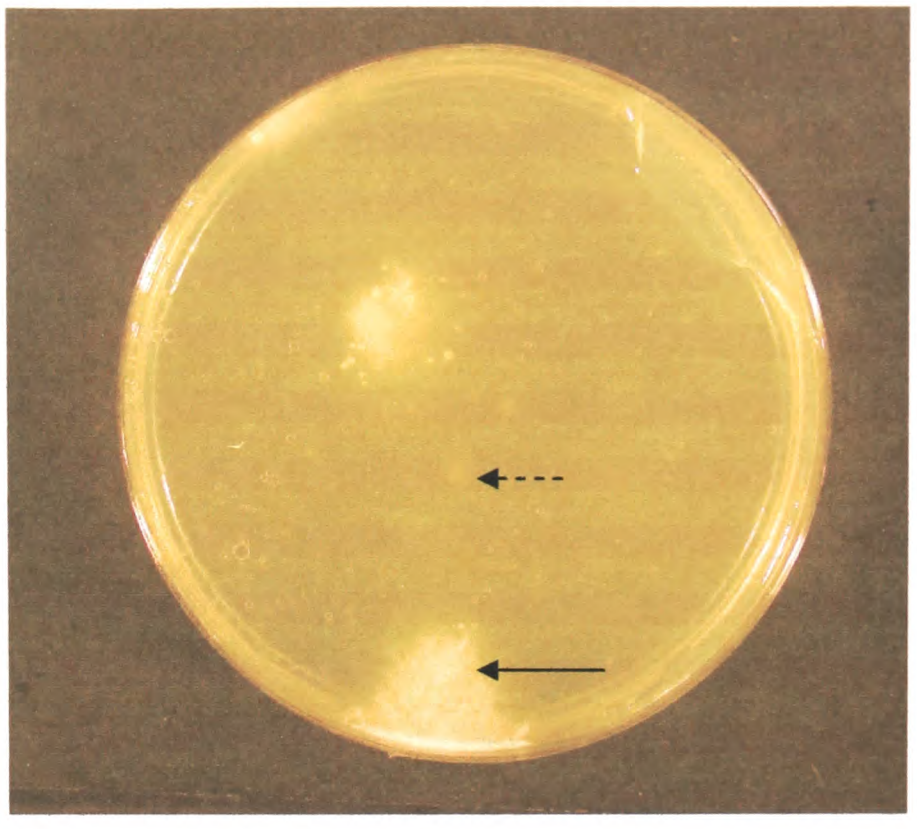
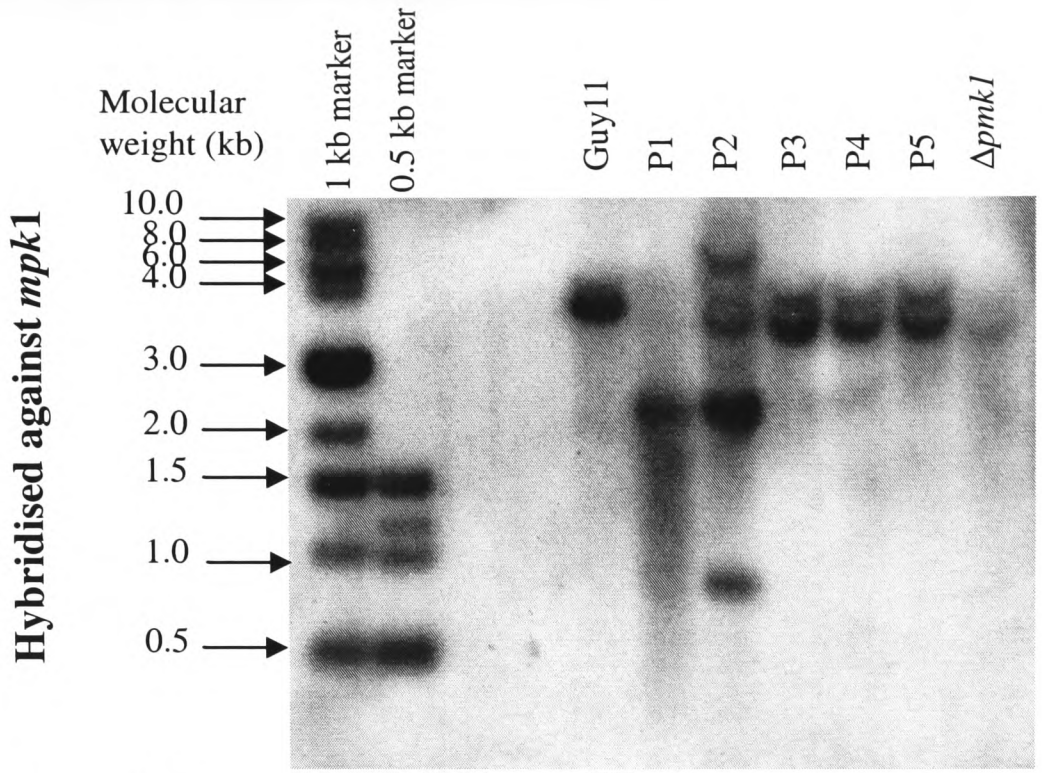


Figure 6.5. Regenerated protoplasts growing on chlorimuron ethyl-containing (50 $\mu g.mL^{-1}$) plates 6 days post-transformation. The solid arrow indicates a colony growing over the surface of the selective media. The broken arrow indicates a regenerating colony growing within the media that has not yet broken through to the surface of the plate.

a)



b)

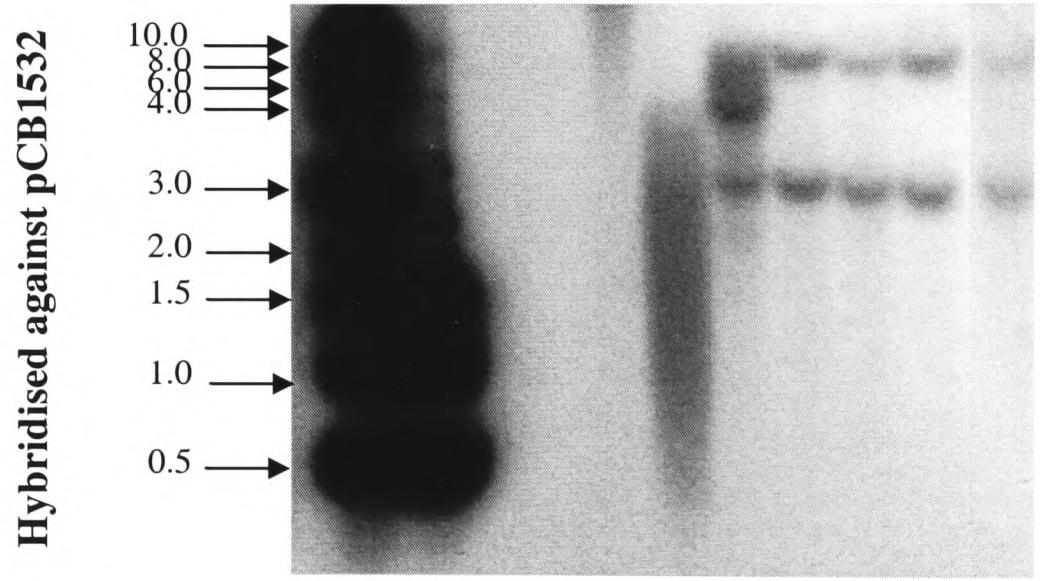


Figure 6.6. Southern blot analysis of selected putative *PMK1* transformants. Genomic DNA was isolated from transformants, restriction endonuclease-digested with *Hind*III and fractionated by electrophoresis in 1% agarose gels. The gels were blotted and the blots were hybridised with either radiolabelled *mpk*1 (a) or pCB1532 (b) DNA, as indicated. In b) the P1 sample has degraded and the Guy11 sample has not digested. a) was exposed for 24 hours and b) was exposed for 6 days. Restriction endonuclease digestion with *Hind*III should yield a 730 bp fragment in transformants.

band of ~5.8 kb which is not seen in either Guy11 or Δ*pmk1*. Both P1 and P2 have a band of ~2.2 kb. However, DNA degradation means that the presence of a 730 bp band in P1 cannot be substantiated. P3, P4 and P5 all have banding patterns comparable to Δ*pmk1*. Hybridising with pCB1532 reveals that P3, P4 and P5 all have banding patterns comparable to Δ*pmk1* (Figure 6.6(b)). P2 also has the ~3.0 kb band of P3, P4, P5 and Δ*pmk1*, but also has a band of 5.2 kb, expected with integration of the transformation vector. Additionally, P2 possesses prominent bands of greater than 5.2 kb.

Figures 6.7 (a), (b) and (c) show that the *Xba*I-digested, *mpk*1-hybridised Bg1, Bg2, Bg4, M3 and M7 all have the 354 bp fragment expected with the presence of the *mpk*1 construct. Additional bands are also prominent, including bands of ~1.8 kb in each of Bg1, Bg2, Bg4, Bg5, M3 and M7 and bands of ~5.4 kb in each of Bg1, Bg5 and M7. Bg2 also possesses prominent bands of ~1.4 kb, 2 kb, 6.0 kb, 6.5 kb and 7.5 kb. M7 possesses additional, prominent bands of ~3.5 kb and 4 kb. Hybridising with pCB1532 reveals prominent bands of between 5.2 kb in Bg1, Bg2, Bg5 and M7 expected with integration of the construct (Figures 6.7 (d), (e) and (f)). Bg2 possesses a band of ~1.7 kb and bands of between 2.0 and 10.0 kb whose exact sizes cannot be resolved from the blot in Figure 6.7(d). Bg4 possesses two bands of 6.0 and 9.0 kb respectively, while M7 possesses an additional band of ~3.0 kb.

6.2.5 Phenotypic analysis

From the Southern blot experiments two transformants carrying *M. grisea PMK1*, namely P1 and P2, and three transformants carrying *B. graminis mpk*1, that is, Bg2, M3 and M7, were chosen for further analysis. Specifically, each transformant was characterised phenotypically by looking at mycelial appearance of plate cultures, and as *M. grisea* Guy11 is pathogenic on susceptible varieties of barley (Swiegard *et al.*, 1998), such as cultivar Golden Promise, germination and differentiation of these transformants on barley epidermis was assessed.

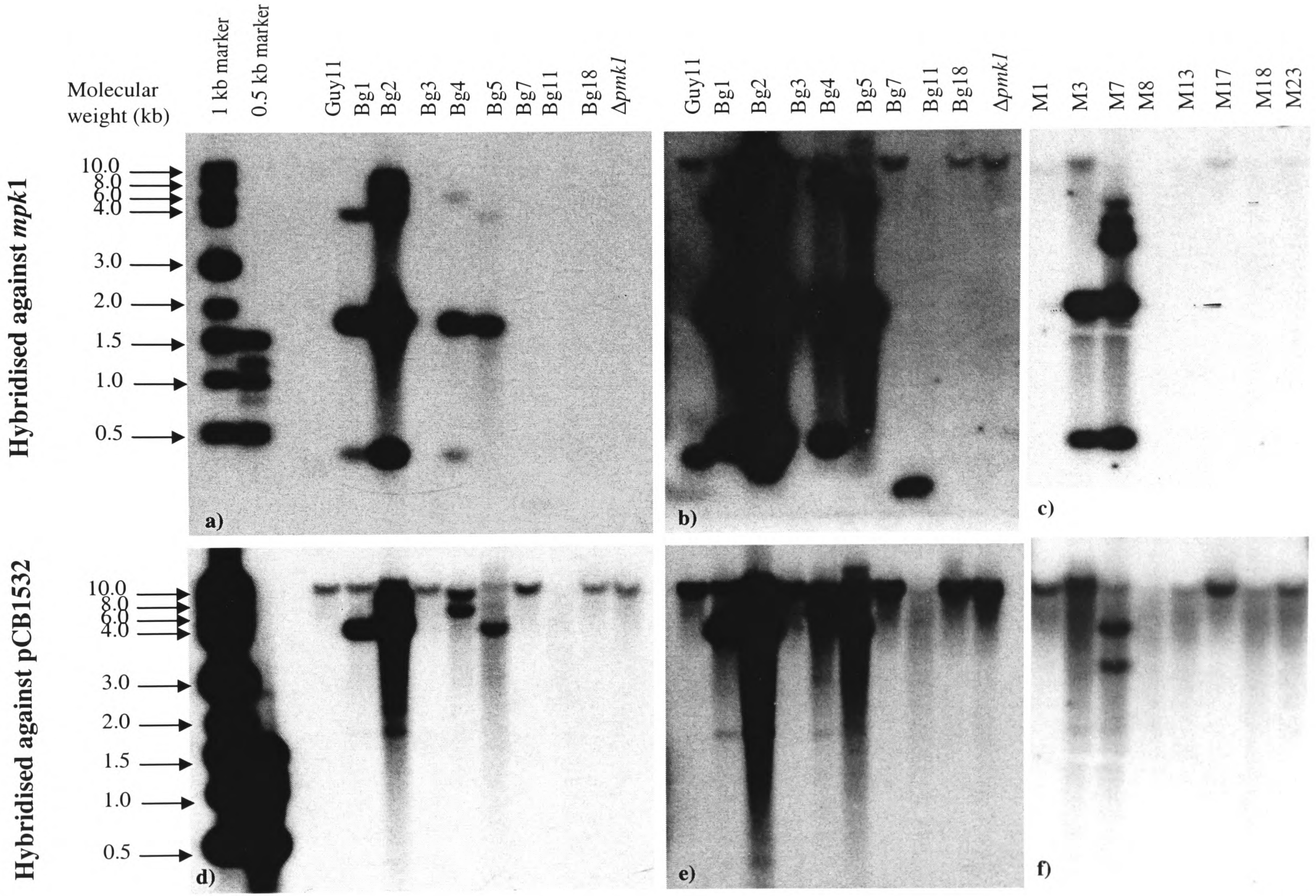


Figure 6.7. Southern blot analysis of selected putative *mpk*1 transformants. Genomic DNA was isolated from transformants, restriction endonuclease-digested with *Xba*I and fractionated by electrophoresis in 1% agarose gels. The gels were blotted and the blots were hybridised with either radiolabelled *mpk*1 (a, b and c) or pCB1532 DNA (d, e and f), as indicated. a) and b) are different exposures of the same blot (molecular weight markers are not shown in b)). a) was exposed for 16 hours (h), b) for 6 days. d) and e) are different exposures of the same blot (molecular weight markers are not shown in e)). d) was exposed for 16 h, e) for 5 days. c) was exposed for 16 h and f) for 6 days. Restriction endonuclease digestion with *Xba*I should yield a 354 bp fragment in transformants.

6.2.5.1 In vitro phenotype

Figure 6.8 shows 10 day-old plate cultures of *M. grisea* wild-type Guy11, Δ*pmk1*, P1, P2, Bg2, M3 and M7 growing on Complete Media (CM). Transformants P1 and P2 (Figure 6.8 (c) and (d)) looked more similar to Guy11 (Figure 6.8(a)) than to the Δ*pmk1* mutant (Figure 6.8(b)), with both P1 and P2 having the distinctive grey/brown colouring of wild-type Guy11. Bg2, M3 and M7 still possessed the characteristic white, ridged appearance of Δ*pmk1*.

6.2.5.2 Germination and differentiation on barley epidermis

P1, P2, Bg2, M3 and M7 were tested for their abilities to differentiate on epidermal peels, from the susceptible barley cultivar Golden Promise, compared with Guy11 and Δ*pmk1*. A time-course of development was performed with conidia being scored for germination (6 replicates of 50 conidia) and differentiation (6 replicates of 50 germinated conidia) at 0, 2, 4, 8, and 12 hpi. Differentiation is defined as the production of an elongated germ tube (EGT), a swollen germ tube (SwGT) or an appressorial germ tube (AGT). Statistical significance was determined using the General Linear Model (GLM) following an arcsine transformation.

Figure 6.9 shows the time-courses of germination of P1 and P2 (Figure 6.9(a)) and Bg2, M3 and M7 (Figure 6.9(b)) over 12 hours compared to Guy11 and Δ*pmk1*. Table 6.1 gives P-values to show the significant differences in germination between the transformants and Guy11 and Δ*pmk1*.

Germination by P1 and P2 was initially slower than Guy11 and Δ*pmk1*, with a mean of around 12% of conidia having germinated by 2 hours post inoculation (hpi) for P1 and P2 compared to a mean of 48% and 36% for Guy11 and Δ*pmk1*, respectively (P=0.000 for each of P1 and P2 when compared with both Guy11 and Δ*pmk1*, Table 6.1). At 4 hpi, the difference in germination level between P1 and P2 when compared with both Guy11 and Δ*pmk1* was still significant (Table 6.1), with a mean of around 86% of conidia having germinated for both Guy11 and

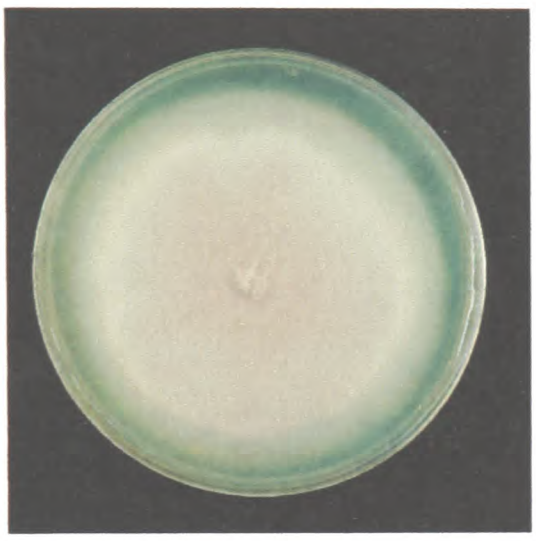
a)



b)



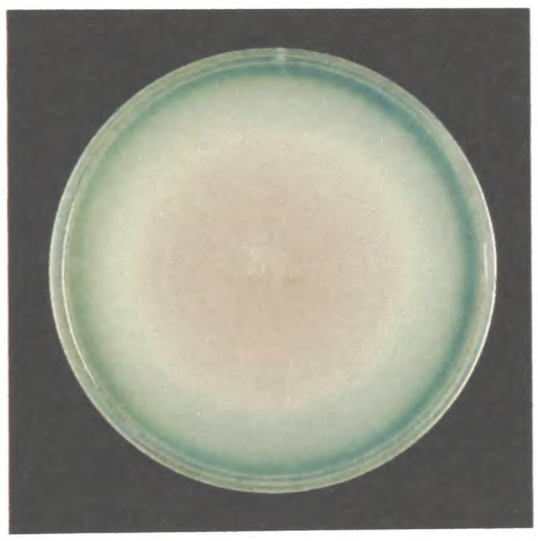
c)



e)



d)



f)



g)

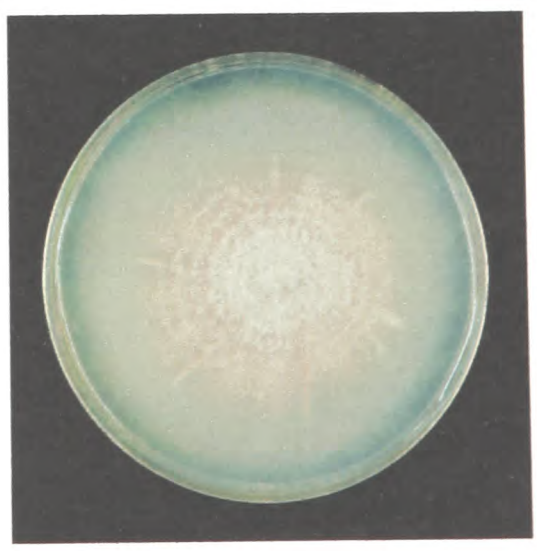
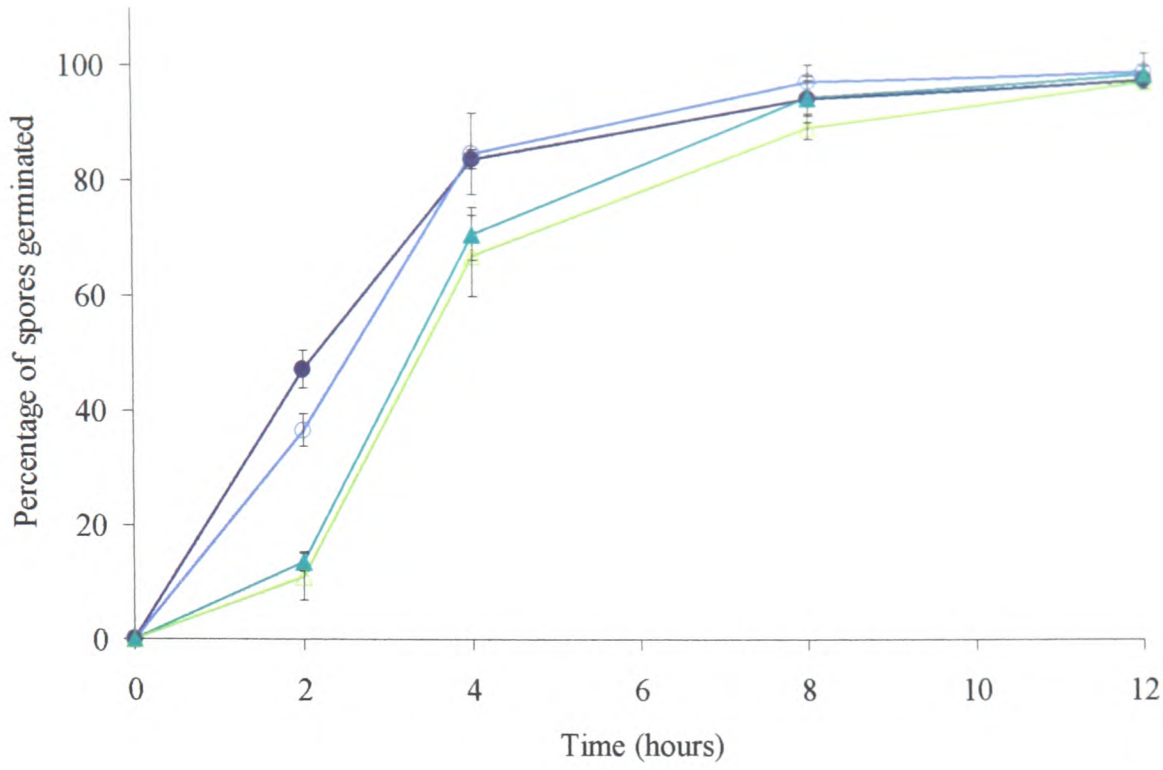


Figure 6.8. Ten day-old cultures of *Magnaporthe grisea* growing on Complete Medium (CM). a) Wild-type: Guy11; b) mitogen-activated protein (MAP) kinase mutant Δ*pmk1*; c) and d) are P1 and P2, respectively, that is, Δ*pmk1* transformed with *M. grisea* wild-type *PMK1*; e), f) and g) are Bg2, M3 and M7, respectively, that is, Δ*pmk1* transformed with *Blumeria graminis* f.sp. *hordei mpk*1.

a)



b)

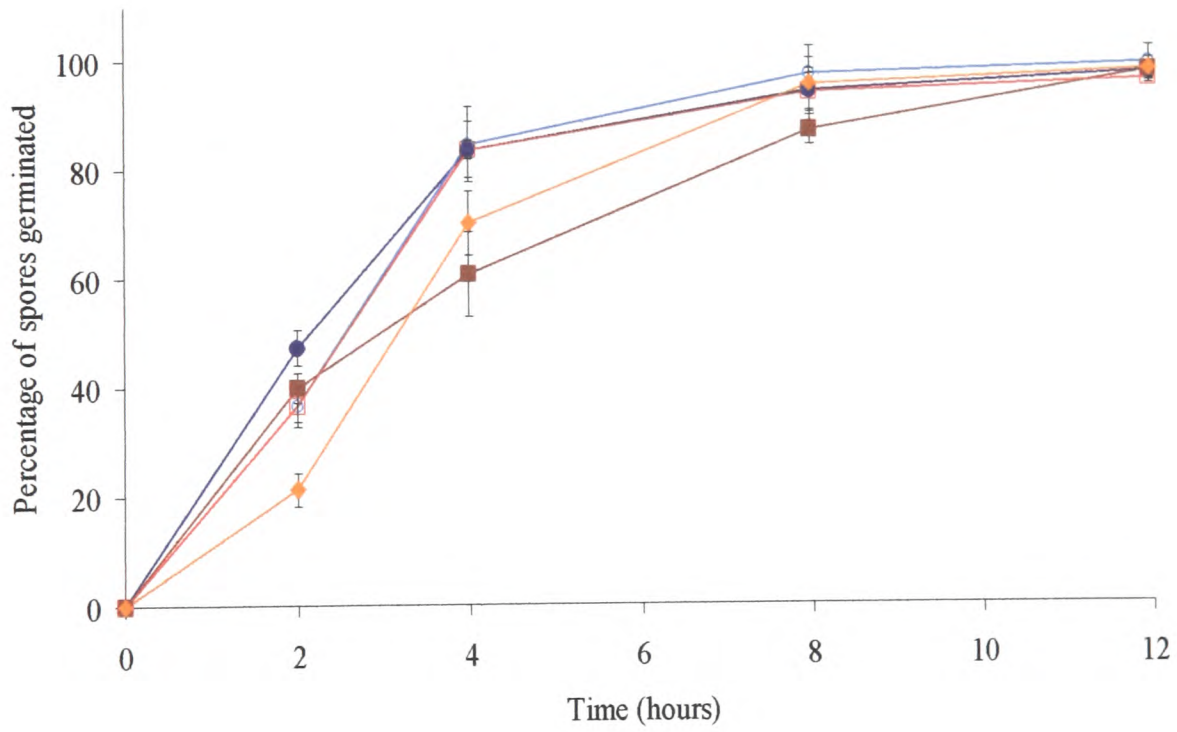


Figure 6.9. Time-course of germination of *Magnaporthe grisea* conidia Guy11and Δ*pmk1* (a and b), P1 and P2 (a), M3 and M7 (b) on barley epidermal peels. ● corresponds to Guy11 and ○ corresponds to Δ*pmk1* in both (a) and (b). ▲ corresponds to P1 and △corresponds to P2 in (a). ■ corresponds to Bg2, □ correspond to M3 and ◆ corresponds to M7 in (b). For each time point, 6 x 50 germlings were scored for germination. The mean ± standard error is shown.

Time (hpi)	Guy11				*Δpmk1*			
	2	4	8	12	2	4	8	12
P1	0.000***	0.018*	0.855	0.238	0.000***	0.010**	0.194	0.145
P2	0.000***	0.006**	0.375	0.918	0.000***	0.004**	0.058	0.058
Bg2	0.006**	0.000***	0.025*	0.651	0.227	0.000***	0.001**	0.055
M3	0.000***	0.773	0.747	0.633	0.993	0.875	0.056	0.023*
M7	0.000***	0.012*	0.672	0.526	0.000***	0.007**	0.257	0.111

Table 6.1. P-values to show to show the significant differences in germination on barley epidermal peels between the *Magnaporthe grisea* transformants P1, P2, Bg2, M3 and M7 and the wild-type Guy11 and mutant *Δpmk1* over a 12 hour time-course. Hpi designates "hours post inoculation". For each strain and time point, 6 x 50 conidia were scored for germination. * indicates $p \leq 0.05$, ** indicates $p \leq 0.01$ and *** indicates $p \leq 0.000$.

Δ*pmk1* compared to a mean of 72% and 64% for P1 and P2 respectively. By 8 hpi, there was no significant difference in the level of germination for P1 and P2, when compared to Guy11 and Δ*pmk1*, with Guy11 and P1 having a mean germination of 96%, Δ*pmk1* having a mean germination of 98%, and P2 having a mean germination of 90%.

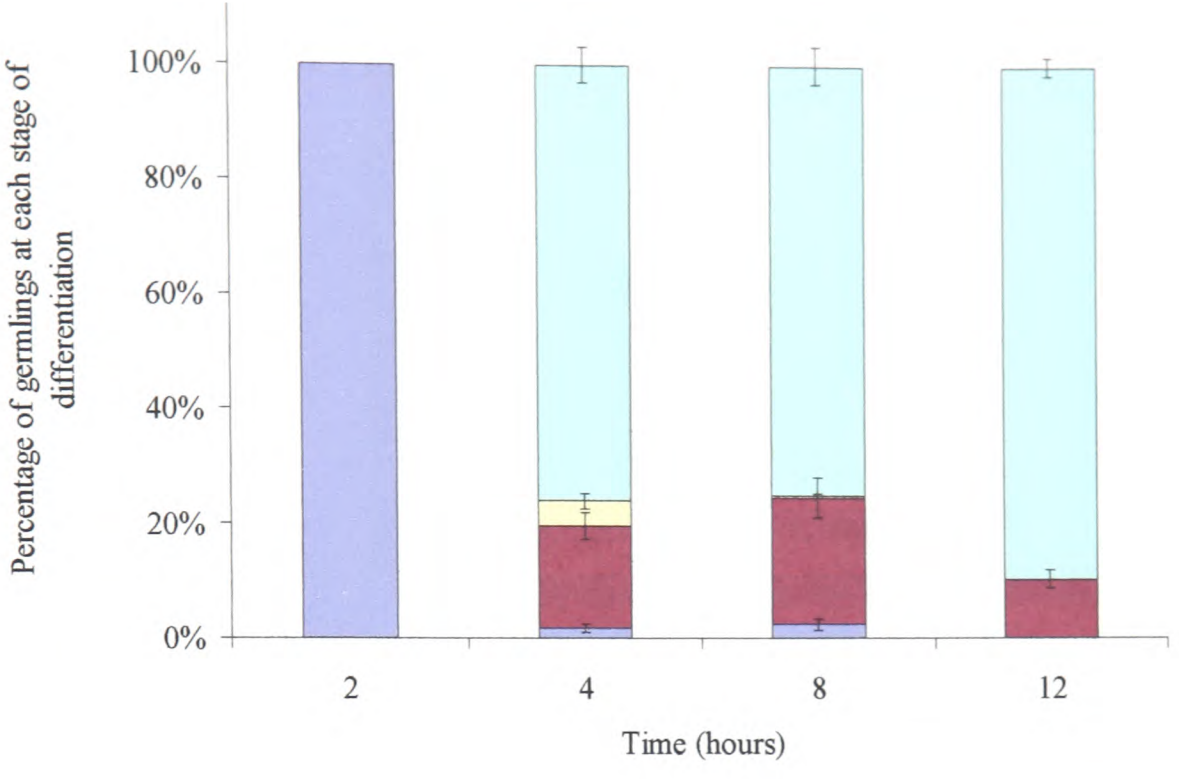
Comparison of germination levels of Bg2, M3 and M7 with Guy11 and Δ*pmk*1 revealed that at 2 hpi, Bg2, M3 and M7 all had significantly different germination levels to Guy11 (Table 6.1). That is, a mean germination of 40%, 36% and 22% respectively compared to 48% for Guy11. However, there was no significant difference between the germination levels of Δ*pmk1*, Bg2 and M3. By 4 hpi, both Bg2 and M7 had significantly different germination levels to Guy11 and Δ*pmk1*. However, by 8 hpi, only Bg2 had germination levels that significantly differed to Guy11 and Δ*pmk1*, with Bg2 having a mean germination of 88% compared to 96% and 98% for Guy11 and Δ*pmk1* respectively.

Figure 6.10 shows the time-courses of differentiation on barley epidermal peels of Guy11 (Figure 6.10(a)), Δ*pmk1* (Figure 6.10(b)), P1 (Figure 6.10(c)), P2 (Figure 6.10(d)), Bg2 (Figure 6.10(e)), M3 (Figure 6.10(f)) and M7 (Figure 6.10(g)) over 12 hours. P-values are given above graphs (c) to (g) and show the significant differences in differentiation between the transformants and Guy11 and Δ*pmk1*. Figure 6.11 shows micrographs of Guy11, Δ*pmk1*, P1, P2, Bg2, M3 and M7 at 8 and 12 hpi.

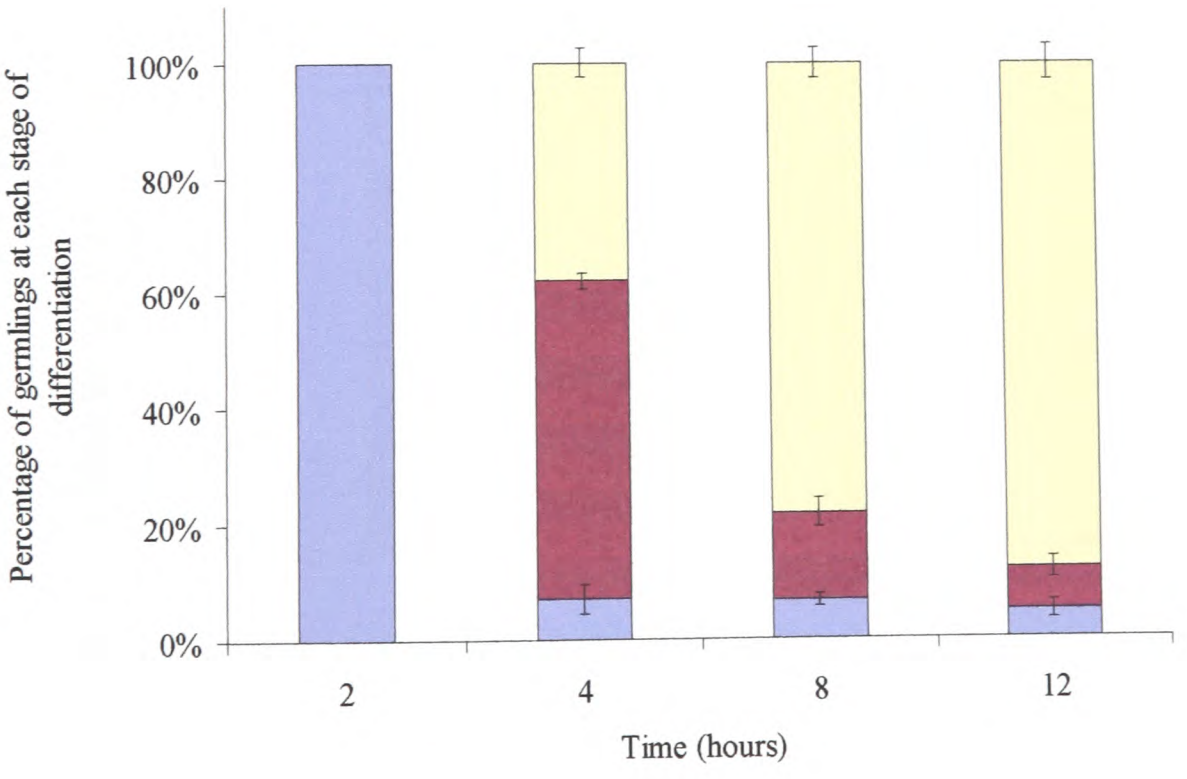
By 4 hpi, both P1 and P2 transformant germlings have differentiated appressoria (Figure 6.10 (c) and (d)). However, significantly fewer P1 germlings have differentiated appressoria (a mean of 28% of germlings) compared to P2 germlings (a mean of 54% germlings) (P=0.002) or the wild-type Guy11 (a mean of 76% of germlings) (P=0.000). The difference in production of appressoria by P2 germlings compared to Guy11 germlings was also highly significant (P=0.000). By 8 hpi, P1 and P2 germlings have still differentiated significantly fewer appressoria than Guy11. However, by 12 hpi, there is no significant

Figure 6.10.

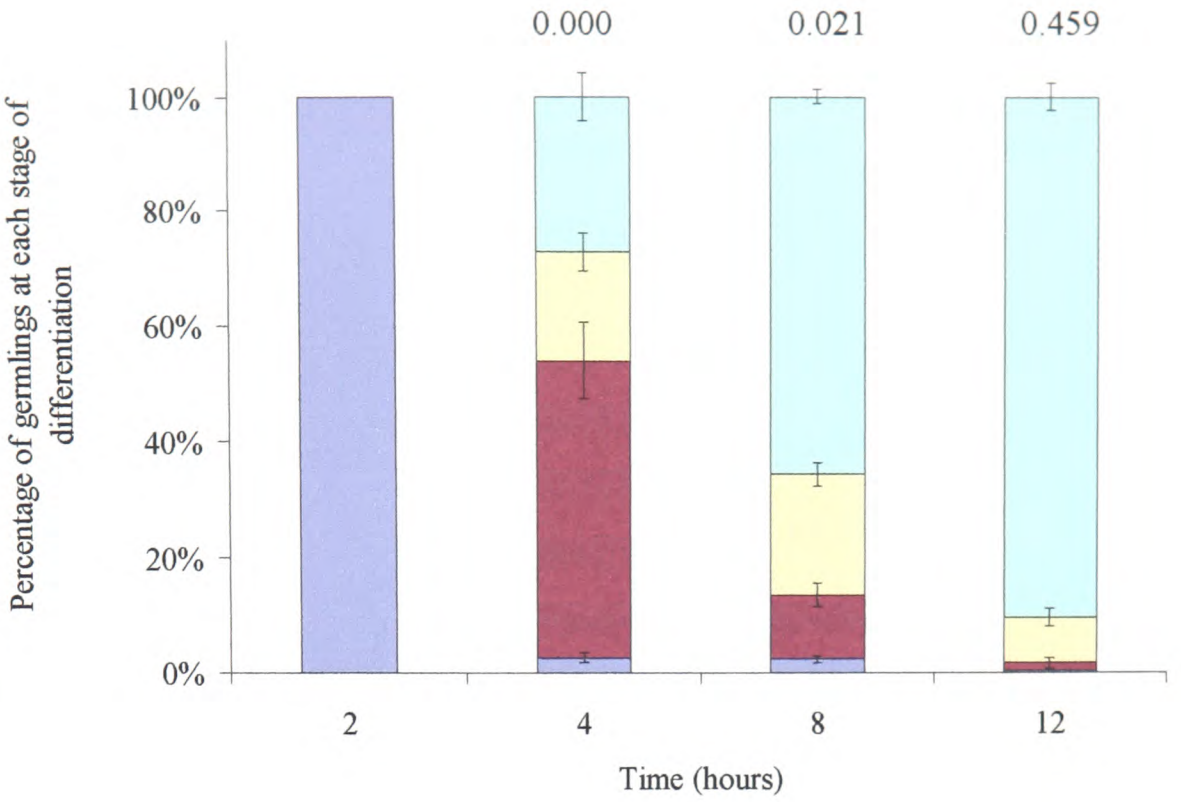
a)



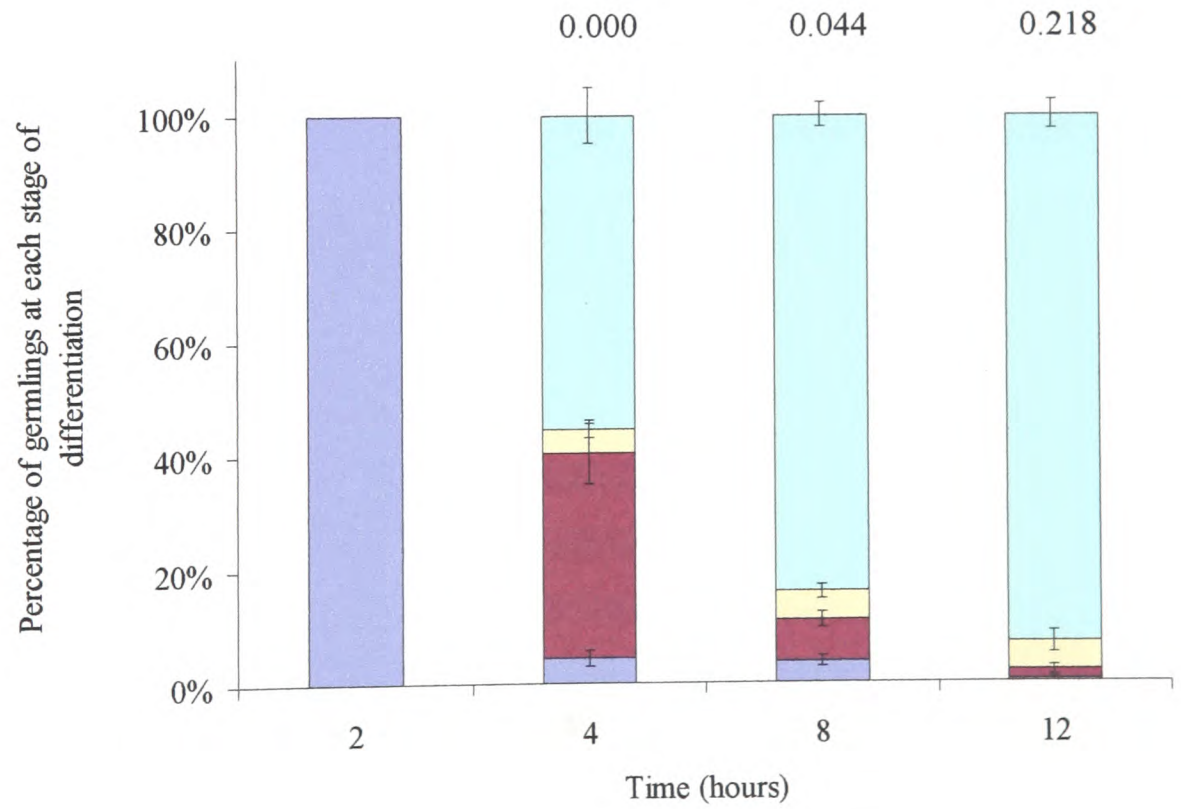
b)



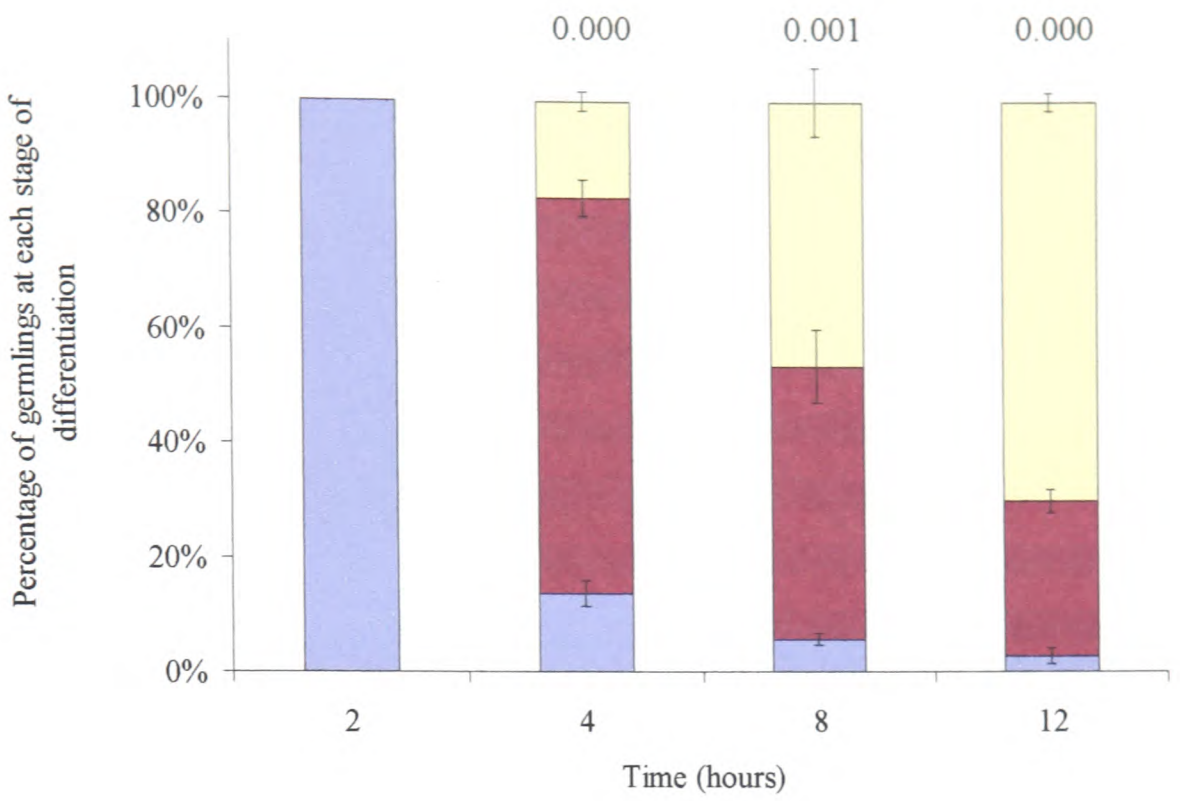
c)


0.000
0.021
0.459
100%
80%
60%
40%
20%
0%
Percentage of germlings at each stage of differentiation
2
4
8
12
Time (hours)

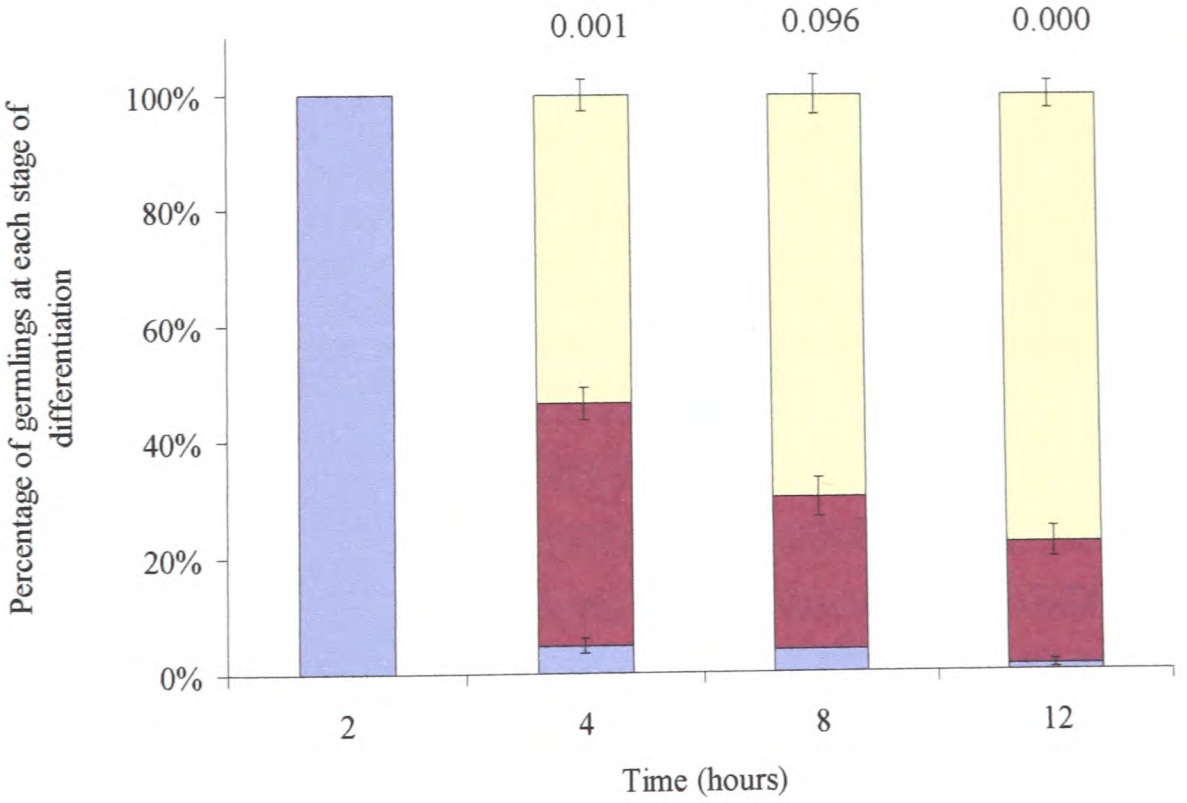
d)


0.000
0.044
0.218
100%
80%
60%
40%
20%
0%
Percentage of germlings at each stage of differentiation
2
4
8
12
Time (hours)

e)


0.000
0.001
0.000
100%
80%
60%
40%
20%
0%
Percentage of germlings at each stage of differentiation
2
4
8
12
Time (hours)

f)


0.001
0.096
0.000
100%
80%
60%
40%
20%
0%
Percentage of germlings at each stage of differentiation
2
4
8
12
Time (hours)

g)

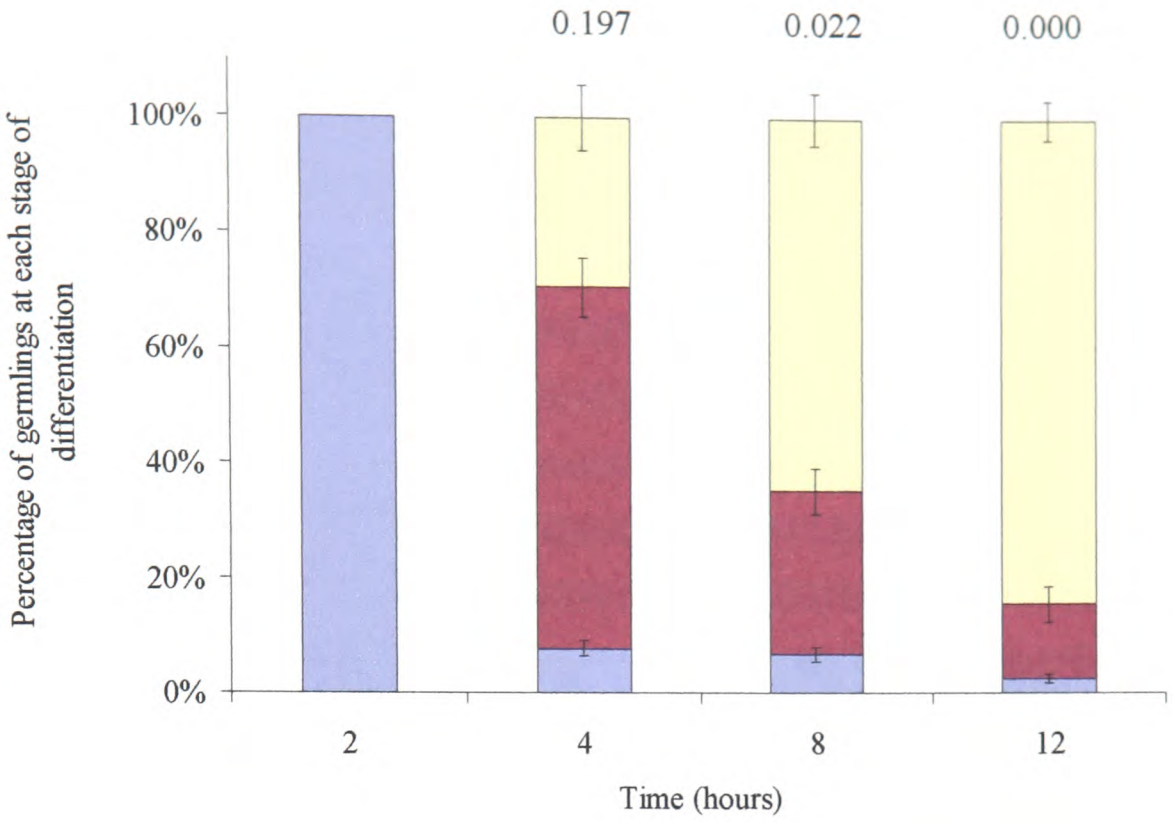


Figure 6.10. Time-courses of differentiation of *Magnaporthe grisea* (a) wild-type Guy11, (b) mutant Δ*pmk1* and transformants, (c) P1, (d) P2, (e) Bg2, (f) M3 and (g) M7 conidia on barley epidermal peels. ■ corresponds to conidia with short germ tubes, ■ corresponds to conidia having differentiated elongated germ tubes, ■ corresponds to conidia having differentiated a swollen germ tube and ■ corresponds to differentiation of an appressorium. In each experiment, 6 x 50 conidia were scored for extent of differentiation and the mean values of 50 conidia are illustrated. The mean percentage differentiation ± standard error is shown. P-values are given above bars: c) and d) P-values show the significant differences between number of appressoria produced by Guy11and the corresponding time-point for P1 and P2, respectively; e), f) and g) P-values showing the significant differences between number of swollen germ tubes produced by Δ*pmk1* and the corresponding time-point for Bg, M3 and M7, respectively, are given above each bar.

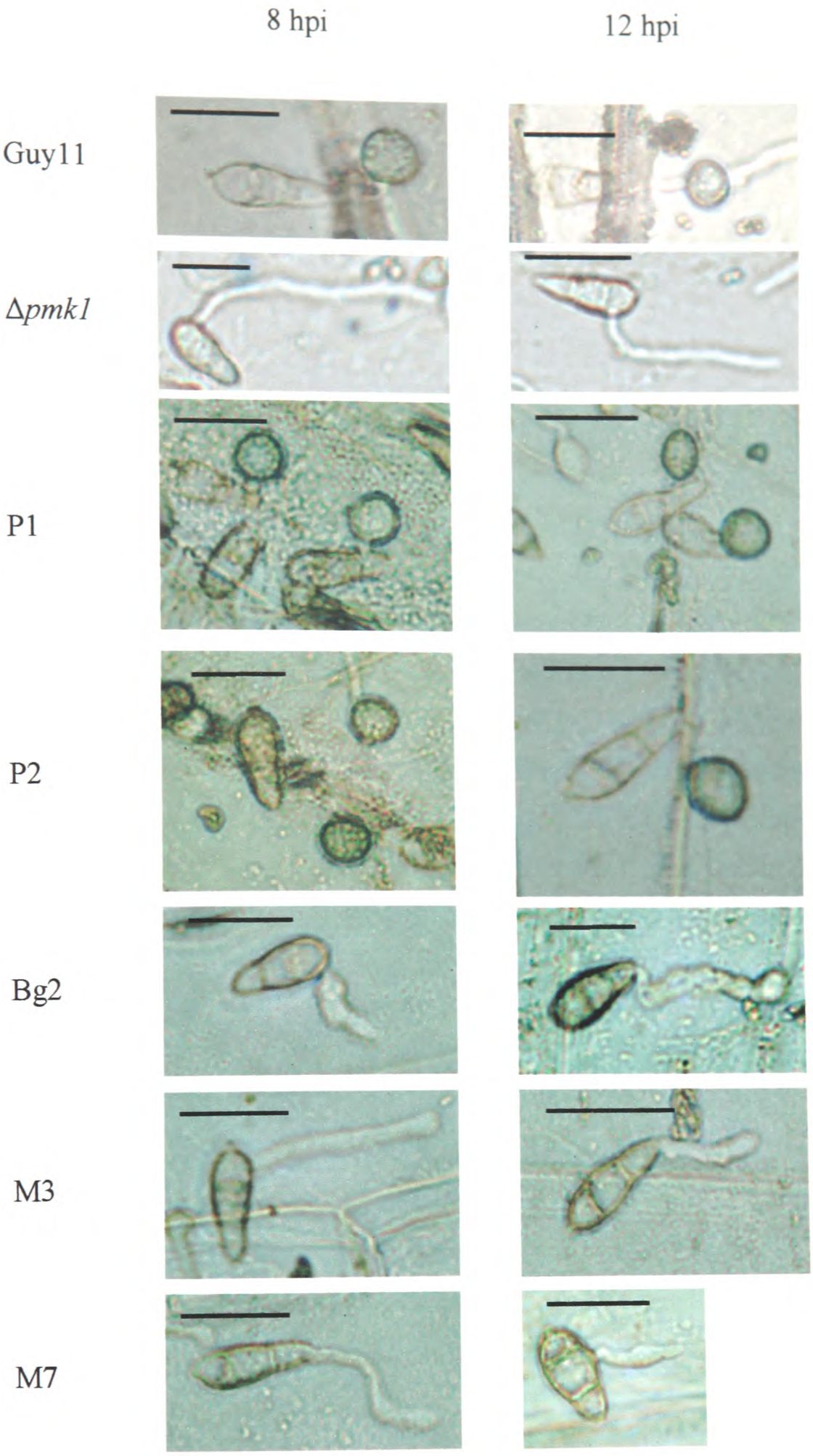


Figure 6.11. Light micrographs of *Magnaporthe grisea* wild-type Guy11, mitogen-activated protein kinase mutant Δ*pmk*1 and transformants P1, P2, Bg2, M3 and M7 on barley epidermal peels at 8 and 12 hours post inoculation (hpi). The bar indicates a length of 20 μm. Magnification x400.

difference in the number of germlings differentiating appressoria between Guy11, P1 and P2.

Bg2, M3 and M7, by 4 hpi, have differentiated swollen appressorial germ tubes (SwGTs) (Figure 6.10 (e), (f) and (g)), but no appressoria, unlike P1 and P2. Compared to Δ*pmk1*, which by 4 hpi had differentiated a mean of 38% SwGTs, there is a significant difference in the number of SwGTs elaborated by Bg2 and M3, with Bg2, M3 and M7 differentiating means of 18%, 54% and 30% SwGTs, where P=0.000, P=0.001 and P=0.197, respectively. By 8 hpi, still no appressoria had been produced by Bg2, M3 and M7 (Figure 6.11) with numbers of SwGTs produced by Bg2 and M7 being significantly different to Δ*pmk1* (Figure 6.10 (e) and (g)). By 12 hpi, whereas Δ*pmk1* has elaborated a mean of 88% SwGTs, Bg2, M3 and M7 still have significantly lower numbers of germlings that have differentiated SwGTs, with means of 78%, 84%, 70% SwGTs being produced. Figure 6.11 also shows that by 12 hpi Bg2, M3 and M7 still resemble Δ*pmk1* more than Guy11 in that no appressoria have been elaborated.

6.2.6 Expression analysis of transformants

Phenotypic analysis revealed that the transformants P1 and P2 were able to complement the Δ*pmk1* defect by producing melanized appressoria, and so must be expressing *PMK1*. However, Bg2, M3 and M7 were unable to produce appressoria on the barley leaf surface. Therefore, further analysis was required to assess whether there was any transcription of the *B. graminis mpk*1 gene in the *M. grisea* transformants. Thus, the end-point RT-PCR method as described by Zhang and Gurr (2000) was implemented to determine whether there was *B. graminis mpk1* expression in the Bg2 transformant.

First strand cDNA was synthesised from total RNA extracted from *M. grisea* Guy11, Δ*pmk1*, Bg2 and *Blumeria graminis* f.sp *hordei* that had been harvested from cellulose membrane at 24 hpi. This time point was selected to correspond with a stage in both *M. grisea* and *B. graminis* when appressoria would be mature. The *B. graminis* and *M. grisea* β-*tubulin* gene transcripts were followed as

internal controls. Figure 6.12 shows that there is expression of *B. graminis* β-*tubulin* in the *B. graminis* sample, and *M. grisea* β-*tubulin* expression in Guy11, Δ*pmk1* and Bg2 harvested from cellulose membrane. *PMK1* expression was only detected in Guy11 and *mpk*1 expression was only detected in *B. graminis*. Transcripts were not normalised to the control, however, this was not necessary for this experiment.

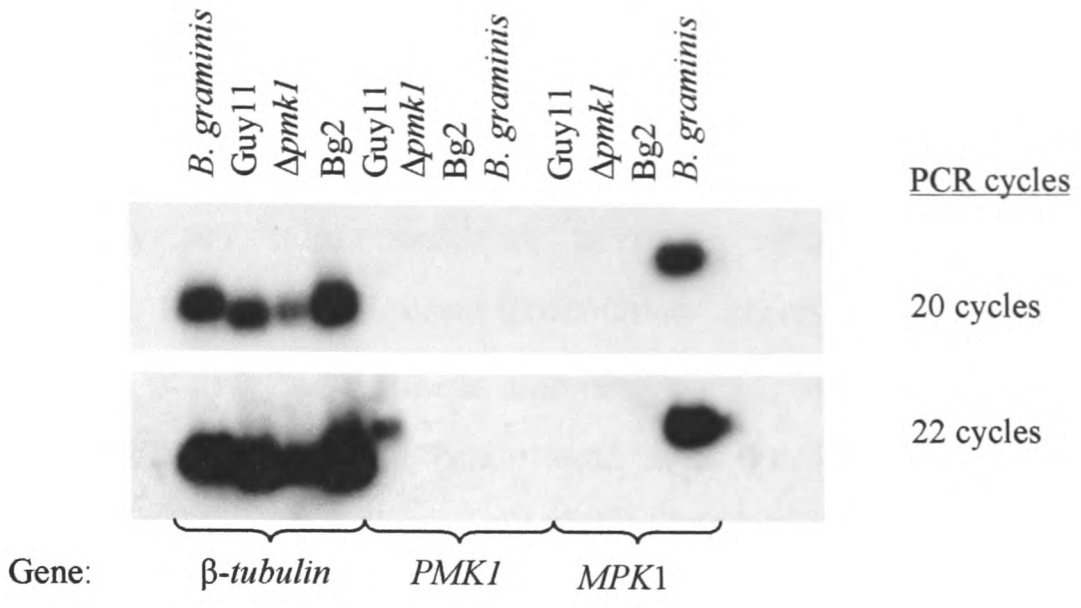


Figure 6.12. Expression of β-*tubulin*, *PMK1* and *mpk*1 in *Blumeria graminis* f.sp. *hordei* and *Magnaporthe grisea* wild-type Guy11, mutant Δ*pmk1* and transformant Bg2 on cellulose membrane, 20 hours post inoculation.

6.3 DISCUSSION

Being a highly specialised, obligately biotrophic pathogen has meant that *Blumeria graminis* f.sp. *hordei* has proved extremely difficult to characterise with molecular genetics. However, the accessibility of highly tractable, nonobligate phytopathogenic fungi, has allowed such pathogens as the rice blast fungus, *Magnaporthe grisea*, to be adopted as "surrogate" systems for the introduction of DNA through heterologous complementation experiments. Therefore, in this study, the *M. grisea* MAP kinase mutant, Δ*pmk1*, was exploited to determine whether the *M. grisea PMK1* homologue in *B. graminis*, that is, *mpk*1, could functionally complement the Δ*pmk1* defect in *M. grisea*.

Functional analysis with the biotrophic, highly organ-specific, non-appressoria-forming grass and cereal pathogen, *Claviceps purpurea* showed that a complete copy of *CPMK1*, together with 1.0 kb and 1.5 kb of its 5' and 3' flanking regions, respectively, was able to fully restore the wild-type phenotype of the *M. grisea* Δ*pmk1* mutant (Mey *et al.*, 2000a). In addition, *CMK1* from *Colletotrichum lagenarium,* a melanized appressorium-forming, nonobligate pathogen of cucumber, could also restore the *M. grisea* Δ*pmk1* mutant to wild-type phenotype, under the control of 3.5 kb of 5' upstream region (Takano *et al.*, 2000). Also, complementation experiments with the *C. purpurea cpmk2* coding region, together with 1.6 kb and 2.9 kb of its 5' and 3' flanking regions, respectively, were able to restore a wild-type phenotype to the *M. grisea mps1* mutant. However, in complementation experiments with the *M. grisea* Δ*cpka* mutant, Bindslev *et al.* (2001) employed the *M. grisea MPG1* promoter, which leads to high levels of gene expression during conidial germination and appressorium development (Talbot *et al.*, 1993; Kershaw *et al.*, 1998), in order to express the *B. graminis BKA1* gene in *M. grisea* Δ*cpka* mutant. Full restoration of pathogenicity and appressorium maturation kinetics were observed with the *MPG1/ BKA1* construct, however, only 1 out of 58 transformants tested displayed complementation (Bindslev *et al.*, 2001). This low frequency was hypothesised as being due to the toxicity of high-level expression of the *BKA1* gene (Bindslev *et al.*, 2001).

Therefore, for complementation experiments with *mpk*1, a transformation vector, containing *B. graminis mpk*1 under the control of its own regulatory regions, was constructed, along with a control vector containing the *M. grisea PMK1* coding region and its regulatory domains.

6.3.1 Transformants

Southern analysis of the five Δ*pmk1* mutants putatively transformed with *PMK1* DNA confirmed the presence of *PMK1* in P1 and P2. Hybridisation with *PMK1* DNA gave rise to the predicted 730 bp *Hind*III restriction-digested fragment consistent with the integration of *PMK1* into the *M. grisea* genome in P2. However, DNA degradation of the P1 sample meant that presence of the predicted 730 bp fragment in P1 could not be verified. Additional hybridising fragments in P2 indicated ectopic insertions of *PMK1*. Presence of a 5.2 kb band in the vector-hybridised blot revealed integration of vector DNA in P2.

Of the 38 putative *mpk*1-transformed protoplast colonies that regenerated on the selective media, 16 were chosen for further analysis. Five of the 10 putative *PMK1*-transformed colonies were also chosen. Southern analysis, followed by hybridisation with *mpk*1 DNA, confirmed the presence of the *mpk*1 transformation DNA. Bg1, Bg2, Bg4, M3 and M7 all gave rise to a ~350 bp *Xba*I restriction-digested fragment consistent with the integraton of *mpk*1 into the *M. grisea* Δ*pmk1* genome. However, the presence of additional hybridising fragments in each of Bg1, Bg2, Bg4, Bg5, M3 and M7 indicated ectopic insertions of *mpk*1. Hybridisation with vector DNA revealed integration of the vector in Bg1, Bg2, Bg5 and M7.

The high frequency of ectopic integrations observed in the *mpk*1 and *PMK1* transformants may be due to the method of selection used to identify transformed colonies, that is, the sulfonylurea resistance gene on the transformation vector. Sulfonylureas (specifically, chlorimuron ethyl, the active ingredient of the herbicide Classic^{reg}) inhibit acetolactate synthase (Sweigard *et al.*, 1997). The sulfonylurea-resistant allele used to create the selection vector, pCB1532, was

modified from *M. grisea ILV1*, a sulfonylurea-resistant acetolactate synthase, involved in isoleucine and valine synthesis (Sweigard *et al.*, 1997). Therefore, it is possible that the *mpk*1 transformation vector integrated preferentially into the *M. grisea* genome at sites of high homology, such as at the *ILV1* site, in preference to the Δ*pmk1* site.

6.3.2 Phenotypic analysis

Magnaporthe grisea strain Guy11 has a distinctive mycelial phenotype. Specifically, it has a grey/brown colouration, caused by melanisation of the cell wall (Figure 6.8(a)). However, this is not characteristic of the Δ*pmk1* mutant, which appears white with concentric ridges (Figure 6.8(b), implying that *PMK1* may be involved in melanin biosynthesis. In support of this notion, Takano *et al.* (2000) reported that *Colletotrichum lagenarium CMK1*, a homologue of *M. grisea PMK1*, plays a role in gene expression required for appressorial melanisation since three melanin genes showed no or slight expression in the *cmk1* mutant. However, the expression of these genes was induced normally during mycelial melanisation (Takano *et al.*, 2000).

Observations of plate-cultures of transformants selected for *in vitro* phenotypic analysis revealed that *PMK1* transformants, P1 and P2, looked more similar to Guy11 than the wild-type, Guy11. *Mpk*1 transformants Bg2, M3 and M7, however, still possessed the characteristic white, ridged appearance of Δ*pmk1*, indicating that there had been no complementation of the Δ*pmk1* defect. Indeed, time-courses of development revealed that P1 and P2 were able to differentiate appressoria by 4 hpi, indicating that the Δ*pmk1* defect had been complemented in these transformants. Bg2, M3 and M7, however, had not elaborated appressoria by 12 hpi and maintained the Δ*pmk1* phenotype, indicating that complementation of Δ*pmk1* in Bg2, M3 and M7 had not been successful.

6.3.3 Expression analysis

Expression analysis revealed that there was no expression of *B. graminis mpk*1 in the *M. grisea* transformant, Bg2, indicating further that this transformant was

either inactive, or that *mpk*1 expression was too low to be detected. However, material for the expression analysis was not harvested from the host plant surface due to limitations on the amount of tissue that can be collected from plant surfaces. Rather, differentiating *M. grisea* tissue for expression studies was harvested from the artificial surface of cellulose membrane, which is capable of inducing appressorium formation in *M. grisea* (see Chapter 3 for further details). Thus, we cannot be sure that gene expression profiles resulting from using such an artificial surface would give the same results as using the host surface.

6.3.4 Alternative transformation vector

Time constraints precluded further studies, but to prevent the problems encountered in this work with ectopic integration of the transformation vector, an alternative selection mechanism could be used which does not rely of a gene which has significant homology to sequences within the *M. grisea* genome. The *bar* gene, which confers bialophos resistance, was successfully used in Δ*pmk1* complementation experiments in *C. lagenarium* (Takano *et al.*, 2000) and in Δ*mps1* complementation experiments in *C. purpurea* (Mey *et al.*, 2002b). Mey *et al.* (2002a) employed a glufosinate resistance cassette construct in *C. purpurea.*

Alternatively, a transformation vector could be made comprising the *B. graminis* *mpk*1 gene under the control of the *M. grisea PMK1* promoter and terminator. Inclusion of *PMK1* flanking regions outside of the region precisely deleted by Xu and Hamer (1996) in Δ*pmk1* would increase the probability of homologous integration of the *mpk*1 construct.

6.3.5 Summary

In this chapter, the rice blast fungus, *Magnaporthe grisea*, was adopted as a "surrogate" host in which to perform complementation experiments. The *Magnaporthe grisea* MAP kinase mutant, Δ*pmk1*, was used to functionally analyse the *Blumeria graminis* f.sp *hordei* MAP kinase gene, *mpk*1. To do this, the *mpk*1 promoter was sequenced and a construct made comprising the *mpk*1 gene under the control of the *mpk*1 promoter. A control construct, that is, the

PMK1 gene under the control of the *PMK1* promoter, was also made. Both constructs were transformed into *M. grisea* Δ*pmk1*. Southern analysis identified transformants for phenotypic studies. These showed that whereas Δ*pmk1* was complemented by *M. grisea PMK1* in control experiments, *B. graminis mpk*1 failed to complement Δ*pmk1*. Expression studies showed that there was no expression of *mpk*1 in an *mpk*1 transformant.

CHAPTER 7
DISCUSSION

7.1 INFECTION STRUCTURE FORMATION

Phytopathogenic fungi face the daunting challenge of recognising a susceptible host, breaching its barriers, overcoming its defences and proliferating on or in host tissues. For this purpose, fungi have evolved diverse strategies for invasion. For instance, *Cladosporium fulvum* hyphae enters through open stomata, with a subsequent increase in diameter of the hyphae upon successful penetration (Mendgen, 1996). Root pathogens such as *Fusarium oxysporum* or *Rhizoctonia solani* aggregate hyphae that may form infection cushions before individual hyphae penetrate with minor modifications of their morphology (Dean, 1997). A more elaborate mechanism for entering host tissues is displayed by the rice blast fungus *Magnaporthe grisea*, which differentiates appressoria from which penetration hyphae develop. However, the most sophisticated differentiation is observed by the obligate biotrophs including *Blumeria graminis* f.sp. *hordei*, which differentiate appressoria, followed by elaboration of a specialised feeding structure, the haustorium, thus establishing an intimate relationship with the host.

The subsequent discussion will focus on infection structure formation in *B. graminis* f.sp. *hordei* as well as the "model" fungus *M. grisea*, which has been exploited herein as a "surrogate host" and provides an interesting biological comparison. The development of infection structures involves a complex morphogenetic program that results in rapid differentiation of a highly specialized structure (Dean, 1997). In *B. graminis*, infection structure differentiation requires the perception of multiple external signals and the integration of multiple signal transduction events in order to coordinate the sequential stages of development, that is, germination and maturation of the primary germ tube (PGT) and emergence and differentiation of the second-formed germ tube into an appressorium. Compared to the regulation of appressorial differentiation in other phytopathogenic fungi, such as *M. grisea*, *B. graminis* infection structure differentiation is a highly complex process. Whilst both of these pathogens require

similar surface signals to trigger appressorial differentiation, including surface hydrophobicity and cuticle-derived substances, each of these signals alone is sufficient to promote high levels of appressorium differentiation in *M. grisea* (Gilbert *et al.*, 1996), whereas each signal provided alone leads to lower levels of differentiation of *B. graminis* than observed on the leaf.

A prerequisite for infection structure formation is germination. Factors affecting germination vary depending on the fungus. High levels of conidial germination (*ca.* 92-98%) are observed in *M. grisea* irrespective of the nature of the substratum, with germination being observed in liquid suspension (Jelitto *et al.*, 1994). By contrast, *B. graminis* germination is regulated by the nature of the conidium-surface contact, with low levels of germination (*ca.* 20-40%) observed in air-borne suspension and on surfaces such as glass and water agar. However, substratum features, such as surface hydrophobicity, increase the proportion of the germinated population (up to *ca.* 70%). Indeed, in this study, comparison of infection structure development of *B. graminis* and *M. grisea* revealed that on epidermal peels, *B. graminis* germination levels did not exceed 80%, with germination levels being much lower on cellulose membrane and water agar. In contrast, regardless of the surface, *M. grisea* reached germination levels of close to 100%.

Differentiation of appressoria in *M. grisea* appears to require a single signalling step. The default pathway of the germinated *M. grisea* conidia in the absence of inductive signals is germ tube elongation (Lee and Dean, 1993; Gilbert *et al.*, 1996). However, upon perception of an inductive signal, germ tube elongation is arrested and appressorium differentiation is triggered, with no further signals being required for completion of the differentiation process. In contrast, germ tube elongation is not the default pathway of germinated conidia in *B. graminis*, with elongation of the second-formed germ tube requiring additional perception of signals, mediated through the PGT. Further perception of signals by the EGT is required to arrest EGT elongation and initiate appressorium formation. Additional signalling through the appressorial germ tube (AGT) tip is required for completion of the formation of the appressorium.

Why has *B. graminis* f.sp. *hordei* evolved a highly complex regulation of infection structure differentiation compared to other phytopathogens such as *M. grisea*? The answer to this question remains obscure, however, one suggestion lies in the evolution of the differing modes of nutrition of these fungi. To elaborate, there are two schools of thought to explain the evolution of different modes of fungal nutrient acquisition, with the ancestral organisms being either saprotrophs or biotrophs (Cooke and Whipps, 1980). The first school of thought is that saprotrophs represent the primitive fungal group, in which case necrotrophy and biotrophy would have evolved with increasing nutritional specialisation and dependence on the host (Jeffries and Young, 1994). Alternatively, the second school suggests that the primitive mode of nutrition is biotrophy. In this case evolution would have been towards a progressive loss of nutritional specialisation (Cooke and Whipps, 1980). The host range of *M. grisea*, which is a facultative biotroph, is greater than *B. graminis* f.sp. *hordei*, which infects barley alone. Therefore, considering the first school of thought, *M. grisea* may not be as nutritionally specialised as *B. graminis*, but would be less dependent on its hosts. Alternatively, *M. grisea* may be considered more nutritionally adaptable to different environments, having lost dependence on its host.

Another reason for the greater complexity of regulation of differentiation by *B. graminis* may not have any evolutionary benefit, but may be a consequence of the development of the PGT. The PGT appears to be a unique feature of *B. graminis* infection structure differentiation and no other powdery mildew species has evolved a PGT. It is thought to have a role in water uptake and may be an adaptation to allow development on hosts in the arid environment of the Middle East, the centre of origin of cereal agriculture (Carver and Bushnell, 1983). The greater complexity of appressorial differentiation may have resulted as a consequence of this adaptation.

In this work, the proportion of *M. grisea* germlings that completed appressorial formation on the barley leaf surface was significantly higher than the *B. graminis* germlings. However, due to the prolific numbers of conidia produced by a

sporulating fungal colony, it is not essential for every *B. graminis* conidium to initiate a new colony, therefore the lower infection rate may not be a hindrance to the rapid spread of the mildew epidemic.

In *B. graminis*, once the AGT has elaborated, penetration of the host cuticle occurs via the infection peg, formed beneath the hooked tip of the appressorium (Kunoh *et al.*, 1978). Penetration is thought to be mediated by the build up of turgor pressure (2-3 MPa) within the AGT (Pryce-Jones *et al.*, 1999) and also by the localised action of degradatory enzymes (Edwards and Allen, 1970) including esterases (Nicholson *et al.*, 1988; Kunoh *et al.*, 1990), cutinase (Pascholati *et al.*, 1992), hydrolytic enzymes such as esterases, lipases, protease, phosphatases, 1, 3-β-glucanase, chitinase, amylase (Fric and Wolf, 1994) and pectinases (Suzuki *et al.*, 1999). In particular, cellulase has been implicated in acting at the site of the infection peg to hydrolyse the barley epidermal cell wall in preparation for the forceful penetration of the papilla (Edwards and Allen, 1970; Pryce-Jones *et al.*, 1999). In *M. grisea*, mechanical force, of up to 8 MPa, appears to be the primary means by which *M. grisea* breaches the plant cuticle and wall layers. Experiments have shown that cutinase is dispensible for pathogenicity (Sweigard *et al.*, 1992) and appressoria are able to puncture inert plastic surfaces (Howard *et al.*, 1991). It is possible, however, that as the penetration peg is forced through the surface leaf layers its passage is aided by the secretion of enzymes that pre-soften the wall layers (Talbot and Foster, 2001).

After penetration of the host cell wall and production of a haustorium within the epidermal cells, *B. graminis* grows ectopically over the barley leaf surface through the production of elongating secondary hyphae. *M. grisea*, though, does not produce "true" haustoria (Heath *et al.*, 1992). Instead, infection hyphae are produced within the first epidermal cells encountered and the fungus then takes upon a beaded, bulbous appearance as it grows throughout the first and adjacent epidermal cells, with long runner hyphae spreading out from the site of infection (Talbot, 1995).

7.2 SIGNAL TRANSDUCTION

Fungi employ sophisticated signal transduction processes to sense and respond to specific environmental cues that drive changes in cell morphology and physiology. The mechanisms that regulate these processes possess highly conserved components contained within cyclic adenosine monophosphate (cAMP) signal transduction cascades and protein kinase pathways. These pathways have been best characterised in mammalian cells and the model yeasts *Saccharomyces cerevisiae* and *Schizosaccharomyces pombe*.

In this study, signal transduction pathways were investigated in *Blumeria graminis* f.sp *hordei* in order to examine the signal transduction events involved in infection structure differentiation. Previous studies have supported roles for cAMP/PKA signal transduction cascades (Hall *et al.*, 1999; Hall and Gurr, 2000; Kinane *et al.*, 2000; Zhang *et al.*, 2001; Bindslev *et al.*, 2001) in *B. graminis* appressorial formation. However, cAMP alone is not sufficient to promote progression through the differentiation process. Therefore, additional signalling pathways are required, such as a MAP kinase cascade, or signalling via PKC.

7.2.1 Protein kinase C

PKCs have been identified in phytopathogenic fungi and have been implicated in differentiation processes, including infection structure formation (Staples and Hoch, 1987; Dickman *et al.*, 1995; Warwar and Dickman, 1996; Thines *et al.*, 1997a, b). Studies into the role of PKC in *B. graminis* signalling were initiated upon the identification of two *B. graminis* PKC genes, designated *pkc*1 and *pkc*-like, by Ziguo Zhang (University of Oxford). Analysis of the PKC1 and PKC-like amino acid sequences revealed that PKC1 resembles mammalian and fungal PKCs generally, and carries an extended N-terminal domain containing two putative rho motifs, characteristic of all euascomycete PKCs sequenced to date. Nothing is currently known about rho proteins in *B. graminis*. However, in *S. cerevisiae*, RHO1 is required for the dynamic spatial and temporal localisation of PKC1 to sites of polarised growth and cell wall damage, resulting in the maintenance of cell wall integrity and the regulation of actin cytoskeleton polarity

(Nonaka *et al.*, 1995; Zhao *et al.*, 1998; Perez and Calonge, 2002). Moreover, this process is thought to act via a MAP kinase signalling cascade (Lee *et al.*, 1993), which will be discussed in more detail below.

PKC-like was found to represent a truncated PKC-like gene, comprising a protein kinase domain with ATP-binding site and a serine/threonine active site signature sequence. Thus PKC-like is reminiscent of a short *pkc*-like gene identified in *Colletotrichum trifolii* (Dickman *et al.*, 1995) which shows increased expression levels upon germination.

Chapter 4 revealed PKC activity could be detected in *B. graminis* conidia. However, insufficient protein from specific stages of *B. graminis* development, and a lack of sensitivity of the PKC activity assay used, precluded a complete time-course of analysis of PKC activity during infection structure formation. Nevertheless, the PKC activity assay was successfully employed to assess a range of serine/threonine kinase antagonists and PKC agonists for their effects on *B. graminis* PKC activity. In addition, a cAMP-dependent protein kinase (PKA) assay was used to assess the specificity of the antagonists to *B. graminis* PKC.

Pharmacological inhibitors for the study of the filamentous fungal differentiation have been successfully employed in *Neurospora crassa* (Arpaia *et al.*, 1999) and *C. trifolii* (Dickman *et al.*, 1995). However, this approach could not be used to assess the function of *B. graminis* PKCs since no inhibitor was found that was potent or specific enough. *B. graminis* PKC1 possesses the highly-conserved catalytic and regulatory domains of the mammalian and other fungal PKCs, that is, the target sites of the inhibitors investigated in this study. However, *B. graminis* PKC1 and PKC-like represent novel forms when compared to the mammalian PKCs, which may mean that the tertiary structure of these proteins is unlike that of the mammalian targets and thus the mammalian PKC-targeting inhibitors cannot gain access to their target sites. This would explain the lack of potency seen with some inhibitors. However, the assay revealed that some inhibitors did affect *B. graminis* PKC activity, but were also inhibitory to PKA and so were not PKC specific. Indeed, this was the case with chelerythrine

chloride, one of the inhibitors successfully employed in studies with *N. crassa* (Arpaia *et al.*, 1999). However, Arpaia *et al.* (1999) did not assess whether the inhibitors used in their study also affected other kinases in *N. crassa*.

Application of exogenous diacylglycerol (DAG) had no effect on PKC activity or germling morphogenesis in *B. graminis*. However, application of the PKC agonist, phorbol ester, caused an increase in *B. graminis* infection structure differentiation and also an increase in *B. graminis* PKC activity when applied *in vivo*, implicating PKC in *B. graminis* germling differentiation. Phorbol esters are not as rapidly metabolised as DAGs, and so this may explain why an effect was seen on *B. graminis* differentiation and PKC activity with phorbol ester and not DAG. However, exogenously-applied DAG has been successfully used in studies with *Uromyces appendiculatus* germlings to stimulate mitosis and partial infection structure development (Staples and Hoch, 1987) and Thines *et al.* (1997a, b) invoked the activation of PKC in *M. grisea* appressorium differentiation by the addition of DAG. Therefore, perhaps DAG is not able to pass through the cell wall to affect PKC in *B. graminis*, whereas it can in *M. grisea* and in *U. appendiculatus*. Indeed, DAG uptake may have been hindered even more in *B. graminis* because it could not be applied directly to the *B. graminis* conidia, rather it was applied to agar beneath cellulose membrane onto which conidia were inoculated. However, there was no effect of DAG on PKC activity in the PKC assay either, although, crude protein extracts were used which might have contained other proteins which could preferentially bind DAG, or, as already mentioned, the DAG could have been metabolised before an effect on PKC could be seen.

Brose and Rosenmund (2002) have proposed that eukaryotic cells possess an array of proteins, other than PKCs, that are receptive to phorbol esters and DAGs. In addition, they caution that PKC inhibitors may not be sufficiently specific alone to define PKC-mediated physiological effects unequivocally. Therefore, if pharmacological studies are to be used in the future to study *B. graminis* differentiation, then, because of the lack of specificity identified in this study, perhaps inhibitors should be designed that are specific to *B. graminis* PKC.

Expression studies of *pkc*1 in this study revealed a peak in *pkc*1 transcript levels just prior to PGT emergence, which correlates with results from *N. crassa* where *PKC* transcript levels were low in dormant spores but elevated during germination (Oved and Yarden, 1996). For *pkc*-like, the real-time transcript levels were greatest in the mature PGT-stage tissue which agrees with expression data from *C. trifolii*, which reveals high levels of transcript abundance during germination for a PKC-like gene (Dickman *et al.*, 1995). However, the real-time profile does not entirely reflect the end-point RT-PCR profile of Zhang *et al.* (2001). This could be due to differences in the techniques including methods of tissue collection and the point at which transcript levels are measured, *i.e.* during the exponential phase of amplification for real-time PCR, but during plateau phase of end-point RT-PCR where reagents could be limiting. However, real-time and end-point profiles have consistently agreed for other *B. graminis* genes analysed, including for *mpk*1 and *mpk*2 (in this study), catalase B (*cat*B) (Zhang *et al.*, submitted), catalase peroxidase (*cpx*), superoxide dismutase (*sod*1), glutathione peroxidase (*gpx*1: AAL56984) and alternative oxidase (*aox*) (C. Henderson, *pers. comm.*). Additionally, the use of β-*tubulin* as a constitutively expressed control in *B. graminis* has recently been supported by a second gene (C. Henderson, *pers. comm.*), that is, elongation factor α, identified through serial analysis of gene expression (SAGE) (Thomas *et al.*, 2002).

7.2.2 Mitogen-activated protein kinase pathways

Three MAP kinases have been identified in *B. graminis* f.sp. *hordei*, *mpk*1, *mpk*2 and *hog*1 (Zhang and Gurr, 2000; unpublished). The work presented in Chapter 5 revealed that MPK1 and MPK2, in phylogenetic terms, are closely related to other phytopathogenic fungal MAP kinases. Specifically, MPK1 has high homology to fungal MAP kinases clustering with PMK1 (Pathogenicity MAP Kinase) from the "model" fungus, *Magnaporthe grisea*, and MPK2 has a high homology to fungal MAP kinases clustering with *M. grisea* MPS1 (MAP Kinase for Penetration and Sporulation). Let us consider some of the PMK1 and MPS1 homologues characterised in phytopathogenic fungi for further indications as to the potential role of MAP kinase signalling in *B. graminis*.

7.2.2.1 PMK1 homologues

The role of MAP kinase signalling in the regulation of appressorium formation in phytopathogenic fungi was first proposed following isolation of the *PMK1* MAP kinase gene from *M. grisea*. *PMK1* is required for the regulation of appressorium formation in response to surface signals and is also necessary for invasive growth or viability in rice plants (Xu and Hamer, 1996).

PMK1 homologues have been described in several plant-pathogenic fungi (Lev *et al*, 1999; Takano *et al*, 2000; Di Pietro *et al*., 2000; Ruiz-Roldan *et al*., 2001; Zheng *et al*., 2001; Mey *et al*., 2002a) and in most cases they play an essential role in pathogenesis (Xu and Hamer, 1996). Indeed *M. grisea* Δ*pmk1* mutants are impaired in appressoria formation, penetration and invasive growth. However, even in phytopathogenic fungi that have drastically different pathogenic strategies to *M. grisea*, *PMK1* homologues appear to have a conserved role. Indeed, in *Claviceps purpurea*, which is highly organ-specific, does not produce appressoria and is a biotroph, deletion of the *PMK1* homologue, *CPMK1*, results in a phentoype which is almost identical to that of *M. grisea* Δ*pmk1* (Mey *et al*., 2002a). This indicates that either the basic penetration mechanisms could be related, or, alternatively, such MAP kinase cascades could represent evolutionarily old signalling pathways involved in sensing the hosts surface and initiating penetration programmes that have divergently adapted to different hosts/organs involved.

M. grisea PMK1 is required for appressorial formation and pathogenicity alone, but not for other developmental functions (Xu and Hamer, 1996). However, this is in contrast to other phytopathogenic fungi where *PMK1* homologues are thought to be involved in several developmental pathways, each responsive to different signals. For instance, in the melanised appressorium-forming pathogen, *C. lagenarium*, *CMK1* is required for pathogenicity, but in contrast to *M. grisea*, is also involved in the regulation of conidiation and germination (Takano *et al*., 2000). Moreover, addition of yeast extract to Δ*cmk1* mutants rescues germination, indicating the presence of a *CMK1*-independent pathway for the regulation of conidial germination. In *C. heterotrophus*, *CHK1* is also required for conidiation

as well as pathogenicity (Lev *et al.*, 1999), and Δ*chk1* mutants are defective in mating when both partners lack a functional copy of the gene. *P. teres PTK1* mutants are deficient in conidiophore differentiation and conidiation, and appressorium formation (Ruiz-Rolan *et al.*, 2001). Therefore, these examples emphasise the different functions of similar signalling MAP kinase pathways in phytopathogenic fungi, even though all of them play crucial roles in fungal pathogenesis.

Interestingly, although *C. heterotrophus CHK1* is more similar to *PMK1* than to *MPS1*, it has some functions of both genes: sexual and asexual sporulation (*MPS1*); pathogenicity (both); appressorium formation (*PMK1*); aerial hypha formation and a function related to viability or cell wall integrity (*MPS1*). Lev *et al.* (1999) therefore propose that there is a "division of labour" among MAP kinase families which is dependent on the species. Indeed, a MAP kinase belonging to a particular family could have been recruited for a specific set of functions in different species. For instance, relative to *C. heterotrophus*, *M. grisea* has evolved a more specialised method of infection, *i.e.* the production of large, melanized appressoria. Thus, *PMK1* acquired a specialised function in *M. grisea*, whereas *MPS1* retained a more general set of functions. *CHK1* became, or remained, functionally more similar to *MPS1*, which has a wide set of developmental roles (Lev *et al.*, 1999). This hypothesis of recruitment of homologous genes for divergent sets of functions may be a general phenomenon in the evolution of ascomycetes. Support for such a hypothesis comes from studies of fungal a transcription factor with a Myb-like DNA binding domain. The *Neurospora* homologue of an *Aspergillus* regulator of conidiation can complement *Aspergillus* mutants in this gene, *flbD*, whereas deletion of the *Neurospora* gene had no major effects on development (Shen *et al.*, 1998). The Myb-like DNA-binding domain is shared between the two species, whereas the remainder of the protein is more divergent (Shen *et al.*, 1998).

7.2.2.2 MPS1 homologues

Before the isolation of *B. graminis* MPS1, few *M. grisea* MPS1 homologues had been isolated. Recently, however, a number of MPS1 homologues have been

characterised and these reveal that MPS1-type homologues are involved in a diversity of processes (Kojima, 2002; Mey *et al.*, 2002b; Hou *et al.*, 2002). *M. grisea* MPS1 is involved in pathogenicity, conidiation, mating, aerial hypha formation and cell wall integrity (Xu *et al.*, 1998). MPS1 may have a similar role to that of SLT2 in *S. cerevisiae* where control of cell wall growth in response to membrane stress is mediated by a PKC pathway that activates the MAP kinase, SLT2/MPK1 (Costogan *et al.*, 1992; Lee *et al.*, 1995; Davenport *et al.*, 1995). Indeed, elaboration of the penetration peg prior to plant penetration is likely to cause considerable membrane stress (Howard, 1997). Therefore, MPS1 may be involved in the maintenance of cell wall integrity and in cell wall remodeling during this process. Additionally, MPS1 may be necessary for polarization of the actin cytoskeleton to facilitate the formation of a penetration hypha. Moreover, *PDE1*, a gene putatively encoding a P-type ATPase has been implicated in regulating membrane integrity and has been shown to be involved in penetration peg formation in *M. grisea* (Balhadère and Talbot, 2001).

Considering other phytopathogenic fungi, *C. lagenarium MAF1* is essential for invasive growth and conidiation (Kojima *et al.*, 2002). However, in contrast with *M. grisea* Δ*mps1* mutants, *C. lagenarium* Δ*maf1* mutants are essential for appressorium formation (Kojima *et al.*, 2002). Additionally, unlike *MPS1*, *MAF1* is dispensable for cell wall integrity, which suggests that either *MAF1* redundantly regulates cell wall integrity with one or more unidentified signalling pathways, or *MAF1* is not involved in the maintenance of cell wall integrity (Kojima *et al.*, 2002). *Fusarium graminearum MGV1*, like *M. grisea MPS1*, is required for cell wall integrity, the development of aerial hyphae, and possibly hyphal fusion and heterokaryon formation (Hou *et al.*, 2002). Conidiation is not affected since *F. graminearum* forms conidiophores in submerged culture or very close to the surface of solid media, rather than on aerial hyphae as with *M. grisea*. However, virulence is severely reduced in *F. graminearum* Δ*mgv1* mutants and this is thought to be a consequence of either a reduction in the vegetative growth rate of the fungus, or, more likely, that the Δ*mgv1* mutants are defective in producing virulence factors required for efficient colonisation of the host tissues (Hou *et al.*, 2002). Hou *et al.* (2002) demonstrated that the ability of Δ*mgv1* mutants to

produce trichothecene mycotoxins in infected plants is greatly reduced and this may contribute to reduced levels of disease. Curiously, even though *C. purpurea* has arguably the most different lifestyle to that of *M. grisea*, being an obligate biotroph and organ-specific, *C. purpurea CPMK2* appears to be more similar to *M. grisea MPS1* in the processes it regulates than the other characterised *MPS1* homologues, with *CPMK2* known to be involved in virulence, conidiation and cell wall integrity.

7.2.2.3 MAP kinase signalling in Blumeria graminis f.sp. hordei

The absence of a practicable transformation system for the functional analysis of *B. graminis* f.sp. *hordei* genes means that characterisation of *B. graminis mpk*1 and *mpk*2 through the study of deletion mutants is as yet not possible. However, the work in Chapter 5 indicated that MAP kinase pathways are involved in the differentiation of *B. graminis* infection structures. Indeed, MAP kinase activity was detected in *B. graminis* spore protein extracts. However, insufficient protein from specific stages of *B. graminis* development, and a lack of sensitivity of the assay used, precluded a complete time-course of analysis of MAP kinase activity during infection structure formation. Indeed the assay employed an antibody to Thr202/Tyr204 of human p44 MAP kinase. An alignment of MAP kinase amino acid sequences in Chapter 5 reveals a high level of conservation generally of amino acid residues around the MAP kinase TEY activation domain between the *B. graminis* and human MAP kinases. However, the region is not 100% conserved. Therefore, employing an antibody raised specifically to the *B. graminis* MAP kinases might provide a more sensitive assay.

Due to the reasons given, the MAP kinase assay could not be employed to assess the agonists and antagonists of the MAP kinase signalling pathway for their effects on *B. graminis* MAP activity. However, *in vivo* experiments revealed that the MAP kinase kinase (MEK) inhibitor, PD98059, inhibited *B. graminis* germling differentiation when applied to spores inoculated onto barley epidermal peels. However, germination was not affected by the inhibitor, therefore, we can speculate that the MAP kinase signalling pathway affected by the inhibitor does not have a role in germination, just as the *M. grisea* PMK1 pathway is not

required for germination (Xu and Hamer, 1996). However, it was impossible to elucidate which *B. graminis* MAP kinase pathway was being targeted by PD98059. Although, Kim *et al.* (2000) revealed that application of PD98059 to *C. gloeosporioides* wild-type conidia caused blockage in developmental changes that mimicked those caused by disrupting the *C. gloeosporioides* MEK gene, *CgMEK1*, including a loss of ability to form appressoria and a loss of virulence.

Even though inhibition of *B. graminis* infection structure formation was inhibited by PD98059, there was no effect on application of the MEK inhibitor U0126, even though this inhibitor is considered more potent than PD98059 (Favata *et al.*, 1998). However, U0126 is known to be highly selective for MEK1 and MEK2 in 3T3 fibroblasts (Favata *et al.*, 1998). Thus, perhaps this high level of selectivity in mammalian cells means that the inhibitor is not likely to affect *B. graminis* MAP kinase signalling. Little is known about MEKs in phytopathogenic fungi and indeed, no MEKs have been identified in *B. graminis*. However, Kim *et al.* (2000) revealed that *C. gloeosporioides* CgMEK1 shares 51, 44, 40, and 35% identity with *U. maydis* FUZ7 (Banuett and Herskowitz, 1994) and *S. cerevisiae* STE7 (Teague *et al.*, 1986), PBS2 (Boguslawski and Polazzi 1987) and MKK2 (Irie *et al.*, 1993), respectively. We can speculate that the lack of selectivity of U0126 for *B. graminis* is due to differing structural conformations between the human MEKs and *B. graminis* MEKs. Alternatively, U0126 might not able to pass through the cell wall to affect *B. graminis*, especially since it could not be applied directly to the *B. graminis* conidia, rather, it was applied in solution beneath barley epidermal peels onto which conidia were inoculated.

Application of the MAP kinase agonist N-Hexanoyl-D-*erythro*-sphingosine had no effect on *B. graminis* germination or differentiation whereas Thines *et al.* (1997) observed an increase in appressorial formation when N-Hexanoyl-D-*erythro*-sphingosine was applied to *M. grisea*. Again, there might have been problems with the level of specificity, or else the sphingosine might not have been taken up by *B. graminis* since it was not applied directly to conidia and was applied to agar beneath cellulose membrane, onto which spores were inoculated.

Importantly, expression data was presented in Chapter 5 for *mpk*1 and *mpk2* and revealed that *mpk*1 expression peaks during appressorium elongation and swelling, and that *mpk*1 appears to be expressed earlier than *mpk*2, hinting at roles in appressorium formation and plant penetration, respectively. Moreover, *mpk*1 and *mpk2* expression peaks at the same time as other *B. graminis* genes which are thought to be involved in penetration of the plant, including those implicated in protection against host-derived stress including catalase B (*cat*B), alternative oxidase (*aox*) and glutathione peroxidase (*gpx*1), and enzymes implicated in penetration including an extracellular alkaline protease and an extracellular 1, 3-β glucanase (Z. Zhang and C. Henderson, *pers. comm.*).

7.2.2.4 The function of Blumeria graminis f.sp. hordei mpk1

Due to the lack of a transformation system that would allow deletion of the *mpk*1 gene in *B. graminis*, the highly tractable *M. grisea* transformation system was employed for investigations into the potential role of *B. graminis mpk*1 (Chapter 6). However, attempts to functionally complement the *M. grisea* Δ*pmk1* mutant with a copy of *B. graminis mpk*1, under the control of its own promoter, were unsuccessful. Indeed, transcript analysis revealed that there was no *mpk*1 gene expression in transformed *M. grisea* Δ*pmk1* germlings, collected from cellulose membrane, an artificial surface which induces appressorial formation in wild-type *M. grisea* strain Guy11.

Mey *et al.* (2002a) considered that complementation of the *M. grisea* Δ*pmk1* mutant with *C. purpurea CPMK1* would not be effective, extrapolating from the findings that with various hydrophobin genes used for complementation of the Δ*mpg1* mutant of *M. grisea*, an *M. grisea* promoter fusion was a prerequisite for successful complementation in most cases (Kershaw *et al.*, 1998). However, under the control of their own promoters, both *CPMK1* and *CPMK2* from *C. purpurea* were able to complement *M. grisea* Δ*pmk1* and Δ*mps1* mutants respectively even though *C. purpurea* and *M. grisea* differ drastically in their pathogenic strategies (Mey *et al.*, 2002a, b). This indicates that conservation between the *C. purpurea* and *M. grisea* pathways is high enough to allow correct expression of the *C.*

purpurea genes in *M. grisea*, even under the control of the *C. purpurea* promoters, and thus full complementation of the Δ*pmk1* deficiency.

Little is known about the transcriptional regulation of the MAP kinase *PMK1* and *MPS1* homologues in phytopathogenic fungi, yet, differences in the temporal expression patterns of the *PMK1*-like genes has been blamed for the partial complementation of the *Fusarium oxysporum* Δ*fmk1* mutant by *M. grisea PMK1* (Di Pietro *et al.*, 2001). Moreover, the low complementation frequency observed in experiments where the *M. grisea* Δ*cpka* mutant was transformed with *B. graminis BKA1* under the control of the *M. grisea MPG1* promoter was attributed to levels of *BKA1* expression that were too high and so were toxic (Bindslev *et al.*, 2001). However, *M. grisea PMK1* is considered to be constitutively expressed at low levels in *M. grisea*, with a high increase in expression occurring during appressorial formation (Tenjo *et al.*, 1999). In contrast, *C. lagenarium CMK1* is thought to be expressed constantly in each developmental stage, yet it fully restores the ability of *M. grisea PMK1* to form appressoria (Takano *et al.*, 2000), indicating that the regulatory pathways controlling expression of both genes in the two pathogens are similar enough to allow complementation. Although, expression analysis of *C. lagenarium CMK1* was only performed in vegetative mycelia and conidia, with expression levels at other stages being based on speculation alone (Takano *et al.*, 2000).

In comparison to studies of the *PMK1* and *MPS1* homologues performed in other phytopathogenic fungi, the work herein demonstrates the most extensive analysis of expression of these MAP kinases, covering six time points from the ungerminated conidial state, through germination, appressorial differentiation and beyond. An increase in our understanding of such profiles in other fungi may yield data for use in functional analysis, such as knowing when to switch genes on and off at critical time-points when using inducible promoters. Indeed, differences in expression requirements may provide one explanation for the lack of complementation of *M. grisea* Δ*pmk1* with *B. graminis mpk*1. Although, other reasons include that there was preferential introduction of the *B. graminis mpk*1 construct into the genome in a manner that meant *mpk*1 could not be expressed.

Indeed, the level of ectopic integration of the construct was somewhat promiscuous, as it was in the control experiment (the introduction of *M. grisea PMK1* into *M. grisea* Δ*pmk1*). However, complementation was achieved in the control, probably due to a high level of homology surrounding *PMK1* in the construct, which allowed integration of the construct into/close to Δ*pmk1* lesion, therefore allowing expression of *PMK1* and complementation of the defect.

Suggestions were put forward in Chapter 6 for alternative constructs that might alleviate the problems encountered with ectopic integration, including using an alternative selection method, or placing the *B. graminis mpk1* gene under the control of the *M. grisea* regulatory regions, with inclusion of *PMK1* flanking regions outside the region precisely deleted by Xu and Hamer (1996) in Δ*pmk1*. This would increase the probability of homologous integration of the *mpk*1 construct.

7.2.3 Upstream effectors, downstream targets and interacting pathways

In contrast to yeast and higher eukaryotes, the analysis of MAP kinase cascades in filamentous fungi is still in its infancy. Little is known about the upstream and downstream components of the phytopathogenic fungal MAP kinases. Among the few upstream elements known to be involved in *PMK1*-like signalling are the MAP kinase kinase *ubc5* from *U. maydis* (Andrews *et al.*, 2000), the MAP kinase kinase *CgMEK1* from *Colletotrichum gloeosporioides* (Kim *et al.*, 2000) and the MAP kinase kinase kinase *ubc4* from *U. maydis* (Andrews *et al.*, 2000).

In *C. lagenarium*, expression studies have revealed that Δ*cmk1* shows no, or only slight, expression of three melanin genes, suggesting that *CMK1* plays a role in gene expression required for appressorial melanisation (Takano *et al.*, 2000). In *F. oxysporum*, transcript levels of an endopectate lyase were greatly reduced in Δ*fmk1* mutants (Di Pietro, 2001). Recently, the *C. heterotrophus CHK1* signalling pathway was found to be involved in the regulation of two cellulase-encoding genes (Lev and Horwitz, 2003).

In several filamentous fungi cAMP has been found to act in parallel with the *PMK1*-like pathways to trigger fungal differentiation and pathogenesis. Analysis of the interaction between the cAMP response pathway and MAP kinase signalling during pre-penetration phase development has been carried out in *Ustilago maydis*. In this fungus, cAMP signalling and the *ubc3* MAP kinase signalling pathway are involved in mating, dimorphic switching and virulence (Xu, 2000). Mutants of the adenylate cyclase gene, *uac1*, which are blocked in cAMP synthesis, grow filamentously instead of budding and are altered in mating response and virulence. However, the constitutive filamentous phenotype can be suppressed by mutations in the *ubc3* gene, but the pathogenicity defect remains unaffected (Xu, 2000). It is thought that the cAMP pathway is critical for maintaining budding growth in haploid cells, whereas the MAP kinase pathway is important for promoting filamentous growth. During plant infection the two pathways act in synergy, but the molecular mechanism of the pathway remains unclear (Xu, 2000).

In *M. grisea* addition of cAMP induced the early stages of appressorium formation in Δ*pmk1* mutants, even though they failed to produce appressoria (Xu and Hamer, 1996). Based on this observation, it has been proposed that *PMK1* operates downstream of the original cAMP signal for appressorium formation, although a direct interaction between components of these pathways has yet to be confirmed (Dean, 1997; Xu, 2000). Furthermore, Thines *et al.* (2000) revealed that the *M. grisea PMK1* pathway appears to control the transfer of lipid (triacylglycerol) and storage carbohydrate (glycogen) reserves to the appressorium following conidial germination, and that PKA controls the breakdown of these reserves ultimately into glycerol, with the result that there is an increase in turgor generation required for cuticle penetration. The results obtained by Thines *et al.* (2000) indicated that enzymes such as glycogen phorphorylase and triacylglycerol lipases are targets of the PKA/MAP kinase signalling pathway during appressorial development, consistent with the regulation of such enzymes in mammals (Lee *et al.*, 2003). To add yet more complexity, another consequence of triacylglycerol degradation is the probable release of second messengers such as DAG, which stimulates appressorium formation in *M. grisea* on non-inductive surfaces (Thines

et al., 1997) and can restore appressorium formation to Δ*pth11* mutants (DeZwann *et al.*, 1999). The *PTH11*-encoded receptor is thought to respond to surface hydrophobicity and therefore generation of cAMP downstream of *PTH11* might not only stimulate appressorium formation but also lipid degradation and the release of diacylglycerol to further stimulate cellular differentiation (Thines *et al.*, 2000).

Therefore, to summarise the process of appressorium formation in *M. grisea*, following mobilisation of the glycogen and triacylglycerol reserves to the developing appressorium, under the control of *PMK1*, glycerol is generated as a result of the action of the PKA pathway. Following glycerol accumulation, there is an increase in turgor pressure required for cuticle penetration, localised dissolution of the cell wall and formation of the penetration peg. These processes are likely to be regulated by the action of PKA and stimulation of a signalling pathway involving *MPS1* (Xu *et al.*, 1998, Thines *et al.*, 2000).

7.3 THE FUTURE FOR SIGNAL TRANSDUCTION WORK IN *BLUMERIA GRAMINIS* F.SP. *HORDEI*

Out of all the phytopathogenic fungi studied to date, it is *M. grisea* that has provided the most "complete" model of the signal transduction pathways involved in appressorium formation, and perhaps the most relevant system when it comes to studying appressorium formation in *B. graminis*. However, as has already been mentioned, *B. graminis* is highly intractable with no practicable transformation system for functional genomics.

A stable DNA-mediated transformation system has been described in *B. graminis* (Chaure *et al.*, 2000). However, this technique has proven to be difficult to implement due to the arbitrary biolistic discharge of plasmid-coated gold bullets into colonies emerging from the leaf surface. Moreover, it is work intensive and with no tight, inducible promoter switch, there is no means of controlling expression. This is especially important when working with obligate biotrophs,

such as *B. graminis*, where deletion of genes involved in pathogenicity often give rise to a lethal phenotype. Further attempts have been made at developing transformation systems for *B. graminis* including using a "glass fingers" approach, which employs silicon carbide "whiskers" to deliver genes into conidia (Zhang, *pers comm.*). However, using this latter method, gene expression was found to be transient, with a high level of spore wounding and insufficient regeneration of germlings.

Double-stranded (ds) RNA interference (RNAi) is a recent technological advance that enables the reduction of gene expression at the post-transcriptional level, and might allow regulation of gene expression in organisms such as *B. graminis* where gene disruption is difficult (reviewed in Cottrell and Doering, 2003). Indeed, RNAi can produce cells with reduced expression of essential genes, yielding phenotypes which cannot be studied using a traditional disruption approach. Additionally, the effects of RNAi can be reversed, permitting in depth study of gene function, and several unrelated genes can be targeted, allowing epistasis analysis and investigations of multiple processes (Cottrell and Doering, 2003). There is great interest in applying RNAi to pathogenic fungi because other RNA silencing processes have been well described in non-pathogenic fungi, such as quelling in *Neurospora crassa* (Cogoni, 2001), and antisense interference in *N. crassa* (Tentler *et al.*, 1997), *Cryptococcus neoformans* (Gorlach *et al.*, 2002) and *Candida albicans* (De Backer *et al.*, 2001). Since RNA silencing mechanisms share common functions and machinery, it is likely that RNAi will be useful in investigations of pathogenic fungi. However, in the fungi, RNAi has only been described in *C. neofomans*, where RNAi was targeted to the *CAP59* gene (Liu *et al.*, 2002). Attempts at RNA silencing in *M. grisea* have, so far, been unsuccessful (Xu, *pers. comm.*).

With such tools to study functional genomics in *B. graminis*, we would be able to study the upstream and downstream components of signalling pathways and advance our study of the interplay between signal transduction pathways and their roles during morphogenesis, pathogenicity and cell integrity. Within the confines of what is currently practicable in *B. graminis* f.sp. *hordei*, this study has

implicated PKC signalling in germling morphogenesis through *in vivo* and *in vitro* studies with phorbol ester, a PKC agonist, and expression analyses. Phylogenetic, inhibitor and expression work has also implicated MAP kinase signalling in infection structure formation.

REFERENCES

Adachi K and Hamer JE. 1998. Divergent cAMP signaling pathways regulate growth and pathogenesis in the rice blast fungus *Magnaporthe grisea*. *Plant Cell*. **10:** 1361-1374.

Agrios GN. 1997. Plant Pathology. (San Diego, CA.: Academic Press).

Aist JR and Bushnell WR. 1991. Invasion of plants by powdery mildew fungi and cellular mechanisms of resistance. (New York, NY: Plenum Press).

Alessi DR, Cuenda A, Cohen P, Dudley DT and Saltiel AR. 1995. PD 098059 is a specific inhibitor of the activation of mitogen-activated protein kinase kinase *in vitro* and *in vivo*. *J. Biol. Chem.* **270:** 27489-27494.

Alonso-Monge R, Navarro-Garcia F, Molero G, Diez-Orejas R, Gustin M, Pla J, Sanchez M and Nombela C. 1999. Role of the mitogen-activated protein kinase Hog1p in morphogenesis and virulence of *Candida albicans*. *J. Bacteriol.* **181:** 3058-3068.

Altschul SF, Madden TL, Schäffer AA, Zhang J, Zhang Z, Miller W and Lipman DJ. 1997. Gapped BLAST and PSI-BLAST: a new generation of protein database search programs. *Nucleic Acids Res.* **25:** 3389-3402.

Ambra R and Macino G. 2000. Cloning and characterization of PKC-homologous genes in the truffle species *Tuber borchii* and *Tuber magnatum*. *FEMS Microbiol. Lett.* **189:** 45-53.

Andrews DL, Egan JD, Mayorga ME and Gold SE. 2000. The *Ustilago maydis ubc4* and *ubc5* genes encode members of a MAP kinase cascade required for filamentous growth. *Mol. Plant Microbe Interact.* **13:** 781-786.

Aquino-Pinero E and Rodriguez-del Valle N. 2002. Characterization of a protein kinase C gene in *Sporothrix schenckii* and its expression during the yeast-to-mycelium transition. *Med. Mycol.* **40:** 185-199.

Arellano M, Valdivieso MH, Calonge TM, Coll PM, Duran A and Perez P. 1999. *Schizosaccharomyces pombe* protein kinase C homologues, pck1p and pck2p, are targets of rho1p and rho2p and differentially regulate cell integrity. *J. Cell Sci.* **112:** 3569-3578.

Arpaia G, Cerri F, Baima S and Macino G. 1999. Involvement of protein kinase C in the response of *Neurospora crassa* to blue light. *Mol. Gen. Genet.* **262:** 314-322.

Asaoka Y, Nakamura S, Yoshida K and Nishizuka Y. 1992. Protein kinase C, calcium and phospholipid degradation. *Trends Biochem. Sci.* **17:** 414-417.

Ausubel FM, Brent R, Kingston RE, Moore DD, Smith JA, Seidman JG and Strahl K. (Eds.) 1987. Current Protocols on Molecular Biology. (John Wiley, N.Y.), pp. 233.

Balhadere PV and Talbot NJ. 2001. *PDE1* encodes a P-type ATPase involved in appressorium-mediated plant infection by the rice blast fungus *Magnaporthe grisea*. *Plant Cell.* **13:** 1987-2004.

Banuett F. 1998. Signalling in the yeasts: an informational cascade with links to the filamentous fungi. *Microbiol Mol. Biol. Rev.* **62:** 249-274.

Banuett F and Herskowitz I. 1994. Identification of Fuz7, a *Ustilago maydis* MEK/MAPKK homolog required for a locus-dependent and -independent steps in the fungal life cycle. *Genes Dev.* **8:** 1367-1378.

Barry OP and Kazanietz MG. 2001. Protein kinase C isozymes, novel phorbol ester receptors and cancer chemotherapy. *Curr. Pharm. Des.* **7:** 1725-1744.

Beckerman JL and Ebbole DJ. 1996. *MPG1*, a gene encoding a fungal hydrophobin of *Magnaporthe grisea*, is involved in surface recognition. *Mol. Plant Microbe Interact.* **9:** 450-456.

Bélanger RR and Labbé C. 2002. Control of powdery mildews without chemicals: Prophylactic and biological alternatives for horticultural crops. In: The Powdery Mildews: A Comprehensive Treatise, RR Belanger, WR Bushnell, AJ Dik and TLW Carver, eds (St Paul, MN.: APS Press), pp. 256-267.

Bencina M, Panneman H, Ruijter GJ, Legisa M and Visser J. 1997. Characterization and overexpression of the *Aspergillus niger* gene encoding the cAMP-dependent protein kinase catalytic subunit. *Microbiology.* **143:** 1211-1220.

Bindslev L, Kershaw MJ, Talbot NJ and Oliver RP. 2001. Complementation of the *Magnaporthe grisea* Δ*cpka* mutation by the *Blumeria graminis* PKA-c gene: Functional genetic analysis of an obligate plant pathogen. *Mol. Plant Microbe Interact.* **14:** 1368-1375.

Blatter RHE, Brown JKM and Wolfe MS. 1998. Genetic control of the resistance of *Erysiphe graminis* f.sp. *hordei* to five triazole fungicides. *Plant Pathol.* **47:** 570-579.

Blumer S. 1967. Echte Mehltaupilze (Erysiphaceae). (Jena, Germany:G. Fischer).

Boguslawski G and Polazzi JO. 1987. Complete nucleotide sequence of a gene conferring polymyxin B resistance on yeast: Similarity of the predicted polypeptide to protein kinases. *Proc. Natl. Acad. Sci. USA.* **84**: 5848-5852.

Bonman JM, Khush GS and Nelson RJ. 1992. Breeding rice for resistance to pests. *Ann. Rev. of Phytopathol.* **30:** 507-528.

Bosemeyer B. 1995. Protein kinases – Structure and function. *FEBS Lett.* **369:** 57-61.

Bourett TM and Howard RJ. 1990. *In vitro* development of penetration structures in the rice blast fungus *Magnaporthe grisea. Can. J. Bot.* **68:** 329-342.

Braun U. 1995. The powdery mildews (Erysiphales) of Europe. (Jena, Germany; Gustav Fischer Verlag).

Braun U, Cook RTA, Inman AJ and Shin HD. 2002. The taxonomy of the powdery mildew fungi. In The Powdery Mildews: A Comprehensive Treatise, RR Belanger, WR Bushnell, AJ Dik and TLW Carver, eds (St Paul, MN.: APS Press), pp. 13-55.

Brose N and Rosenmund C. 2002. Move over protein kinase C, you've got company: alternative cellular effectors of diacylglycerol and phorbol esters. *J. Cell Sci.* **115:** 4399-4411.

Brown JKM. 1994. Chance and selection in the evolution of barley powdery mildew. *Trends Microbiol.* **2:** 470-475.

Bruno KS, Aramayo R, Minke PF, Metzenberg RL and Plamann M. 1996. Loss of growth polarity and mislocalization of septa in a *Neurospora* mutant altered in the regulatory subunit of cAMP-dependent protein kinase. *EMBO J.* **15:** 5772-5782.

Bruns RF, Miller FD, Merriman RL, Howbert JJ, Heath WF, Kobayashi E, Takahashi I, Tamaoki T and Nakano H. 1991. Inhibition of protein kinase C by Calphostin C is light-dependent. *Biochem. Biophys. Res. Commun.* **176:** 288-293.

Bryngelsson T and Collinge DB. 1992. Biochemical and molecular analyses of the response of barley to infection by powdery mildew. In Barley: genetics, biochemistry, molecular biology and biotechnology, PR Shrewry, ed (Wallingford, UK: CABI).

Buhr TL and Dickman MB. 1997. Gene expression analysis during conidial germ tube and appressorium development in *Colletotrichum trifolii. Appl. Environ. Microbiol.* **63:** 2378-2383.

Büschges R, Hollricher K, Panstruga R, Simons G, Wolter M, Frijters A, van Daelen R, van der Lee T, Diergaarde P, Groenendijk J, Topsch S, Vos P, Salamini F and Schulze-Lefert P. 1997. The barley *Mlo* gene: a novel control element of plant pathogen resistance. *Cell.* **88:** 695-705.

Bushnell WR. 2002. The role of powdery mildew research in understanding host-parasite interaction: past, present, and future. In The Powdery Mildews: Comprehensive Treatise, RR Belanger, WR Bushnell, AJ Dik and TLW Carver, eds (St Paul, MN.: APS Press), pp. 1-12.

Bushnell WR and Bergquist SE. 1975. Aggregation of host cytoplasm and the formation of papillae and haustoria in powdery mildew of barley. *Phytopathol.* **65:** 310-318.

Bushnell WR and Zeyen RJ. 1976. Light and electron microscope studies of cytoplasmic aggregates formed in barley cells in response to *Erysiphe graminis. Can. J. Bot.* **54:** 1647-1655.

Bussink HJ and Osmani SA. 1999. A mitogen-activated protein kinase (MPKA) is involved in polarized growth in the filamentous fungus, *Aspergillus nidulans. FEMS Microbiol. Lett.* **173:** 117-125.

Caffrey DR, O'Neill LA and Shields DC. 1999. The evolution of the MAP kinase pathways: coduplication of interacting proteins leads to new signaling cascades. *J. Mol. Evol.* **49**: 567–582.

Canagarajah BJ, Khokhlatchev A, Cobb MH and Goldsmith EJ. 1997. Activation mechanism of the MAP kinase ERK2 by dual phosphorylation. *Cell.* **90:** 859-869.

Carver TLW and Bushnell. 1983. The probable role of primary germ tubes in water uptake before infection *by Erysiphe graminis. Physiol. Plant Pathol.* **23:** 229-240.

Carver TLW and Ingerson SM. 1987. Responses of *Erysiphe graminis* germlings to contact with artificial and host surfaces. *Physiol. Mol. Plant Pathol.* **30:** 359-372.

Carver TLW, Thomas BJ and Ingerson-Morris SM. 1995a. The surface of *Erysiphe graminis* and the production of extracellular material at the fungus/host interface during germling and conidial development. *Can. J. Bot.* **73:** 272-287.

Carver TLW, Ingerson-Morris SM, Thomas BJ and Zeyen RJ. 1995b. Early interactions during powdery mildew interaction. *Can. J. Bot.* **73:** 632-639.

Carver TLW, Ingerson SM and Thomas BJ. 1996. Influence of host surface features on development of *Erysiphe graminis* and *Erysiphe pisi.* In Plant Cuticles - an integrated functional approach. G Kersteins, ed, (Bios Scientific Pub., Oxford, UK.), pp 255-266.

Carver TLW, Kunoh H, Thomas BJ and Nicholson R. 1999. Release and visualisation of the extracellular matrix of conidia of *Blumeria graminis. Mycol. Res.* **103:** 547-560.

Chaure P, Gurr SJ and Spanu P. 2000. Stable transformation of *Erysiphe graminis* an obligate biotrophic pathogen of barley. *Nat. Biotechnol.* **18:** 205-207.

Chen B, Gao S, Choi GH and Nuss DL. 1996. Extensive alteration of fungal gene transcript accumulation and elevation of G-protein-regulated cAMP levels by a virulence-attenuating hypovirus. *Proc Natl. Acad. Sci. USA.* **93:** 7996-8000.

Chijiwa T, Mishima A, Hagiwara M, Sano M, Hayashi K, Inoue T, Naito K, Toshioka T and Hidaka H. 1990. Inhibition of forskolin-induced neurite outgrowth and protein phosphorylation by a newly synthesized selective inhibitor of cyclic AMP-dependent protein kinase, N-[2-(p-bromocinnamylamino)ethyl]-5-isoquinolinesulfonamide (H-89), of PC12D pheochromocytoma cells. *J. Biol Chem.* **265:** 5267-5272.

Choi W and Dean RA. 1997. The adenylate cyclase gene *MAC1* of *Magnaporthe grisea* controls appressorium formation and other aspects of growth and development. *Plant Cell.* **9:** 1973-1983.

Cogoni C. 2001. Homology-dependent gene silencing mechanisms in fungi. *Annu. Rev. Microbiol.* **55:** 381-406.

Cooke RC and Whipps JM. 1980. The evolution of modes of nutrition in fungi parasitic on terrestrial plants. *Biol. Rev.* **55:** 341-362.

Costigan C, Gehrung S and Snyder M. 1992. A synthetic lethal screen identifies *SLK1*, a novel protein-kinase homologue implicated in yeast-cell morphology and cell-growth. *Mol. Cell. Biol.* **12:** 1162–1178.

Cottrell TR and Doering TL. 2003. Silence of the strands: RNA interference in eukaryotic pathogens. *Trends Microbiol.* **11:** 37-43.

Courey AJ and Tjian R. 1988. Analysis of Sp1 *in vivo* reveals multiple transcriptional domains, including a novel glutamine-rich activation motif. *Cell.* **55:** 887-898.

Csank C, Schroppel K, Leberer E, Harcus D, Mohamed O, Meloche S, Thomas DY and Whiteway M. 1998. Roles of the *Candida albicans* mitogen-activated protein kinase homolog, Cek1p, in hyphal development and systemic candidiasis. *Infect. Immun.* **66:** 2713-2721.

Dangl JL and Jones JD. 2001. Plant pathogens and integrated defence responses to infection. *Nature.* **411:** 826-833.

Davenport KR, Sohaskey M, Kamada Y, Levin DE and Gustin MC. 1995. A second osmosensing signal-transduction pathway in yeast-hypotonic shock activates the *PKC1* protein kinase-regulated cell integrity pathway. *J. Biol. Chem.* **270:** 30157–30161.

Dean RA. 1997. Signal pathways and appressorium morphogenesis. *Annu. Rev. Phytopathol.* **35:** 211-234.

De Backer MD, Nelissen B, Logghe M, Viaene J, Loonen I, Vandoninck S, de Hoogt R, Dewaele S, Simons FA, Verhasselt P, Vanhoof G, Contreras R and Luyten WH. 2001. An antisense-based functional genomics approach for identification of genes critical for growth of *Candida albicans. Nat. Biotechnol.* **19:** 235-241.

Deising HB, Werner S and Wernitz M. 2000. The role of fungal appressoria in plant infection. *Microbes Infect.* **2:** 1631-1641.

de Jong JC, McCormack BJ, Smirnoff N and Talbot N. 1997. Glycerol generates turgor in rice blast. *Nature.* **389:** 244-245.

Devoto A, Piffanelli P, Nilsson I, Wallin E, Panstruga R, von Heijne G and Schulze-Lefert P. 1999. Topology, subcellular localization, and sequence diversity of the Mlo family in plants. *J Biol Chem.* **274:** 34993-5004.

DeZwaan TM, Carroll AM, Valent B and Swiegard JA. 1999. *Magnaporthe grisea* Pth11p is a novel plasma membrane protein that mediates appressorium differentiation in response to inductive substrate cues. *Plant Cell.* **11:** 2013-2030.

Dickman MB, Buhr TL, Warwar V, Truesdell GM and Huang CX. 1995. Molecular signalling during the early stages of alfalfa anthracnose. *Can. J. Bot.* **73:** S1169 – S1177.

Di Pietro A, Garcia-MacEira FI, Meglecz E and Roncero MI. 2001. A MAP kinase of the vascular wilt fungus *Fusarium oxysporum* is essential for root penetration and pathogenesis. *Mol. Microbiol.* **39:** 1140-1152.

Dixon KP, Xu JR, Smirnoff N and Talbot NJ. 1999. Independent signaling pathways regulate cellular turgor during hyperosmotic stress and appressorium-mediated plant infection by *Magnaporthe grisea. Plant Cell.* **11**: 2045–2058.

Dudley DT, Pang L, Decker SJ, Bridges AJ and Saltiel AR. 1995. A synthetic inhibitor of the mitogen-activated protein kinase cascade. *Proc. Natl. Acad. Sci.* USA. **92:** 7686-7689.

Duncia JV, Santella JB 3rd, Higley CA, Pitts WJ, Wityak J, Frietze WE, Rankin FW, Sun JH, Earl RA, Tabaka AC, Teleha CA, Blom KF, Favata MF, Manos EJ, Daulerio AJ, Stradley DA, Horiuchi K, Copeland RA, Scherle PA, Trzaskos JM, Magolda RL, Trainor GL, Wexler RR, Hobbs FW and Olson RE. 1998. MEK inhibitors: the chemistry and biological activity of U0126, its analogs, and cyclization products. *Bioorg. Med. Chem. Lett.* **8:** 2839-2844.

Edwards HH and Allen PJ. 1966. Distribution of the products of photosynthesis between powdery mildew and barley. *Plant Physiol.* **41:** 683-688.

Edwards HH and Allen PJ. 1970. A fine-structure of the primary infection process during infection of barley by *Erysiphe graminis* f.sp. *hordei. Phytopathol.* **60:** 1504-1509.

Ellis J and Jones J. 1998. Structure and function of proteins controlling strain specific pathogen resistance in plants. *Curr. Opin, Plant Biol.* **1:** 288-293.

English JM and Cobb MH. 2002. Pharmacological inhibitors of MAPK pathways. *Trends in Pharmacological Sci.* **23:** 40-45.

Engh RA, Girod A, Kinzel V, Huber R and Bossemeyer D. 1996. Crystal structures of catalytic subunit of cAMP-dependent protein kinase in complex with isoquinolinesulfonyl protein kinase inhibitors H7, H8, and H89. Structural implications for selectivity. *J. Biol. Chem.* **271:** 26157-26164.

Favata MF, Horiuchi KY, Manos EJ, Daulerio AJ, Stradley DA, Feeser WS, Van Dyk DE, Pitts WJ, Earl RA, Hobbs F, Copeland RA, Magolda RL, Scherle PA, Trzaskos JM. 1998. Identification of a novel inhibitor of mitogen-activated protein kinase kinase. *J. Biol. Chem.* **273:** 18623-18632.

Filippi MC and Prabhu AS. 1997. Integrated effect of host plant resistance and fungicidal seed treatment on rice blast control in Brazil. *Plant Disease.* **81:** 351-355.

Fox D and Smulian AG. 1999. Mitogen-activated protein kinase *Mkp1* of *Pneumocystis carinii* complements the *slt2*Delta defect in the cell integrity pathway of *Saccharomyces cerevisiae. Molecular Microbiology.* **34:** 451-62.

Francis SA, Dewey FM and Gurr SJ. 1996. The role of cutinase in germling development and infection by *Erysiphe graminis* f. sp. *hordei. Physiol. Mol. Plant Pathol.* **49:** 201–211.

Fric F and Wolf G. 1994. Hydrolytic enzymes of ungerminated and germinated conidia of *Erysiphe graminis* DC f.sp. *hordei* Marchal. *J. Phytopathol.* **140:** 1-10.

Gao SJ and Nuss DL. 1996. Distinct roles for two G protein α sub-units in fungal virulence, morphology, and reproduction revealed by targeted gene disruption. *Proc. Natl. Acad. Sci. USA.* **93:** 14122–14127.

Garrill A, Jackson SL, Lew RR and Heath IB. 1993. Ion channel activity and tip growth: tip-localized stretch-activated channels generate an essential Ca^{2+} gradient in the oomycete *Saprolegnia ferax. Eur. J. Cell Biol.* **60:** 358-365.

Gair R, Jenkins JEE and Lester E. 1991. Barley diseases. In Cereal pests and diseases. (Ipswich, UK: Farming Press Ltd.).

Gay JL, Martin M and Ball E. 1985. The impermeability of powdery mildew conidia and their germination in arid environments. *Plant Pathol.* **34:** 353-362.

Gilbert RD, Johnson AM, and Dean RA. 1996. Chemical signals responsible for appressorium formation in the rice blast fungus *Magnaporthe grisea. Physiol. Mol. Plant Pathol.* **48:** 335-346.

Gold S, Duncan G, Barrett K and Kronstad J. 1994. cAMP regulates morphogenesis in the fungal pathogen *Ustilago maydis. Genes Dev.* **8:** 2805-2816.

Goni FM and Alonso A. 1999. Structure and functional properties of diacylglycerols in membranes. *Progr. Lipid Res.* **38**: 1-48.

Gorlach JM, McDade HC, Perfect JR and Cox GM. 2002. Antisense repression in *Cryptococcus neoformans* as a laboratory tool and potential antifungal strategy. *Microbiology.* **148(Pt 1):** 213-219.

Green JR, Carver TLW and Gurr SJ. 2002. The formation and function of infection and feeding structures. In The Powdery Mildews: A Comprehensive Treatise, RR Belanger, WR Bushnell, AJ Dik and TLW Carver, eds (St Paul, MN.: APS Press), pp. 66-83.

Gurr SJ, Unkles S and Kinghorn J. 1987. The structure and organisation of nuclear genes of filamentous fungi. In *Gene structure in eukaryotic microbes.* JR Kinghorn, ed (IRL Press, Oxford and Washington) pp 93-139.

Gustin MC, Albertyn J, Alexander M, and Davenport K. 1998. MAP kinase pathways in the yeast. *Saccharomyces cerevisiae. Microbiol. Mol. Biol. Rev.* **62:** 1264–300.

Gschwendt M, Kittstein W and Marks F. 1991. Protein kinase C activation by phorbol esters: do cysteine-rich regions and pseudosubstrate motifs play a role? *Trends Biochem. Sci.* **16:** 167-169.

Gschwendt M, Dieterich S, Rennecke J, Kittstein W, Mueller HJ and Johannes FJ. 1996. Inhibition of protein kinase C mu by various inhibitors. Differentiation from protein kinase C isozymes. *FEBS Lett.* **392:** 77-80.

Hagiwara M, Inagaki M, Watanabe M, Ito M, Onodo K, Tanaka T and Hidaka H. 1987. Selective modulation of calcium-dependent myosin phosphorylation by novel protein kinase inhibitors, isoquinolinesulfonamide derivates. *Mol. Pharmacol.* **32:** 7-12.

Hardie G. 1988. Pseudosubstrates turn off protein kinases. *Nature.* **335:** 592-593.

Hall A. 1994. Small GTP-binding proteins and the regulation of the actin cytoskeleton. *Annu. Rev. Cell Biol.* **10:** 31-54.

Hall AA. 1999. Signal transduction during infection structure differentiation by barley powdery mildew. Thesis for the degree of Doctor of Philosophy, University of Oxford.

Hall AA and Gurr SJ. 2000. Initiation of appressorial germ tube differentiation and appressorial hooking: distinct morphological events regulated by cAMP signalling in *Blumeria graminis* f.sp *hordei*. *Physiol. Mol. Plant Pathol.* **56:** 39-46.

Hall AA, Bindslev L, Rouster J, Rasmussen SW, Oliver R and Gurr SJ. 1999. Involvement of cAMP and protein kinase A in conidial differentiation by *Erysiphe graminis* f. sp. *hordei*. *Mol. Plant Microbe Interact.* **12:** 960-968.

Hamer JE and Holden DW. 1997. Linking Approaches in the Study of Fungal Pathogenesis: A Commentary. *Fungal Genet. Biol.* **21:** 11-16.

Hamer JE and Talbot NJ. 1998. Infection-related development in the rice blast fungus *Magnaporthe grisea*. *Curr. Opin. Microbiol.* **1:** 693-697.

Hamer JE, Howard RJ, Chumley FG and Valent V. 1988. A mechanism for surface attachment in spores of a plant pathogenic fungus. *Science*. **239:** 288-290.

Hanahan D. 1985. Techniques for transformation of *E.coli*. In DNA Cloning. Volume 1. DM Glover, ed (Oxford, Washington DC:IRL Press), pp 109-136.

Hanks SK and Hunter T. 1995. Protein kinases 6. The eukaryotic protein kinase superfamily: kinase (catalytic) domain structure and classification. *FASEB J.* **9:** 576-596.

Hanks S, Quinn A and Hunter T. 1988. The protein kinase family: Conserved features and deduced phylogeny of the catalytic domains. *Science*. **241:** 42-52.

Hardison JR. 1944. Specialisation of pathogenicity in *Erysiphe graminis* on wild and cultivated species. *Phytopathol.* **34:** 1-20.

Hawksworth DL, Kirk PM, Sutton BC and Pegler DN. 1995. Dictionary of the Fungi. GC Ainsworth ed (GR Biby, Wallingford, UK: CAB Int. 8th ed.), pp 616.

Heath MC. 2000. Nonhost resistance and nonspecific plant defenses. *Curr. Opin. Plant Biol.* **3:** 315-319.

Heath MC, Valent B, Howard RJ, and Chumley FG. 1990. Interactions of two strains of *Magnaporthe grisea* with rice, goosegrass and weeping lovegrass. *Can. J. Bot.* **68:** 1627-1637.

Heath MC, Howard RJ, Valent B, and Chumley FG. 1992. Ultrastructural interactions of one strain of *Magnaporthe grisea* with goosegrass and weeping lovegrass. *Can. J. Bot.* **70:** 779-787.

Herbert JM, Augereau JM, Gleye J and Maffrand JP. 1990. Chelerythrine is a potent and specific inhibitor of protein kinase C. *Biochem. Biophys. Res. Commum.* **172:** 993-999.

Herskowitz I. 1995. MAP kinase pathways in yeast: for mating and more. *Cell.* **80:** 187–97.

Hidaka H, Inagaki M, Kawamoto S and Sasaki Y. 1984. Isoquinolinesulfonamides, novel and potent inhibitors of cyclic nucleotide dependent protein kinase and protein kinase C. *Biochemistry.* **23:** 5036-5041.

Hiura U. 1978. Genetic basis of *formae speciales* in *Erysiphe graminis*. In Powdery Mildews. DM Spencer, ed (London, UK; Academic Press Ltd).

Hoch HC and Staples RC. 1985. Evidence that cAMP initiates nuclear division and infection structure formation in the bean rust fungus, *Uromyces phaseoli*. *Exp. Mycol.* **8:** 37-46.

Hoch HC and Staples RC. 1991. Signalling for infection structure formation in fungi. In The fungal spore and disease initiation in plants and animals. GT Cole HC Hoch, eds (Plenium Press Pub., New York, USA), pp 25-46.

Hoch HC, Staples RC, Whitehead B, Comeau J and Wolf ED. 1987. Signalling for growth orientation and cell differentiation by surface topography in *Uromyces*. *Science* **235:** 1659-1662.

Hodgkin MN, Pettitt TR, Martin A, Michell RH, Pemberton AJ and Wakelam MJ. 1998. Diacylglycerols and phosphatidates: which molecular species are intracellular messengers? *Trends Biochem. Sci.* **23**: 200-204.

Holloman DW and Wheeler IE. 2002. Controlling powdery mildews with chemistry. In The Powdery Mildews: A Comprehensive Treatise, RR Belanger, WR Bushnell, AJ Dik and TLW Carver, eds (St Paul, MN.: APS Press), pp. 249-255.

Holloman DW, Wheeler IE, Dixon K, Longhurst C, and Skylakakis G. 1997. Defining the resistance risk of the new powdery mildew fungicide quinoxyfen. *Pesticide Sci.* **51:** 347-351.

Holloway PJ. 1970. Surface factors affecting the wetting of leaves. *Pesticide Sci.* **1:** 156-163.

Hou Z, Xue C, Peng Y, Katan T, Kistler HC and Xu JR. 2002. A mitogen-activated protein kinase gene (MGV1) in *Fusarium graminearum* is required for female fertility, heterokaryon formation, and plant infection. *Mol. Plant Microbe Interact.* **15:** 1119-1127.

Howard RJ. 1994. Cell biology and pathogenesis. In Rice Blast Disease. RS Zeiger, SA Leong and PS Teng, eds (CAB International, Wallingford, UK), pp 3-22.

Howard RJ. 1997. Breaching the outer barrier-cuticle and cell wall penetration. In: The Mycota. V Plant Relationships, Part A. GC Carroll and P Tudzynski, ed (Berlin/Heidelberg: Springer-Verlag), pp. 43-60.

Howard RJ and Ferrari MA. 1989. Role of melanin in appressorium formation. *Exp. Mycol.* **13:** 403-418.

Howard RJ and Valent B. 1996. Breaking and entering: host penetration by the fungal rice blast pathogen *Magnaporthe grisea. Annu. Rev. Microbiol.* **50:** 491-512.

Howard RJ, Ferrari MA, Roach DH and Money NP. 1991. Penetration of hard substrates by fungus employing enormous turgor pressures. *Proc. Natl. Acad. Sci. USA*. **88:** 11281-11284.

Huckelhoven R, Fodor J, Preis C and Kogel KH. 1999. Hypersensitive cell death and papilla formation in barley attacked by the powdery mildew fungus are associated with hydrogen peroxide but not with salicylic acid accumulation. *Plant Physiol.* **119:** 1251-1260.

Huber SM, Lottspeich F and Kamper J. 2002. A gene that encodes a product with similarity to dioxygenases is highly expressed in teliospores of *Ustilago maydis*. *Mol. Genet. Genomics*. **267:** 757-771.

Hurley JH, Newton AC, Parker PJ, Blumberg PM and Nishizuka Y. 1997. Taxonomy and function of C1 protein kinase C homology domains. *Protein Sci.* **6:** 477-80.

Hwang BK, Kim KD and Kim YB. 1989. Carbohydrate composition and acid invertase activity in rice leaves infected with *Pyricularia oryzae*. *J. Phytopathol.* **125:** 124-132.

Inukai T, Zeigler RS, Sarkarung S, Bronson M, Dung LV, Kinoshita T and Nelson RJ. 1996. Development of pre-isogenic lines for rice blast-resistance by marker-aided selection from a recombinant inbred population. *Theoretical and Applied Genetics*. **93:** 560-567.

Irie K, Takase M, Lee KS, Levin DE, Araki H, Matsumoto K and Oshima Y. 1993. *MKK1* and *MKK2*, which encode *Saccharomyces cerevisiae* mitogen-activated protein kinase-kinase homologs, function in the pathway mediated by protein kinase C. *Mol. Cell Biol.* **13**: 3076-3083.

James WC, Teng PS and Nutter FW. 1991. Estimated losses of crops from plant pathogens. In: CRC Handbook of Pest Management in Agriculture. D Pimentel, ed (Boca Raton, USA: CRC Press).

Jelitto TC, Page HA and Read ND. 1994. Role of external signals in regulating the pre-penetration phase of the rice blast fungus, *Magnaporthe grisea*. *Planta*. **194:** 471-477.

Jeffries P and Young TWK. 1994. Interfungal parasitic relationships. (CAB International, Wallingford, UK).

Jenkyn JF and Bainbridge A. 1978. Biology and pathology of cereal powdery mildews. In The Powdery Mildews. DM Spencer, ed (London: Academic Press Ltd.), pp. 248-321.

Johannes FJ, Prestle J, Eis S, Oberhagemann P and Pfizenmaier K. 1994. PKCmu is a novel, atypical member of the protein kinase C family. *J. Biol. Chem.* **269:** 6140-6148.

Johnson JL and Lapadat R. 2002. Mitogen-activated protein kinase pathways mediated by ERK, JNK, and p38 protein kinases. *Science*. **298:** 1911-1912.

Jones JD. 2001. Putting knowledge of plant disease resistance genes to work. *Curr. Opin. Plant Biol.* **4:** 281-287.

Jørgensen JH. 1992. Discovery, characterisation and exploitation of *Mlo* powdery mildew resistance in barley. *Euphytica*. **63:** 141-153.

Kase H, Iwahashi K, Nakanishi S, Matsuda Y, Yamada K, Takahashi M, Murakata C, Sato A, Kaneko M. 1987. K-252 compounds, novel and potent inhibitors of protein kinase C and cyclic nucleotide-dependent protein kinases. *Biochem. Biophys. Res. Commun.* **142:** 436-440.

Kemp BE and Pearson RB. 1991. Intrasteric regulation of protein kinases and phosphatases. *Biochim Biophys Acta.* **1094:** 67-76

Keranen LM, Dutil EM and Newton AC. 1995. Protein kinase C is regulated *in vivo* by three functionally distinct phosphorylations. *Curr Biol.* **5:** 1394-1403.

Kershaw MJ, Wakley G and Talbot NJ. 1998. Complementation of the *mpg1* mutant phenotype in *Magnaporthe grisea* reveals functional relationships between fungal hydrophobins. *EMBO J.* **17:** 3838-3849.

Kim YK, Li D and Kolattukudy PE. 1998. Induction of Ca^{2+}-calmodulin signalling by hard-surface contact primes *Colletotrichum gloeosporoides* conidia to germinate and form appressoria. *J. Bacteriol.* **180:** 5144–5150.

Kim YK, Kawano T, Li D, Kolattukudy PE. 2000. A mitogen-activated protein kinase kinase required for induction of cytokinesis and appressorium formation by host signals in the conidia of *Colletotrichum gloeosporioides*. *Plant Cell.* **12:** 1331-1343.

Kinane J, Dalvin S, Bindslev L, Hall AA, Gurr SJ and Oliver R. 2000. Evidence that the cAMP pathway controls emergence of both primary and appressorial germ tubes of barley powdery mildew. *Mol. Plant Microbe Interact.* **13:** 494-502.

Kobayashi I, Tanaka C, Yamaoka N and Kunoh H. 1991. Morphogensis of *Erysiphe graminis conidia* on artificial membranes. *Trans. Mycol. Soc. Japan.* **32:** 187-198.

Kojima K, Kikuchi T, Takano Y, Oshiro E and Okuno T. 2002. The mitogen-activated protein kinase gene MAF1 is essential for the early differentiation phase of appressorium formation in *Colletotrichum lagenarium. Mol. Plant Microbe Interact.* **15**: 1268-76.

Kolattukudy PE, Li D, Beng-Shin H and Flaishman MA. 1995. Host signals in fungal gene expression involved in penetration into the host cell. *Can. J. Bot.* **73:** S1160-S1168.

Kronstad J. 1997. Virulence and cAMP in smuts, blights and blasts. *Trends in Plant Sci.* **2:** 193-199.

Kronstad J, Bakkeren G, Gold S, Yee A, Laity C, Duncan G, Barrett K, Glasson L, Campbell R and Athwal G. 1995. Control of filamentous growth by mating and cyclic-amp in Ustilago. *Can. J. Bot.* **73 (Suppl 1):** S258-S265.

Kronstad J, De Maria AD, Funnell D, Laidlaw RD, Lee N, de Sa MM and Ramesh M. 1998. Signaling via cAMP in fungi: interconnections with mitogen-activated protein kinase pathways. *Arch Microbiol.* **170:** 395-404.

Kultz, D. 1998. Phylogenetic and functional classification of mitogen and stress-activated protein kinase. *J. Mol. Evol.* **46:** 571-588.

Kunoh H. 1982. Primary germ tubes of *Ersiphe graminis* conidia. In Plant Infection: The Physiological and Biochemical Basis. Y Asada, WR Bushnell, S Ouchi and CP Vance, eds (Springer-Verlag, Berlin). pp. 45-59.

Kunoh H and Ishikazi H. 1975. Silicon levels near penetration sites of fungi on wheat, barley and cucumber and morning glory leaves. *Physiol. Plant Pathol.* **5:** 283-297.

Kunoh H, Tsuzuki T and Ishizaki H. 1978. Cytological studies of early stages of powdery mildew in barley and wheat. IV. Direst ingress from superficial primary germ tubes and appressoria of *Erysiphe graminis hordei* on barley leaves. *Physiol. Plant Pathol.* **13:** 327-333.

Kunoh H, Itoh O, Kohno M and Ishizaki H. 1979. Are primary germ tubes of conidia unique to *Erysiphe graminis*? *Ann. Phytopathol. Soc. Jpn.* **45:** 675-682.

Kunoh H, Nicholson RL, Yoshioka H, Yamaoka N and Kobayashi I. 1990. Preparation of the infection court by Erysiphe graminis: dehydradation of the host cuticle. *Physiol. and Mol. Plant Pathol.* **36:** 397-407.

Kwon YH, Hoch HC and Aist JR. 1991. Initiation of appressorium formation in *Uromyces appendiculatus*: organisation of the apex, and the responses involving microtubules and apical vesicles. *Can. J. Bot.* **69:** 2560-2573.

Kyriakis JM, Banerjee P, Nikolakaki E, Dai T, Rubie EA, Ahmad MF, Avruch J and Woodgett JR. 1994. The stress-activated protein kinase subfamily of c-Jun kinases. *Nature.* **369:** 156-160.

Latterell FM and Rossi AE. 1986. Longevity and pathogenic stability of *Pyricularia oryzae. Phytopathology.* **76:** 231-235.

Lee FN and Beaty T. 1999. Evaluation of foliar fungicides for control of neck blast of rice, 1999. *F&N Tests.* **55:** 329.

Lee YH and Dean RA. 1993. cAMP regulates infection structure formation in the plant-pathogenic fungus *Magnaporthe grisea. Plant Cell* **5:** 693-700.

Lee YH and Dean RA. 1994. Hydrophobicity of contact surface induces appressorium formation in *Magnaporthe grisea*. *FEMS Microbiol. Lett.* **115:** 71-75.

Lee KS, Irie K, Gotoh Y, Watanabe Y, Araki H, Nishida E, Matsumoto K and Levin DE. 1993. A yeast mitogen-activated protein kinase homolog (Mpk1p) mediates signalling by protein kinase C. *Mol. Cell. Biol.* **13:** 3067–3075.

Lee N, D'Souza CA and Kronstad JW. 2003. Of Smuts, Blasts, Mildews and Blights: cAMP signaling in phytopathogenic fungi. *Annu. Rev Phytopathol.* **41:** 03.1-03.29.

Lev S and Horwitz BA. 2003. A mitogen-activated protein kinase pathway modulates the expression of two cellulase genes *in Cochliobolus heterostrophus* during plant infection. *Plant Cell.* **15:** 835-844.

Lev S, Sharon A, Hadar R, Ma H and Horwitz BA. 1999. A mitogen-activated protein kinase of the corn leaf pathogen *Cochliobolus heterostrophus* is involved in conidiation, appressorium formation, and pathogenicity: diverse roles for mitogen-activated protein kinase homologs in foliar pathogens. *Proc. Natl. Acad. Sci. USA*. **96**: 13542-13547.

Levin DE, Fields FO, Kunisawa R, Bishop JM and Thorner J. 1990. A candidate protein kinase C gene, PKC1, is required for the *S. cerevisiae* cell cycle. *Cell.* **62:** 213-224.

Lewis TS, Shapiro PS and Ahn NG. 1998. Signal transduction through MAP kinase cascades. *Adv Cancer Res.* **74:** 49-139.

Li D, Rogers LM and Kolattukudy PE. 1997. Cloning and expression of cDNA encoding a mitogen-activated protein kinase from a phytopathogenic filamentous fungus. *Gene.* **195**: 161-166.

Lim LG and Gaunt RE. 1986. The effect of powdery mildew (*Erysiphe graminis* f.sp. *hordei*) and leaf rust (*Puccinia hordei*) on spring barley in New Zealand. II. Apical development and yield potential. *Plant Pathol.* **36:** 123-129.

Liu S and Dean RA. 1997. G protein α-subunit genes control growth, development and pathogenicity of *Magnaporthe grisea*. *Mol. Plant Microbe Interact.* **10:** 1075–1086.

Liu H, Cottrell TR, Pierini LM, Goldman WE and Doering TL. 2002. RNA interference in the pathogenic fungus *Cryptococcus neoformans*. *Genetics*. **160:** 463-470.

Lyngkaer MF and Carver TLW. 1999a. Modification of mlo5 resistance to *Blumeria graminis* attack in barley as a consequence of induced accessibility and inaccessibility. *Physiol. Mol. Plant Pathol.* **44:** 163-147.

Lyngkaer MF and Carver TLW. 1999b. Induced accessibility and inaccessibility to *Blumeria graminis* f.sp. *hordei* in barley epidermal cells attacked by a compatible isolate. *Physiol. Mol. Plant Pathol.* **55:** 161-162.

Mackill AO and Bonman JM. 1986. New hosts of *Pyricularia oryzae*. *Plant Disease*. **70:** 125-127.

Madhani HD and Fink GR. 1998. The control of filamentous differentiation and virulence in fungi. *Trends Cell Biol.* **8:** 348-353.

Manners JM and Gay JL. 1980. Autoradiography of the haustoria of *Erysiphe pisi*. *J. Gen. Microbiol.* **116:** 529-533.

Manners JM and Gay JL. 1982. Transport, localisation and metabolism of ^{14}C-photosynthates at the host-parasite interface of *Pisum sativum* and *Erysiphe pisi*. *New Phytol.* **91:** 221-224.

Marchal E. 1902. De la specialisation du parasitisme chez l'*Erysiphe graminis*. *Compt. Rend. Acad. Sci. Paris*. **135:** 210-213.

Marchetti MA. 1994. Race-specific and rate-reducing resistance to rice blast in US rice cultivars. In: Rice Blast Disease. RS Zeigler, SA Leong, PS Teng, eds (CAB International, Wallingford, UK, in association with IRRI, Manila, Philippines), pp 167-186.

Marchetti MA, McClung AM, Webb BD and Bollich CN. 1996. Registration of B82-761 long-grain rice germplasm resistant to blast and sheath blight. *Crop Science*. **36**: 815.

Mayorga ME and Gold SE. 1999. A MAP kinase encoded by the *ubc3* gene of *Ustilago maydis* is required for filamentous growth and full virulence. *Mol. Microbiol.* **34**: 485-497.

McKeen WE. 1972. Nuclear movement in *Erysiphe graminis hordei. Can. J. Microbiol.* **18:** 1333-1336.

Mellor H and Parker PJ. 1998. The extended protein kinase C superfamily. *Biochem. J.* **332:** 281-292.

Mendgen K. 1996. Fungal attachment and penetration. In Plant Cuticles - an integrated functional approach. G Kiersten, ed (Bios scientific Pub, Oxford, UK), pp 175-188.

Mey G, Oeser B, Lebrun MH and Tudzynski P. 2002a. The biotrophic, non-appressorium-forming grass pathogen *Claviceps purpurea* needs a Fus3/Pmk1 homologous mitogen-activated protein kinase for colonization of rye ovarian tissue. *Mol. Plant Microbe Interact.* **15:** 303-312.

Mey G, Held K, Scheffer J, Tenberge KB and Tudzynski P. 2002b. CPMK2, an SLT2-homologous mitogen-activated protein (MAP) kinase, is essential for pathogenesis of *Claviceps purpurea* on rye: evidence for a second conserved pathogenesis-related MAP kinase cascade in phytopathogenic fungi. *Mol. Microbiol.* **46:** 305-318.

Morawetz R, Lendenfeld T, Mischak H, Muhlbauer M, Gruber F, Goodnight J, de Graaff LH, Visser J, Mushinski JF and Kubicek CP. 1996. Cloning and characterisation of genes (*pkc*1 and *pkc*A) encoding protein kinase C homologues from *Trichoderma reesei* and *Aspergillus niger*. *Mol. Gen. Genet.* **250:** 17-28.

Motoyama T, Nakasako M, Yamaguchi I, Lyr H, Russell PE, Dehne HW and Sisler HD. 1999. Molecular action mechanism of a new melanin biosynthesis inhibitor. In: Modern fungicides and antifungal compounds II. 12th International Reinhardsbrunn Symposium, Friedrichroda, Thuringia, Germany, 24th-29th May 1998, 111-119.

Mott HR, Carpenter JW, Zhong S, Ghosh S, Bell RM and Campbell SL. 1996. The solution structure of the Raf-1 cysteine-rich domain: a novel ras and phospholipid binding site. *Proc. Natl. Acad. Sci. USA*. **93:** 8312-8317.

Muller P, Aichinger C, Feldbrugge M and Kahmann R. 1999. The MAP kinase *kpp*2 regulates mating and pathogenic development in *Ustilago maydis*. *Mol. Microbiol.* **34:** 1007-1017.

Nalefski EA and Falke JJ. 1996. The C2 domain calcium-binding motif: structural and functional diversity. *Protein Sci.* **5**: 2375-2390.

Navarro-Garcia F, Sanchez M, Pla J and Nombela C. 1995. Functional characterization of the *MKC1* gene of *Candida albicans*, which encodes a mitogen-activated protein kinase homolog related to cell integrity. *Mol. Cell Biol.* **15:** 2197-2206.

Nevoigt E and Stahl U. 1997. Osmoregulation and glycerol metabolism in the yeast *Saccharomyces cerevisiae. FEMS Microbiol. Rev.* **21:** 231-241.

Newton AC. 1989. Genetic adaptation of *Erysiphe graminis* f.sp. *hordei* to barley with partial resistance. *J. Phytopathol.* **126:** 133-148.

Newton AC. 1993. Interaction of proteins with lipid headgroups: lessons from protein kinase C. *Annu. Rev. Biophys. Biomol. Struc.* **22:** 1-25.

Newton AC. 2001. Protein kinase C: structural and spatial regulation by phosphorylation, cofactors, and macromolecular interactions. *Chem. Rev.* **101:** 2353-2364.

Nicholson RL. 1996. Adhesion of fungal propagules. In: Histology, Ultrastructure and Molecular Cytology of Plant-Microorganism Interactions. M Nicole, V Gianinazzi-Pearson eds (Amsterdam: Kluwer), pp. 117–34.

Nicholson RL and Epstein L. 1991. Adhesion of fungi to the plant surface: prerequisite for pathogenesis. In: The Fungal Spore and Disease Initiation in Plants and Animals. GT Cole, HC Hoch ed (New York: Plenum.), pp. 3-23.

Nicholson RL, Yoshida H, Yamaoka N and Kunoh H. 1988. Preparation of the infection court by *Erysiphe graminis*. II. Release of esterase enzyme from conidia in response to contact stimulus. *Exp. Mycol.* **12:** 336-349.

Nishizuka Y. 1992. Intracellular signaling by hydrolysis of phospholipids and activation of protein kinase C. *Science.* **258:** 607-614.

Nishizuka Y. 1995. Protein kinase C and lipid signaling for sustained cellular responses. *FASEB J.* **9:** 484-496.

Nonaka H, Tanaka K, and Hirano H. 1995. A downstream target of rho1 small gtp-binding protein is *pkc*1, a homologue of protein kinase C, which leads to activation of the map kinase cascade in *Saccharomyces cerevisiae*. *EMBO J.* **14:** 5931-5938.

Oeser B. 1998. *PKC1*, encoding a protein kinase C, and *FAT1*, encoding a fatty acid transporter protein, are neighbours in *Cochliobolus heterostrophus*. *FEMS Microbiol. Lett.* **165:** 273-280.

Orr JW, Keranen LM and Newton AC. 1992. Reversible exposure of the pseudosubstrate domain of protein kinase C by phosphatidylserine and diacylglycerol. *J. Biol. Chem.* **267:** 15263-15266.

Ou SH. 1985. Rice diseases. (Kew, Surrey: Commonwealth Mycological Institute, CAB) pp. 109-201.

Oved S and Yarden O. 1996. Differential expression of class C protein kinases during early development of *Neurospora crassa*. The Seventeenth Congress of the Israeli Phytopathological Society, Bet. Dagan, Israel. Phytoparasitica. pp 164.

Page RDM. 1996. TREEVIEW: An application to display phylogenetic trees on personal computers. *Computer Applications in the Biosciences.* **12:** 357-358.

Paravicini G, Mendoza A, Antonsson B, Cooper M, Losberger C and Payton MA. 1996. The *Candida albicans PKC1* gene encodes a protein kinase C homolog necessary for cellular integrity but not dimorphism. *Yeast.* **12:** 741-56.

Pappa H, Murray-Rust J, Dekker LV, Parker PJ and McDonald NQ. 1998. Crystal structure of the C2 domain from protein kinase C-delta. *Structure.* **6:** 885-894.

Pascholati SF, Yoshioka H, Kunoh H and Nicholson RL. 1992. Preparation of the infection court by *Erysiphe graminis* f.sp. *hordei*: cutinase is a component of the conidial exudates. *Physiol. and Mol. Plant Pathol.* **41:** 53-59.

Pears C, Schaap, D and Parker P. 1991. The regulatory domain of protein kinase C-epsilon restricts the catalytic domain specificity. *Biochem. J.* **276:** 257-260.

Perez P and Calonge TM. 2002. Yeast protein kinase C. *J. Biochem.* **132:** 513-517.

Peterhansel C, Freialdenhoven A, Kurth J, Kolsch R and Schulze-Lefert P. 1997. Interaction analyses of genes required for resistance responses to powdery mildew in barley reveal distinct pathways leading to leaf cell death. *Plant Cell.* **9:** 1397-1409.

Pfaffl MW. 2001. A new mathematical model for relative quantification in real-time RT-PCR. *Nucleic Acids Res.* **29:** 2002-2007.

Podila GK, Rogers LM and Kolattujudy PE. 1993. Chemical signals from avocado surface wax trigger germination and appressorium formation in *Colletotrichum. Plant Physiol.* **103:** 267-272.

Pouysségur J, Volmat V and Lenormand P. 2002. Fidelity and spatio-temporal control in MAP kinase (ERKs) signalling. *Biochemical Pharmacology.* **64:** 755-763.

Prabhu AS, Filippi MC and Zimmermann FJP. 1996. Genetic control of blast in relation to nitrogen fertilization in upland rice. *Pesquisa Agropecuaria Brasileira.* **31:** 339-347.

Pryce-Jones E, Carver TLW and Gurr SJ. 1999. The roles of cellulase and mechanical force in penetration by *Erysiphe graminis* f.sp. *hordei. Physiol. Mol. Plant Pathol.* **55:** 175-182.

Raines MA, Kolesnick RN and Golde DW. 1993. Sphingomyelinase and ceramide activate mitogen-activated protein kinase in myeloid HL-60 cells. *J. Biol. Chem.* **268:** 14572-14575.

Regenfelder E, Spellig T, Hartmann A, Lauenstein S, Bölker M and Kahmann R. 1997. G proteins in *Ustilago maydis*: transmission of multiple signals. *EMBO J.* **16:** 1934-1942.

Ron D and Kazanietz MG. 1999. New insights into the regulation of protein kinase C and novel phorbol ester receptors. *FASEB J.* **13:** 1658-1676.

Rossman AY, Howard RJ and Valent B. 1990. *Pyricularia grisea*, the correct name for the rice blast fungus. *Mycologia.* **82:** 509-512.

Ruiz-Roldan, MC, Maier FJ and Schafer W. 2001. *PTK1*, a mitogen-activated-protein kinase gene, is required for conidiation, appressorium formation, and pathogenicity of *Pyrenophora teres* on barley. *Mol. Plant Microbe Interact.* **14:** 116-125.

Roumen EC. 1994. A strategy for accumulating genes for partial resistance to blast disease within a conventional breeding program. In: Rice Blast Disease. RS Zeigler, SA Leong, PS Teng, eds (CAB International, Wallingford, UK, in association with IRRI, Manila, Philippines), pp 245-266.

Sambrook J, Fritsch EF and Maniatis T. 1989. Molecular Cloning. A Laboratory Manual. Cold Spring Harbour Press, USA.

Sayers LG, Katayama S, Nakano K, Mellor H, Mabuchi I, Toda T and Parker PJ. 2000. Rho-dependence of *Schizosaccharomyces pombe* Pck2. *Genes Cells.* **5:** 17-27.

Schaeffer HJ and Weber MJ. 1999. Mitogen-activated protein kinases: specific messages from ubiquitous messengers. *Mol. Cell. Biol.* **19:** 2435-2444.

Schulze-Lefert P and Vogel J. 2000. Closing the ranks to attack by powdery mildew. *Trends in Plant Sci.* **5:** 343-348.

Sharkey NA and Blumberg PM. 1985. Kinetic evidence that 1, 2-diolein inhibits phorbol ester binding to protein kinase C via a competitive mechanism. *Biochem. Biophys. Res. Commun*. **133:** 1051-1056.

Sharkey NA, Leach KL and Blumberg PM. 1984. Competitive inhibition by diacylglycerol of specific phorbol ester binding. *Proc. Natl. Acad. Sci. USA*. **81:** 607-610.

Shen WC, Wieser J, Adams TH and Ebbole DJ. 1998. The *Neurospora rca-1* gene complements an *Aspergillus flbD* sporulation mutant but has no identifiable role in *Neurospora* sporulation. *Genetics*. **148:** 1031-1041.

Sherwood JE and Somerville SC. 1990. Sequence of the *Erysiphe graminis* f. sp *hordei* gene encoding beta-tubulin. *Nucleic Acids Research*. **18:** 1052.

Siegel MR. 1981. Sterol-inhibiting fungicides: effects on sterol biosynthesis and sites of action. *Plant Disease*. **65:** 986-989.

Sivapalan A. 1993. Effects of water on germination of powdery mildew conidia. *Mycol. Res*. **24:** 309-333.

Slater SJ, Ho C, Kelly MB, Larkin JD, Taddeo FJ, Yeager MD and Stubbs CD. 1996. Protein kinase C alpha contains two activator binding sites that bind phorbol esters and diacylglycerols with opposite affinities. *J. Biol. Chem*. **271:** 4627-4613.

Soanes DM, Kershaw MJ, Cooley RN and Talbot NJ. 2002. Regulation of the MPG1 hydrophobin gene in the rice blast fungus *Magnaporthe grisea. Mol. Plant Microbe Interact*. **15:** 1253-1267.

Staples RC and Hoch HC. 1987. Infection structures – form and function. *Experimental Mycology*. **11:** 163-169.

Su Y, Dostman WRG, Herberg FW, Durick K, Xuong NH, Ten Eyck L, Taylor SS and Varughese KI. 1995. Regulatory subunit of protein kinase A: structure of deletion mutant with cAMP binding domains. *Science*. **269:** 807-813.

Suzuki S, Komiya Y, Mitsui T, Tsuyumu S and Kunoh H. 1999. Activity of pectinases in conidia and germlings of *Blumeria graminis* and the expression of genes encoding pectinases. *Ann. Phytopath. Soc. Japan*. **65:** 131-139.

Sweigard JA, Chumley FG and Valent B. 1992. Disruption of a *Magnaporthe grisea* cutinase gene. *Mol. Gen. Genet.* **232:** 183-190.

Sweigard JA, Chumley FG, Carroll AM, Farrall L and Valent B. 1997. A series of vectors for fungal transformation. *Fungal Genetics Newsletter*. **44:** 52-53.

Sweigard JA, Carroll AM, Farrall L, Chumley FG and Valent B. 1998. *Magnaporthe grisea* pathogenicity genes obtained through insertional mutagenesis. *Mol. Plant Microbe Interact*. **11:** 404-412.

Takai Y, Kishimoto A, Inoue and M, Nishizuka Y. 1977. Studies on a cyclic nucleotide-independent protein kinase and its proenzyme in mammalian tissues. I. Purification and characteristaion of an active enzyme from bovine cerebellum. *J. Biol. Chem*. **252:** 7603-7609.

Takai Y, Sasaki T, Tanaka K, and Nakanashi H. 1995. Rho as a regulator of the cytoskeleton. *Trends Biochem. Sci*. **20**: 227-231.

Talbot NJ. 1995. Having a blast: exploring the pathogenicity of *Magnaporthe grisea. Trends Microbiol*. **3:** 9-16.

Talbot NJ and Foster AJ. 2001. Genetics and genomics of the rice blast fungus *Magnaporthe grisea*: Developing an experimental model for understanding fungal diseases of cereals. *Adv. Bot. Res.* **34:** 263-287.

Talbot NJ, Ebbole DJ and Hamer JE. 1993. Identification and characterisation of *MPG1*, a gene involved in pathogenicity from the rice blast fungus *Magnaporthe grisea*. *Plant Cell.* **5:** 1575-1590.

Talbot NJ, Kershaw MJ, Wakley GE, de Vries OMH, Wessels JGH and Hamer JE. 1996. *MPG1* encodes a fungal hydrophobin involved in surface interactions during infection-related development of *Magnaporthe grisea*. *Plant Cell.* **8:** 985-99.

Takano Y, Kikuchi T, Kubo T, Hamer JE, Mise K and Furusawa I. 2000. The *Colletotrichum lagenarium* MAP kinase gene CMK1 regulates diverse aspects of fungal pathogenesis. *Mol. Plant Microbe Interact.* **13**: 374–383.

Tamaoki T, Nomoto H, Takahashi I, Kato Y, Morimoto M and Tomita F. 1986. Staurosporine, a potent inhibitor of phospholipid / Ca^{2+} dependent protein kinase. *Biochem. Biophys. Res. Comm.* **135:** 397-402.

Taylor SS, Buechler JA and Yonemoto W. 1990. cAMP-dependent protein kinase: framework for a diverse family of regulatory enzymes. *Annu. Rev. Biochem.* **59:** 971-1005.

Teague MA, Chaleff DT and Errede B. 1986. Nucleotide sequence of the yeast regulatory gene *STE7* predicts a protein homologous to protein kinases. *Proc. Natl. Acad. Sci. USA.* **83:** 7371-7375.

Tenjo F, Xu JR and Hamer JE. 1999. Expression and cellular distribution of *Magnaporthe grisea* MAP kinase *PMK1*. Abstracts of the 20th Fungal Genetics Conference, Asilomar, CA. March 23-28, 1999. p118.

Tentler S, Palas J, Enderlin C, Campbell J, Taft C, Miller TK, Wood RL and Selitrennikoff CP. 1997. Inhibition of *Neurospora crassa* growth by a glucan synthase-1 antisense construct. *Curr Microbiol.* **34:** 303-308.

Terhune BT and Hoch HC. 1993. Substrate hydrophobicity and adhesion of *Uromyces* urediospores and germlings. *Exp. Mycol.* **17:** 241-252.

Thieron M, Pontzen R, Kurahashi Y, Lyr H, Russell PE, Dehne HW and Sisler HD. 1999. Molecular action mechanism of a new melanin biosynthesis inhibitor. In: Modern fungicides and antifungal compounds II. 12th International Reinhardsbrunn Symposium, Friedrichroda, Thuringia, Germany, 24th-29th May 1998, 101-109.

Thines E, Eilbert F, Sterner O and Anke H. 1997a. Signal transduction leading to appressorium formation in germinating conidia of *Magnaporthe grisea*: effects of second messengers diacylglycerols, ceramides and sphingomyelin. *FEMS Microbiol. Lett.* **156:** 91-94.

Thines E, Eilbert F and Sterner O. 1997b. Glisoprenin A, an inhibitor of the signal transduction pathway leading to appressorium formation in germinating conidia of *Magnaporthe grisea* on hydrophobic surfaces. *FEMS Microbiol. Lett.* **151:** 219-224.

Thines E, Weber RW and Talbot NJ. 2000. MAP kinase and protein kinase A-dependent mobilization of triacylglycerol and glycogen during appressorium turgor generation by *Magnaporthe grisea*. *Plant Cell.* 12: 1703-1718.

Thomas SW, Glaring MA, Rasmussen SW, Kinane JT and Oliver RP. 2002. Transcript profiling in the barley mildew pathogen *Blumeria graminis* by serial analysis of gene expression (SAGE). *Mol. Plant Microbe Interact.* **15:** 847-856.

Thompson JD, Gibson TJ, Plewniak F, Jeanmougin F and Higgins DG. 1997. The ClustalX windows interface: flexible strategies for multiple sequence alignment aided by quality analysis tools. *Nucleic Acids Res.* **24:** 4876-4882.

Toda T, Shimanuki M and Yanagida M. 1993. Two novel protein kinase C-related genes of fission yeast are essential for cell viability and implicated in cell shape control. *EMBO J.* **12:** 1987-95.

Toda T, Dhut S, Superti-Furga G, Gotoh Y, Nishida E, Sugiura R and Kuno T. 1996. The fission yeast *pmk1+* gene encodes a novel mitogen-activated protein kinase homolog which regulates cell integrity and functions coordinately with the protein kinase C pathway. *Mol. Cell Biol.* **16:** 6752-6764.

Toker A. 1998. Signaling through protein kinase C. *Front Biosci.* **3:** D1134-1147.

Toullec D, Pianetti P, Coste H, Bellevergue P, Grand-Perret T, Ajakane M, Baudet V, Boissin P, Boursier E and Loriolle F. 1991. The bisindolylmaleimide GF 109203X is a potent and selective inhibitor of protein kinase C. *J. Biol. Chem.* **266:** 15771-15781.

Tucker SL and Talbot NJ. 2001. Surface attachment and pre-penetration stage development by plant pathogenic fungi. *Annu. Rev. Phytopathol.* **39:** 385-417.

Tsutakawa SE, Medzihradszky KF, Flint AJ, Burlingame AL and Koshland DE Jr. 1995. Determination of *in vivo* phosphorylation sites in protein kinase C. *J Biol. Chem.* **270:** 26807-26812.

Urban M, Bhargava T and Hamer JE. 1999. An ATP-driven efflux pump is a novel pathogenicity factor in rice blast disease. *EMBO J.* **18:** 512-521.

Urech PA, Staub T and Voss G. 1997. Resistance as a concomitant of modern crop protection. *Pesticide Sci.* **51:** 227-234.

Valent B. 1990. Rice blast as a model system for plant pathology. *Phytopathology.* **80:** 33-36.

Valvarde AM, Sinnet-Smith J, Van Lint J and Rozengurt E. 1994. Molecular cloning and characterisation of protein kinase D: a target for diacylglycerol and phorbol esters with a distinctive catalytic domain. *Proc. Natl. Acad. Sci. USA.* **91:** 8572-8576.

von Ropenack E, Parr A and Schulze-Lefert P. 1998. Structural analyses and dynamics of soluble and cell wall-bound phenolics in a broad spectrum resistance to the powdery mildew fungus in barley. *J Biol. Chem.* **273:** 9013-9022.

Wahl I, Eshed NS, Segal A and Sobel Z. 1978. Significance of wild relatives of small grains and other wild grasses in cereal powdery mildews. In: The Powdery Mildews. DM Spencer, ed (London, UK: Academic Press Ltd).

Wakelam MJ. 1998). Diacylglycerol - when is it an intracellular messenger? *Biochim. Biophys. Acta.* **1436:** 117-126.

Way KJ, Chou E and King GL. 2000. Identification of PKC-isoform-specific biological actions using pharmacological approaches. *Trends Pharmacol. Sci.* **21:** 181-187.

Webster J. 1993. Introduction to the fungi. (Cambridge UK: Cambridge University Press).

Wheeler IE, Hollomon DW, Gustafson G, Mitchell JC, Longhurst C, Zhang Z and Gurr SJ. 2003. Quinoxyfen perturbs signal transduction in barley powdery mildew (*Blumeria graminis* f.sp. *hordei*). *Mol. Plant Path.* **4:** 177-186.

Whitmarsh AJ and Davis RJ. 1998. Structural organization of MAP-kinase signalling modules by scaffold proteins in yeast and mammals. *Trends Biochem. Sci.* **23:** 481-485.

Wolfe MS. 1984. Trying to understand and control powdery mildew. *Plant Pathol.* **33:** 451-466.

Wolfe MS and Schwarzbach E. 1978. The recent history of the evolution of barley powdery mildew in Europe. In: The Powdery Mildews, DM Spencer, ed (London, UK: Academic Press Ltd.), pp 129-157.

Woolacott B and Archer SA. 1984. The influence of the primary germ tube on infection of barley by *Erysiphe graminis* f.sp. *hordei*. *Plant Pathol.* **33:** 225-231.

Wösten HAB, Ásgeirdóttir SA, Krook JH, Drenth JHH and Wessels JGH. 1994. The fungal hydrophobin Sc3p self-assembles at the surface of aerial hyphae as a protein membrane constituting the hydrophobic rodlet layer. *Eur. J. Cell Biol.* **63:** 122–129

Xu JR. 2000. MAP kinases in fungal pathogens. *Fungal Genet. Biol.* **31:** 137-152.

Xu JR and Hamer JE. 1996. MAP kinase and cAMP signaling regulate infection structure formation and pathogenic growth in the rice blast fungus *Magnaporthe grisea*. *Genes Dev.* **10:** 2696-2706.

Xu JR, Urban M, Sweigard JA and Hamer JE. 1997. The *CPKA* gene of *Magnaporthe grisea* is essential for appressorial penetration. *Mol. Plant Microbe Interact.* **10:** 187-194.

Xu JR, Staiger CJ and Hamer JE. 1998. Inactivation of the mitogen-activated protein kinase Mps1 from the rice blast fungus prevents penetration of host cells but allows activation of plant defense responses. *Proc. Natl. Acad. Sci. USA.* **95:** 12713-12718.

Xiao JZ, Oshima A, Kamakura T, Ishiyama T and Yamaguchi I. 1994a. Extracellular glycoprotein(s) associated with cellular differentiation in *Magnaporthe grisea*. *Mol. Plant Microbe Interact.* **7:** 639-644.

Xiao JZ, Watanabe T, Kamakura T, Ohshima A and Yamaguchi I. 1994b. Studies on cellular-differentiation of *Magnaporthe grisea* - physicochemical aspects of substratum surfaces in relation to appressorium formation. *Physiol. Mol. Plant Pathol.* **44:** 227-236.

Yang A and Dickman MB. 1997. Regulation of cAMP and cAMP dependent protein kinase during conidial germination and appressorium formation in *Colletotrichum trifolii*. *Physiol. Mol. Plant Pathol.* **50:** 117-127.

Yang Z and Dickman MB. 1999. *Colletotrichum trifolii* mutants disrupted in the catalytic subunit of cAMP-dependent protein kinase are non-pathogenic. *Mol. Plant Microbe Interact.* **12:** 1753-1790.

Ypema HL and Gold RE. 1999. Kresoxim-methyl. Modifications of a naturally occurring compound to produce a new fungicide. *Plant Disease*. **83:** 4-17.

Zeyen RJ and Bushnell WR. 1979. Papilla response of barley epidermal cells caused by *Erysiphe graminis*: rate and method of deposition determined by microcinematography and transmission electron microscopy. *Can. J. Bot.* **47:** 898-913.

Zeyen RJ Carver TLW and Lyngkaer MF. 2002. Epidermal Cell Papillae. In: The Powdery Mildews: A Comprehensive Treatise, RR Belanger, WR Bushnell, AJ Dik and TLW Carver, eds (St Paul, MN.: APS Press), pp. 107-125.

Zhang F, Strand A, Robbins D, Cobb MH and Goldsmith EJ. 1994. Atomic structure of the MAP kinase ERK2 at 2.3 Å resolution. *Nature.* **367:** 704-711.

Zhang G, Kazanietz MG, Blumberg PM and Hurley JH. 1995. Crystal structure of the cys2 activator-binding domain of the protein kinase C delta in complex with phorbol ester. *Cell.* **81:** 917-924.

Zhang Z and Gurr SJ. 2000. Walking into the unknown: a 'step down' PCR-based technique leading to the direct sequence analysis of flanking genomic DNA. *Gene.* **253:** 145-150.

Zhang Z and Gurr SJ. 2001. Expression and sequence analysis of the *Blumeria graminis* mitogen-activated protein kinase genes *mpk*1 and *mpk*2. *Gene.* **266:** 57-65.

Zhang Z, Hall A, Perfect E and Gurr SJ. 2000. Differential expression of two *Blumeria graminis* chitin synthase genes. *Mol. Plant Pathol.* **1:** 125-138.

Zhang Z, Priddey G and Gurr SJ. 2001. The barley powdery mildew protein kinase C gene, *pkc*1 and *pkc*-like gene, are differentially expressed during morphogenesis. *Mol. Plant Pathol.* **2:** 327-337.

Zhang Z, Henderson C and Gurr SJ. H_2O_2 scavenger activity in the true obligate barley powdery mildew pathogen. *Submitted.*

Zheng L, Campbell M, Murphy J, Lam S and Xu JR. 2000. The *BMP1* gene is essential for pathogenicity in the gray mold fungus. *Botrytis cinerea. Mol. Plant Microbe Interact.* **13:** 724-732.

Zhao M, New L and Kato Y. 1998. Activation of MEF2A by map kinase p38. *FASEB J.* **12:** 448.

Zhou XL, Stumpf MA, Hoch HC and Hung C. 1991. A mechanosensitive channel in whole cells and in membrane patches of the fungus *Uromyces. Science.* **253:** 1415-1417.

Zhou SC, Zhu XY, Jiang YF, Yang QY, Ke W, Miao RW and Wu-Shang Z. 1999. Incorporation of the rice blast durable resistance into hybrid rice. *Chinese Journal of Rice Science.* **13:** 69-72.

```
CCAAATACCT GCCGTACTGG CTCGTCGTGT TACTGTCGTG ATCGTTTCCC GATTGTGAAC
---------------------►  Primer A
CAGACATGTC AGATACGATA GCCCGGCAAT AAGAGGTAGC AACATTGTAG CAGACCGTAA
ATGTATTAAT ACCACCTGTC AATACTATTG TGTTGCTACT TTGGTATCTA CCTAGGTACC
TATCTAGGTA CCAACCTACC CACCTACCTG GCTTACCTCC TTCAAGGTAC CTCCTTATCC
AGGTTGTAGC TCCCATCTGC TCATCTGGTA TCCACACAGA GAGACTTCCC AAGGCCACCT
TCTCCTTTTT CGGCCCTTCC TTTCCCAGCC AGCCCAGACC ACCTGTCCTG GGCCGACTGA
CCGACCTACT TGTTATTACC TACCTACCGA CAGGACATCC CCTACCTTAC CTTACAACCA
CGTACCAACG ATCATTAACG ACTGGACTGG ACGGGGTTTG ATTAATTGTC ACTGTCATTC
TCGTTGGTCC ATCCGTCCCA AGTCACCCAG GAGAGAAAAG GCACGCGGGT CAGGTTGCCT
GCCTAACCAG AATTGAAAGG TCCCTCTTCA GTAAAAAAGA CGGCGCTTGG ACGGCTTTCC
TGCCTGGGTC TTGACGATCA AGCACGGTGG CCGAGCTTTC TATTTTATTT TATTTTTTAT
TCTTATTATT TTTTTCACAT CGCCCTGCAG CCCAAGGAAG CAGCTGCACA ATCTCCGCTG
CCGCCTCCAT CGAGACTAGG TTATTGAACT ACTGCACTAC CTACACCACA GCTTTATTGG
CACGTTGCGA CTGTACTTGC TGCGGCCAAG GAACCAACAA AGGCACCAAA CTTTTTGAAT
TATTTTCTAT CTTTTTTCCC CATTTGCCTT TTGTTTTTTG TACTTGTCCC TGGGAATTTC
GCCACTTCCC ATTGAGCGCA GGTCCCTGAG CCCAAGTCGA CAACCTTCGG TGCACCGTCG
CACCTTACCC GCAATTCAAC AGCCCAAGTC TCCCCGCTAG ACAAACCCCG CTCCGCTTTC
CTGAACCAGA GCAGGCGGCA TCATCGCCAG CTCCTTTCAG CGCCGCCATG TCTCGCGCCA
ATCCACCAAG CAACTCTTCG GGGTCTCGCA AGATCTCATT CAACGTAAGC GAGCAATACG
ACATCCAGGA TGTCGTGGGC GAGGGCGCTT ATGGAGTCGT TTGGTAAGTA CACCTCTGCC
GGAACCGAAC ACCGCATCTT GCCTGGACCT GCTCCGCAAC ATCCAAAGAA TGGCTGTACA
ATTTGGTCAG GACGGTAACC TTTCAAACTT TGCGTCGCTT AATGGCTGAC ATGACCGGTG
GGCGTTTTGG TCTGTTGTAG CTCTGCGATC CATAAGCCTT CGGGCCAAAA GGTTGCCATA
AAGAAGATCA CCCCGTTCGA TCATTCTATG TTCTGCCTAC GAACCCTCCG CGAGATGAAG
CTGCTCCGGT ACTTCAACCA CGAGAACATC ATTTCCATCC TCGACATCCA GAAGCCCCGA
AGCTACGAGA CCTTCAACGA GGTGTACCTG ATCCAGGAGC TCATGGAGAC TGACATGCAC
CGTGTCATCC GCACCCAAGA CCTATCCGAC GATCACTGCC AGTACTTCAT CTACCAGACT
CTGCGTGCTC TCAAGGCAAT GCACTCGGCA AACGTGCTTC ACCGTGATCT GAAGCCCTCG
AATCTCCTTC TCAACGCCAA CTGTGATTTG AAGGTTTGCG ATTTTGGTCT GGCTCGTTCT
GCCGCCTCGC AAGAGAACAA CTCGGGTTTC ATGACAGAAT ACGTCGCTAC GCGTTGGTAC
CGTGCTCCCG AGATCATGTT GACCTTTAAG GAGTACACCA AGGCTATTGA CGTGTGGTCT
GTTGGCTGCA TTCTGGCTGA AATGCTCAGC GGAAAGCCTT TGTTCCCCGG AAAGGACTGT
AAGTTACAAT GGCGTTCCTC TGTATTGAGT GTGCTACTTG CTCCCGCCCC AGAGTGTGCT
GCACCGTAGA CACGATGTTC TCCCCAGTAC TGACACTTGA TACTTTGTTA GACCACCACC
AGCTCACGCT GATTCTTGAC GTTCTCGGCA CACCCACCAT GGAGGACTAC TATGGTATCA
AGTCCCGCCG TGCAAGGGAG TACATTCGCT CGCTGCCGTT CAAGAAAAAG GTTCCTTTCA
GGACACTCTT CCCCAAGACT TCGGATCTCG CCTTGGACCT GTTGGAGAAG TTGCTTGCCT
TTAACCCCGT CAAGCGCATC ACCGTCGAGG AAGCTTTGAA GCACCCTTAC CTTGAGCCGT
ACCATGACCC CGATGATGAA CCCACCGCAC CGCCGATTCC CGAGGAGTTC TTTGATTTCG
ATAAGCACAA GGATAACCTG AGCAAAGAGC AGCTCAAGCA GTTCATCTAC CAGGAAATTA
TGCGGTAATG CGGCGAGCGG TCCATGGTCA TTGGCTTGTT TGACAGGCAG CCCACAGGCA
TTGGCGTCGA GCGAAGGAAC TAGACGTCTC GCAGTGGTGG CTGCGGCAGA GCGTTCGCGT
GCGGTAGCAG GGGTGAAATG GGACAGATCC CGTGGGATAT GTTCAAGATG GCATATCAGG
ATGTGCATGG GGCTATCAGG GAGATCGATC TGCTGTAAGC TGCCAGAGCC TGCAAAAGAT
CATTCCTTGG TTTTTTTCTA TATCCACTAT CAACCACATT TAACACCACA TCTTACATTT
TCCACCTCAT CCCTCACAAT ACCACATGCT GTCTTGACAC CGACCATCCT CGACTTCAGA
CTTGTGTATC CTCAAGTTTA CATGGAGGCT GCTGTGGCAA TCACGCGCAA ACTTGAAAGG
CATAAGTTTG TTTACTGGTG AAGGCGGGCG GATCTGTGTA TTCGTGGATT GCTGTGCCGA
GCGGAGCTTT CAAGACAAAG GGAATAATTG TATATGAGCA ATTTCTGAGT GTGATTTACT
ATGCGCCATC CCCGCCGGCA CTCACAATTA A
   Primer B  ◄--------------------
```

Appendix 1. *Magnaporthe grisea PMK1* promoter and gene sequences. Primers (A and B) used to obtain the promoter and gene for transformation experiments are indicated with arrows. The start codon (ATG) is given in red. The *Hind*III restriction digest site used in Southern analysis is indicated (blue).

```
GAATAAGATG CTGCTCATGC CTCAGGCTCG GTCCTCATGG CATAACCTAA AGGCCAGCAT
--------------------► Primer C
TGTCTGTCTC ATATACCAGC TTTCCCTTGA TTGCCCCGCG TATCAGATTA GGCGAGATCC
ACTTCAAGAG TTGAGGTAGC CTTCATCGAA GTTCTAGAGT ACCGGACGTC AATTGAGCTT
CACAGCGAGC CAAGGCCTCG CAGCTCTTGT TTAGCAGTAT CCTTTGAAAA TATTTTGATA
TCACGTCTCC ATTCATTTCG TACATCTTTA ATCTAACTGG CCTCAGCTTT GTTTGAGGTC
TGGTTTACCC AAGCGTTGAC CAGACTAGTC CATCAGATTC GGAACGCGAC TACGGAAGTT
GCAGCTTAGT GGAGGTAGTG CCTGCTCTGC TACTACAAAT GCTCGAGGGA CCGAGCGCAA
  Primer F ◄----------------
TTGCTGCAGG TAGCTGACAG GCGAAACTTG GACTCTAGGG GTATAAGCTG AGGACAACAA
CGACAATCCA TAACAGCAAA GTTCAATCTA GAATAGCTGC AAACTACATC GACTTGAGCT
ATTCCTTTAA CTTCCGCACC CTTTGCTCGT AGGCTGCTTG TGAGAGACGA AACATCTCGC
GCTTTCATTG CTATTGCTGC AACTGTCTGC TGTCCACATC TCTCGCCACT CTTCTCTGCT
YTGACATCTC CTACCCTGAG ACCTTGCTCA TTCAATAGTA ATAGCTCATC TTTTACAACA
TCCCCTTACT ACTACCGGTC ATCTGTCAGC TTTCAAGCTG CATCTATCTA ATATTCAAGA
CTTGCAAGCG AACACCAGAG TTGTCTTTTT CCTAATTTCA CCAACCCCTC CTCTTTAGAT
AGGAACAGCT TTCATACACG CTTTCAGATC GTCAAAGGCA CTTTCAAGAT GTCGACCCGT
GCCCCTAATG CTACGACAGG ATCGCGTAAG ATCTCATTCA ACGTAAGTGA GCAGTATGAT
ATTCAAGATG TTGTGGGAGA GGGTGCCTAT GGTGTTGTCT GGTGAGTCTC ACTCAGCCTG
AATACCCCAC CATTTAAAGA TGGTATTGTC ACGATACGCT GCTCAACTCT TTCCTGACAT
CTATCTTCAT TGACTCTACC CTCAAATTTT GAAGAAATAT TCTTTTAATT CTATTTTCTA
CAGCTCAGCT CTTCACAAGC CCACAGGACA AAAGGTTGCT ATCAAAAAAA TTACTCCATT
CGACCATTCT ATGTTCTGTC TGAGAACATT GCGAGAGATG AAGCTGCTTC GATACTTCAA
TCATGAAAAT ATCATCTCAA TTTTGGATAT TCAAAAGCCT CGCAGCTTTG ACTCTTTCAC
CGAGGTTTAC TTGATTCAGG TATATACAAA TCTTAAATAC AAAATCAAGA AAACCCCTGC
TTGCTCTAAT CATAGATAGC AAGAGACGAC TAACAACAGT CTACAGGAGC TTATGGAAAC
CGACATGCAC AGAGTAATTC GCACTCAAGA TCTCTCAGAT GATCATTGCC AGTATTTTAT
ATACCAGACT CTTCGTGCAC TTAAAGCTAT GCATTCCGCC AACGTCTTAC ACCGTGATCT
TAAGCCCTCC AACCTTCTTA TAAATGCCAA CTGCGATCTT AAGGTTTGCG ATTTTGGACT
AGCTCGATCT GCTGCCTCAC AAGAGGATTG TTCTGGATTC ATGACTGAAT ATGTGGCGAC
TCGCTGGTAT CGTGCGCCTG AAATCATGTT GACCTTTAAA GAATATACAA AAGCAATTGA
TGTATGGTCT GTTGGGTGTA TCTTGGCAGA GATGCTGAGC GGAAAACCTT TGTTCCCGGG
AAAAGATTGT ACGTTTCACA AACACACACC TACATATACA AATTCATTGC GTATACCTCT
AACATGATGA AGACCATCAC CAATTAACAC TAATCCTTGA TGTTCTCGGC ACCCCCACTA
TGGAGGACTA TTATGGCATC AAATCTCAGT CTGTGCTCGC GAATATATTC GATCCCTTCC
ATTCAAGAAG AAGATTCCCT TCAAACAAAT GTTTCCCCAA AACGTCTGAT TTAGCACTTG
ATCTATTAGA AAAGTTATTA GCCTTCAATC CAGTCAAGAG AATAACTGTT GACGAGGCCC
TTCAACATCC GTACTTAGAA CCTTATCATG ATCCCGAGGA TGAGCCAACT GCCGATCCAA
TTCCCGAGGA ATTCTTCGAC TTTGACAAAA ACAAGGACAA TTTGAGCAAA GAACAGCTCA
AAGAACTAAT CTTTCAGGAA ATTATGCGGT AGTACCGTTA TGAGCAGGTT CAACAGAGGC
TATGTAATTT ACTTTGTGTG TATCGTGGAT CCGATTAATT CCC
                Primer D  ◄--------------------
```

Appendix 2. *Blumeria graminis* f.sp. *hordei mpk*1 promoter and gene sequences. Primers (C and D) used to obtain the promoter and gene for transformation experiments are indicated with arrows. The start codon (ATG) is given in red. The *Xba*I restriction digest sites used in Southern analysis are indicated (blue).